DEVELOPMENT OF A NEW ADAPTIVE HARMONIC BALANCE METHOD
AND ITS COMPARISON

A THESIS SUBMITTED TO
THE GRADUATE SCHOOL OF NATURAL AND APPLIED SCIENCES
OF
MIDDLE EAST TECHNICAL UNIVERSITY

BY

ONUR SERT

IN PARTIAL FULFILLMENT OF THE REQUIREMENTS
FOR
THE DEGREE OF MASTER OF SCIENCE
IN
MECHANICAL ENGINEERING

FEBRUARY 2018

Approval of the thesis:

DEVELOPMENT OF A NEW ADAPTIVE HARMONIC BALANCE METHOD AND ITS COMPARISON

submitted by **ONUR SERT** in partial fulfillment of the requirements for the degree of **Master of Science in Mechanical Engineering Department, Middle East Technical University by,**

Prof. Dr. M. Gülbin Dural Ünver
Dean, Graduate School of **Natural and Applied Sciences** _____

Prof. Dr. M. A. Sahir Arıkan
Head of Department, **Mechanical Engineering** _____

Assoc. Prof. Dr. Ender Ciğeroğlu
Supervisor, **Mechanical Engineering Dept., METU** _____

Examining Committee Members:

Assoc. Prof. Dr. Yiğit Yazıcıoğlu
Mechanical Engineering Dept., METU _____

Assoc. Prof. Dr. Ender Ciğeroğlu
Mechanical Engineering Dept., METU _____

Assist. Prof. Dr. Mehmet Bülent Özer
Mechanical Engineering Dept., METU _____

Assist. Prof. Dr. Kıvanç Azgın
Mechanical Engineering Dept., METU _____

Assoc. Prof. Dr. S. Çağlar Başlamışlı
Mechanical Engineering Dept., Hacettepe University _____

Date: _____02.02.2018_____

I hereby declare that all information in this document has been obtained and presented in accordance with academic rules and ethical conduct. I also declare that, as required by these rules and conduct, I have full cited and referenced all material and results that are not original to this work.

Name, Last name : Onur SERT

Signature   :

ABSTRACT

DEVELOPMENT OF A NEW ADAPTIVE HARMONIC BALANCE METHOD AND ITS COMPARISON

Sert, Onur

M.Sc., Department of Mechanical Engineering

Supervisor: Assoc. Prof. Dr. Ender Ciğeroğlu

February 2018, 208 pages

Nonlinear systems are encountered in many areas of science. In order to study these systems on a theoretical level, many approaches regarding the solution of nonlinear equation systems have been developed.

Harmonic Balance Method (HBM) is one of the most powerful and popular methods for solving nonlinear differential equations in frequency domain. The main idea of the method is representation of the time-periodic response and nonlinear internal forces in terms of Fourier series and balancing each harmonic term. In order to avoid solving an infinite system of equations, one needs to truncate this series at some point. The number of terms to be included in the series is a compromise between the computational effort and the required solution accuracy. In order to overcome this challenge, numerous adaptive algorithms for automatically selecting the harmonics to be included in the solution are developed. These methods are called Adaptive Harmonic Balance Methods (AHBMs).

In this thesis, it is aimed to investigate and compare the effectiveness of AHBMs that are currently in use for mechanical vibration problems and to introduce new AHBMs

as an alternative to the existing ones. For this purpose, firstly the mathematical backgrounds of all the methods are investigated in detail. Then, using the scripts developed in MATLAB$^{®}$, AHBMs and the classical HBM are employed in order to perform nonlinear response analysis of selected lumped parameter systems. Error analyses are done and comparisons of computational time requirements are obtained in order to show the differences between various methods and effectiveness of the newly proposed methods.

Keywords: Harmonic balance method, adaptive harmonic balance method, harmonic selection, vibrations of nonlinear systems

ÖZ

YENİ BİR ADAPTİF HARMONİK DENGELEME YÖNTEMİ GELİŞTİRİLMESİ VE KARŞILAŞTIRILMASI

Sert, Onur

Yüksek Lisans, Makina Mühendisliği Bölümü

Tez Yöneticisi: Doç. Dr. Ender Ciğeroğlu

Şubat 2018, 208 sayfa

Doğrusal davranış göstermeyen sistemler pek çok bilimsel disiplinde yer almaktadır. Bu sistemleri teorik düzeyde inceleyebilmek adına, doğrusal olmayan denklemlerin çözümü için birçok yöntem geliştirilmiştir.

Harmonik Dengeleme Yöntemi (HDY) doğrusal olmayan denklemlerin frekans düzleminde çözümü için kullanılan en etkili ve popüler yöntemlerden biridir. Yöntemin ana fikri, periyodik davranışların Fourier serisi olarak ifade edilmesine dayanmaktadır. Sonsuz büyüklükte bir denklem sistemi çözmek zorunda kalmaktan kaçınmak için, bu serinin bir noktada sona erdirilmesi gerekmektedir. Bu noktanın seçimi, istenen çözümün hassasiyeti ve maliyeti arasında bir denge kurmayı gerektirmektedir. Bu güçlüğü aşmak ve çözüme dahil edilecek terimleri otomatik olarak belirlemek için çeşitli Adaptif Harmonik Dengeleme Yöntemleri geliştirilmiştir.

Bu tezde, literatürde yer alan ve mekanik titreşimler alanında kullanılan Adaptif Harmonik Dengeleme Yöntemlerini araştırmak, bunların arasında bir karşılaştırma

yapmak ve yeni Adaptif Harmonik Dengeleme Yöntemleri önermek amaçlanmıştır. Bu amaç doğrultusunda, öncelikle var olan yöntemlerin ve önerilen yeni metodların matematiksel arka planları ayrıntılı olarak açıklanmıştır. MATLAB$^{®}$ programında hazırlanan kodlar kullanılarak, hem adaptif harmonik dengeleme yöntemleri hem de klasik harmonik dengeleme yöntemi ile örnek sistemlerin doğrusal olmayan titreşim cevapları hesaplanmıştır. Hata analizleri ve çözüm için harcanan süre karşılaştırmaları yapılarak yöntemlerin farklılıkları ve önerilen yeni yöntemlerin etkileri gösterilmiştir.

Anahtar Kelimeler: Harmonik dengeleme yöntemi, adaptif harmonik dengeleme yöntemi, harmonik seçimi, doğrusal olmayan titreşimler

To my family

and to the memory of Arda Taylan

ACKNOWLEDGEMENTS

TABLE OF CONTENTS

LIST OF TABLES

TABLES

xvi

LIST OF FIGURES

FIGURES

LIST OF SYMBOLS

a	Control parameter for Yümer's Method
$[A]$	Flexibility matrix
$[C]$	Viscous damping matrix
$[D]$	Generalized damping matrix
E_r^d	Total spectral energy ratio for Grolet's Method
$\{F_{ext}(t)\}$	External forcing vector
f_N	Nonlinear force
$\{f_N(t,q,\dot{q})\}$	Nonlinear internal forcing vector
h	Structural damping
i	Unit imaginary number
$[H]$	Structural damping matrix
$[H]^d$	Localized harmonic number matrix for Grolet's Method
$[I]$	Identity matrix
$\{I\}_m$	Index vector for Grolet's method
$[J]$	Jacobian matrix
$[\bar{J}]$	Modified Jacobian matrix for arc length continuation
$\{J\}^d$	Localized index vector for Grolet's method
k	Stiffness
$[K]$	Stiffness matrix
m	Mass
$[M]$	Mass matrix
M^m	Maximum number of equations for Grolet's Method
N	Normal force

N_{iter}	Number of iterations
N_{opt}	Optimum number of iterations for adaptive step size
N_h^m	Maximum number of harmonics
$\{q\}$	Vector of unknowns for arc length continuation
$\{q(t)\}$	Displacement vector
$\{\dot{q}(t)\}$	Velocity vector
$\{\ddot{q}(t)\}$	Acceleration vector
R	Family of algebraic equations to be solved
$\bar{R}$	Modified family of algebraic equations for arc length continuation
s	Step size
t	Time
T	Period
$[T(t)]$	Matrix of harmonic response components
$u(t)$	Input motion for dry friction element
$\{u\}^d$	Localized Fourier coefficient vector for Grolet's Method
$U(t)$	Potential energy
U_m	Mean potential energy
$w(t)$	Slip motion for dry friction element
x	Generalized displacement
$\{x\}$	Vector of unknowns for Newton's method and fixed point iteration
$[\alpha(\omega)]$	Receptance matrix
δ	Gap
ε	Control parameter for Jaumoille's Method
ε^d	Fraction of spectral energy for Grolet's Method
ε_s	Step size modifier

$\bar{\varepsilon}_s$	Modified step size modifier
ε_t	Control parameter for PRB-AHBM
λ	Relaxation factor
μ	Friction coefficient
ρ_b	Backward control parameter for Grolet's Method
ρ_d	Fraction of residual energy for Grolet's Method
ρ_f	Forward control parameter for Grolet's Method
ω	Frequency
$\{Z\}$	Fourier coefficient vector for Jaumoille's Method

Subscripts and Indices

0	Bias term
c	Cosine component
f	nonlinear forcing
im	Imaginary part
j	Equation or variable number
k	Harmonic number
L	Linear
NL	Nonlinear
pr	Pseudo-response
r	Reduced
re	Real part
s	Sine component

Superscripts

i	Iteration number
d	DOF number

Abbreviations

AFT	Alternating frequency time method
AHBM	Adaptive harmonic balance method
DOF	Degree of freedom
EHBM	Elliptic harmonic balance method
EOM	Equation of motion
FB-AHBM	Forcing based adaptive harmonic balance method
FFT	Fast Fourier Transform
HBM	Harmonic balance method
IHBM	Incremental harmonic balance method
IFFT	Inverse fast Fourier transform
MDOF	Multi degree of freedom
ODE	Ordinary differential equation
PRB-AHBM	Pseudo-response based adaptive harmonic balance method
SDOF	Single degree of freedom

CHAPTER 1

INTRODUCTION

1.1 Motivation

All real engineering structures involve clearances, cracks, parts that rub or hit against each other etc. These phenomena make all real structures nonlinear by nature. For many engineering applications, the nonlinear effects inside the system in consideration are negligibly small. Therefore, linear mathematical models are able to approximate the behavior of the system with a high degree of accuracy. On the contrary, other applications involve nonlinearities that affect the dynamical behavior of the system greatly; therefore the use of nonlinear mathematical models becomes a must. In addition to these highly nonlinear systems, advancements in technology introduce new materials, smaller systems and new reasons for engineers to seek for better precision. Moreover, with the advances in computer technology better computational facilities come into the picture. Therefore, we can say that nowadays both the need and the means to employ nonlinear models in dynamic analyses seem to rise.

Mathematical methods to solve nonlinear equations are vital in nonlinear vibrations research. The most common methods for solving the nonlinear differential equations are dependent on performing numerical integration over the time domain. These methods are generally named as time marching methods [1]. But time marching methods are known to require significant amount of computational effort and computational time [2]. In addition to this, for vibration problems, most of the time steady-state response is sought which is in the frequency domain rather than time domain response. In this case the time marching methods require even more

computational time to reach to the steady-state response. Hence, when one is after the steady-state response, computationally more "efficient" methods that can operate directly in the frequency domain are favorable.

Harmonic Balance Method (HBM) is one of the methods that fit to the description given above. It can operate in the frequency domain and is highly advantageous when the frequency response of a time-periodic system is sought. By employing HBM, one can convert nonlinear ordinary differential equations (ODEs) into a set of nonlinear algebraic equations, which are much easier to solve. Therefore, method is computationally more economical than time marching methods and it turns out that it is capable of representing very strong nonlinearities with sufficient accuracy [3]. The mathematical basis of the method is to represent periodic phenomena as truncated Fourier series with finite number of harmonics. This makes it suitable for many kinds of nonlinear problems in many different areas of engineering.

Despite its advantages, for large systems, even when HBM is used, one can end up with a significant number of equations to be solved simultaneously or extensive computational time spent in vain. In order to overcome this difficulty and increase the power of HBM even more, Adaptive Harmonic Balance Methods (AHBMs) come into picture, which can eliminate the use of unnecessary harmonics. Together with a condensation method [2, 4] , AHBMs have the potential to drastically decrease the computational time and the storage space required to solve a nonlinear system. For this purpose numerous AHBMs were introduced to the literature by different researchers in the recent years [4 – 9].

1.2   Literature Survey

This section consists of two parts. The first part includes the HBM, its application areas and multiple variants of HBM. The second sub-section gives an overview of the AHBMs currently available in literature. The adaptive methods which are

developed for nonlinear response analysis of vibratory systems will be discussed in much more detail in the following chapters.

1.2.1 Harmonic Balance Method in Nonlinear Dynamic Response Analysis

HBM is one of the most well known means for analyzing structures involving strong nonlinearities [10]; therefore, it has been used extensively in the analysis of nonlinear systems. HBM are used in several different areas including nonlinear circuit analysis [7, 11]; computational fluid dynamics [9, 12 − 15], nonlinear oscillators [16, 17]; rotor dynamics [18 − 21]; mathematical modeling of friction in bladed disks [22 − 25]; gear dynamics [26, 27]; mathematical modeling of cracks [19, 20, 28], dynamic modeling of structural joints [4, 29]; nonlinear dynamic modeling of aircraft landing gears [30], passive vibration control [31, 32]; energy harvesting [33]; flutter phenomenon [34]; nonlinear identification [35]; vibrations of carbon nanotubes [36, 37]; acoustics [38, 39] and even evaluation of periodic chemical processes [40]. In this thesis, applications of HBM in the field of nonlinear vibrations will be the focus of attention.

HBM was first introduced by Nayfeh and Mook [10]. The basic definition and the formulation of HBM based on the general form of EOM for nonlinear vibrations, has been explained at an introductory level by numerous works [10,, 41]. In these works, the formulations generally include the harmonic and super harmonic components of the response only. Groll and Ewins [18] present a more general formulation which includes sub-harmonics. The book section presented by Sarrouy and Sinou gives an overview of the HBM formulation, together with condensation, path following and solution methods [2]. The method presented by Cameron and Griffin [42] can also be considered as an important contribution to the general HBM formulation. In their paper, Cameron and Griffin investigated Alternating Frequency Time (AFT) method, which is capable of calculating the Fourier coefficients of nonlinear forces by applying an Inverse Fast Fourier Transform (IFFT) − Fast Fourier Transform (FFT) procedure. Then, the coefficients calculated by AFT can be directly used in the HBM

equations. The method is applicable where the Fourier integrals for nonlinear forcing coefficients are too difficult or impossible to evaluate.

One of the most important variants of the HBM is the so called Incremental Harmonic Balance Method (IHBM) introduced by Cheung and Lau [43]. The method is actually equivalent to applying Galerkin Procedure and Newton's Method in consecutive order [44]. Once the vibration response of the system at a single frequency point is known, a small increment is added to the frequency and kept constant, so that the solution at the neighboring point can be found. After that, the incremental increase in the response that corresponds to the increase in frequency is calculated numerically by Newton's Method. The same procedure can be followed by incrementing a component of the response and calculating the frequency values that correspond to it as well. It has later been shown by Ferri [45] that this method is actually equivalent to the so called Harmonic Balance Newton Raphson Method (HBNR). Later on, the IHBM has been studied extensively and further developed. Cheung et al. [46] applied this method to systems having cubic nonlinearity. A variant of the method was derived and used in the analysis of dry friction by Pierre et al. [47]. Lau and Zhang [48] came up with a generalized form of this method so as to study piecewise linear systems. Leung and Chui [49] modified the method and reversed the order of linearization and incrementization in order to locate bifurcations. Lau and Yuen [50] worked on Hopf bifurcation and limit cycle problems with the help of IHBM. Raghothama and Narayanan used IHBM to analyze a two dimensional airfoil with cubic pitching stiffness, undergoing plunge and pitching motions in incompressible flow [51], to study bifurcation and chaos in a geared rotor bearing system [52] and on an articulated loading platform [53]. Similarly, in 2002, Xu, Lu and Cao [54] studied bifurcation and chaos in a harmonically excited oscillator by IHBM. In 2004, Pušenjak and Oblak [55] extended the IHBM to include multiple time scales so that analysis of a system undergoing almost periodic oscillations, under the effect of excitations with incommensurable frequencies. The formulation includes sub-harmonics and the

method uses arc-length continuation to overcome bifurcations. Also, in the same paper they came up with a modification of the method that enables the analysis of autonomous systems as well. In 2005, Sze Chen and Huang [44] applied IHBM for the first time for axially moving beams. In the same year, Zhou and Zhang used IHBM for the response calculation of a wheel shimmy system having both Coulomb and quadratic damping [30]. In 2006, Fu, Wong and Wang [36] used IHBM in a carbon nanotube study. The extension of a method for nonlinear response analysis of spur gear pairs was derived by Shen, Yang and Liu [27]. Another extention for flutter analysis was presented by Cai, Liu and Li [33]. In 2012, Chen, Liu and Meng [56] used IHBM for a statistical study on flutter. In 2013, Lu et al. studied the nonlinear dynamics of a submerged floating structure with the IHBM [57]. They introduced an FFT procedure instead of Galerkin procedure into the method.

Another variant of the HBM is the Elliptic Harmonic Balance Method (EHBM). It was originally introduced by Yuste [58]. The main idea of this method is to use Jacobi elliptic functions instead of circular trigonometric functions in the assumed solution. Yuste made case studies on nonlinear oscillator problems. Later on, the method has been studied by other researchers for studies on elementary systems showing strong nonlinear behavior. Margallo et al. [59] used the method for their study on van der Pol equations. Yuste and Bejarano [60] and Margallo and Bejarano [61] worked on various improvements on the method. Later on, by using EHBM, Alex [62] performed studies on the Duffing oscillator. Also Belhaq and Lakrad [63, 64] employed the method for analyzing mixed parity oscillators and showed that the method is more suitable than the classical HBM for this analysis. In 2008, Cveticanin et al. [65] obtained the periodic solution for the generalized Rayleigh equation with EHBM. In 2009, Chen and Liu [66] extended EHBM for the first time to analyze a 2-DOF oscillator.

Variants of HBM developed by Kim and Noah [67], and Kim and Choi [3] are worth mentioning. In 1996, Kim and Noah [67] developed an alternative HBM for a

nonlinear Jeffcott rotor model. In the 2-DOF model they investigated, the cross-coupling stiffness term caused frequencies which are not integer multiples of the excitation frequency to appear in the response. Therefore, in order to account for these frequencies and obtain the quasi-periodic responses correctly, they substituted double truncated Fourier series into the EOM. They also used the AFT approach for calculating the Fourier coefficients of the nonlinear forcing created by the cross-coupling stiffness. In 1997, Kim and Choi [3] developed a generalized multiple HBM for the analysis of aperiodic, self excited oscillations of Jeffcott rotor having piecewise linear nonlinearity at the bearing support. Again in this paper, the rotor model undergoes self excited vibrations due to the cross-coupled stiffness. Therefore multiple excitations having incommensurable frequencies occur in the system. To formulate the HBM under this kind of an excitation, the authors used multiple Fourier series to express the response of each DOF. For the sake of convenience, they used multiple time scales and introduced the hyper-time concept. Their results show that the new method produces sufficiently accurate results when compared to the numerical integration results. In their literature review paper, using the concepts introduced by Kim and Choi, Sarrouy and Sinou [2] formulated a HBM in a generalized and compact way. Also Guskov et. al [21] did a similar work and presented a compact formulation with the name Generalized Harmonic Balance Method. They also performed case studies for rotor dynamics.

In 2005 Kim, Rook and Singh [68] introduced a new HBM variant. Their method is especially derived for calculating super and sub harmonics, exposing both the stable and unstable responses of torsional systems having clearance type of nonlinearities. As a new development at that time, their method included arc-length continuation and stability analysis. Their results include case studies that verify the method as well as some results that were not seen in the literature before. In 2006, Dunne and Hayward [69] introduced the so called Split Frequency Harmonic Balance Method. In this method, a multi harmonic Fourier series is assumed as the solution. Then, the lower frequency terms and the higher frequency terms are grouped together, splitting

the series into two. The lower harmonics are calculated numerically as always whereas the higher frequencies are not solved directly but are updated. The overall error in the equation system is continuously reduced by including more and more harmonics in the lower frequency group, where case studies were presented on a SDOF oscillator. In 2009, Coudeyras, Sinou and Nacivet [70] developed an extension of the HBM, namely the Constrained HBM. This method was derived for systems having flutter instability and its main purpose is to constrain the HBM so that the unwanted solutions are suppressed. This way the so called stationary nonlinear vibrational response for self-exciting structured can be found. The case studies performed with a disc brake show that the method produces satisfactory results but the accuracy depends greatly on the number of harmonics. Again in 2009 Bonello and Hai [71] introduced the Receptance HBM. Their method focused on nonlinear dynamic models of aero-engine assemblies with nonlinear bearings. The method requires the linear receptance matrix to be given as an input, in order to construct nonlinear equation of motion of the system Where the Finite Element Analysis (FEA) of the engine must be done as a priori. In 2009 LaBryer and Attar [72] presented the High Dimensional HBM for large-scale problems. Unlike all other HBM variants, this method actually performs in the time domain. By defining a Discrete Fourier Transform (DFT) operator, they were able to switch from frequency domain to the time domain easily. The authors claim that, working in the time domain makes the method possible to be integrated into an existing FEA program, thus enabling that program to be computationally more efficient and more accurate in nonlinear vibration analysis. Their case studies indicate that the method yields sufficient results and works faster than time marching methods. In 2011, Leung and Guo [73] introduced the Forward Residue Harmonic Balance Method for systems with fractional derivative damping. In the same year they presented the Residue Harmonic Balance Method for the solution of nonlinear jerk equations [74]. The results of their study showed that the new method yields better results than the previously known methods. In 2013, Xiao, Zheng and Cao [75] used Residue Harmonic Balance Method for their studies on the van der Pol oscillator. In 2013,

7

Didier, Sinou and Faverjon [76] introduced the Stochastic Harmonic Balance Method for the solution of nonlinear dynamic systems with non-regular nonlinearities and in the existence of uncertainties. The results of the newly proposed method and a known solution procedure combining Multi-Dimensional Harmonic Balance Method and Monte Carlo simulations are compared with each other, which validated the new method.

1.2.2 Adaptive Harmonic Balance Methods in Literature

The methods which are developed to select the harmonics that are dominant in the system, and to keep unnecessary harmonics out of the solution process will be summarized here. In these methods, unlike the ones described in the previous section, the total number of harmonics to be included in the assumed periodic solution is not constant. The number of harmonics is subject to change according to the criteria used. The main purpose in Adaptive Harmonic Balance Method (AHBM) is to increase the computational efficiency of the solution process, since unnecessary harmonics used in the solutions has a drastic effect in the increase of computational time.

The first AHBM was developed by Gourary et al. [8], in which authors analyzed nonlinear electrical circuits. They transformed the equation set to be solved to a form such that the terms which correspond to the linear nodes (the nodes which do not have a nonlinear element attached to them) are zero and the terms which correspond to the nonlinear terms have almost zero higher harmonics. Therefore they proposed a new method that does not include linear harmonics in the equations to be solved and further reduces this equation set by decreasing the number of harmonics for weakly nonlinear nodes. In order to decide the degree of nonlinearity, they used the "nodal residual norm" concept. They calculated the norm of the vector which contains the Fourier coefficients for each node. They decreased the number of harmonics until the norm becomes less than a pre-determined threshold value. The harmonics to be excluded from the solution are selected by the contribution they make to the total

8

value of the norm whereas the ones with the minimal contribution are excluded from the solution.

In 2004, Maple et al. introduced another AHBM method [9]. They worked on the nonlinear CFD analyses of a supersonic/subsonic diverging nozzle with unsteady periodic outflow conditions. The adaptive method they derived is based upon the concept of "spectral energy". In this method, the energy level that corresponds to the last harmonic included in the solution is continuously calculated and monitored. This value is divided to the total energy. This calculation is done for each cell in the CFD mesh separately. If the ratio of the two energy levels at a specific cell turns out to be higher than an allowed value set by the user, this means that the last harmonic is considerably high. Therefore more harmonics need to be added to the solution. This process continues until the energy levels of last harmonics become lower than the threshold value. The method turned out to be very efficient, causing a decrease in the computational effort up to 86%.

In 2005, Zhu and Christofferssen [7] developed an AHBM where they investigated the nonlinear behavior of a bipolar oscillator in an electric circuit. Similar to Maple et. al. [9], they monitored the amplitudes of each harmonic in order to force convergence on the system which allowed them to reach steady state solution earlier.

In 2010, during his research on nonlinear vibrations and mistuning identification of bladed disks, Yümer [6] introduced a new AHBM. Unlike the researchers before him, Yümer derived a so-called global method where the number of harmonics to be included in the solution is the same for every DOF in the system. In this method, the adaptiveness is achieved by monitoring the absolute values of the terms inside the nonlinear forcing vector. Yümer stated that his method works pretty well when the parameters are chosen wisely.

Again in 2010, in their study on nonlinear bolted joint models, Jaumoillé et. al. [4] introduced another AHBM, which, is a global method similar to Yümer's. The method is an incremental method, in which the response of system is calculated with a certain number of harmonics, then the number of harmonics is increased by one and the solution is performed again until a stopping criterion based on the approximate strain energy is reached. Authors demonstrated their method on a bolted joint model with two beams and two LuGre friction models. The results showed that their method works pretty well for the problems with friction nonlinearity.

In 2012, Grolet and Thouverez developed a different AHBM [5]. In this method, similar to the method of Maple et. al. [9] adaptiveness is achieved by monitoring the spectral energy of each harmonic in the tangent predictor. It allows utilizing different number of harmonics at different DOFs. Moreover, different from the most of the methods described above, it is not an incremental method.

The three AHBMs which are derived for structural dynamics problems will be discussed in more detail in Chapter 3.

1.3 Objective

In this study, it is aimed to introduce a new AHBM and compare it to the other methods available in the literature. This is accomplished by firstly describing the mathematical background of these methods in detail. Then, each of these methods will be employed for the response calculation of selected nonlinear systems. The results are then compared to each other in terms of computational time and accuracy. The systematic approach used for the error analysis is also explained in detail so that the objectiveness of the comparison can be demonstrated. In brief, the aim throughout the thesis is to introduce a new AHBM and demonstrate the contribution it makes to the current literature.

1.4 Scope of the Thesis

The outline of the thesis is as follows:

In Chapter 2, the nonlinear response analysis of dynamic structures is presented. Firstly, the general structure of a nonlinear EOM is described. Secondly, the means available for the solution of this nonlinear EOM are summarized. Later on, the continuation methods that give us the means to obtain the nonlinear response curves are mentioned. In addition, some of the nonlinearity types from the literature are presented. Finally, some explanatory case studies are given.

In Chapter 3, the details of the AHBM methods developed for nonlinear vibration analyses are presented. Firstly, the methods from the literature are investigated and explanatory case studies are given. Then, similarly, the newly proposed methods are explained and are illustrated on examples.

In Chapter 4, case studies performed for the comparison of AHBMs are presented. Firstly, the basics of the error analysis procedure derived for this comparison is explained. Then results found from detailed case studies are given.

In Chapter 5, a brief summary of the work done, discussions, conclusions and possible future extensions of this work are given.

CHAPTER 2

NONLINEAR VIBRATION ANALYSIS

2.1 The Nonlinear Equation of Motion

The most general form of the equation of motion for a nonlinear dynamic system can be written as follows

$$[M]\{\ddot{q}(t)\} + [D]\{\dot{q}(t)\} + [K]\{q(t)\} + \{f_N(t, q, \dot{q})\} = \{F_{ext}(t)\}, \tag{2.1}$$

where $\{q(t)\}$ is the displacement vector, $[M]$ is the mass matrix, $[D]$ is the damping matrix (including all the damping and gyroscopic effects in the system), $[K]$ is the stiffness matrix which may include structural damping matrix, $\{f_N(t, q, \dot{q})\}$ is the nonlinear internal forcing vector and $\{F_{ext}(t)\}$ is the external forcing vector. Different from a linear system, a nonlinear internal forcing vector, due the forces that occur in the nonlinear elements is introduced. The existence of this term prevents the principle of superposition and principle of proportionality from being valid for nonlinear systems, thus making linear analysis techniques inapplicable for nonlinear systems [77].

2.2 Harmonic Balance Method

As mentioned before, Harmonic Balance Method (HBM) is one of the most powerful and popular techniques to solve the nonlinear equation set defined by Equation (2.1) in frequency domain. The mathematical basis of this method has been investigated by García-Saldaña and Gasull [78]. Since investigation of a theoretical basis for HBM is well beyond the scope of this thesis, the mathematical background will not

be explained here. Only the application of this method to Equation (2.1) will be given.

If the external forcing is periodic, it is expected to have a periodic response; hence, one can express both the external forcing and the response of the systems by using Fourier series as follows

$$\{F_{ext}(t)\} = \{F_0\} + \sum_{k=1}^{\infty}\{F_{sk}\}\sin(k\omega t) + \sum_{k=1}^{\infty}\{F_{ck}\}\cos(k\omega t), \tag{2.2}$$

$$\{q(t)\} = \{q_0\} + \sum_{k=1}^{\infty}\{q_{sk}\}\sin(k\omega t) + \sum_{k=1}^{\infty}\{q_{ck}\}\cos(k\omega t), \tag{2.3}$$

where $\{F_0\}$, $\{F_{sk}\}$ and $\{F_{ck}\}$ are $(n\times 1)$ vectors containing the known time independent bias terms and k^{th} harmonic coefficients of the sine and cosine components of the external forcing, respectively. Similarly, $\{q_0\}$, $\{q_{sk}\}$ and $\{q_{ck}\}$ are $(n\times 1)$ displacement vectors for the bias component, and, sine and cosine components of the kth harmonic, respectively. Since it is the dynamic response we are after, the elements of $\{q_0\}$, $\{q_{sk}\}$ and $\{q_{ck}\}$ are the unknowns to be determined.

Although the series expressions given in Equation (2.2) and Equation (2.3) are mathematically correct, they are not practically applicable for numerical computation. Therefore, these series must be truncated at some point. Utilizing m harmonics external forcing and displacement vectors can be written as

$$\{F_{ext}(t)\} = \{F_0\} + \sum_{k=1}^{m}\{F_{sk}\}\sin(k\theta) + \sum_{k=1}^{m}\{F_{ck}\}\cos(k\theta), \tag{2.4}$$

$$\{q(t)\} = \{q_0\} + \sum_{k=1}^{m}\{q_{sk}\}\sin(k\theta) + \sum_{k=1}^{m}\{q_{ck}\}\cos(k\theta). \tag{2.5}$$

14

where, $\theta = \omega \cdot t$. Taking the time derivatives of the displacement vector, velocity and acceleration vectors are obtained as

$$\{\dot{q}(t)\} = \sum_{k=1}^{m}(k\omega)\{q_{sk}\}\cos(k\theta) - \sum_{k=1}^{m}(k\omega)\{q_{ck}\}\sin(k\theta), \tag{2.6}$$

$$\{\ddot{q}(t)\} = -\sum_{k=1}^{m}(k\omega)^{2}\{q_{sk}\}\sin(k\theta) - \sum_{k=1}^{m}(k\omega)^{2}\{q_{ck}\}\cos(k\theta). \tag{2.7}$$

Similarly, the nonlinear forcing vector can be expressed as follows

$$\{f_{N}(t,q,\dot{q})\} = \{f_{N0}\} + \sum_{k=1}^{m}\{f_{Nsk}\}\sin(k\theta) + \sum_{k=1}^{m}\{f_{Nck}\}\cos(k\theta), \tag{2.8}$$

where, $\{f_{N0}\}$, $\{f_{Nsk}\}$ and $\{f_{Nck}\}$ are $(n \times 1)$ vectors containing the bias component and sine and cosine component of the kth harmonic of the nonlinear internal forcing vector. Since the nonlinearities in a dynamic system are attached to the DOFs, the nonlinear internal forces are not only dependent on time but also the response and in some cases derivatives of the response as well. Therefore, the series expression for the nonlinear forces must be consistent with the response expression. In other words, $\{f_{N0}\}$, $\{f_{Nsk}\}$ and $\{f_{Nck}\}$ must be found in terms of $\{q_{0}\}$, $\{q_{sk}\}$ and $\{q_{ck}\}$.

The most commonly used method for achieving this is as follows: The Fourier series expressions for the response are inserted into the nonlinear forcing vector. Then, having found the nonlinear forces in time domain, one needs to "project" these forces onto the Fourier basis, $(1, \sin(k\theta), \cos(k\theta))$ where $k = 1, 2, \ldots, m$. This projection can be done by evaluating the following inner products [2]:

$$\{f_{N0}\} = \frac{1}{2\pi} \int\limits_0^{2\pi} f_N(t,q,\dot{q}) d\theta$$

$$\{f_{Nsk}\} = \frac{1}{\pi} \int\limits_0^{2\pi} f_N(t,q,\dot{q}) \sin(k\theta) d\theta \ .$$

(2.9)

$$\{f_{Nck}\} = \frac{1}{\pi} \int\limits_0^{2\pi} f_N(t,q,\dot{q}) \cos(k\theta) d\theta$$

If the integrals given in Equation (2.9) can be evaluated, an analytical expression for the Fourier series representation of $\{f_N(t,q,\dot{q})\}$ can be found. If the integrals cannot be evaluated analytically, they can be calculated numerically. However, if the nonlinear forces cannot be expressed in closed form, as mentioned in Chapter 1, the elements of the nonlinear forcing vector can be obtained by using the AFT method [2, 42].

Assuming that all harmonics in the calculation of the nonlinear forcing are used, substituting Equations (2.4) - (2.8) into Equation (2.1) the following relation is obtained

$$[M]\left(-\sum_{k=1}^{m}(k\omega)^2\{q_{sk}\}\sin(k\theta) - \sum_{k=1}^{m}(k\omega)^2\{q_{ck}\}\cos(k\theta)\right)$$

$$+[D]\left(\sum_{k=1}^{m}(k\omega)\{q_{sk}\}\cos(k\theta) - \sum_{k=1}^{m}(k\omega)\{q_{ck}\}\sin(k\theta)\right)$$

$$+[K]\left(\{q_0\} + \sum_{k=1}^{m}\{q_{sk}\}\sin(k\theta) + \sum_{k=1}^{m}\{q_{ck}\}\cos(k\theta)\right) \qquad . \qquad (2.10)$$

$$+\{f_{N0}\} + \sum_{k=1}^{m}\{f_{Nsk}\}\sin(k\theta) + \sum_{k=1}^{m}\{f_{Nck}\}\cos(k\theta) = \{F_0\} + \sum_{k=1}^{m}\{F_{sk}\}\sin(k\theta)$$

$$+\sum_{k=1}^{m}\{F_{ck}\}\cos(k\theta)$$

Combining the sine and cosine coefficients:

16

$$\sum_{k=1}^{m}\left[\sin\left(k\theta\right)\left(-\left(k\omega\right)^{2}\left[M\right]\{q_{sk}\}-\left(k\omega\right)\left[D\right]\{q_{ck}\}+\left[K\right]\{q_{sk}\}+\{f_{Nsk}\}\right)\right]$$

$$+\sum_{k=1}^{m}\left[\cos\left(k\theta\right)\left(-\left(k\omega\right)^{2}\left[M\right]\{q_{ck}\}+\left(k\omega\right)\left[D\right]\{q_{sk}\}+\left[K\right]\{q_{ck}\}+\{f_{Nck}\}\right)\right]. \qquad (2.11)$$

$$+\left[K\right]\{q_{0}\}+\{f_{N0}\}=\{F_{0}\}+\sum_{k=1}^{m}\{F_{sk}\}\sin\left(k\theta\right)+\sum_{k=1}^{m}\{F_{ck}\}\cos\left(k\theta\right)$$

Equation (2.11) can only be satisfied if the coefficients of bias terms and terms of $\sin\left(k\theta\right)$ and $\cos\left(k\theta\right)$ on both sides are balanced, resulting in

$$[K]\{q_{0}\}+\{f_{N0}\}=\{F_{0}\}, \qquad (2.12)$$

$$\left([K]-\left(k\omega\right)^{2}[M]\right)\{q_{sk}\}-\left(k\omega\right)[D]\{q_{ck}\}+\{f_{Nsk}\}=\{F_{sk}\}, \qquad (2.13)$$

$$\left([K]-\left(k\omega\right)^{2}[M]\right)\{q_{ck}\}+\left(k\omega\right)[D]\{q_{sk}\}+\{f_{Nck}\}=\{F_{ck}\}. \qquad (2.14)$$

Combining Equations (2.13) and (2.14) a matrix equation for the kth harmonic can be obtained as

$$\begin{bmatrix} [K]-\left(k\omega\right)^{2}[M] & -\left(k\omega\right)[D] \\ \left(k\omega\right)[D] & [K]-\left(k\omega\right)^{2}[M] \end{bmatrix}\begin{Bmatrix} \{q_{sk}\} \\ \{q_{ck}\} \end{Bmatrix}+\begin{Bmatrix} \{f_{Nsk}\} \\ \{f_{Nck}\} \end{Bmatrix}=\begin{Bmatrix} \{F_{sk}\} \\ \{F_{ck}\} \end{Bmatrix}. \qquad (2.15)$$

Repeating Equation (2.15) for $k=1,2,\ldots,m$ and combining all, system of nonlinear algebraic equations are obtained.

$$
\begin{bmatrix}
[K] & [0] & [0] & \cdots & [0] \\
[0] & \left[\Lambda(\omega)\right] & [0] & \cdots & [0] \\
[0] & [0] & \left[\Lambda(2\omega)\right] & \cdots & [0] \\
\vdots & \vdots & \vdots & \ddots & \vdots \\
[0] & [0] & [0] & \cdots & \left[\Lambda(m\omega)\right]
\end{bmatrix}
\begin{Bmatrix}
\{q_0\} \\
\{q_{s1}\} \\
\{q_{c1}\} \\
\{q_{s2}\} \\
\{q_{c2}\} \\
\vdots \\
\{q_{sm}\} \\
\{q_{cm}\}
\end{Bmatrix}
+
\begin{Bmatrix}
\{f_{N0}\} \\
\{f_{Ns1}\} \\
\{f_{Nc1}\} \\
\{f_{Ns2}\} \\
\{f_{Nc2}\} \\
\vdots \\
\{f_{Nsm}\} \\
\{f_{Ncm}\}
\end{Bmatrix}
=
\begin{Bmatrix}
\{F_0\} \\
\{F_{s1}\} \\
\{F_{c1}\} \\
\{F_{s2}\} \\
\{F_{c2}\} \\
\vdots \\
\{F_{sm}\} \\
\{F_{cm}\}
\end{Bmatrix},
\qquad (2.16)
$$

where

$$
\left[\Lambda(\omega)\right] =
\begin{bmatrix}
[K] - \omega^2 [M] & -\omega[D] \\
\omega[D] & [K] - \omega^2 [M]
\end{bmatrix}.
\qquad (2.17)
$$

As mentioned at the beginning of the previous section, $[D]$ includes all the damping and gyroscopic effects in the system. This kind of a notation was preferred in order to keep the formulation general. For specific cases, Equation (2.16) can still be used by modifying Equation (2.17). For example, for a system which has both inherent structural damping and viscous damping but no gyroscopic effects, Equation (2.17) takes the following form:

$$
\left[\Lambda(\omega)\right] =
\begin{bmatrix}
[K] - \omega^2 [M] & -\omega[C] - [H] \\
\omega[C] + [H] & [K] - \omega^2 [M]
\end{bmatrix}
\qquad (2.18)
$$

where $[C]$ is the viscous damping matrix and $[H]$ is the structural damping matrix.

The n nonlinear differential equations of motion in time domain are now converted to $n(2m+1)$ algebraic equations with $n(2m+1)$ unknowns and one free parameter, ω. In order to obtain the response for a certain frequency spectrum, one needs to

18

solve this nonlinear equation system for different values of ω. Matrix equation given by Equation (2.16) can be easily generated for any number harmonics due its simple structure.

In the formulation given above, Fourier series approximations contain the bias term, the first harmonic and the super harmonics. It is also possible to include sub-harmonics in the formulation by introducing an integer υ [18].

$$\{q(t)\} = \{q_0\} + \sum_{k=1}^{m} \{q_{sk}\} \sin\left(\frac{k}{\upsilon}\theta\right) + \sum_{k=1}^{m} \{q_{ck}\} \cos\left(\frac{k}{\upsilon}\theta\right). \tag{2.19}$$

In this thesis, in order not to complicate the formulations further and since the sub-harmonics are not the main area of interest, they will not be included in the equations. But they may be of importance in nonlinear vibration analyses where the systems in consideration exhibit self-excited vibrations [21, 70]. Furthermore, in these kinds of problems there may also be a need to use multiple Fourier series representations having more than one basic frequency as well as using multiple time scales [3]. Since the adaptive methods are investigated with simpler dynamic models in this thesis, these advanced formulations will not be included either; however, developed methods can be applied to the case of sub- and super-harmonics without any modification.

2.3   Numerical Solution of Nonlinear Algebraic Equation Systems

In the previous section, the conversion of nonlinear ordinary differential equations to nonlinear algebraic equations via HBM is described. In order to achieve the ultimate goal and obtain the dynamic response, the equation set given in Equation (2.16) must be solved. In this section, the numerical methods for solving more than one nonlinear equations simultaneously are briefly presented. The emphasis is on the most widely used methods in structural dynamics.

2.3.1 Fixed Point Iteration

Assuming the equation system for which the solution is sought is of the form:

$$R(\{x\}) = \{0\},$$
(2.20)

where $\{x\}$ is the vector containing the variables to be solved and R is the family of functions which are to be solved simultaneously.

The fixed point iteration actually deals with finding the fixed points of a function. That is, solving for the $\{x\}$ values satisfying such an equation:

$$\{x\} = G(\{x\}).$$
(2.21)

If the equation system defined in Equation (2.20) can be rearranged into the form given in Equation (2.21), one can simply use fixed point iteration for root finding. In fact, many nonlinear problems are formulated as or can be converted into the fixed point problem. The conversion is mostly done by algebraic manipulation or by simply adding $\{x\}$ to both sides of the equation system.

The recurrence formula for fixed point iteration is as follows:

$$\{x\}^{i+1} = G\left(\{x\}^{i}\right),$$
(2.22)

where $\{x\}^{i}$ is the iterate from the previous solution step and $\{x\}^{i+1}$ is the iterate for the next step. When the error between two iterates become too small, the solution procedure ends.

One of the most important points in the application of this method is that, the rate of convergence of the method is greatly affected by the selection of G. Although they are the same equation systems written differently, different formulations for G can cause the iterations to converge at a different speed or even to diverge. The criteria for G ensuring linear convergence of the fixed point iteration have been explained by Kelley [79].

Another factor that greatly affects the convergence is relaxation proposed by [23].

$$\{x\}_{new}^{i+1} = \lambda \{x\}_{calc}^{i+1} + (1-\lambda)\{x\}^{i}. \tag{2.23}$$

Here λ is a weighting factor which can takes a value between 0 and 2. $\{x\}_{calc}^{i+1}$ is the calculated value of the next iterate from Equation (2.22). By calculating a weighted sum of the last two iterates and using this sum instead of the one found from Equation (2.22) one can greatly enhance the method's capability to converge. If $0 < \lambda < 1$, the modification is called underrelaxation and it can convert a divergent system into a convergent one. If $1 < \lambda < 2$, overrelaxation takes place, improving the convergence rate of an already convergent system.

2.3.2 Newton's Method

Newton's Method is one of the most effective and widely used numerical methods for obtaining the roots of nonlinear equation systems. Its application to functions with a single variable has been known since the 17th century. Later on, its application for multi variables, nonlinear equations and its alternatives were introduced.

Iterative solution formula by using Newton's Method is as follows:

$$\{x\}^{i+1} = \{x\}^{i} - \left[J\left(\{x\}^{i}\right) \right]^{-1} R\left(\{x\}^{i}\right), \tag{2.24}$$

21

where $\{x\}^i$ and $\{x\}^{i+1}$ are the previous and current iterates, respectively. R is the equation system given in Equation (2.20) and J is the Jacobian matrix. Assuming we have n equations and n unknowns, denoting the jth variable in vector $\{x\}$ by x_j and the jth equation in R as R_j, the Jacobian is defined as:

$$J = \begin{pmatrix} \dfrac{\partial R_1}{\partial x_1} & \dfrac{\partial R_1}{\partial x_2} & \cdots & \dfrac{\partial R_1}{\partial x_n} \\ \dfrac{\partial R_2}{\partial x_1} & \dfrac{\partial R_2}{\partial x_2} & \cdots & \dfrac{\partial R_2}{\partial x_n} \\ \vdots & \vdots & \ddots & \vdots \\ \dfrac{\partial R_n}{\partial x_1} & \dfrac{\partial R_n}{\partial x_n} & \cdots & \dfrac{\partial R_n}{\partial x_n} \end{pmatrix}. \tag{2.25}$$

The partial derivatives in Equation (2.25) can be very difficult or impossible to calculate analytically. In such cases it can be computed numerically. The computation is generally done by using forward difference formula [79, 80]. The formula is simply a way of perturbing the equation system in the direction of a single variable, finding the difference between the perturbed system and the initial point and finally performing a division to compute the gradient numerically. By following this procedure for every single variable, one can construct the Jacobian column by column.

Provided that the initial guess is sufficiently close to the solution and the convergence criteria are satisfied, Newton's method converges to the solution quadratically. The convergence criteria are explained in detail and mathematically proved by Kelley [80]. However, although Newton's Method usually converges within a few iterations, it can be time consuming and computationally expensive. The main reason for this is the computation of the Jacobian matrix at every iteration. If an analytical Jacobian is not available and the numerical Jacobian is too costly, some alternative methods can be preferred.

One of these alternative methods is the Chord Method [77, 79]. In this method, the Jacobian is calculated for the first iteration only and the same Jacobian is used throughout the iterations. A similar method is the Shamanskii Method [77, 79]. In this method, the Jacobian is updated at every l iterations. The usage of these methods generally increase the number of iterations required for convergence. But, if the calculation of the Jacobian is expensive, performing a few more iterations with an outdated Jacobian reduces the overall computational effort; hence, these methods become computationally economical.

The quasi-Newton methods also provide alternatives to Newton's Method. These methods are actually extensions of the secant method to multi variable problems. The most famous one of these methods is Broyden's Method [81]. In this method, instead of calculating the Jacobian, an approximation to the Jacobian is calculated and then it is subjected to a rank-one update as the iterations go on. If the initial guess is close to the real solution, this method can perform very well [79].

In addition to the methods described above, the methods that belong to family of methods known as the Newton-Krylow methods are strong alternatives for the solution of computational physics problems [77, 79].

For obtaining the nonlinear response of dynamic systems within the scope of this thesis, applying Newton's method along with a path following scheme is the common application in the literature and it is known to give very good results [2, 5, 77]. Therefore, for the studies mentioned in this thesis, Newton's method with a path following scheme is used.

2.4   Path Following Methods

In order to obtain the frequency response, one needs to solve Equation (2.16) for different values of the free parameter, i.e. frequency, ω.

Studying the nonlinear response curve given in Figure 2.1, one can see that the curve bends to the right. This is due to the existence of a hardening cubic stiffness. Between the turning points B and E, the unstable region is located. The existence of this region causes multiple solutions to coexist for a specific frequency interval. Without a proper path following method, the best results that could be obtained from the response calculations for this case are the curve segments from A to B and from C to D by performing a forward frequency sweep or segments from D to E and from F to A by performing a backward frequency sweep. Path following using Newton's Method with ω as the continuation parameter fails to follow the path in the case of turning points where multiple solutions exist. Moreover, the initial guesses for the Newton's Method tend to perform poorly at the jump locations due to large differences in the previous and current solutions indicated by points B and C or E and F ; hence, the method usually diverges and cannot find a solution [77].

Using a proper path following method provides the means to vary ω systematically which makes it possible to find multiple solutions located at a single frequency value. This is achieved by following the path even it turns back or intersects itself by using an appropriate path following method. The application of a path following method consists of two parts:

1. After a solution for the current frequency step ω^i is obtained, generation of initial guess for the next frequency step ω^{i+1} from the previous frequency steps,
2. Correction of the initial guess until the iterations converge.
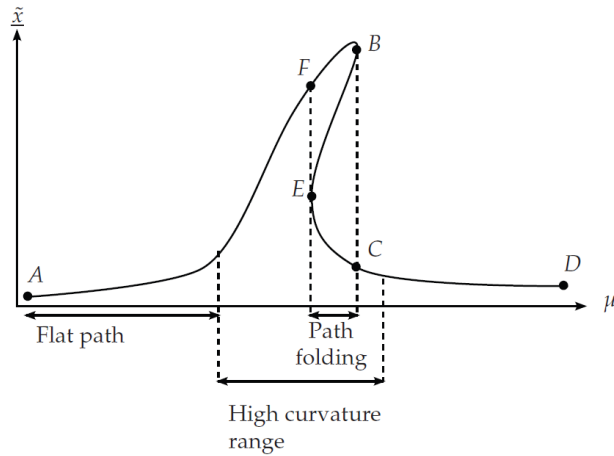
Figure 2.1 A Typical Response Curve for a Duffing Oscillator with Cubic Stiffness Nonlinearity [2]

2.4.1 Generation of Initial Guess

All the numerical methods that can be used for the solution of Equation (2.16) require an initial guess that is sufficiently close to the actual solution. However, finding this initial guess is not a simple task. A systematic approach that can automatically come up with accurate initial guesses for every single point on the curve is required in order to obtain the frequency response curves of a nonlinear system. Therefore the graphical methods used for locating the roots of a function with a single variable or trial and error procedures are not applicable in this situation. Using the solution of the linear part of Equation (2.16) as an initial guess is not applicable since the nonlinear effects may become more and more dominant where the nonlinear solution becomes significantly different than the linear solution. The predictors presented here overcome the mentioned difficulties. The main idea behind them is to predict the next point on a response curve by following the curve's trend at the previous solution points.

The first predictor to be mentioned is the secant predictor. It locates the initial guess for the next frequency step on the line that connects the two previous solution points.

25

It is a simple method and performs well when the curvature of the response curve is not very large [2]. A graphical representation is given in Figure 2.2.

The second predictor to be mentioned is the tangent predictor. This predictor locates the initial guess for the next step on the tangent line passing from the previous solution point. In most of the cases, it performs very well. Therefore, this method is preferred for the studies in this thesis. A graphical representation is given in Figure 2.2. More detailed formulation about this predictor is given in Section 2.4.2.1.
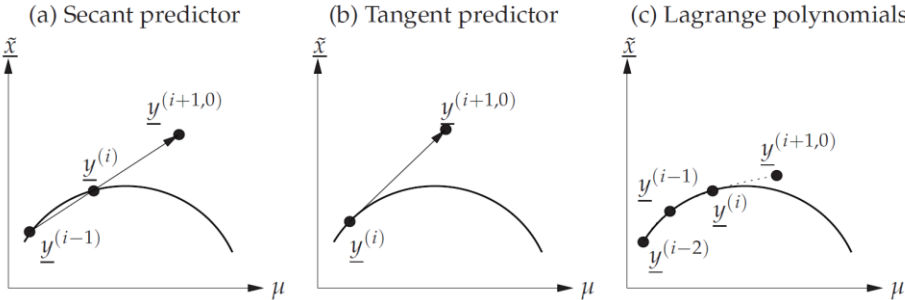
Figure 2.2 A Graphical Representation of the Predictor Methods [2]

The final predictor to be mentioned uses the previous $d+1$ solution points to form a Lagrange polynomial of degree d. Then, this polynomial can be extrapolated so that an initial guess can be calculated for the next frequency point. In order not to increase the computational cost, d is generally kept around 2 or 3 [2]. A graphical representation is given in Figure 2.2.

So far, determination of the direction for the initial guess by different predictors has been mentioned but the matter of how far these guesses will be located has not been explained yet. For this, the arc length s, in other words the distance between two

successive solution points, is used. Using the same notation as in Equation (2.16) arc length can be defined as

$$s = \sqrt{\left(\{x\}^{i+1} - \{x\}^{i}\right)^{T} \left(\{x\}^{i+1} - \{x\}^{i}\right) + \left(\omega^{i+1} - \omega^{i}\right)^{2}} \ . \tag{2.26}$$

All the predictors locate the initial guess point, namely $\left(\{x\}^{i+1}, \omega^{i+1}\right)$ away from the previous solution point by a predetermined amount, s, set by the user.

2.4.2 Correction Methods

Having determined the location of the initial guess, the problem for obtaining the curves similar to the one given in Figure 2.1 is now reduced to making that initial guess converge on the actual solution curve. There are numerous correction methods available for this task, such as the Moore-Penrose pseudo inverse method or the pseudo arc length method [2]. But only the arc length continuation method will be explained in detail here.

2.4.2.1 The Arc Length Continuation Method

In the arc length continuation method, the arc length given in Equation (2.26) is introduced to Equation (2.16) as the new path following parameter. The frequency ω becomes an unknown to be solved, instead of a free parameter. Therefore Newton's Method becomes capable of tracing solution path, which can turn back. Denoting the unknown Fourier coefficient vector by $\{x\}$, the new unknown vector becomes

$$\{q\} = \begin{Bmatrix} \{x\} \\ \omega \end{Bmatrix}. \tag{2.27}$$

27

Since a new unknown is introduced to the equation system, a new equation must be introduced as well. This new equation is the equation of a hyper-sphere located at the previous solution point, having a radius of s.

$$h\left(\{x\},\omega,s\right)=\left(\{x\}^{i+1}-\{x\}^{i}\right)^{T}\left(\{x\}^{i+1}-\{x\}^{i}\right)+\left(\omega^{i+1}-\omega^{i}\right)^{2}-s^{2}=0. \tag{2.28}$$

In Section 2.4.1 the predictors which place an initial guess at a predetermined distance of s from the previous solution point were described. In fact such an initial guess is located on the surface of the hyper sphere defined by Equation (2.28). Now, adding Equation (2.28) into the equation system defined by Equation (2.16), the numerical solution scheme is actually being forced to converge onto the actual response curve by following the surface of the hyper-sphere. As a result, starting from the initial guess all the successive iteration points are to be located on the hyper-sphere, eventually converging onto the nonlinear response curve. This behavior is illustrated in Figure 2.3. This is the reason why the family of methods containing the arc length continuation is called correction methods [2]. They "correct" the initial guess.
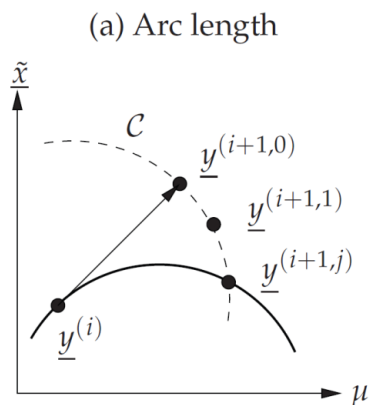
(a) Arc length

Figure 2.3 Illustration of Arc Length Continuation [2]

28

The arc length continuation method and HBM can be integrated into Newton's Method as follows:

First, writing Equation (2.16) in the residual form:

$$\{R(\{x\},\omega))\} = \begin{bmatrix} [K] & [0] & [0] & \cdots & [0] \\ [0] & [\Lambda(\omega)] & [0] & \cdots & [0] \\ [0] & [0] & [\Lambda(2\omega)] & \cdots & [0] \\ \vdots & \vdots & \vdots & \ddots & \vdots \\ [0] & [0] & [0] & \cdots & [\Lambda(m\omega)] \end{bmatrix} \begin{Bmatrix} \{q_0\} \\ \{q_{s1}\} \\ \{q_{c1}\} \\ \{q_{s2}\} \\ \{q_{c2}\} \\ \vdots \\ \{q_{sm}\} \\ \{q_{cm}\} \end{Bmatrix} + \begin{Bmatrix} \{f_{N0}\} \\ \{f_{Ns1}\} \\ \{f_{Nc1}\} \\ \{f_{Ns2}\} \\ \{f_{Nc2}\} \\ \vdots \\ \{f_{Nsm}\} \\ \{f_{Ncm}\} \end{Bmatrix} - \begin{Bmatrix} \{F_0\} \\ \{F_{s1}\} \\ \{F_{c1}\} \\ \{F_{s2}\} \\ \{F_{c2}\} \\ \vdots \\ \{F_{sm}\} \\ \{F_{cm}\} \end{Bmatrix} = \begin{Bmatrix} \{0\} \\ \{0\} \\ \{0\} \\ \{0\} \\ \{0\} \\ \vdots \\ \{0\} \\ \{0\} \end{Bmatrix}. \quad (2.29)$$

Then, the recursive formula for Newton's Method given in Equation (2.24) can be written as:

$$\{q\}_k^{i+1} = \{q\}_k^i - \begin{bmatrix} \dfrac{\partial R(\{x\},\omega)}{\partial \{x\}} & \dfrac{\partial R(\{x\},\omega)}{\partial \omega} \\ \dfrac{\partial h(\{x\},\omega)}{\partial \{x\}} & \dfrac{\partial h(\{x\},\omega)}{\partial \omega} \end{bmatrix}_{\substack{\{x\}=\{x\}_k^i \\ \omega=\omega_k^i}}^{-1} \begin{Bmatrix} R\left(\{x\}_k^i,\omega_k^i\right) \\ h\left(\{x\}_k^i,\omega_k^i,s\right) \end{Bmatrix}. \quad (2.30)$$

where the superscript i denotes the ith iteration and subscript k denotes k^{th} frequency point. R and h are given in Equation (2.29) and Equation (2.28), respectively.

The tangent predictor for arc length continuation becomes:

$$\{q\}_{k+1} = \{q\}_k - \left[\bar{J}\left(\{q\}_k,s\right)\right]^{-1} \frac{\partial \bar{R}\left(\{q\}_k,s\right)}{\partial s} s, \quad (2.31)$$

where $\left[\bar{J}\left(\{q\}_{k},s\right) \right]$ and $\bar{R}\left(\{q\}_{k},s\right)$ are the new Jacobian matrix and the new residual vector obtained in addition of the arc-length equation, respectively.

During the application of arc length continuation, if the radius of the hyper-sphere (also called the step size) defined in Equation (2.28) is too small, the solution scheme may compute too many points on the response curve unnecessarily. On the other hand if the step size is too large, the solution scheme may have difficulty in tracking the response curve around the turning points and sharp corners. In order to find an optimum solution between the computational time and accuracy, the step size can be adjusted automatically by an adaptive algorithm. One of the simplest and most effective ways to make the step size adaptive is to adjust the step size according to the number of iterations at the previous point. De Niet [82] proposed an approach, based on the following ratio

$$\varepsilon_{s} = \frac{N_{opt}}{N_{iter}}.$$
(2.32)

In this approach, if ε is greater than 1, it means that the number of iterations, N_{iter}, is lower than the optimum number of iterations, N_{opt}. Therefore the numerical solution scheme is having no trouble in terms of convergence and the step size can be increased. If ε is lower than 1, it means that the solution scheme performs more than necessary number of iterations to converge onto the desired curve. In order to decrease the amount of iterations, the step size should be decreased.

Increasing or decreasing the step size rapidly may also cause problems in terms of convergence and accuracy. In order to slow down the increase or decrease rate, De Niet suggested the following normalization:

$$\varepsilon_s = \begin{cases} 0.5 & if & \varepsilon_s \leq 0.5 \\ \varepsilon_s & if & 0.5 < \varepsilon_s < 2 \\ 2 & if & \varepsilon_s \geq 2 \end{cases}.$$ (2.33)

To change the step size for the next step, the normalized ratio was multiplied with the previous step size value as

$$s_{i+1} = \overline{\varepsilon}_s s_i.$$ (2.34)

During the studies presented in the thesis, it was seen that under certain circumstances De Niet's method also caused the step size to change rapidly. Therefore a modified version of this method is proposed

$$\overline{\varepsilon}_s = \begin{cases} 0.5 & if & \varepsilon_s \leq 0.5 \\ \varepsilon_s & if & 0.5 < \varepsilon_s \leq 1 \\ 1 & if & 1 < \varepsilon_s < 2 \\ 2 & if & \varepsilon_s \geq 2 \end{cases},$$ (2.35)

$$s^{i+1} = \sqrt[3]{\overline{\varepsilon}_s}\, s^i.$$ (2.36)

It can be seen from the formulation that the selection of optimum number of iterations affects the accuracy greatly. De Niet suggested that for Newton's Method, N_{opt} should be kept around 5. But for other numerical solution methods, this number needs to be altered. Since Newton's Method is the selected numerical solution scheme for this thesis, N_{opt} is taken as 5.

2.5   Condensation Methods

For a system with n DOFs, an application of multi harmonic HBM with m harmonics included in the solution yields Equation (2.16) which contains $n(2m+1)$

nonlinear algebraic equations. When the multi harmonic responses of systems with many DOFs are sought, this number can become very large. Dealing with many equations removes the computational time advantage of HBM compared to timed domain methods and may result in the failure of the solver as well. Therefore it is necessary to keep the number of equations to be solved to a minimum. For this purpose, two methods are used.

2.5.1   Receptance Method

Receptance method, which was originally proposed by Menq et. al. [83] for the analysis of bladed disk systems with dry friction dampers, basically isolates the equations related to the DOFs which have a nonlinear element connected to them from the rest of the equations. If all the DOFs in a system have at least one nonlinear element connected to them, then the isolated equations become no different than the original equation system. In this case, the computational advantage of the receptance method disappears.

Considering the equation of motion given in Equation (2.1), with the matrix $[D]$ replaced with combined structural and viscous damping for harmonic motion can be written as follows :

$$[M]\{\ddot{q}(t)\}+[C]\{\dot{q}(t)\}+([K]+i[H])\{q(t)\}+\{f_N(t,q,\dot{q})\}=\{F_{ext}(t)\}. \qquad (2.37)$$

For the case where a multi harmonic solution is sought for the equation of motion, we can write the following complex matrix equation for the kth harmonic [77] as:

$$([K]-(k\omega)^2[M]+i[H]+i(k\omega)[C])\{q_k\}+\{f_{Nk}\}=\{F_k\}, \qquad (2.38)$$

where $\{q_k\}$, $\{f_{Nk}\}$ and $\{F_k\}$ are $n \times 1$ vectors containing the complex Fourier coefficients of the response, nonlinear forcing and the external forcing. Multiplying

32

both sides of Equation (2.38) with the receptance matrix, $\left[\alpha\left(k\omega\right)\right]$, the following

relation is obtained

$$\left\{q_k\right\} + \left[\alpha\left(k\omega\right)\right]\left\{f_{Nk}\right\} = \left[\alpha\left(k\omega\right)\right]\left\{F_k\right\}, \tag{2.39}$$

where

$$\left[\alpha\left(\omega\right)\right] = \left[-\omega^2\left[M\right] + i\omega\left[C\right] + i\left[H\right] + \left[K\right]\right]^{-1}. \tag{2.40}$$

As mentioned in the beginning of this section, the DOFs in a dynamic system can be divided into two groups; one being the nonlinear DOFs and the other one being the linear DOFs. The nonlinear DOFs are the ones which have at least one nonlinear element connected to them. The aim here is to isolate the equations belonging to the nonlinear DOFs, from those belonging to the linear DOFs. For this purpose, reordering DOFs as linear and nonlinear DOFs and partitioning the matrices, Equation (2.39) can be written as

$$\left\{\begin{matrix}\left\{q_k\right\}_L \\ \left\{q_k\right\}_{NL}\end{matrix}\right\} + \left[\begin{matrix}\left[\alpha_{LL}\left(k\omega\right)\right] & \left[\alpha_{LN}\left(k\omega\right)\right] \\ \left[\alpha_{NL}\left(k\omega\right)\right] & \left[\alpha_{NN}\left(k\omega\right)\right]\end{matrix}\right]\left\{\begin{matrix}\left\{0\right\} \\ \left\{f_{Nk}\right\}_{NL}\end{matrix}\right\} = \left[\begin{matrix}\left[\alpha_{LL}\left(k\omega\right)\right] & \left[\alpha_{NL}\left(k\omega\right)\right] \\ \left[\alpha_{NL}\left(k\omega\right)\right] & \left[\alpha_{NN}\left(k\omega\right)\right]\end{matrix}\right]\left\{\begin{matrix}\left\{F_k\right\}_L \\ \left\{F_k\right\}_{NL}\end{matrix}\right\}, \tag{2.41}$$

where the subscript *L* denotes the linear DOFs and the subscript *NL* denotes the nonlinear DOFs. Note that the vector containing the Fourier coefficients for the nonlinear forcing has zeros on the first line. This is because the linear DOFs have no connection to the nonlinear elements; therefore they have no nonlinear internal force applied on them. Expanding the second row of Equation (2.41), the equations related to the nonlinear DOFs can be isolated as follows

$$\left\{q_k\right\}_{NL} + \left[\alpha_{NN}\left(k\omega\right)\right]\left\{f_{Nk}\right\}_{NL} = \left[\alpha_{NL}\left(k\omega\right)\right]\left\{F_k\right\}_L + \left[\alpha_{NN}\left(k\omega\right)\right]\left\{F_k\right\}_{NL}. \tag{2.42}$$

33

The desired equation system is obtained but it is still in complex form. In order to solve this equation system with the methods described in the previous sections, one needs a real equation system rather than a complex one. Separating real and imaginary parts and arranging the equations the following result for the kth harmonic is obtained

$$\left\{ \begin{array}{c} \{q_{sk}\}_{NL} \\ \{q_{ck}\}_{NL} \end{array} \right\} + \left[\begin{array}{cc} \left[\alpha_{NNre}(k\omega)\right] & \left[-\alpha_{NNim}(k\omega)\right] \\ \left[\alpha_{NNim}(k\omega)\right] & \left[\alpha_{NNre}(k\omega)\right] \end{array} \right] \left\{ \begin{array}{c} \{f_{Nsk}\}_{NL} \\ \{f_{Nck}\}_{NL} \end{array} \right\} - \ldots$$

$$\left[\begin{array}{cccc} \left[\alpha_{NLre}(k\omega)\right] & \left[\alpha_{NNre}(k\omega)\right] & \left[-\alpha_{NLim}(k\omega)\right] & \left[-\alpha_{NNim}(k\omega)\right] \\ \left[\alpha_{NLim}(k\omega)\right] & \left[\alpha_{NNim}(k\omega)\right] & \left[\alpha_{NLre}(k\omega)\right] & \left[\alpha_{NNre}(k\omega)\right] \end{array} \right] \left\{ \begin{array}{c} \{F_{sk}\}_L \\ \{F_{sk}\}_{NL} \\ \{F_{ck}\}_L \\ \{F_{ck}\}_{NL} \end{array} \right\} = \left\{ \begin{array}{c} \{0\} \\ \{0\} \\ \{0\} \\ \{0\} \end{array} \right\}, \quad (2.43)$$

or, in a more compact form:

$$\left\{ \begin{array}{c} \{q_{sk}\}_{NL} \\ \{q_{ck}\}_{NL} \end{array} \right\} - \left[\beta(\omega)\right] \left\{ \begin{array}{c} \{F_{sk}\}_L \\ \{F_{sk}\}_{NL} \\ \{F_{ck}\}_L \\ \{F_{ck}\}_{NL} \end{array} \right\} - \left\{ \begin{array}{c} \{0\} \\ \{f_{Nsk}\}_{NL} \\ \{0\} \\ \{f_{Nck}\}_{NL} \end{array} \right\} = \left\{ \begin{array}{c} \{0\} \\ \{0\} \\ \{0\} \\ \{0\} \end{array} \right\}, \quad (2.44)$$

where

$$\left[\beta(\omega)\right] = \left[\begin{array}{cccc} \left[\alpha_{NLre}(\omega)\right] & \left[\alpha_{NNre}(\omega)\right] & -\left[\alpha_{NLim}(\omega)\right] & -\left[\alpha_{NNim}(\omega)\right] \\ \left[\alpha_{NLim}(\omega)\right] & \left[\alpha_{NNim}(\omega)\right] & \left[\alpha_{NLre}(\omega)\right] & \left[\alpha_{NNre}(\omega)\right] \end{array} \right], \quad (2.44)$$

where subscript *re* indicates the real part, subscript *im* indicates the imaginary part, subscript *s* indicates sine and subscript *c* indicates cosine terms. For the bias terms, present in non-symmetric nonlinearities, Equation (2.44) takes the following form:

34

$$\{q_0\}_{NL} - \begin{bmatrix} [A_{NL}] & [A_{NN}] \end{bmatrix} \begin{Bmatrix} \{F_0\}_L \\ \{F_0\}_{NL} - \{f_{N0}\}_{NL} \end{Bmatrix} = \{0\}, \qquad (2.45)$$

where *A* is the inverse of the stiffness matrix. Writing Equation (2.44) for all the harmonics and including Equation (2.45), one can obtain the following generalized expression for *m* harmonics:

$$\begin{Bmatrix} \{q_0\}_{NL} \\ \{q_{s1}\}_{NL} \\ \{q_{c1}\}_{NL} \\ \vdots \\ \{q_{sm}\}_{NL} \\ \{q_{cm}\}_{NL} \end{Bmatrix} - [B_N(\omega)] \left(\begin{Bmatrix} \{F_0\}_L \\ \{F_0\}_{NL} \\ \{F_{s1}\}_L \\ \{F_{s1}\}_{NL} \\ \{F_{c1}\}_L \\ \{F_{1c}\}_{NL} \\ \vdots \\ \{F_{sm}\}_L \\ \{F_{sm}\}_{NL} \\ \{F_{cm}\}_L \\ \{F_{cm}\}_{NL} \end{Bmatrix} - \begin{Bmatrix} \{0\} \\ \{f_{N0}\}_{NL} \\ \{0\} \\ \{f_{Ns1}\}_{NL} \\ \{0\} \\ \{f_{N1c}\}_{NL} \\ \vdots \\ \{0\} \\ \{f_{Nsm}\}_{NL} \\ \{0\} \\ \{f_{Ncm}\}_{NL} \end{Bmatrix} \right) = \begin{Bmatrix} \{0\} \\ \{0\} \\ \{0\} \\ \vdots \\ \{0\} \\ \{0\} \end{Bmatrix}, \qquad (2.46)$$

where

$$[B_N(\omega)] = \begin{bmatrix} [A_{NL}] & [A_{NN}] & [0] & [0] & \cdots & [0] \\ [0] & [0] & [\beta(\omega)] & [0] & \cdots & [0] \\ [0] & [0] & [0] & [\beta(2\omega)] & \cdots & [0] \\ \vdots & \vdots & \vdots & \vdots & \ddots & \vdots \\ [0] & [0] & [0] & [0] & \cdots & [\beta(m\omega)] \end{bmatrix}. \qquad (2.47)$$

The set of equations given in Equation (2.46) needs to be solved by a numerical continuation scheme. If Newton's Method is to be used together with arc length continuation, one needs replace the right hand side of Equation (2.29) with the left

35

hand side of Equation (2.46) and use the new *R* inside the expressions given in Equation (2.30) and Equation (2.31).

For the linear DOFs, Expanding the first row of Equation (2.41):

$$\{q_k\}_L = \left[\left[\alpha_{LL}(k\omega)\right] \quad \left[\alpha_{LN}(k\omega)\right]\right] \left\{ \begin{array}{c} \{F_k\}_L \\ \{F_k\}_{NL} - \{f_{Nk}\}_{NL} \end{array} \right\}. \tag{2.48}$$

Following a similar procedure as done for the nonlinear DOFs, one can obtain the following equation

$$\left\{ \begin{array}{c} \{q_0\}_L \\ \{q_{s1}\}_L \\ \{q_{c1}\}_L \\ \vdots \\ \{q_{sm}\}_L \\ \{q_{cm}\}_L \end{array} \right\} = \left[B_L(\omega)\right] \left(\left\{ \begin{array}{c} \{F_0\}_L \\ \{F_0\}_{NL} \\ \{F_{s1}\}_L \\ \{F_{s1}\}_{NL} \\ \{F_{c1}\}_L \\ \{F_{1c}\}_{NL} \\ \vdots \\ \{F_{sm}\}_L \\ \{F_{sm}\}_{NL} \\ \{F_{cm}\}_L \\ \{F_{cm}\}_{NL} \end{array} \right\} - \left\{ \begin{array}{c} \{0\} \\ \{f_{N0}\}_{NL} \\ \{0\} \\ \{f_{Ns1}\}_{NL} \\ \{0\} \\ \{f_{N1c}\}_{NL} \\ \vdots \\ \{0\} \\ \{f_{Nsm}\}_{NL} \\ \{0\} \\ \{f_{Ncm}\}_{NL} \end{array} \right\} \right), \tag{2.49}$$

where

$$\left[B_N(\omega)\right] = \begin{bmatrix} \left[A_{NL}\right] & \left[A_{NN}\right] & \left[0\right] & \left[0\right] & \cdots & \left[0\right] \\ \left[0\right] & \left[0\right] & \left[\gamma(\omega)\right] & \left[0\right] & \cdots & \left[0\right] \\ \left[0\right] & \left[0\right] & \left[0\right] & \left[\gamma(2\omega)\right] & \cdots & \left[0\right] \\ \vdots & \vdots & \vdots & \vdots & \ddots & \vdots \\ \left[0\right] & \left[0\right] & \left[0\right] & \left[0\right] & \cdots & \left[\gamma(m\omega)\right] \end{bmatrix}, \tag{2.50}$$

and

36

$$[\gamma(\omega)] = \begin{bmatrix} [\alpha_{LLre}(k\omega)] & [\alpha_{LNre}(k\omega)] & [-\alpha_{LLim}(k\omega)] & [-\alpha_{LNim}(k\omega)] \\ [\alpha_{LLim}(k\omega)] & [\alpha_{LNim}(k\omega)] & [\alpha_{LLre}(k\omega)] & [\alpha_{LNre}(k\omega)] \end{bmatrix}. \tag{2.51}$$

After solving Equation (2.46), solutions of Equation (2.48), i.e. linear DOFs, can be obtained by performing the matrix multiplication given in Equation (2.49). As a result, the receptance method leaves the equations regarding the linear DOFs out of the numerical solution process, hence causing a considerable decrease in the total number of equations to be solved for the case size of the nonlinear DOFs is significantly smaller than the total DOFs of the system. Even though receptance method decreases the number of nonlinear equations to be solved significantly compared to the total DOFs of the system, the resulting number of equation may still be very high. For such cases or for the cases where the nonlinearities are distributed though out the system, modal superposition approach introduced by Cigeroglu et. al [84] provides an alternative to the receptance method.

2.6 Nonlinearity Types

In this section the nonlinear elements that are used in this thesis are introduced and mathematical formulations required for the calculation of the Fourier coefficients are given, which are used in the HBM.

2.6.1 Cubic Stiffness

Cubic stiffness is one of the most widely used nonlinearity in nonlinear structural dynamics [85]. It is actually a massless spring that does not obey Hooke's law. Instead, the force exerted by the spring is proportional to the cube of the displacement which is:

$$f_N(x) = k_c x^3, \tag{2.52}$$

where k_c is the stiffness of the nonlinear element in N/m^3. This term can take negative values as well as positive values. If it is negative, the nonlinear element is

said to have softening behavior; whereas if it is positive, the element is said to have hardening behavior. These phenomena are illustrated in Figure 2.4.

Fourier coefficients for the nonlinear force exerted by a cubic stiffness element can be obtained by assuming a multi harmonic response as follows

$$x(\theta) = x_0 + \sum_{k=1}^{m} \left[x_{sk} \sin(k\theta) + x_{ck} \cos(k\theta) \right].$$
(2.53)

Here, $x(\theta)$ represents the relative displacement between the ends of the cubic stiffness element. In case the cubic stiffness element is connected between the ground and a DOF, this relative displacement reduces to the displacement of that DOF.
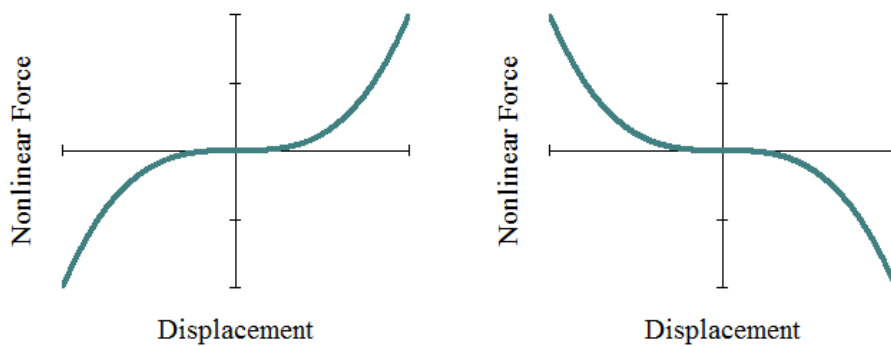
Figure 2.4 Cubic stiffness elements showing hardening (left) and softening (right) behavior

Using the expressions given in Equation (2.9) the Fourier coefficients for the bias term and the kth harmonic term can be obtained as:

$$f_{N0} = \frac{1}{2\pi} \int_0^{2\pi} k_c \left[x(\theta) \right]^3 d\theta$$

$$f_{Nsk} = \frac{1}{\pi} \int_0^{2\pi} k_c \left[x(\theta) \right]^3 \sin(k\theta) d\theta \; . \qquad (2.54)$$

$$f_{Nck} = \frac{1}{\pi} \int_0^{2\pi} k_c \left[x(\theta) \right]^3 \cos(k\theta) d\theta$$

The integrals given in Equation (2.54) can be calculated analytically and the resulting expressions can be embedded into a computer code. However if the number of harmonics included in the solution is large, the analytic approach requires considerable amount of algebraic manipulation due to the cubic term. Senjarovic and Fan [86] have proposed a useful formulation that can be used in these integrals. However, in this thesis, the integrals given in Equation (2.54) are calculated numerically.

Finally, it should be noted that the cubic stiffness nonlinearity is an odd symmetric nonlinearity. If a dynamic system includes only odd symmetric nonlinearities and excited by an external forcing with only odd numbered harmonics, the multi harmonic response can be represented by a Fourier series having only the odd harmonics as

$$x(\theta) = \sum_{k=1,3,5...}^{m} \left[x_{sk} \sin(k\theta) + x_{ck} \cos(k\theta) \right]. \qquad (2.55)$$

In this case, bias forcing term, $\{f_{N0}\}$, in Equation (2.54) is equal to zero and $\{f_{Nsk}\}$ and $\{f_{Nck}\}$ terms are nonzero only for the odd values of k. Therefore the bias term and the even numbered harmonics of the nonlinear forcing do not need to be considered.

2.6.2 Piecewise Linear Stiffness

The relation between force and displacement for this element is described as follows:

$$f_N(x) = \begin{cases} k_2 x + (k_1 - k_2)\delta & if \quad x \geq \delta \\ k_1 x & if \quad -\delta < x < \delta \\ k_2 x - (k_1 - k_2)\delta & if \quad x \leq -\delta \end{cases} \qquad (2.56)$$

Special cases occur when k_1 or k_2 is zero. $k_1 = 0$ case is known as the saturation nonlinearity, whereas $k_2 = 0$ case is known as the backlash nonlinearity. These nonlinearities can be observed around pre-loaded bearing locations and external store mounting structures in aircrafts [85]. Graphical representations of these nonlinearities are given in Figure 2.6.
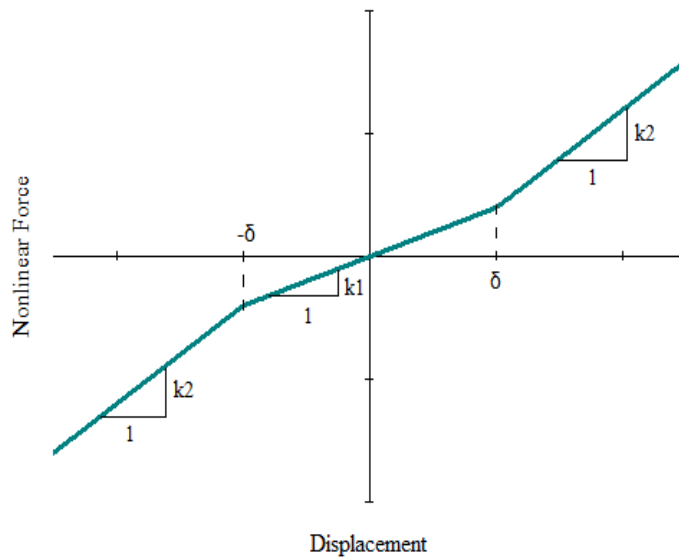
Figure 2.5 Behavior of piecewise linear stiffness nonlinearity
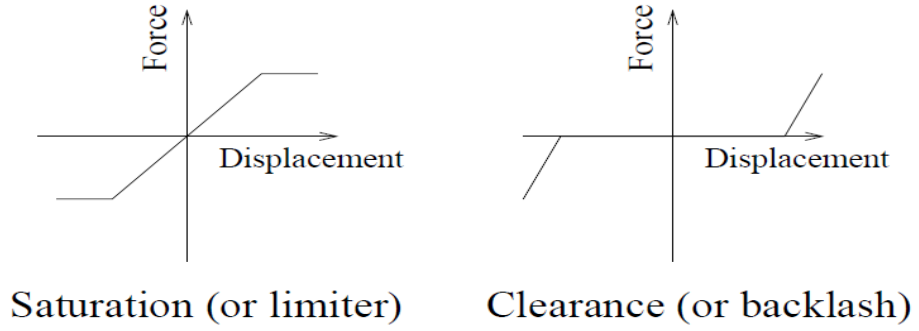
Figure 2.6 Special cases of piecewise linear stiffness [85]

When using the multi harmonic HBM for nonlinear response analysis, the Fourier coefficients for nonlinear force exerted by a piecewise linear stiffness element can be determined as follows:

Assuming a multi harmonic relative displacement between the ends of the piecewise linear stiffness nonlinearity as defined in Equation (2.53), and substituting this into Equation (2.56), Fourier coefficients of the nonlinear force can be obtained as

$$
\begin{aligned}
f_{N0} &= \frac{1}{2\pi}\int_0^{2\pi} f_N(\theta)\,d\theta \\[2ex]
f_{Nsk} &= \frac{1}{\pi}\int_0^{2\pi} f_N(\theta)\sin(k\theta)\,d\theta \\[2ex]
f_{Nck} &= \frac{1}{\pi}\int_0^{2\pi} f_N(\theta)\cos(k\theta)\,d\theta
\end{aligned}
\qquad (2.57)
$$

In order to evaluate these integrals, the points where the definition of the integrand changes, i.e. transition angles, must be located. These points correspond to the roots of the following equations, in the interval $[0, 2\pi]$:

$$x(\theta) - \delta = 0$$
$$x(\theta) + \delta = 0$$
(2.58)

When the number of harmonics included in in the solution is more than 1, solution of Equation (2.58) cannot be obtained analytically; hence, numerical methods should be used. In order to locate all the roots in the interval $[0, 2\pi]$, an incremental search can be performed. Chapra [87] presented a very useful incremental search algorithm together with a MATLAB$^{®}$ script. After the determination of the transition angles and their corresponding states, one can partition the integrals given in Equation (2.57) into a sum of sub-integrals where the roots become the integral boundaries. Then, each sub integral simply reduces to

$$I_0 = \int_{\theta_j}^{\theta_{j+1}} \left(k_j x(\theta) + c \right) d\theta$$

$$I_{sk} = \int_{\theta_j}^{\theta_{j+1}} \left(k_j x(\theta) + c \right) \sin(k\theta) d\theta \; ,$$
(2.59)

$$I_{ck} = \int_{\theta_j}^{\theta_{j+1}} \left(k_j x(\theta) + c \right) \cos(k\theta) d\theta$$

where the integrand is determined by the behavior of $x(\theta)$ in the interval $\theta_j < \theta < \theta_{j+1}$. For example if $-\delta < x(\theta) < \delta$ for $\theta_j < \theta < \theta_{j+1}$, $k_j = k_1$ and $c = 0$. In this way, every integral and therefore every Fourier coefficient can be calculated analytically and can be embedded inside a computer code.

As for the cubic stiffness nonlinearity, the piecewise linear stiffness nonlinearity is odd symmetric. If a dynamic system contains only odd symmetric nonlinearities and an external forcing with odd harmonics only, the multi harmonic response can be represented by a Fourier series having only odd harmonics. In this case the Fourier series representation of the nonlinear force exerted by a piecewise linear stiffness element contains only odd harmonics.

2.6.3   Gap Nonlinearity

The expression of the nonlinear force for this element is defined as:

$$f_N(x) = \begin{cases} k_g(x-\delta) & if \quad x \geq \delta \\ 0 & if \quad x < \delta \end{cases}.$$
(2.60)
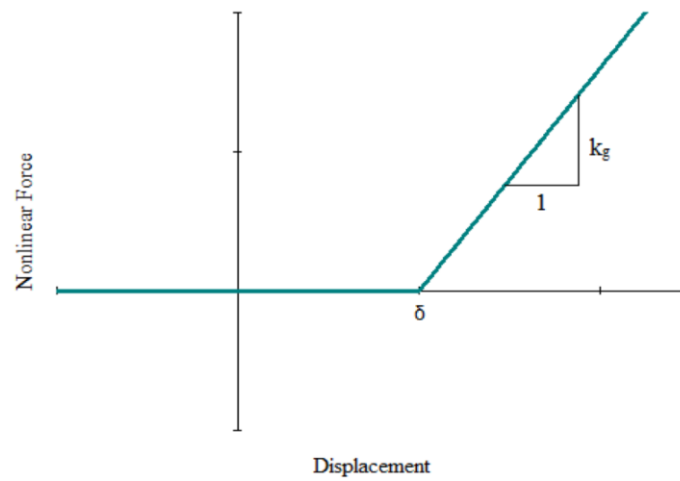
Figure 2.7 The behavior of gap element

This element can be used for modeling special types of clearances and cracks. When k_g becomes too large, the element starts to show almost rigid behavior. In this case, the dynamic model may be used for investigating impact effects. Such systems tend to show very interesting and complex behavior [85].

Assuming a multi harmonic relative displacement between the ends of the gap nonlinearity as defined in Equation (2.53), and substituting this into Equation (2.60), Fourier coefficients of the nonlinear force can be obtained as follows

43

$$f_{N0} = \frac{1}{2\pi} \int_0^{2\pi} f_N(\theta)d\theta$$

$$f_{Nsk} = \frac{1}{\pi} \int_0^{2\pi} f_N(\theta)\sin(k\theta)d\theta \ .$$

(2.61)

$$f_{Nck} = \frac{1}{\pi} \int_0^{2\pi} f_N(\theta)\cos(k\theta)d\theta$$

As described in the previous section, in order to evaluate the integrals given in Equation (2.61), one needs to determine the regions where $x(\theta)$ becomes equal to δ. Therefore, all the roots of the following equation should be determined in the interval $[0, 2\pi]$:

$$x(\theta) - \delta = 0 \ .$$

(2.62)

The locations of the roots can be found by following an incremental search procedure. After the roots are determined, the integrals given in Equation (2.61) can be calculated. These integrals can be evaluated more easily than the ones for a piecewise linear stiffness element because at the regions where $x(\theta)$ is less than δ, the integrals will be automatically zero. For the remaining regions, the sub-integrals reduce to:

$$I_0 = \int_{\theta_j}^{\theta_{j+1}} k_g \left(x(\theta) - \delta \right) d\theta$$

$$I_{sk} = \int_{\theta_j}^{\theta_{j+1}} k_g \left(x(\theta) - \delta \right)\sin(k\theta)d\theta \ ,$$

(2.63)

$$I_{ck} = \int_{\theta_j}^{\theta_{j+1}} k_g \left(x(\theta) - \delta \right)\cos(k\theta)d\theta$$

which can be evaluated analytically. Unlike the nonlinear elements discussed before, the gap nonlinearity is not an odd symmetric nonlinearity. Therefore if a gap element

44

exists in the system, one must include the bias term, even numbered harmonics in addition to the odd numbered harmonics in representation of the nonlinear forcing.

2.6.4 Dry Friction

There are numerous friction models in the literature. For the studies in this thesis, a 1-D Coulomb friction model with constant normal load is used. The graphical representation of the model can be seen in Figure 2.8.
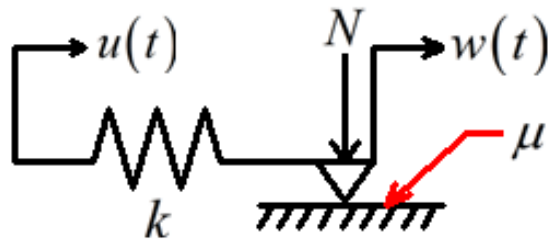
Figure 2.8 The 1-D Dry friction model

In the model, $u(t)$ is the relative input motion. k is the contact stiffness between the rubbing surfaces, N is the constant normal force, μ is the dry friction coefficient and $w(t)$ is the slip motion.

The force on the spring is given as:

$$f_s = k(u - w). \tag{2.64}$$

From Newton's second law of motion, the force on the spring is equal to the friction force.

Details about the physics of the model are explained by Ciğeroğlu [77]. As explained by Ciğeroğlu, the stick state occurs whenever the input motion $u(t)$ changes its direction. That is, it's time derivative, $\dot{u}(t)$ changes its sign. Therefore, at the instant of this sign change, $\dot{u}(t)$ must become zero.

$$\dot{u} = 0. \tag{2.65}$$

Since the systems in consideration are vibratory systems, this direction change in $u(t)$ is bound to happen. This can be proved from a mathematical point of view by using the periodicity of the response and the Mean Value Theorem.

As a result, the element always sticks at some time t. After sticking, the element may or may not begin to slip. If the force in the spring becomes equal to μN, which is the limiting value of friction force, positive slip begins and after this point the friction force stays constant until the transition from positive slip to stick occurs.

Therefore,

$$f_s = k(u - w) = \mu N, \tag{2.66}$$

is valid throughout positive slip.

The same phenomenon occurs after sticking if the force in the spring becomes equal to $-\mu N$, initiating negative slip. After negative slip begins, the friction force stays constant until transition from negative slip to stick occurs.

Therefore, the expression

$$f_s = k(u - w) = -\mu N \tag{2.67}$$

is valid throughout negative slip.

When transition from positive slip to stick occurs, the input motion changes its direction from positive to negative. At the instant of transition, both Equation (2.65) and Equation (2.66) are satisfied. Starting from this first instant $w(t)$ takes a value w_0 and stays constant throughout the stick phase. Denoting the value of $u(t)$ at the same instant as u_0, we can write Equation (2.66) for the start of stick as:

$$k\left(u_0 - w_0\right) = \mu N .$$ (2.68)

Slip motion $w(t)$ is unknown; therefore the nonlinear force expressions must not have $w(t)$ or w_0 in them. By using Equation (2.68), we can eliminate w_0 from the force expression given in Equation (2.64) and obtain the force expression for this particular stick state which occurs after transition from positive slip as:

$$f_s = k(u - u_0) + \mu N$$ (2.69)

This stick state continues until negative slip starts. At the first instant of negative slip, both Equation (2.67) and the stick condition $w(t) = w_0$ are satisfied. Therefore, at this instant Equation (2.67) becomes:

$$k\left(u - w_0\right) = -\mu N .$$ (2.70)

Equating the two w_0 expressions from Equation (2.68) and Equation (2.70), one can obtain the condition for transition from stick to negative slip as:

$$k\left(u - u_0\right) + 2\mu N = 0 .$$ (2.71)

By following a similar procedure, the condition for transition from stick to positive slip can be obtained as:

$$k\left(u - u_0^{'}\right) - 2\mu N = 0,$$ (2.72)

where $u_0^{'}$ is the value of $u(t)$ at the end of negative slip, beginning of stick phase. In addition, the force expression for the stick state which occurs after transition from negative slip to stick can be obtained as:

$$f_s = k(u - u_0^{'}) - \mu N$$ (2.73)

If the force in the spring never becomes equal to $\pm \mu N$, the element always stays in the stick state. For this case, there is no transition from stick to slip; therefore $w(t)$ is always constant and the element behaves completely like a linear spring with stiffness k.

After all, the force exerted by this nonlinear element can be expressed as:

$$f_n = \begin{cases} -\mu N & if \quad \dot{u} \leq 0 \quad and \quad k\left(u - u_0\right) + 2\mu N \leq 0 \\ k(u - u_0^{'}) - \mu N & if \quad \dot{u} \geq 0 \quad and \quad k\left(u - u_0^{'}\right) - 2\mu N < 0 \\ \mu N & if \quad \dot{u} > 0 \quad and \quad k\left(u - u_0^{'}\right) - 2\mu N \geq 0 \\ k(u - u_0) + \mu N & if \quad \dot{u} < 0 \quad and \quad k\left(u - u_0\right) + 2\mu N > 0 \\ ku & if \qquad\qquad\qquad no\_slip \end{cases}$$ (2.74)

For the evaluation of the conditions given in Equation (2.74) one needs to obtain all the roots of Equation (2.65), Equation (2.71) and Equation (2.72), i.e. transition angles, in the interval $[0,2\pi]$ and order them in order to identify where stick, positive slip or negative slip cases are valid. If slip never occurs, i.e. no roots for Equations (2.71) and (2.72) are identified, the last line given in Equation (2.74) must be used.

48

The locations of the roots can be found by following an incremental search procedure. After the roots in the interval $[0, 2\pi]$ are found, one can arrange the integrands and integral boundaries of the following integral expressions according to the obtained roots.

$$\{f_{N0}\} = \frac{1}{2\pi} \int_0^{2\pi} f_N(\theta) d\theta$$

$$\{f_{Nsp}\} = \frac{1}{\pi} \int_0^{2\pi} f_N(\theta) \sin(p\theta) d\theta \qquad (2.75)$$

$$\{f_{Ncp}\} = \frac{1}{\pi} \int_0^{2\pi} f_N(\theta) \cos(p\theta) d\theta$$

Then, analytical integrations can be performed for every value of p in order to calculate the Fourier coefficients for nonlinear forcing. The whole procedure can be embedded inside a computer code.

2.6.5   Case Studies

Three case studies will be presented in this section to exemplify the HBM, arc length continuation method and different types of nonlinearities.

2.6.5.1   Case Study 1: Comparison of Time Integration and HBM

In this case study, the solution of a simple nonlinear problem by in time integration and HBM is presented and the results are compared.

For this study a simple system with a gap nonlinearity is used. The system and its parameters are given in Figure 2.9 and Table 2.1 respectively. The excitation force on the mass is taken as $F = 50\sin(\omega \cdot t)$ N.

Table 2.1 Parameters for Case Study 1

M (kg)	k (N/m)	h (N/m)	δ (m)	k_g (N/m)
1	100	1	5	400
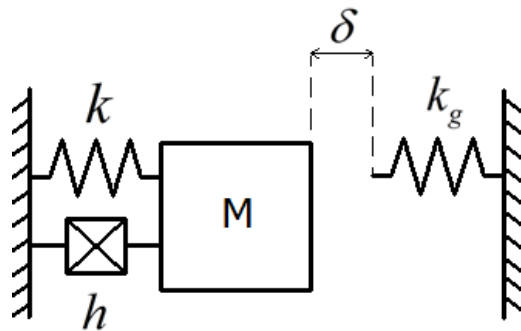
Figure 2.9 The SDOF System Used in Case Study 1

The natural frequency of this system can easily be calculated as 10 rad/s. In order to obtain a satisfactory frequency response plot, response of the system is obtained between 5 and 15 rad/s.

For the time domain solution, ode45 solver of MATLAB® is used. The frequency range of interest is divided into 200 segments. For each frequency step, time response of the system is calculated in ode45 for 200 seconds. It is observed that 200 seconds is long enough for the system to reach steady state. After the solutions are obtained for each frequency, the steady state vibration amplitudes are computed and corresponding frequency values are stored in two different arrays. The frequency response graph is obtained by plotting these stored amplitude and frequency values against each other.

For the frequency domain solution, HBM with 10 harmonics is used, and the resulting nonlinear system of equations is solved with a Newton's Method-arc length continuation scheme. The frequency response obtained from both methods are presented in Figure 2.10.
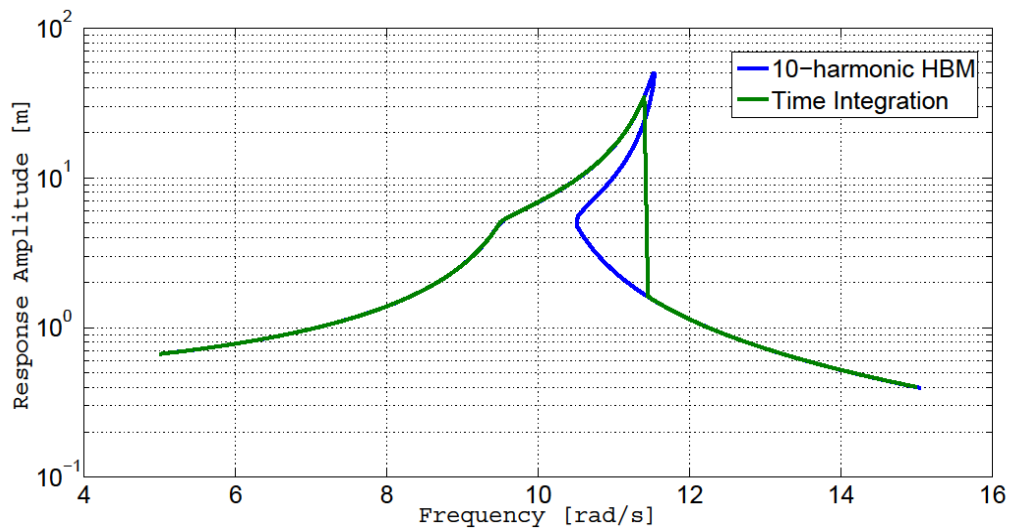
Figure 2.10 Total Nonlinear Response Graphs Obtained from Time Domain Integration and HBM

It can be seen from Figure 2.10 that, the periodic response assumption for the HBM is valid for such problems. Therefore, the method can obtain the steady state response for nonlinear vibration problems with a satisfactory accuracy.

It can also be seen from Figure 2.10 that when multiple solutions coexist for a single frequency, time integration is not able to find all of them. Also, even for one degree of freedom simple system, it requires significant amount of computational time. For example, for the problem presented here, using the default error tolerance and time

51

span options of ode45, the solution time is about 3 minutes and 7 seconds. On the other hand, together with arc length continuation and adaptive step size, HBM is able to obtain the frequency response in only 35 seconds, although the response obtained from HBM is computed at 334 points instead of 201. Therefore, if similar number of points are used (334 points) time response will approximately require 4.5 to 5 minutes. It should be noted that in order to get the complete frequency response time integration should be repeated in the reverse direction, i.e. high to low frequency sweep, which will increase the computational time of the time integration. Moreover, this computational time difference will increase exponentially, if the degrees of freedom of the system under consideration increases. Furthermore, in the unstable region, HBM combined with arc length continuation is able to obtain multiple solutions whereas time integration cannot. As stated before, if the nonlinear frequency response is sought, using a frequency domain method seems much more advantageous.

2.6.5.2   Case Study 2: Application of HBM on a Nonlinear Vibration Problem

For this sub-section, the system in consideration is a cantilever beam model, taken from Cigeroglu [77]. The mass and stiffness matrices of the beam are obtained via the Finite Element Method. The beam is modeled by four 2D beam elements and the resulting mass and stiffness matrices are 8x8; hence, the resulting dynamic model becomes an 8-DOF model.

As the nonlinear elements, a dry friction damper and a gap element is added between the ground and the eighth DOF. The resulting system is illustrated in Figure 2.11. The parameters for the nonlinearities are given in Table 2.2.

Table 2.2 Parameters for Case Study 2

δ (m)	μN (N)	$k_{contact}$ (N/m)	F (N)	k_g (N/m)	mL (kg)	$\dfrac{EI}{L^3}$ (N/m)
2	3	1	1	3	1	1
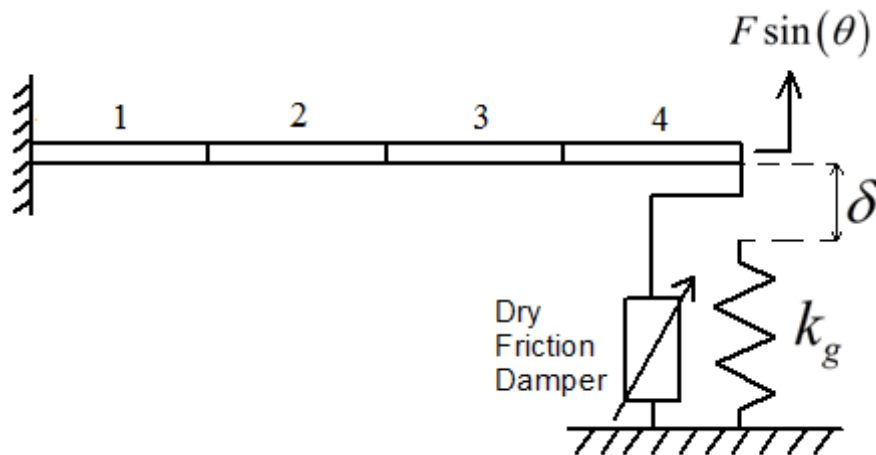
Figure 2.11 A Cantilever Beam Model with a Dry Friction Damper and Gap Nonlinearity Located at the Tip

For the parameter set given, the response calculations are carried out by using 10 harmonics. The frequency response for the eighth DOF around the first natural frequency is given in Figure 2.12, Figure 2.13 and Figure 2.14. The change in the phase angle of the first harmonic of the response throughout the frequency range of interest can be seen in Figure 2.15.

It can be seen from the graphs that the first harmonic is sufficient to represent the total response in most of the frequency region of interest. In these regions, higher harmonics are calculated but eventually they turned out to be zero. Therefore, their

logarithms are undefined. Conversely, near the resonance higher harmonics increase in magnitude. The reason for this is the increase in response amplitude around the resonance region. At some point, it becomes equal to or greater than the gap. After that, the beam starts to hit the discrete spring. This impact excites higher harmonics, an expected behavior of gap nonlinearity. In addition, in the same resonance region, when the displacement is around 3.5 m the force stored in the contact stiffness becomes large enough to overcome friction and the friction element starts to slip. However, away from the resonance, the friction element sticks and the element behaves like a linear spring. In the end, one obtains a nonlinear response curve, which contains a shifted resonance peak, decreased in magnitude and bent to the right, a combination of two types of nonlinearities.
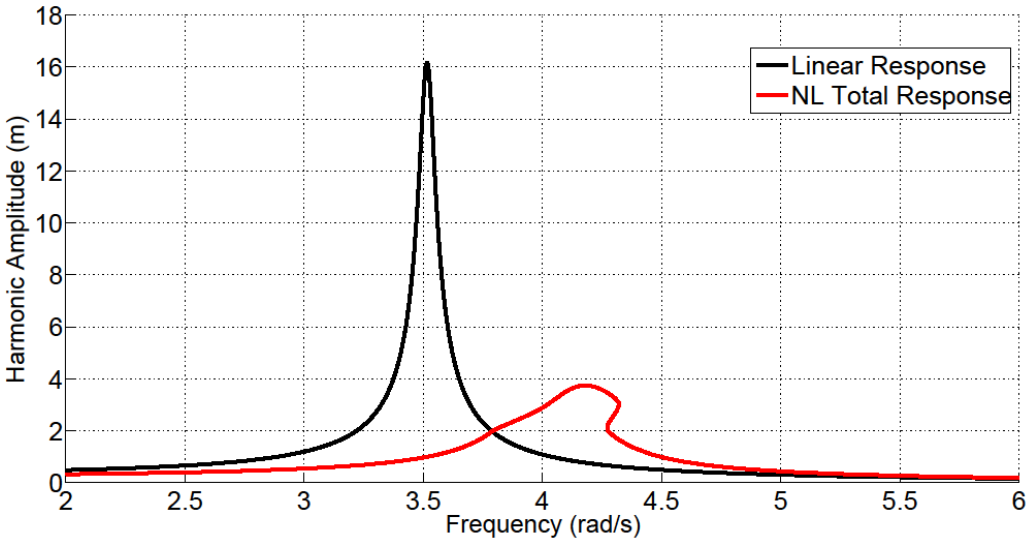
Figure 2.12 Linear and Nonlinear Total Response Curves for 7th DOF

54
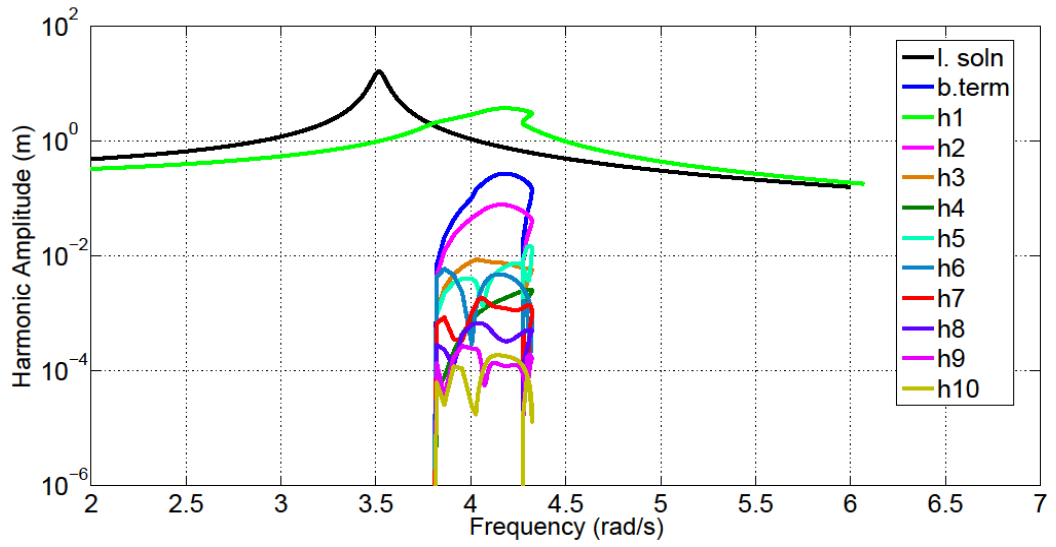
Figure 2.13 Amplitudes of harmonics for 7th DOF
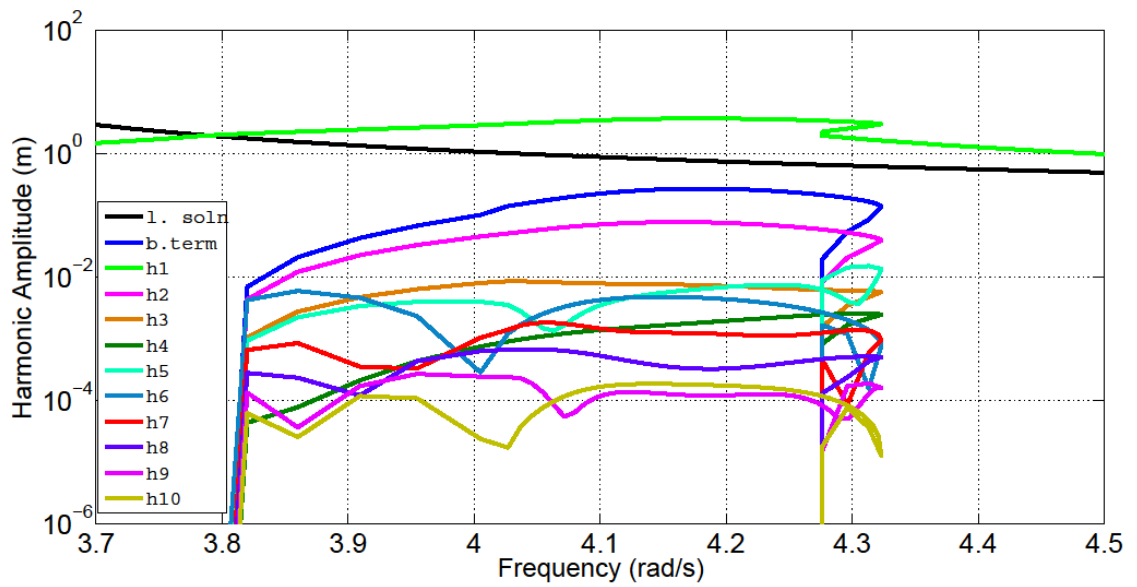
Figure 2.14 Amplitudes of harmonics around resonance for 7th DOF
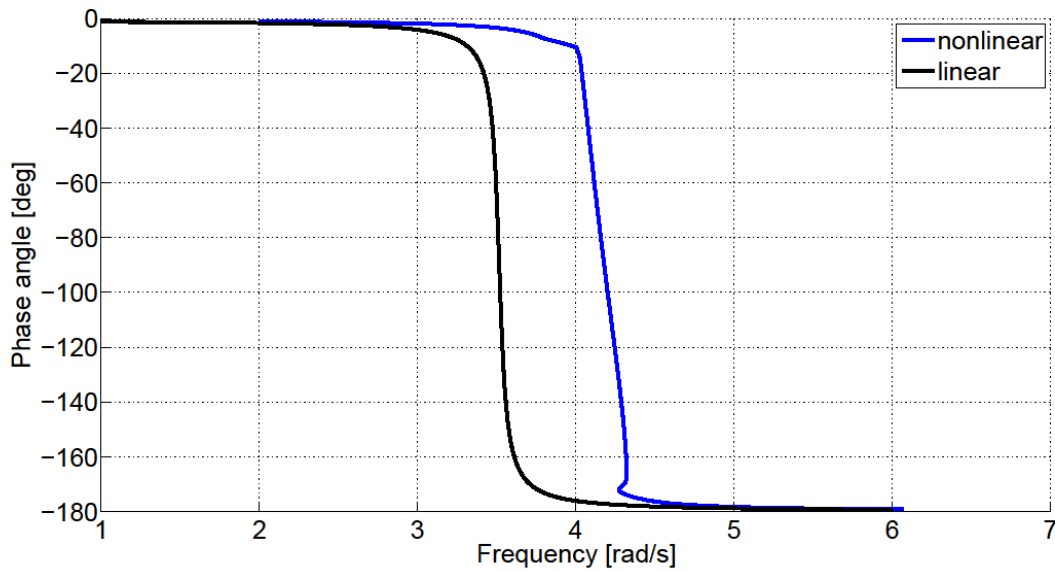
Figure 2.15 Angle Plot for the First Harmonic of 7th DOF

For the second part of this study, parameters given in Table 2.3 are used where μN_2 and $k_{contact2}$ belongs to a second dry friction damper, added between the DOFs 5 and 7. For this case, the results can be seen in Figure 2.16 and Figure 2.17.

It can be seen from Figure 2.17 that since μN_2 is as small as 0.2 N, slip occurs easily at the corresponding damper. Correspondingly, slip-stick behavior begins at relatively low displacement values around 3.5 rad/s and odd-numbered harmonics are excited. As in the previous example, impact starts at the gap element around the resonance and slip begins at the first damper, therefore all 10 harmonics are excited at the same time. As the displacement starts to decrease, effect of the gap element wears out. Around 4.75 rad/s the slip-stick behavior stops at the second damper and only the first harmonic maintains its magnitude.

The change in the phase angle of the first harmonic of the response throughout the frequency spectrum of interest can be seen in Figure 2.18.

Table 2.3 Second Set of Parameters for Case Study 2

δ (m)	μN (N)	$k_{contact}$ (N/m)	F (N)	k_g (N/m)	μN_2 (N)	$k_{contact2}$ (N/m)
2	2	1	1	3	0.2	1
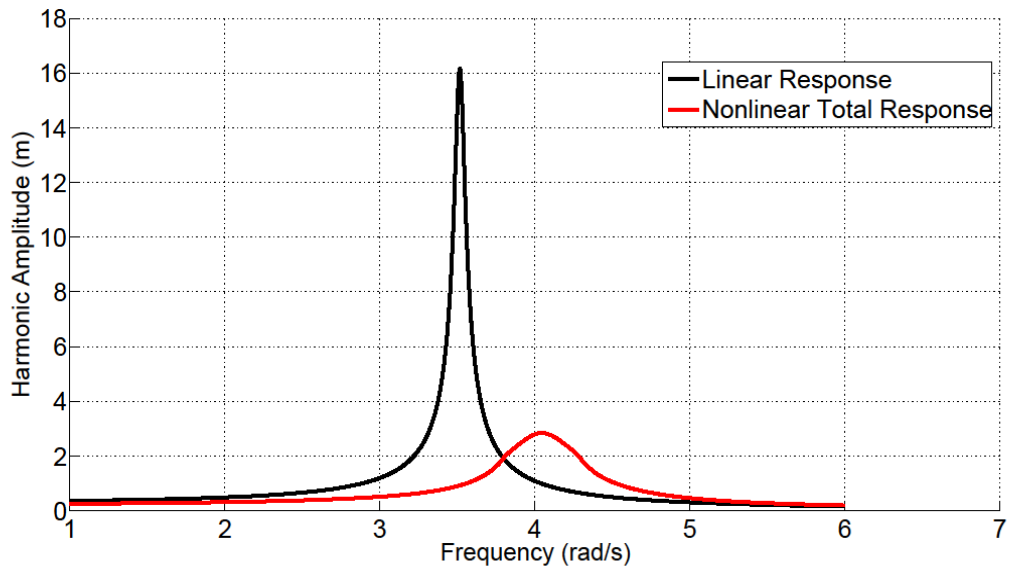
Figure 2.16 Total Response Curves for 7th DOF
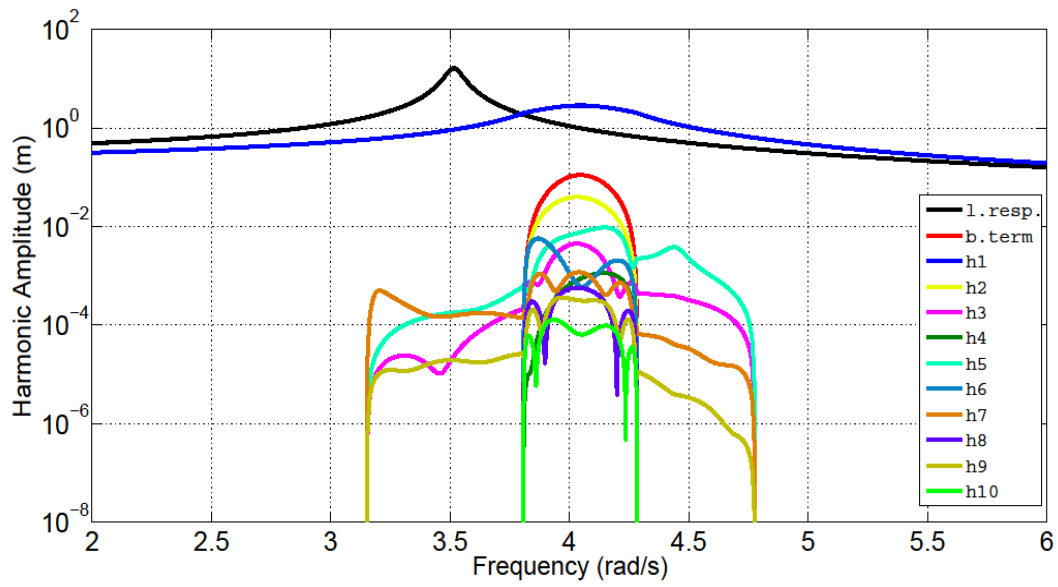
Figure 2.17 Amplitudes of harmonics for 7th DOF
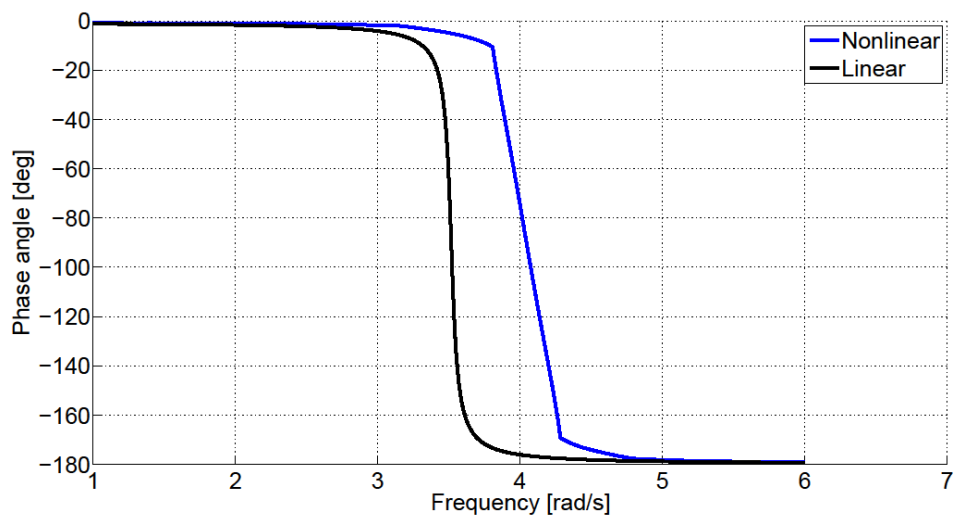
Figure 2.18 Phase Angle Plot for the First Harmonic of 7th DOF

58

2.6.6 Case Study 3

Another case study involving cubic stiffness nonlinearity is presented in this section. The system of interest is shown in Figure 2.19 and the corresponding parameters of the system are given in Table 2.4.

A 5-harmonic solution is performed for the given system. The frequency response and phase angle graphs of the first DOF is are given in Figure 2.20, Figure 2.21 .
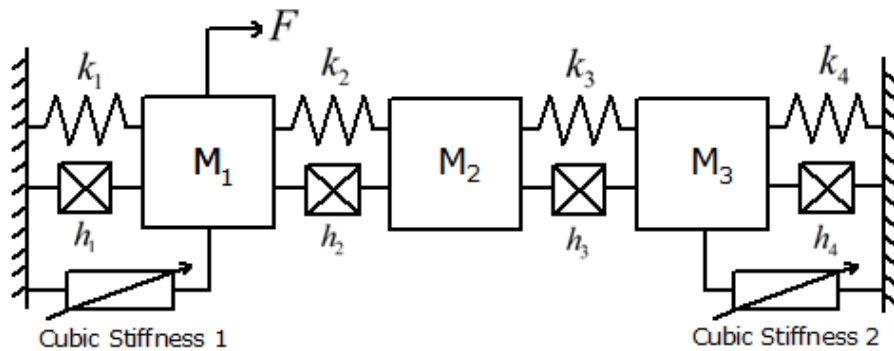
Figure 2.19 The 3-DOF System Used in Case Study 3

Table 2.4 Parameters of the System, Case Study 3

M_1, M_3 (kg)	M_2 (kg)	k_1, k_2, k_3, k_3 (N/m)	h_1, h_2, h_3, h_4 (N/m)	F (N)
1	0.75	1000	10	$30\sin(\theta) + 30\sin(2\theta) + 30\sin(3\theta)$
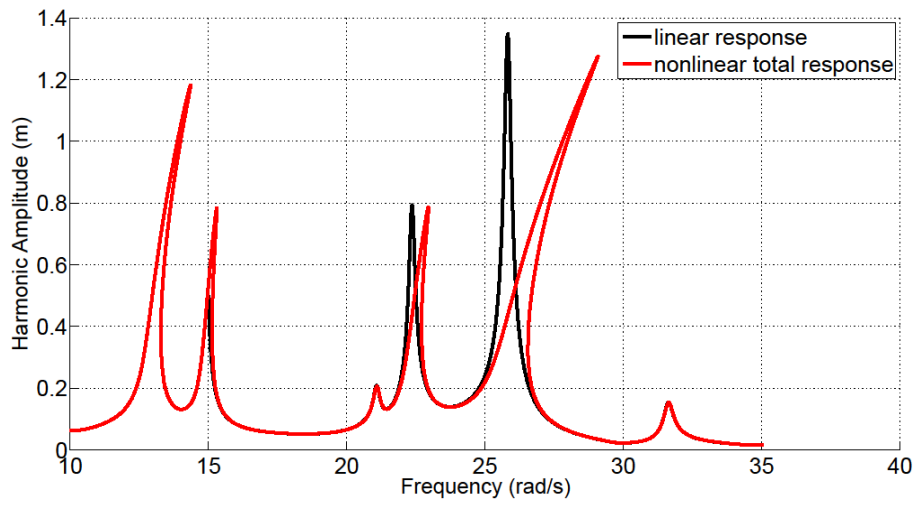
Figure 2.20 Linear and Nonlinear Response Curves for the First DOF
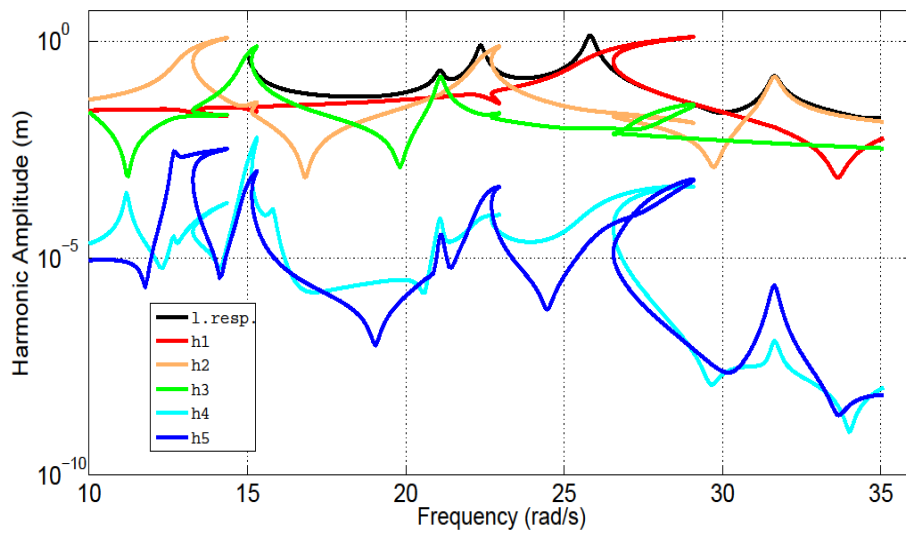
Figure 2.21 Amplitudes of Harmonics for the First DOF

60

CHAPTER 3

ADAPTIVE HARMONIC BALANCE METHODS

3.1   Introduction

In Chapter 2, it is indicated that application of the classical HBM approach yields $n(2m+1)$ algebraic equations, where n is the DOF of the system in consideration and m is the number of harmonics retained in the solution. In addition, in the same chapter reduction methods are introduced. The purpose of these methods is to decrease the number of equations to be solved. But both of the reduction methods presented, perform this reduction without changing the number of harmonics, m. In fact, a further reduction can be obtained by neglecting the harmonics which do not contribute significantly to the total solution; therefore, the computational efficiency of the HBM can be enhanced. The basis of adaptive harmonic balance methods (AHBMs) depends on this idea. In this chapter, the AHBMs available in the field of structural dynamics are discussed and a new adaptive harmonic balance method is presented.

3.2   AHBM 1: Jaumouille´, Sinou and Petitjean's Method

In 2010, Jaumouille´, Sinou and Petitjean [4] introduced an AHBM which is originally intended to be used in analyzing nonlinear bolted joint models. As mentioned in Chapter 1, in order to identify the harmonics that should be used, the method uses the concept of approximate strain energy. It is basically equal to the potential energy stored in the linear springs during the vibratory motion of the system. Potential energy stored in the springs is defined as:

$$U(t) = \frac{1}{2}\{q(t)\}^T [K]\{q(t)\}. \tag{3.1}$$

Using the notation followed by the authors, one can express $\{q(t)\}$, i.e. the displacement vector, as:

$$\{q(t)\} = \{q_0\} + \sum_{k=1}^{m}\{q_{sk}\}\sin(k\theta) + \sum_{k=1}^{m}\{q_{ck}\}\cos(k\theta) = [T(t)]\{Z\}$$

$$[T(t)] = \begin{bmatrix}[I] & [I]\sin(\theta) & [I]\cos(\theta) & \cdots & [I]\sin(m\theta) & [I]\cos(m\theta)\end{bmatrix}, \qquad (3.2)$$

$$\{Z\} = \begin{bmatrix}\{q_0\} & \{q_{s1}\} & \{q_{c1}\} & \cdots & \{q_{sm}\} & \{q_{cm}\}\end{bmatrix}^T$$

where I is $n \times n$ identity matrix. Furthermore, it can be shown that:

$$\frac{1}{T}\int_0^T [T(t)]^T[T(t)]\,dt = [L] = \begin{bmatrix} 2I & [0] & \cdots & [0] \\ [0] & I & \cdots & [0] \\ \vdots & \vdots & \ddots & \vdots \\ [0] & [0] & \cdots & I \end{bmatrix}_{[n(2m+1)]\times[n(2m+1)]}, \qquad (3.3)$$

where T indicates one period and superscript T indicates matrix transpose. In order to suppress the time dependency in Equation (3.1) one can find the mean value of the potential energy for one period as

$$U_m = \frac{1}{T}\int_0^T \left[\frac{1}{2}\{Z\}^T[T(t)]^T[K][T(t)]\{Z\}\right]dt. \qquad (3.4)$$

In order to make use of Equation (3.3) inside Equation (3.4), authors introduce a new identity. For an $n \times n$ matrix $[W]$ and an $n(2m+1) \times 1$ vector $\{Y\}$:

$$[W][T(t)]\{Y\} = [T(t)][N_W]\{Y\}, \qquad (3.5)$$

where

$$N_W = \begin{bmatrix} [W] & [0] & \cdots & [0] \\ [0] & [W] & \cdots & [0] \\ \vdots & \vdots & \ddots & \vdots \\ [0] & [0] & \cdots & [W] \end{bmatrix}.$$

(3.6)

By using the identity given in Equation (3.5), the approximate strain energy expression can be reduced to a matrix multiplication :

$$U_m = \frac{1}{2}\{Z\}^T [L][N_K]\{Z\}.$$

(3.7)

The authors also derived a variant of this formula where the approximate strain energy can be found from the Fourier coefficients of nonlinear DOFs only as

$$U_m = \frac{1}{2}\left[Z_q\right]^T \left[L_q\right]\left[N_{\left[K_{qq}\right]-\left[K_{qp}\right]^T\left[K_{pp}\right]^{-1}\left[K_{pq}\right]}\right]\left[Z_q\right],$$

(3.8)

where $\left[Z_q\right]$ is the matrix containing the Fourier coefficients of the nonlinear DOFs only; $\left[L_q\right]$ is a $q(2m+1) \times q(2m+1)$ identity matrix, where q is the number of nonlinear DOFs. $\left[K_{qq}\right]-\left[K_{qp}\right]^T\left[K_{pp}\right]^{-1}\left[K_{pq}\right]$ is a modified stiffness matrix that acts as the stiffness matrix on the nonlinear DOFs. The details about the derivation of this term can be found in reference [4]. It should be noted that the expression for the approximate strain energy given in Equation (3.8) is valid when a reduction method which decouples the equations of different linear and nonlinear DOFs, such as receptance method is used. Also, the expression is based on the assumption that there are no external forces acting on linear DOFs. Therefore, in case there exist many nonlinear DOFs and/or external forces acting on the linear DOFs, it is necessary to use the basic formula given in Equation (3.7).

The harmonic selection process of this method is relatively simple. Firstly, at every frequency point, the Fourier coefficients for the response are calculated with k harmonics. Then, at the same point, the number of harmonics is increased by 1 and the resulting equation set is solved one more time. This process continues until the relative approximate strain energy difference ratio given below becomes less than a certain threshold value:

$$\varepsilon = \frac{U_m^{k+1} - U_m^k}{U_m^k}, \qquad (3.9)$$

where U_m^k is the approximate strain energy calculated from the response containing k harmonics. When ε becomes less than the threshold value, it means that the contribution from the last added harmonic is small enough. In such a case, the increase of harmonics is stopped and the initial guess for the next frequency step is computed. The starting value of k is set to 1. The whole process is summarized in Figure 3.1.

Since this method assigns the same number of harmonics for all DOFs, it is referred as a global method [5]. Also, since the method increases the number of harmonics one by one, it is referred as an incremental [5] method. In some cases where the strain energy convergence rate is not smooth, the incremental behavior of the method can cause the algorithm to stop before saturation occurs [4]. In addition, for the regions where higher harmonics gain importance, the incremental behavior requires the response to be computed over and over again at the same solution point. Hence, this can increase the computational time considerably. In addition, since the maximum number of harmonics to be retained is not defined in this method, the algorithm may end up calculating excessively many harmonics at certain solution points, which can be unnecessary.

$$\text{with } \tilde{x} = \left\{ \begin{array}{c} Z \\ or \\ Z_q \end{array} \right\} \quad \text{and} \quad \hat{\mathbf{K}} = \left\{ \begin{array}{c} \mathbf{K} \\ or \\ \tilde{\mathbf{K}}_{qq} - {}^T\tilde{\mathbf{K}}_{qp}\tilde{\mathbf{K}}_{pp}^{-1}\tilde{\mathbf{K}}_{pq} \end{array} \right\}.$$
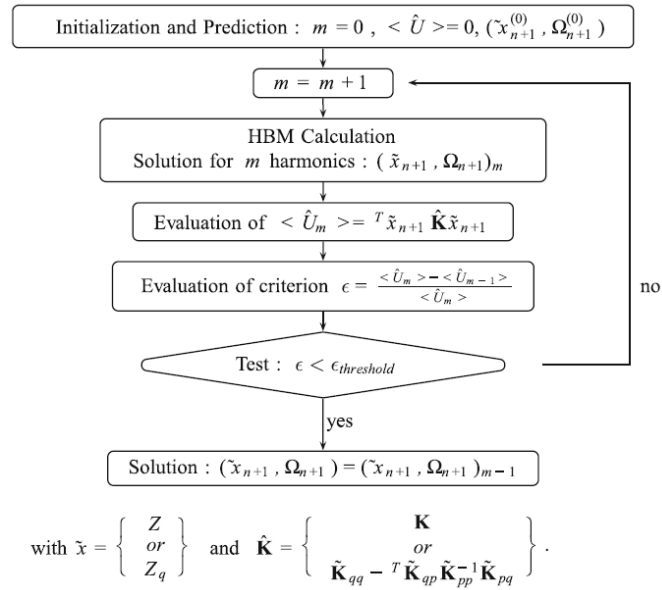
Figure 3.1 Algorithm for the method presented by Jamouillé et. al [4]

3.2.1 Case Study 1: Application of AHBM 1 on a SDOF System

The one DOF system with a gap nonlinearity is given in Figure 3.2.
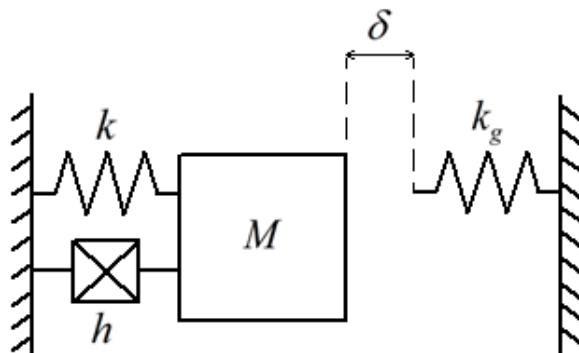
Figure 3.2 A SDOF System with Gap Nonlinearity

External forcing acting on the mass is taken as $F = 50\sin(\omega \cdot t)$ N. The parameters of the system are given in Table 3.1. The responses of the system obtained are given in Figure 3.3 to Figure 3.5. In Figure 3.5, the change in the number of harmonics is shown on the vertical axis, whereas on the horizontal axis, arc length is given. Arc length is basically the length of the response curve. As the numerical solution procedure continues, new frequency points are added to the response curve and the length of the curve increases. One can easily relate the number of harmonics used at a single point with the length of the curve up to that point and obtain a plot such as the one given in Figure 3.5.

It can be seen from the figures that the resonance peak on the linear curve shifted to the right if the displacement amplitude is large enough to close the gap. Furthermore, a second peak formed around 6 rad/s due to the impact effect created by the gap nonlinearity. For the most of the nonlinear response curve, the response is represented by 7 harmonics. But this number increases considerably around the resonances.

Table 3.1 Parameters for Case Study 1

M (kg)	k (N/m)	h (N/m)	δ (m)	k_g (N/m)	$\varepsilon_{threshold}$
1	100	1	0.4	400	10^{-20}
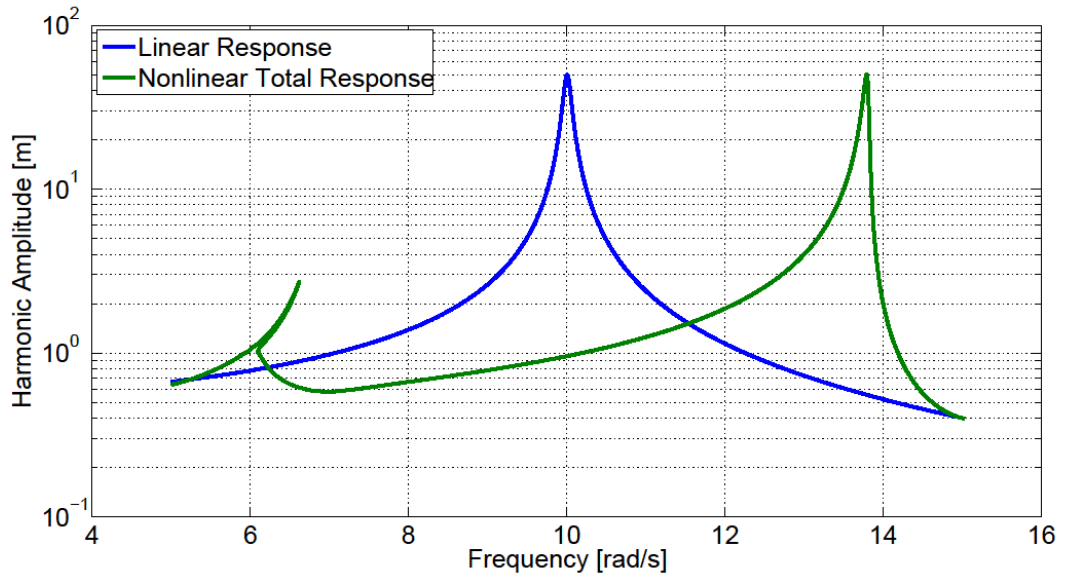
Figure 3.3 Total Nonlinear Response and Linear Response Curves for Case Study 1, $\varepsilon_{threshold} = 10^{-20}$
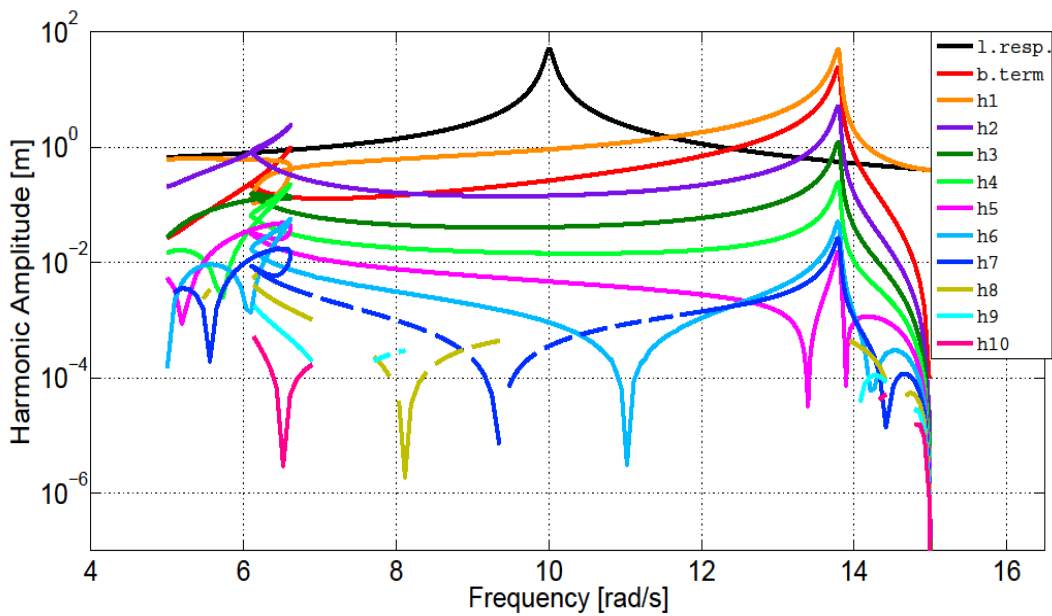
Figure 3.4 Amplitudes of harmonics for Case Study 1 (only the first 10 harmonics are shown for clarity), $\varepsilon_{threshold} = 10^{-20}$
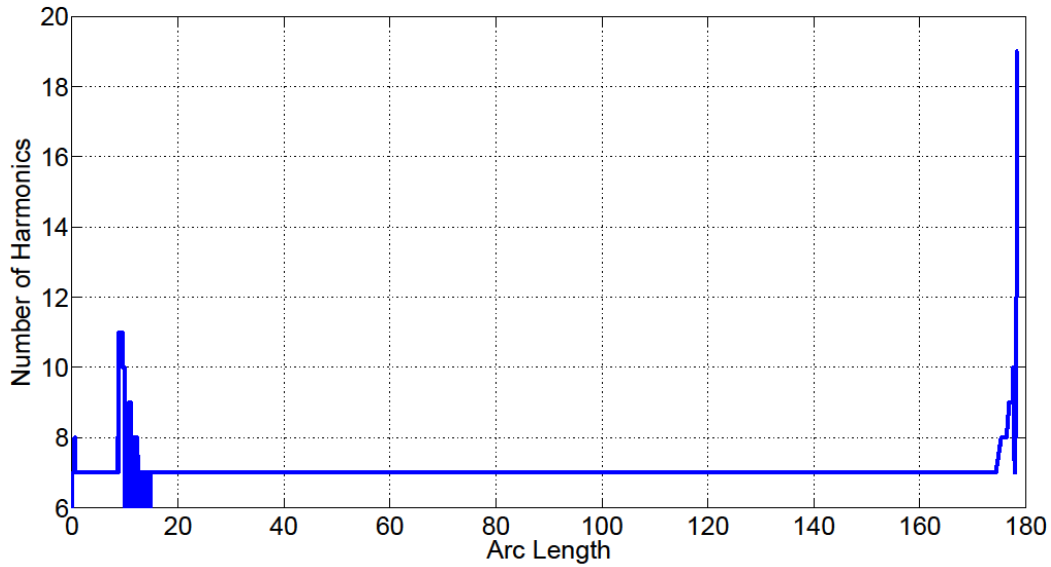
Figure 3.5 Number of Harmonics Used During Solution, $\varepsilon_{threshold} = 10^{-20}$

From the given algorithm of the method, it is expected that setting $\varepsilon_{threshold}$ to a higher value would cause less harmonics to be used in the solution. This effect must become evident especially for systems which have a smooth increase in the amplitudes of higher harmonics. To see this effect, the analysis is repeated by increasing $\varepsilon_{threshold}$ to 10^{-12}. The results are given from Figure 3.6 to Figure 3.8. It can be seen from these figures that the number of harmonics retained in the solution decreased to some amount.
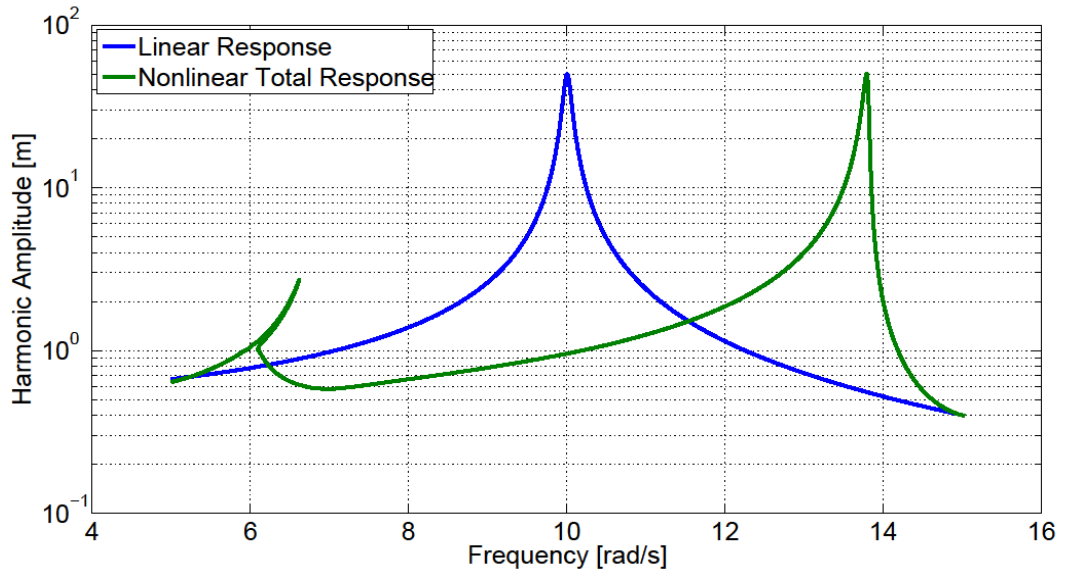
Figure 3.6 Total Nonlinear Response and Linear Response Curves for Case Study 1, $\varepsilon_{threshold} = 10^{-12}$
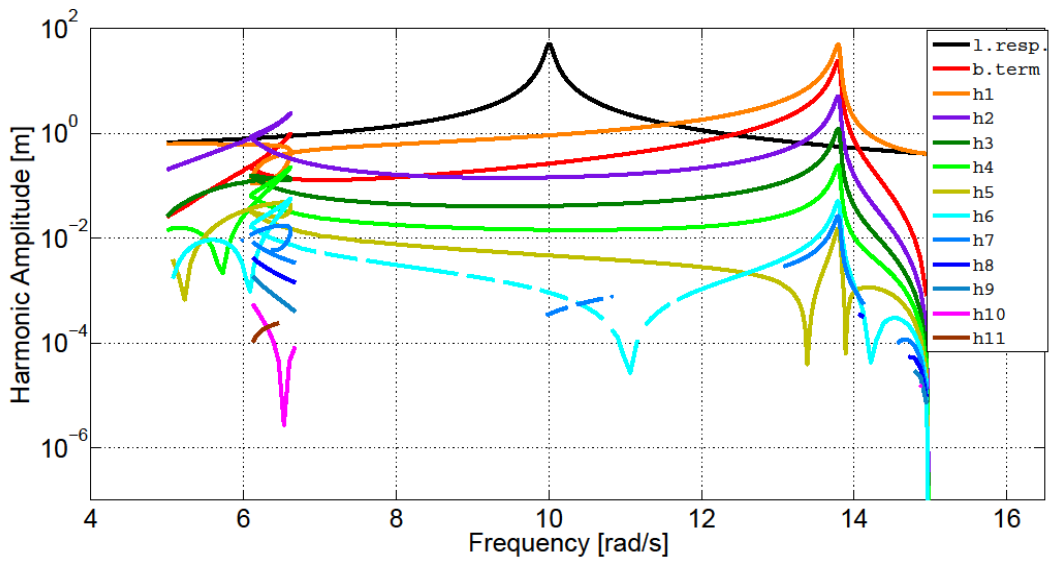
Figure 3.7 Amplitudes of harmonics for Case Study 1, $\varepsilon_{threshold} = 10^{-12}$
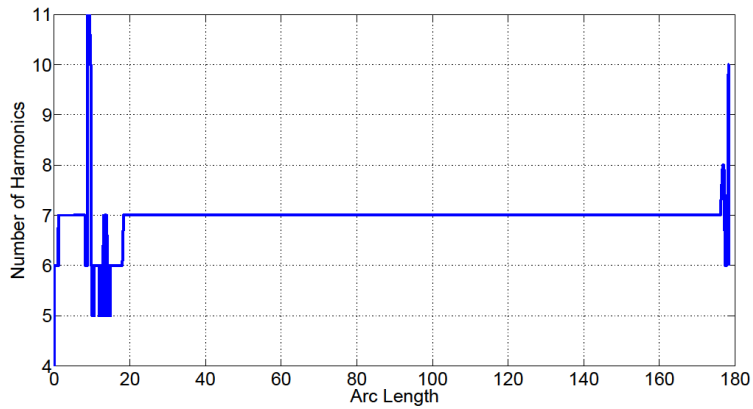
Figure 3.8 Number of Harmonics Used During Solution, $\varepsilon_{threshold} = 10^{-12}$

In the next step, in order to observe the rejection of more harmonics, $\varepsilon_{threshold}$ is further increased to 10^{-6}. The results are given in Figure 3.9 to Figure 3.101. It can be seen from Figure 3.11 that increasing the threshold value decreased the number of harmonics used as expected.
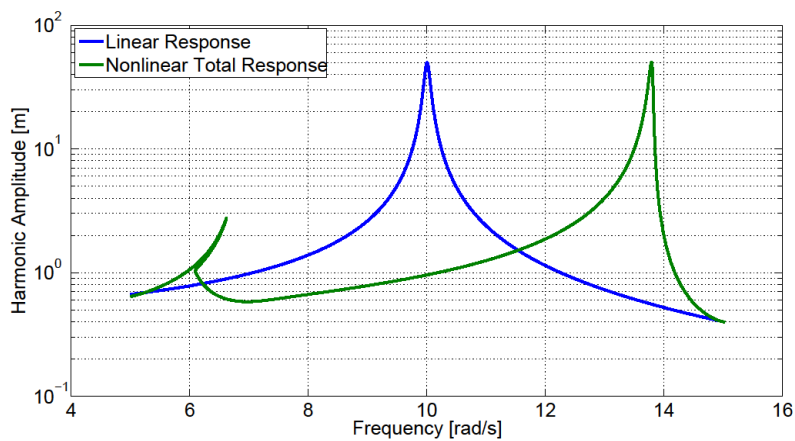
Figure 3.9 Total Nonlinear Response and Linear Response Curves for Case Study 1, $\varepsilon_{threshold} = 10^{-6}$
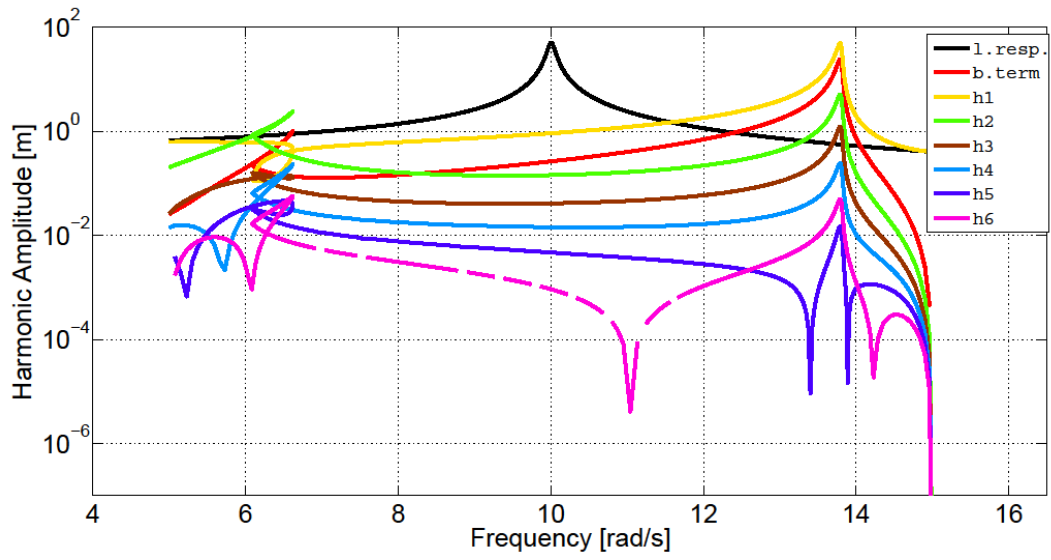
Figure 3.10 Amplitudes of harmonics for Case Study 1, $\varepsilon_{threshold} = 10^{-6}$
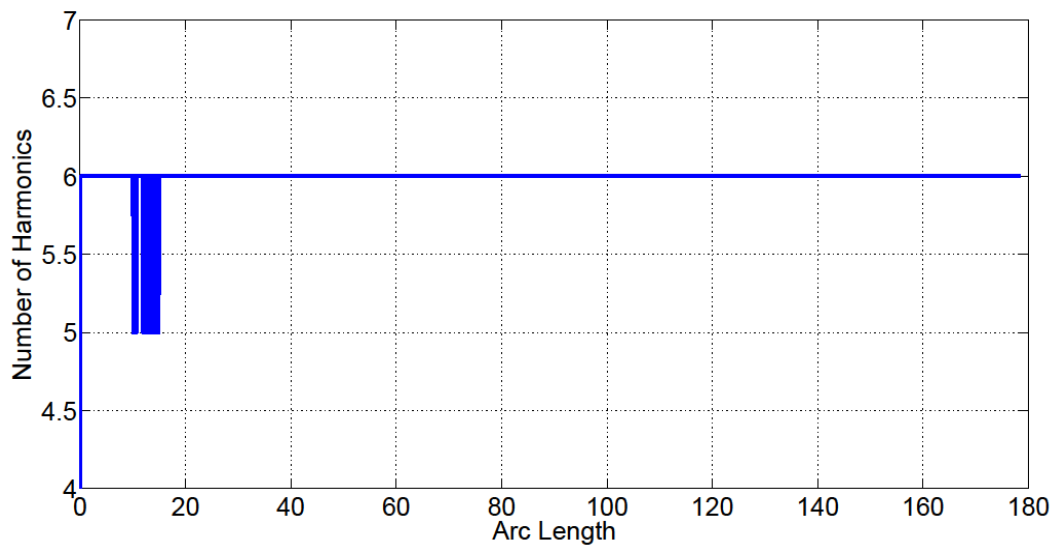
Figure 3.11 Number of Harmonics Used During Solution for Case Study 1,

$\varepsilon_{threshold} = 10^{-6}$

To enhance the study, the parameters of the system are modified as given in Table 3.2. The results obtained for this modified problem are given in Figure 3.12 to Figure 3.14.

It can be seen from Figure 3.12 and Figure 3.13 that increasing the gap causes the system to behave like a linear system until the frequency is closer to the resonance frequency where the vibration amplitude becomes as large as the gap. In the original example, the gap is considerably small and due to the existence of the peak around 6 rad/s this phenomenon is not observable. In addition to that, decreasing the severity of the nonlinearity caused the AHBM to use fewer harmonics throughout the curve. However, it can be seen in Figure 3.14 that around the resonance, the number of harmonics included in the solution increased considerably.

Table 3.2 Modified Parameters for Case Study 1

M (kg)	k (N/m)	h (N/m)	δ (m)	k_g (N/m)	$\varepsilon_{threshold}$
1	100	1	5	100	10^{-20}
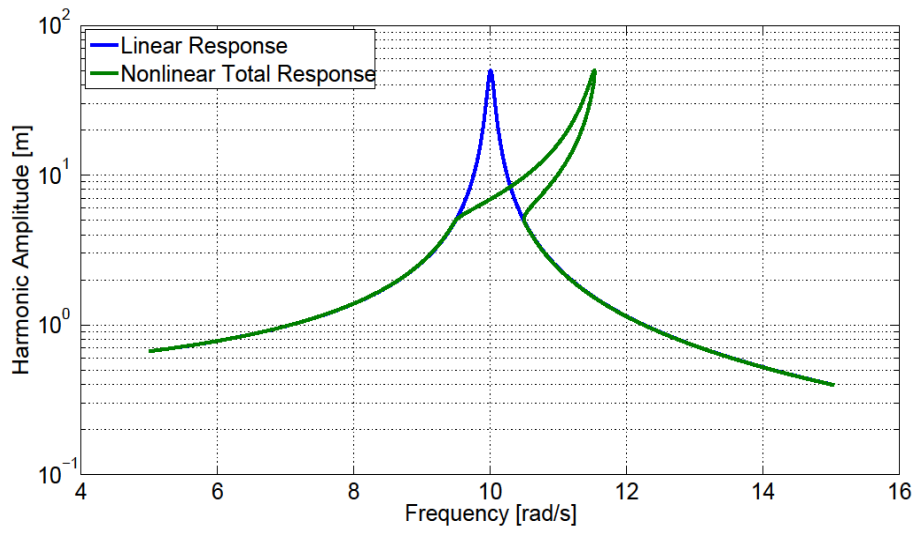
Figure 3.12 Linear and nonlinear total response curves for Case Study 1, modified, $\varepsilon_{threshold} = 10^{-20}$
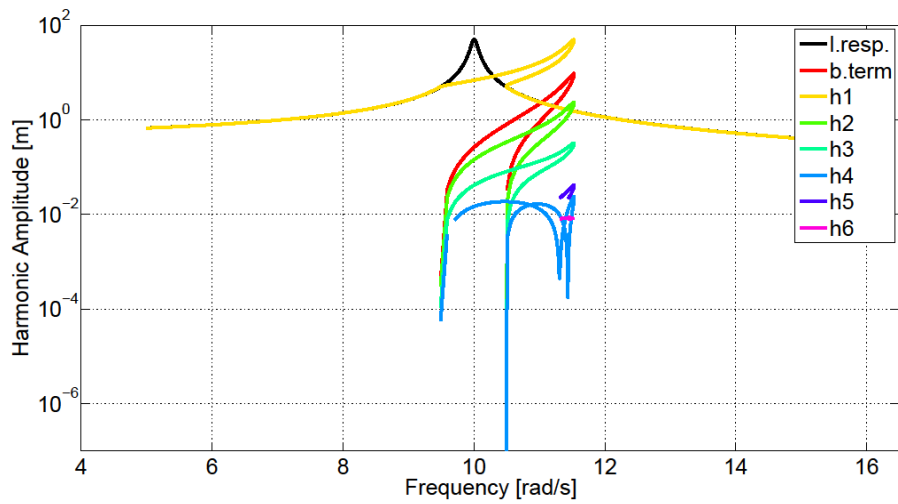
Figure 3.13 Amplitudes of harmonics for Case Study 1, modified, $\varepsilon_{threshold} = 10^{-20}$
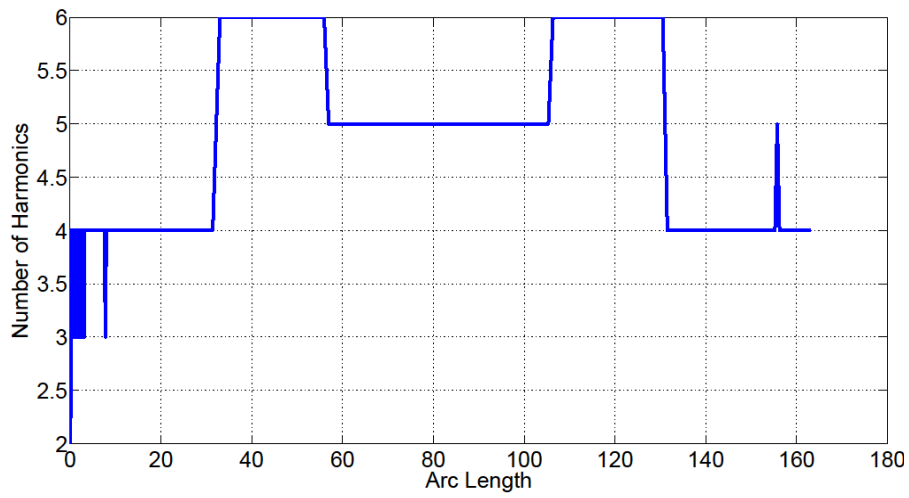
Figure 3.14 Number of Harmonics Used During Solution for Case Study 1, modified, $\varepsilon_{threshold} = 10^{-20}$

Similar to the previous example, increasing $\varepsilon_{threshold}$ to 10^{-1} causes less harmonics to be retained in the solution. The results obtained for this case are given in Figure 3.15 to Figure 3.17.
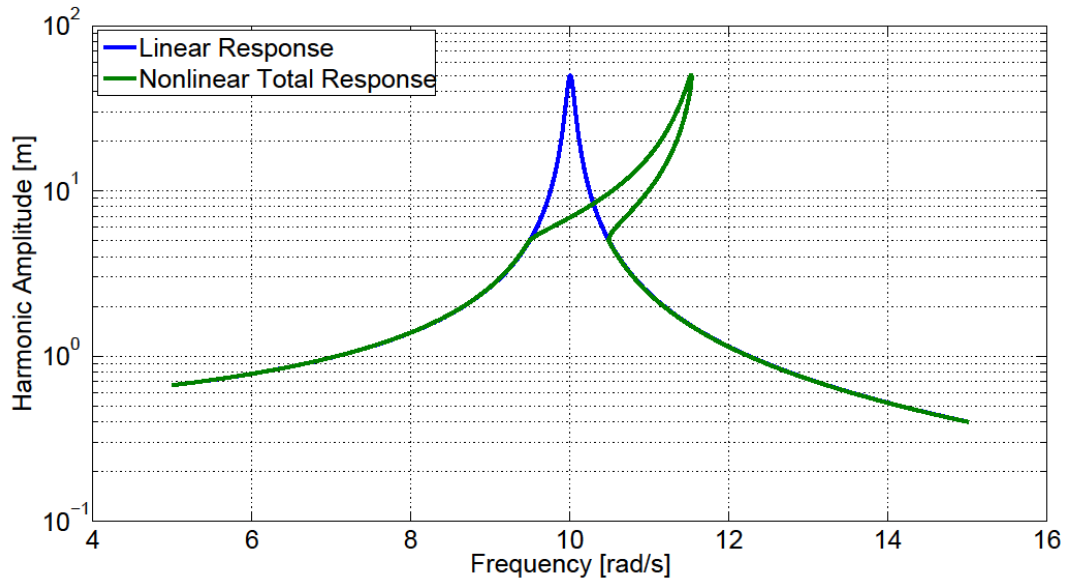
Figure 3.15 Linear and nonlinear total response curves for Case Study 1, modified, $\varepsilon_{threshold} = 10^{-1}$
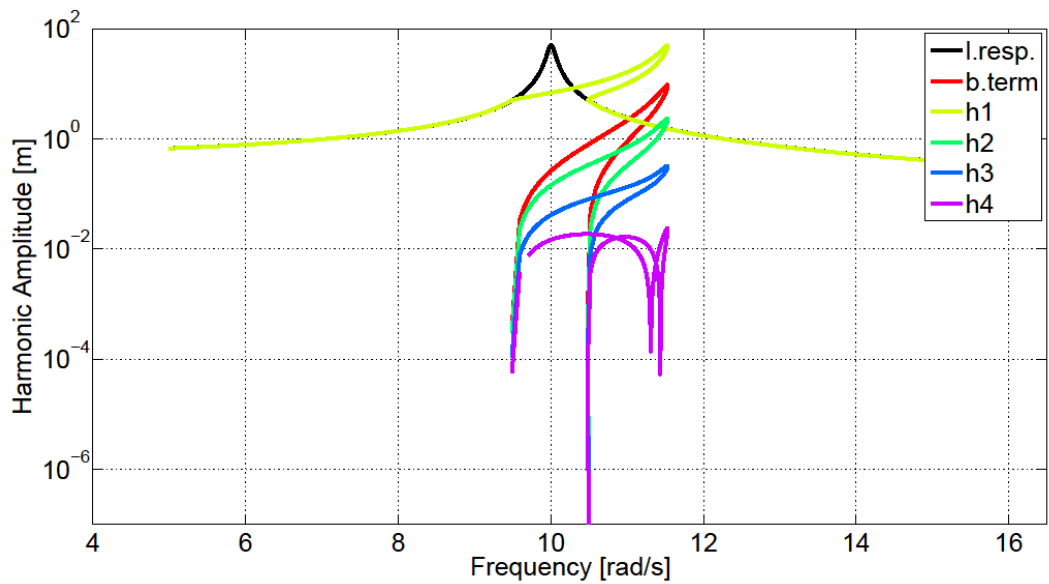
Figure 3.16 Amplitudes of harmonics for Case Study 1, modified, $\varepsilon_{threshold} = 10^{-1}$
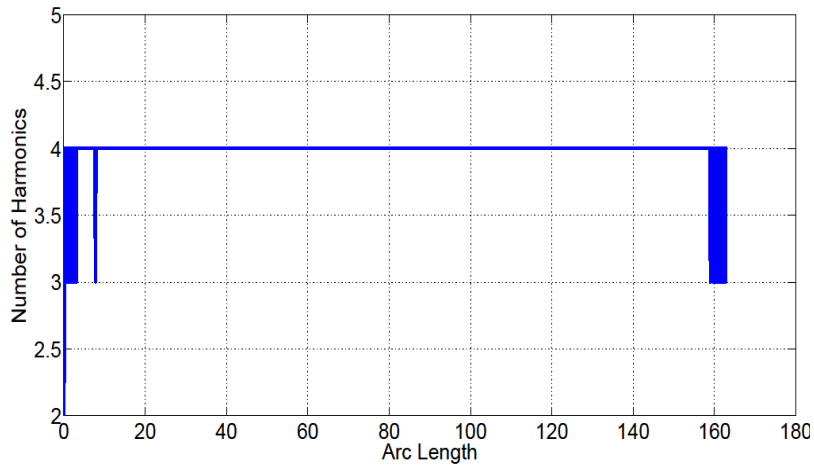
Figure 3.17 Number of Harmonics Used During Solution for Case Study 1, modified, $\varepsilon_{threshold} = 10^{-1}$

3.2.2 Case Study 2: Application of AHBM 1 on a MDOF System

In this section, application of AHBM 1 on a MDOF system with two piecewise linear stiffness elements and under the excitation of a multi-harmonic forcing is demonstrated. The studied system is illustrated in Figure 3.18. Parameters of the system and parameters of the piecewise linear stiffness elements are given in Table 3.3 and Table 3.4, respectively.
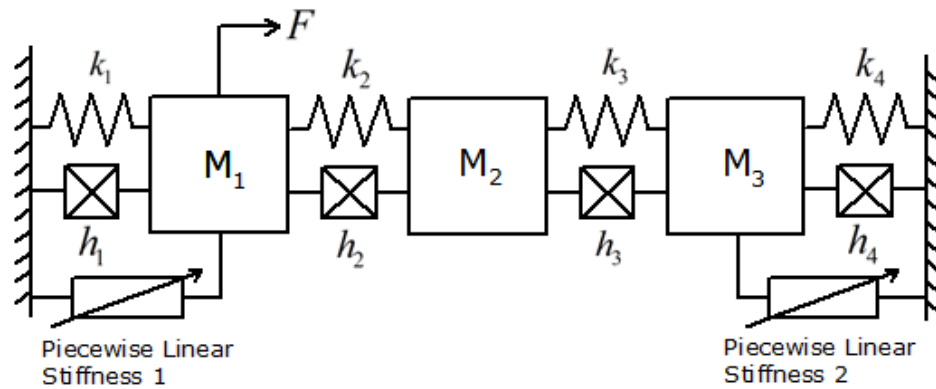
Figure 3.18 A MDOF System with piecewise linear stiffness nonlinearity

For the first analysis, $\varepsilon_{threshold}$ is taken as 10^{-20}. The results around the first natural frequency are given in Figure 3.19 - Figure 3.26. In Figure 3.25 and Figure 3.26 the change in the number of harmonics used is given. Figure 3.26 shows how many harmonics are used at each frequency. At the locations where multiple solutions exist, the graph shows more than one harmonic number located at the same frequency. In Figure 3.25, arc length is used instead of frequency. As mentioned before, arc length is basically the length of the response curve and since the response curve gets only longer as the solution goes on, only one harmonic number corresponds to each arc length value. Hence, the curve given in Figure 3.25 does not turn back. These two types of graphs are given in the following examples of this chapter.

In the results, it is observed from the results obtained that addition of two different piecewise linear stiffness elements to the first and third DOFs increased the overall stiffness in the system, eventually decreasing the overall vibration amplitude. Also the locations of the peaks are shifted due to this increase in stiffness. Due to the hardening behavior of the nonlinear elements shown in Figure 2.5, the response

77

graph bends to the right. It is also important to note that the 2θ component in the excitation causes the response to have even harmonics in addition to the odd ones.

In Figure 3.20, Figure 3.22 and Figure 3.24 only the first 10 harmonics are shown for brevity. However, it can be seen from Figure 3.25 and Figure 3.26 that the number of harmonics retained in the solution increases up to 35 at certain solution points.

Table 3.3 Physical Parameters of the MDOF System

M_1, M_3 (kg)	M_2 (kg)	k_1, k_2, k_3, k_4 (N/m)	h_1, h_2, h_3, h_4 (N/m)	F (N)
1	0.75	1000	10	$30\sin(\theta) + 30\sin(2\theta)$

Table 3.4 Parameters of the Nonlinear Elements

	δ (m)	k_1 (N/m)	k_2 (N/m)
Piecewise Linear Stiffness 1	0.1	1000	2000
Piecewise Linear Stiffness 2	0.05	500	1000
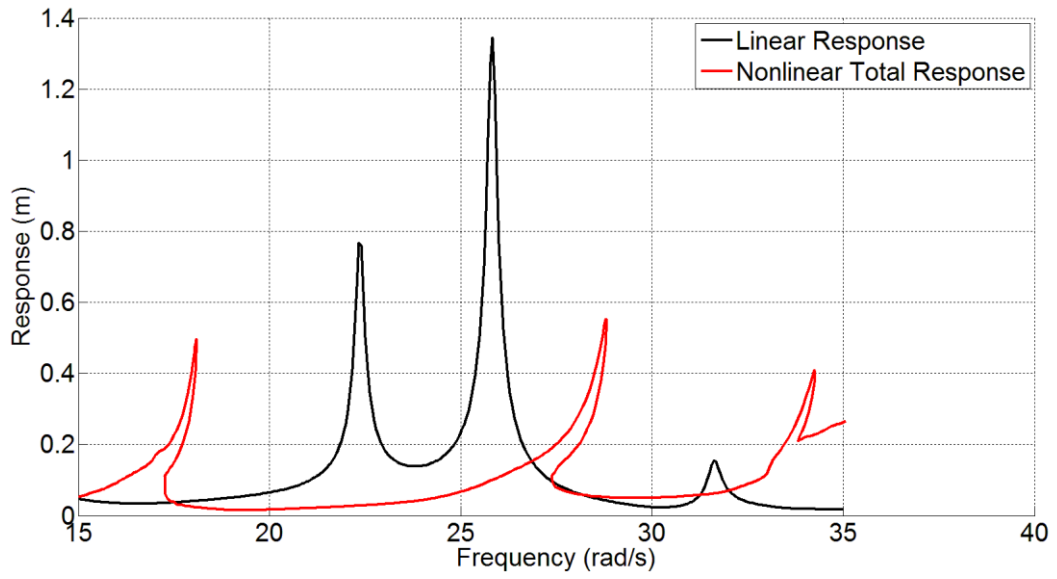
Figure 3.19 Total Response of the first DOF for Case Study 2, $\varepsilon_{threshold} = 10^{-20}$
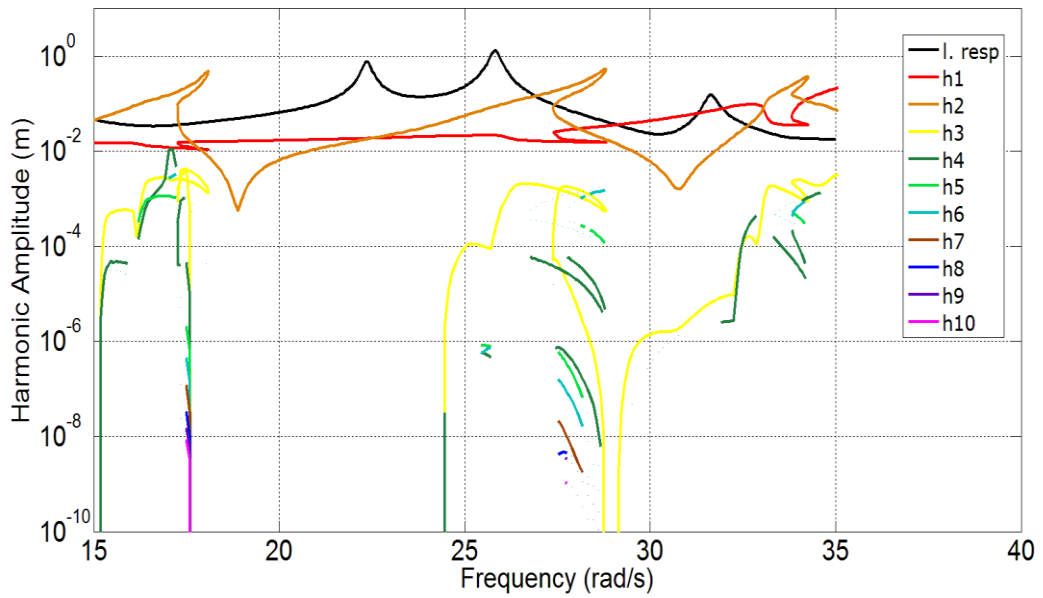
Figure 3.20 Harmonics of the first DOF for Case Study 2, $\varepsilon_{threshold} = 10^{-20}$
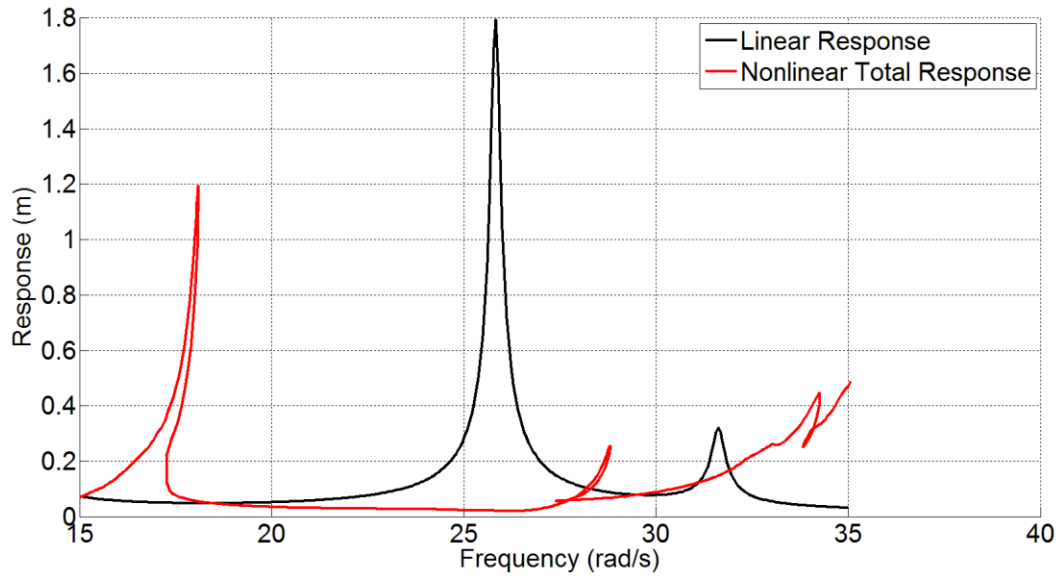
Figure 3.21 Total Response of the second DOF for Case Study 2, $\varepsilon_{threshold} = 10^{-20}$
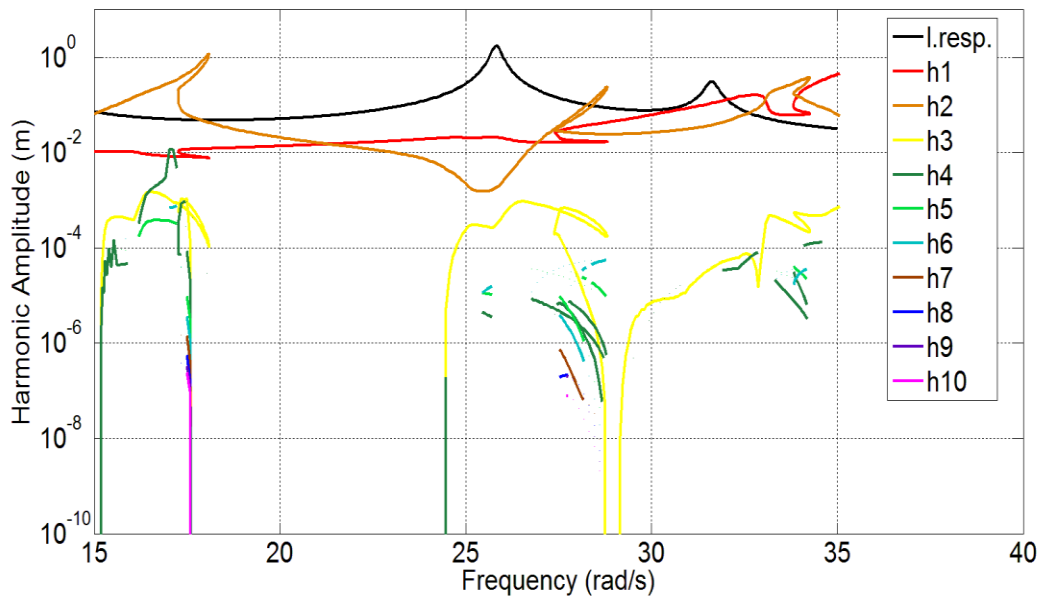
Figure 3.22 Harmonics of the second DOF for Case Study 2, $\varepsilon_{threshold} = 10^{-20}$
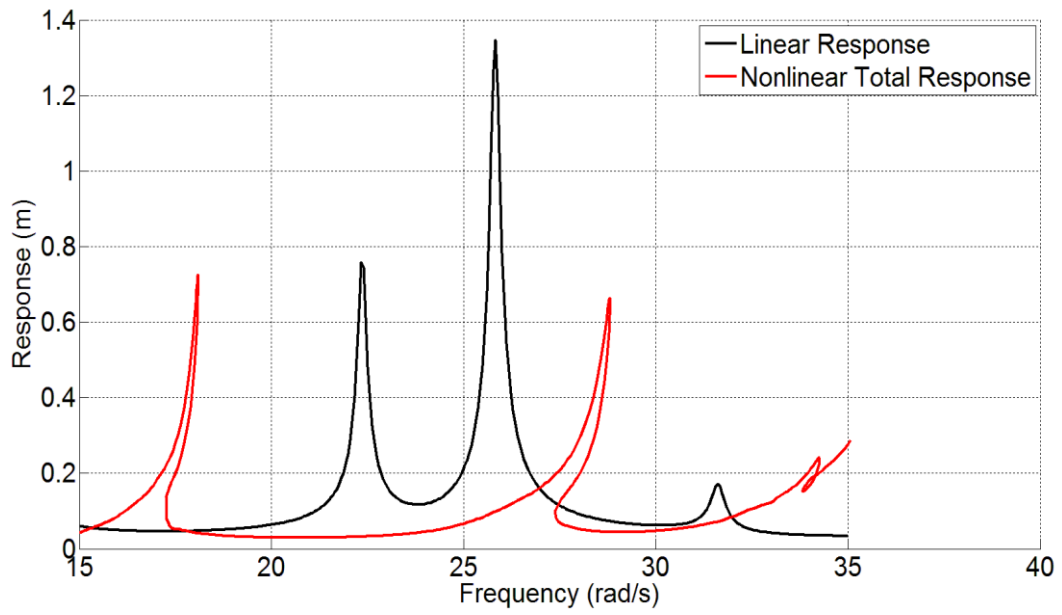
Figure 3.23 Total Response of the third DOF for Case Study 2, $\varepsilon_{threshold} = 10^{-20}$
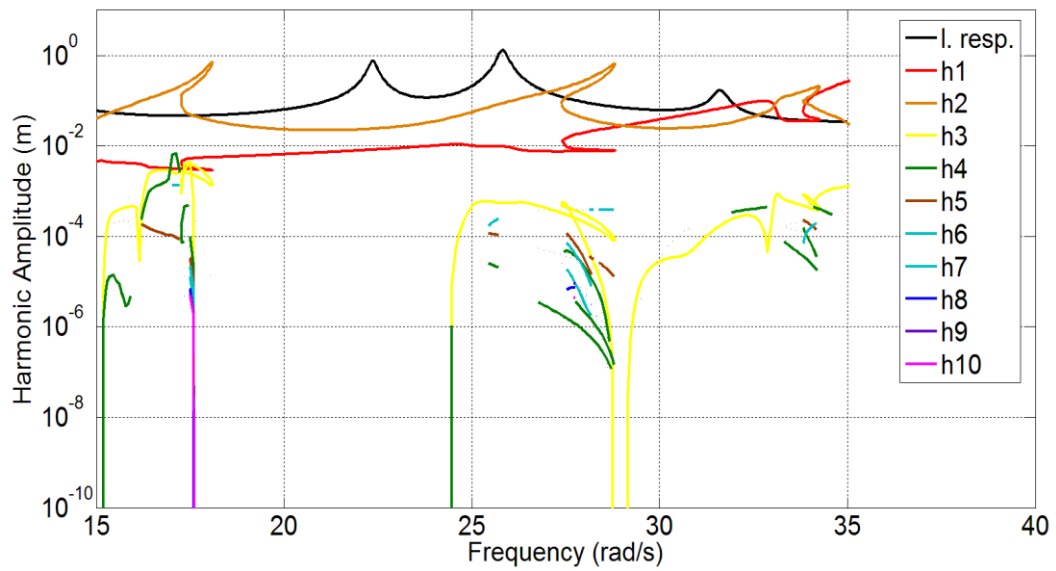
Figure 3.24 Harmonics of the third DOF for Case Study 2, $\varepsilon_{threshold} = 10^{-20}$

81
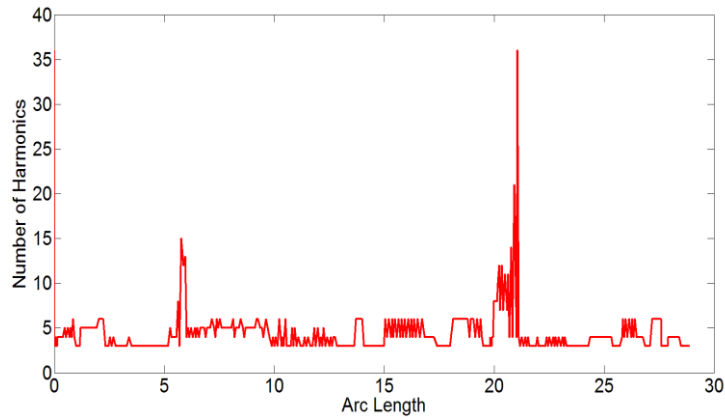
Figure 3.25 Number of harmonics used for Case Study 2, $\varepsilon_{threshold} = 10^{-20}$
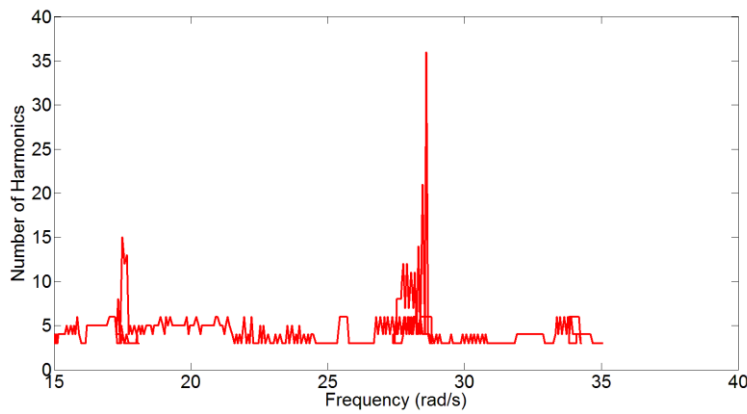
Figure 3.26 Number of harmonics used at each frequency for Case Study 2, $\varepsilon_{threshold} = 10^{-20}$

For the next analysis, the threshold value is increased to 10^{-2} so that the higher harmonics with very small effect on the total response can be eliminated. The results are given in Figure 3.27 to Figure 3.34. It can be seen from the results that a 3-harmonic Fourier series representation is sufficient for obtaining a good approximation to the total response.
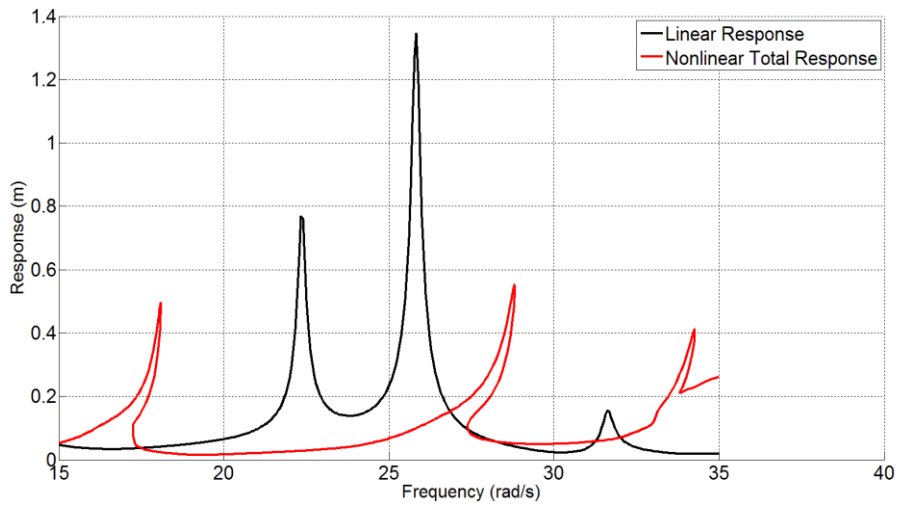
Figure 3.27 Total Response of the first DOF for Case Study 2, $\varepsilon_{threshold} = 10^{-2}$
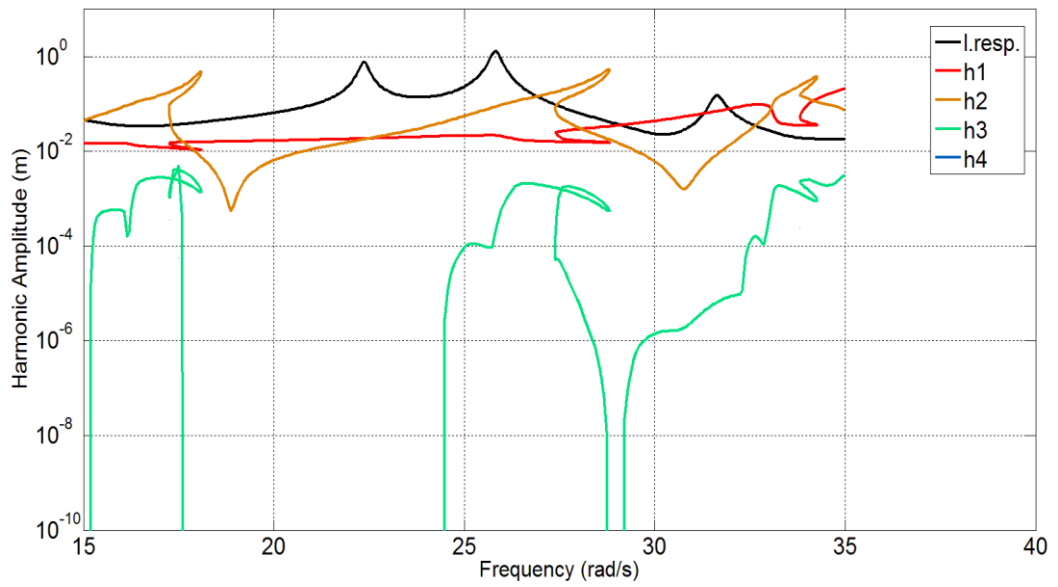
Figure 3.28 Harmonics of the first DOF for Case Study 2, $\varepsilon_{threshold} = 10^{-2}$
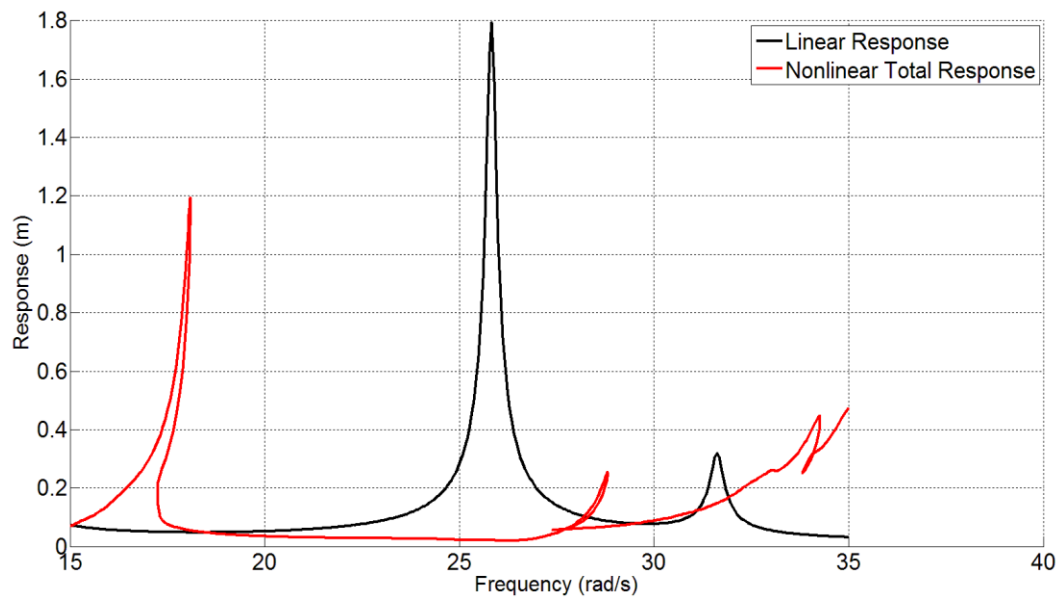
Figure 3.29 Total Response of the second DOF for Case Study 2, $\varepsilon_{threshold} = 10^{-2}$
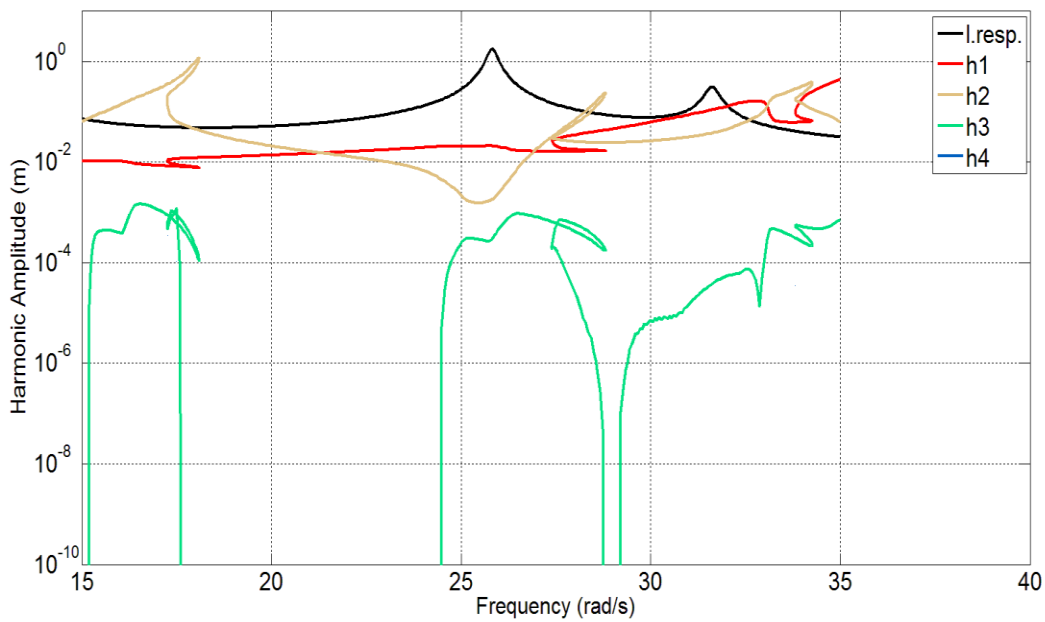
Figure 3.30 Harmonics of the second DOF for Case Study 2, $\varepsilon_{threshold} = 10^{-2}$
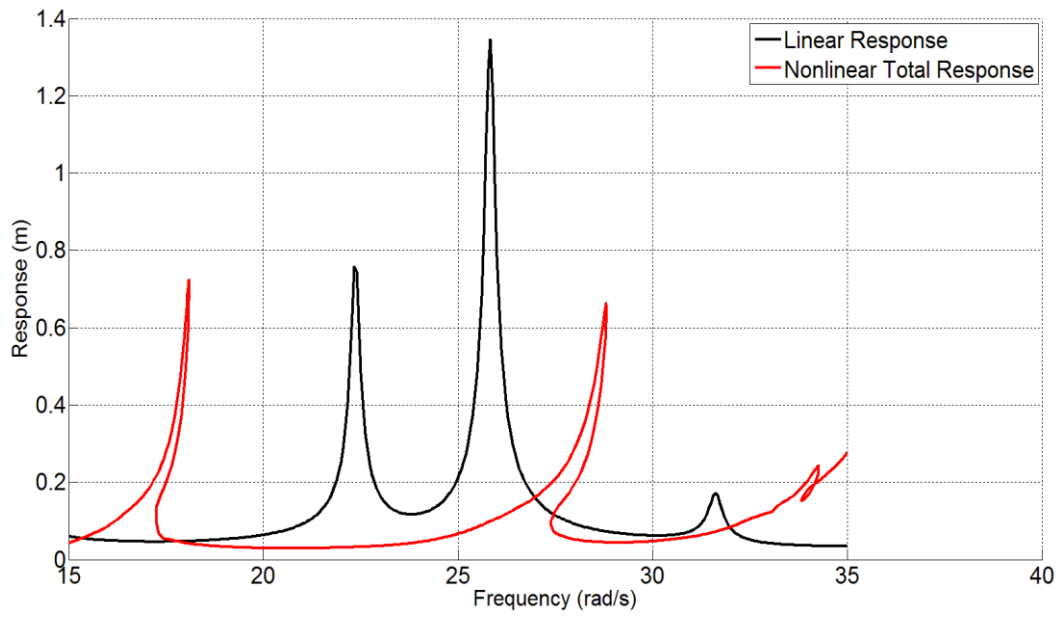
Figure 3.31 Total Response of the third DOF for Case Study 2, $\varepsilon_{threshold} = 10^{-2}$
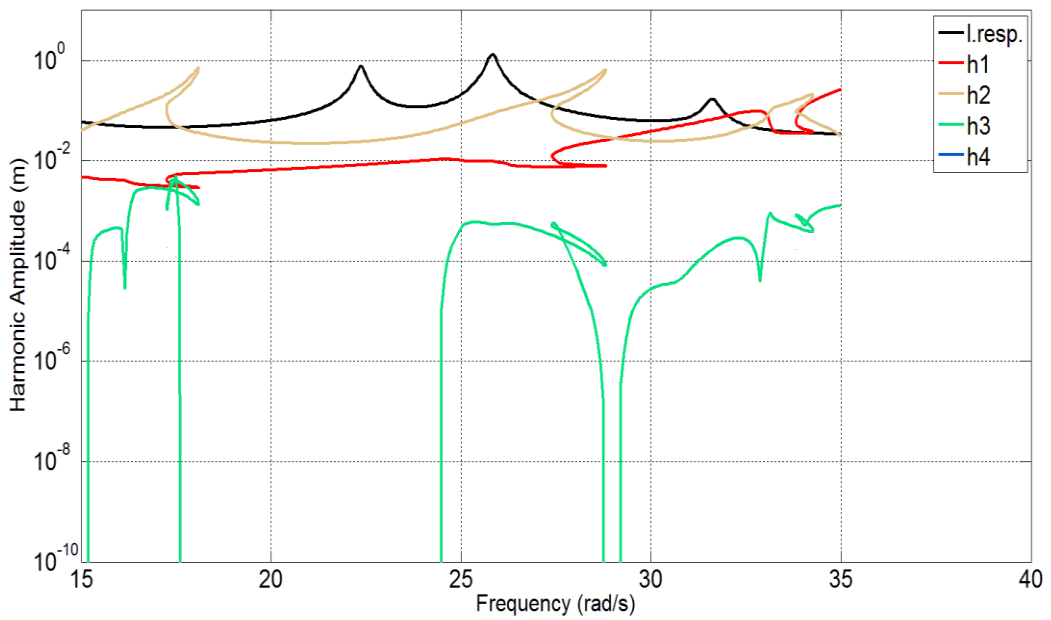
Figure 3.32 Harmonics of the third DOF for Case Study 2, $\varepsilon_{threshold} = 10^{-2}$
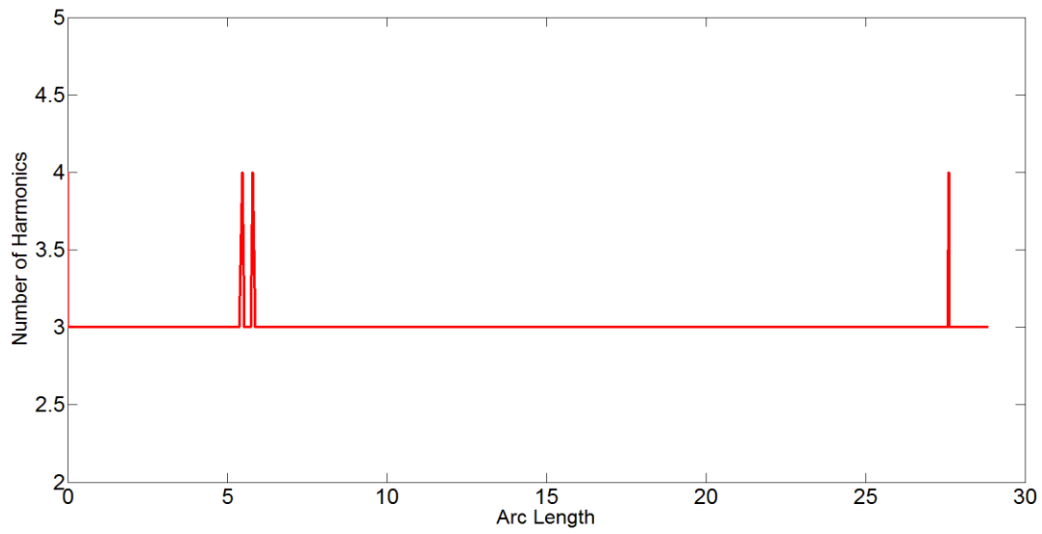
Figure 3.33 Number of harmonics used for Case Study 2, $\varepsilon_{threshold} = 10^{-2}$
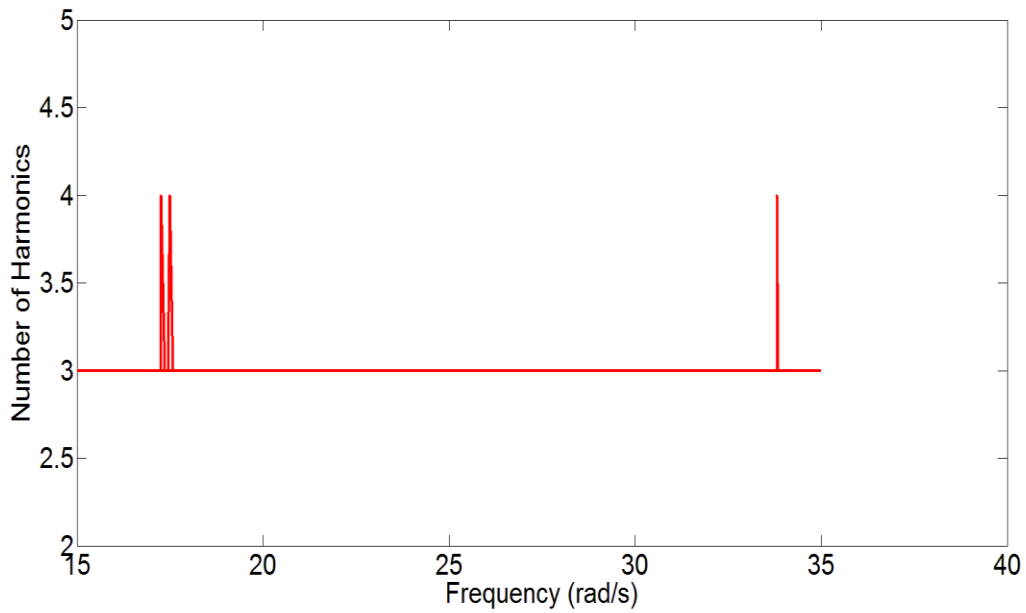
Figure 3.34 Number of harmonics used at each frequency for Case Study 2, $\varepsilon_{threshold} = 10^{-2}$

86

3.3 AHBM 2: Grolet and Thouverez's Method

In 2012, Grolet and Thouverez proposed a new AHBM [5]. Unlike the method described in the previous section; this method is local, that is, the number of harmonics is arranged seperately for each DOF and in addition, the method is not incremental. The number of harmonics for each DOF is not increased one by one in order. Instead, the spectral energies for a predetermined number of harmonics are determined. Then, the ones with relatively high energy are retained in the solution.

3.3.1 Preliminary Definitions

In this method, the harmonic selection process begins by assigning the maximum number of harmonics, N_h^m, that should be included in the response. In case, N_h^m harmonics are used for all DOFs in the system, the nonlinear equation set contains $n\left(2N_h^m+1\right)$ equations and unknowns. Using the notation in Chapter 2, this equation set can be denoted as:

$$R\left(\{x\},\omega\right)=R\left(\{q\}\right)=\{0\}. \tag{3.10}$$

During the application of Grolet and Thouverez's method, each equation in this equation set and therefore each unknown in the unknown vector $\{q\}$ are numbered with the help of an index vector, $\{I\}_m=\begin{bmatrix}1 & 2 & \ldots & M_m\end{bmatrix}^T$ where $M_m=n\left(2N_h^m+1\right)$. For the case where the algorithm decides to reduce the equation system and neglect some of the unknowns, another index vector $\{I\}_r$ is defined. $\{I\}_r$ is a subset of $\{I\}_m$ and it includes only the equation numbers of the retained unknowns, i.e. the harmonic coefficients. It helps to keep track of which equations and unknowns are present in the solution scheme at the current solution step. The reduced equation system can be denoted as:

$$R_r\left(\{x\}_r,\omega\right)=\{0\}, \tag{3.11}$$

where the subscript r stands for reduced. In order to apply the threshold criterion and arrange the harmonic numbers for each DOF separately, the algorithm needs to isolate the Fourier coefficients of different DOFs. For this reason, following vectors are defined for $1 \leq d \leq n$:

$$\{u\}^d = \begin{bmatrix} q_0^d & q_{s1}^d & q_{c1}^d & \cdots & q_{sN_h^m}^d & q_{cN_h^m}^d \end{bmatrix}^T \tag{3.12}$$

$$\{u\}_r^d = \begin{bmatrix} q_0^d & \cdots & q_{sN_r^m}^d & q_{cN_r^m}^d \end{bmatrix}^T, \tag{3.13}$$

where $\{u\}^d$ is the Fourier coefficient vector of DOF d, including all harmonics. $\{u\}_r^d$ is the reduced Fourier coefficient vector of DOF d. $q_{sN_r^m}^d$ and $q_{cN_r^m}^d$ are the sine and cosine components of the last retained harmonic.

In addition to the global index vectors described above, their local counterparts are defined for each DOF. For $1 \leq d \leq n$, the vector $\{I\}_r^d$ is defined. It contains the index numbers, which are taken from $\{I\}_r$ and are related to DOF d only. From here, it can be concluded that one can easily obtain $\{u\}_r^d$ by taking the terms with index numbers stored in the vector $\{I\}_r^d$ from the global unknown matrix $\{q\}$. With a similar approach, the index vector $\{J\}_r^d$ is defined for $1 \leq d \leq n$ which operates on vector $\{u\}^d$. $\{u\}_r^d$ is obtained by extracting the terms with the index numbers stored in $\{J\}_r^d$ from $\{u\}^d$. Finally, the row matrix $[H]_r^d$ is defined in order to store the retained harmonic numbers for each DOF.

In order to make the concepts described above more clear, a simple example will be demonstrated here. Assuming that a two DOF nonlinear system is being analyzed, no condensation method is used, N_h^m is equal to 4, indicating that if all harmonics are retained, there exists a total of 18 unknowns, 9 for each DOF including the bias terms. Assuming at the ith solution point, the $[H]_r^d$ row matrices, which contain the harmonics to be retained for each DOF, turned out to be

$$[H]_r^1 = \begin{bmatrix} 0 & 1 & 3 \end{bmatrix} \quad , \quad [H]_r^2 = \begin{bmatrix} 0 & 2 & 4 \end{bmatrix}, \tag{3.14}$$

where 0 indicates the bias term. In this case, $\{J\}_r^d$ index vectors, which contain the index numbers of Fourier coefficients to be taken from $\{u\}^d$ and stored in $\{u\}_r^d$ vectors, would be:

$$\{J\}_r^1 = \begin{bmatrix} 1 & 2 & 3 & 6 & 7 \end{bmatrix}^T \quad , \quad \{J\}_r^2 = \begin{bmatrix} 1 & 4 & 5 & 8 & 9 \end{bmatrix}^T. \tag{3.15}$$

The first DOF has 2 harmonics and a bias term. From the local coefficient vector $\{u\}^1$, the terms which belong to the bias term, the first harmonic and the third harmonic are located on the lines with indices 1; 2 and 3; 6 and 7, respectively. Similarly, one can find that in the vector $\{u\}^2$, terms that belong to the bias term, second harmonic and the fourth harmonic are located on the lines with indices 1; 4 and 5; 8 and 9, respectively.

Returning back to the global equation system, assuming that the equation system follows the order given in Equation (2.16) and equations that belong to DOF 1 are always written before DOF 2, one can find that the lines that belong to the bias term, first harmonic and third harmonic of DOF 1 are located on the lines with indices 1; 3

89

and 5; 11 and 13, respectively. By using a similar approach, one can find that the indices of DOF 2 are to be 2, 8, 10, 16 and 18. Therefore, the $\{I\}_r^d$ vectors become

$$\{I\}_r^1 = \begin{bmatrix} 1 & 3 & 5 & 11 & 13 \end{bmatrix}^T \quad , \quad \{I\}_r^2 = \begin{bmatrix} 2 & 8 & 10 & 16 & 18 \end{bmatrix}^T. \tag{3.16}$$

Finally the global index vector, which is the combination of the vectors given in Equation (3.16) becomes

$$\{I_r\} = \begin{bmatrix} 1 & 2 & 3 & 5 & 8 & 10 & 11 & 13 & 16 & 18 \end{bmatrix}^T. \tag{3.17}$$

3.3.2 Selection of Harmonics

The harmonic selection process of the method is based on the tangent predictor presented in Section 2.4.1.

Assume that the response has been computed at the solution point i. Due to the nature of AHBM, some harmonics are neglected and the resulting Fourier coefficient vector $\{q\}_r^i$ has less than M_m elements. In order to apply the selection process, it is assumed that the neglected harmonics at the current solution step are equal to zero. An $M_m \times 1$ vector $\{q\}^i$ is formed by adding zeros into $\{q\}_r^i$. From this newly constructed coefficient vector, by using the tangent predictor, an initial guess, $\{q\}_p$, having N_h^m harmonics is computed for the next solution point. After that, as described in the previous section, $\{q\}_p$ is divided into n sub-vectors with $2N_h^m + 1$ elements, each of which belonging to a different DOF. The harmonic selection is performed through these vectors.

Consider the initial guess sub-vector of DOF d, $\{u\}_p^d$. The fraction of spectral energy for the kth harmonic of DOF d is defined as:

$$\varepsilon_k^d = \frac{\left(u_{p_{sk}}^d\right)^2 + \left(u_{p_{ck}}^d\right)^2}{\left\|\{u\}_p^d\right\|} .$$

(3.18)

where $\|.\|$ denotes the Euclidean norm and $u_{p_{sk}}^d$ and $u_{p_{ck}}^d$ are the sine and cosine components of the kth harmonic in $\{u\}_p^d$. With the help of the index vector $\{J\}_r^d$ and the harmonic vector $[H]_r^d$, the total spectral energy ratio of the harmonics that were retained at the ith solution point can be calculated as:

$$E_r^d = \sum_{k \in H_r^d} \varepsilon_k^d .$$

(3.19)

Equation (3.18) and Equation (3.19) imply that if $[H]_r^d$ includes all the possible harmonics, E_r^d becomes 1. This leads to the definition of the fraction of residual energy:

$$\rho_d = 1 - E_r^d .$$

(3.20)

During the harmonic selection procedure, ρ_d is compared to two threshold values ρ_f and ρ_b which satisfy the condition $0 \le \rho_b \le \rho_f \le 1$. If ρ_d turns out to be greater than ρ_f, it means that the amount of energy contained in the neglected harmonics becomes very large. Therefore the neglected harmonics with maximum spectral energy values are included one by one into $[H]_r^d$ until ρ_d falls below ρ_f. This

process is named as the forward procedure. If ρ_d turns out to be less than ρ_b this means that the error committed is much smaller than the allowable error. Therefore the retained harmonics with the minimum spectral energy values are excluded one by one from H_r^d until ρ_d becomes larger than ρ_b. This process is named as the backward procedure. If ρ_d lies between two threshold values, the solution scheme continues with the current harmonics. This process is repeated for every DOF. In the end, from the newly formed $\left[H\right]_r^d$ matrices, the index vectors are updated for the next step and the numerical solution of the response for the next point begins. The whole procedure is illustrated in Figure 3.35.

Selection of values for ρ_b and ρ_f is the major factor that effects the accuracy of the solution. Since the method assumes that the neglected harmonics are zero, it is important to assign sufficiently small values for ρ_b and ρ_f. Otherwise the method may end up neglecting harmonics with significant importance, and thus obtaining a rough estimation for the response [5].

It should also be noted that in the calculation of spectral energy fractions and the steps that followed, the bias term was not included in the formulation. Most of the time, the bias term turns out to be greater than higher harmonics and this can introduce rounding errors and neglecting of important harmonics. For convenience, it is useful to keep the bias term always included in $\left[H\right]_r^d$ and not taking it into account for spectral energy calculations [5].
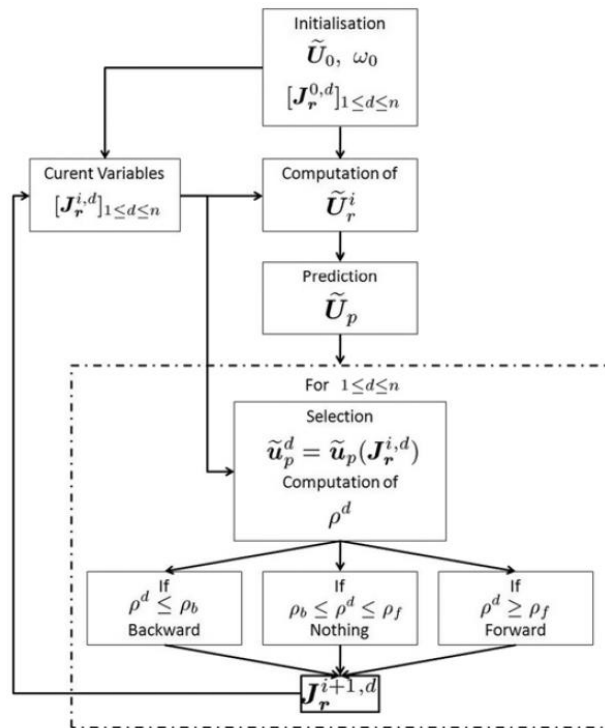
Figure 3.35 The Algorithm for Grolet and Thouverez's Method [5]

3.3.3 Case Study 3: Application of AHBM 2 on a SDOF System

The same system used in Case Study 1 and given in Figure 3.2 is used in Case Study 3 with 3 different parameter sets. The first parameter set is given in Table 3.5.

For this parameter set, the response of the system around the resonance can be found in Figure 3.36, Figure 3.37 and Figure 3.38. From the results it can be seen that, since the control parameters are chosen very small, the method calculated all 10 harmonics throughout the frequency spectrum.

Table 3.5 Parameters Set 1 for Case Study 3

M (kg)	k (N/m)	h (N/m)	δ (m)	k_g (N/m)	ρ_b	ρ_f	N_h^m
1	100	1	0.4	400	10^{-14}	10^{-12}	10
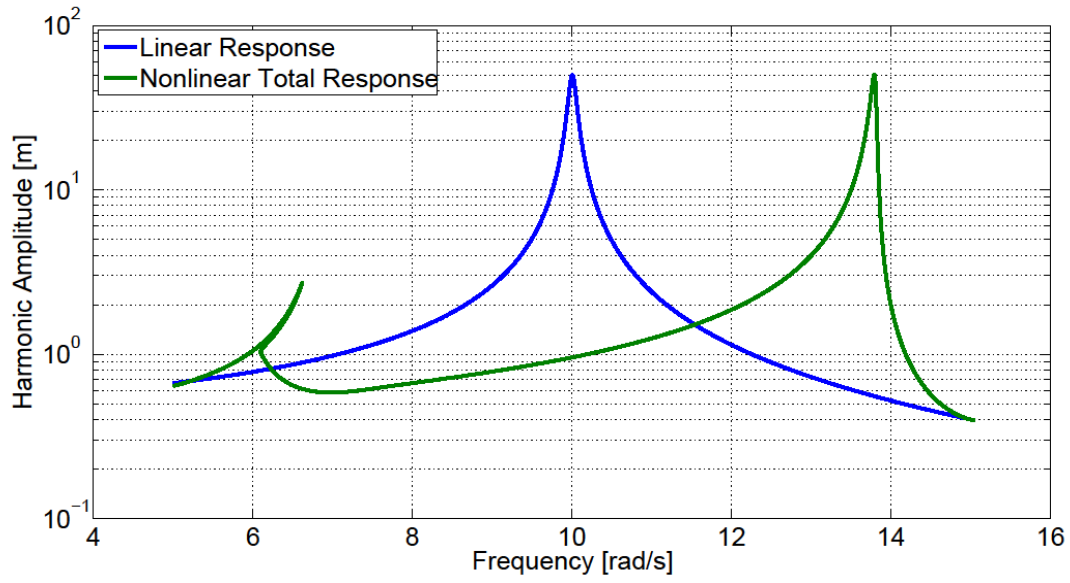
Figure 3.36 Linear and nonlinear total response curves for Case Study 3, Parameter Set 1
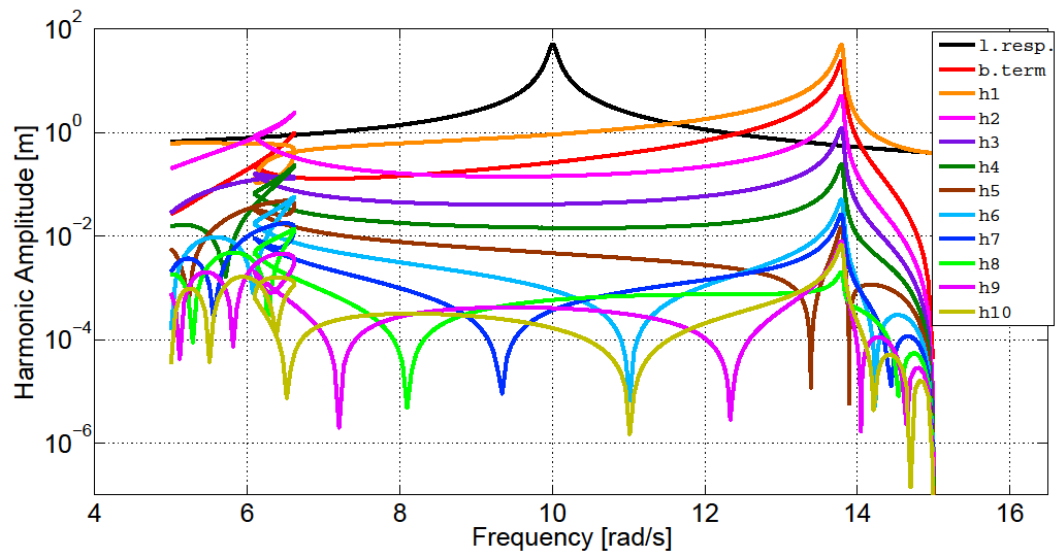
Figure 3.37 Amplitudes of Harmonics for Case Study 3, Parameter Set 1
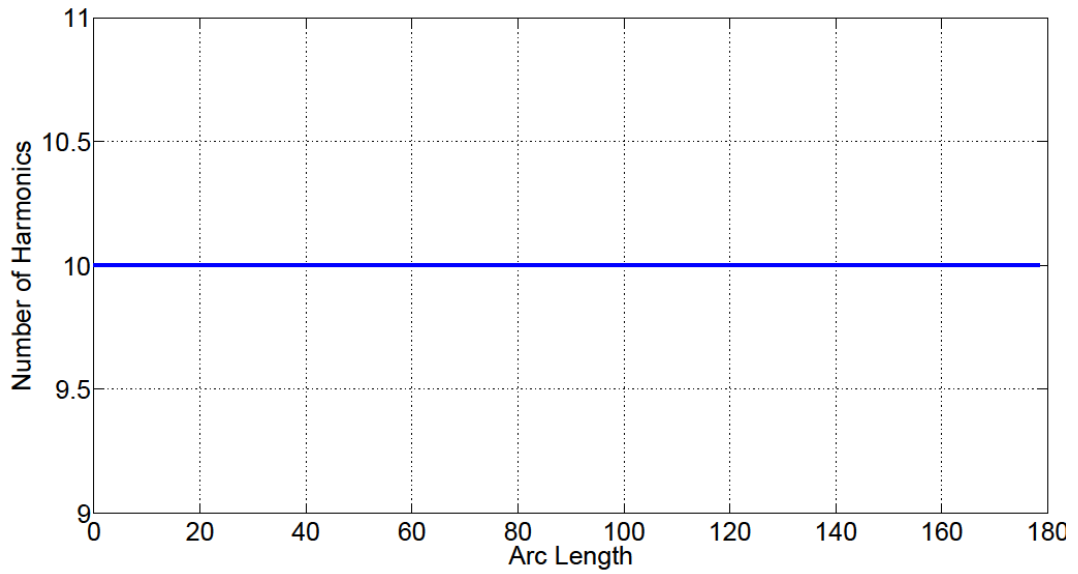
Figure 3.38 Number of Harmonics Used During Solution for Case Study 3,
Parameter Set 1

For the next analysis, the parameters are changed as given in Table 3.6. The results
obtained for this case are given in Figure 3.39, Figure 3.40 and Figure 3.41. The
results show that the number of retained harmonics is decreased for certain parts of
the frequency spectrum.

Table 3.6 Parameters for Case Study 3, Parameter Set 2

M (kg)	k (N/m)	h (N/m)	δ (m)	k_g (N/m)	ρ_b	ρ_f	N_h^m
1	100	1	0.4	400	10^{-12}	10^{-8}	10
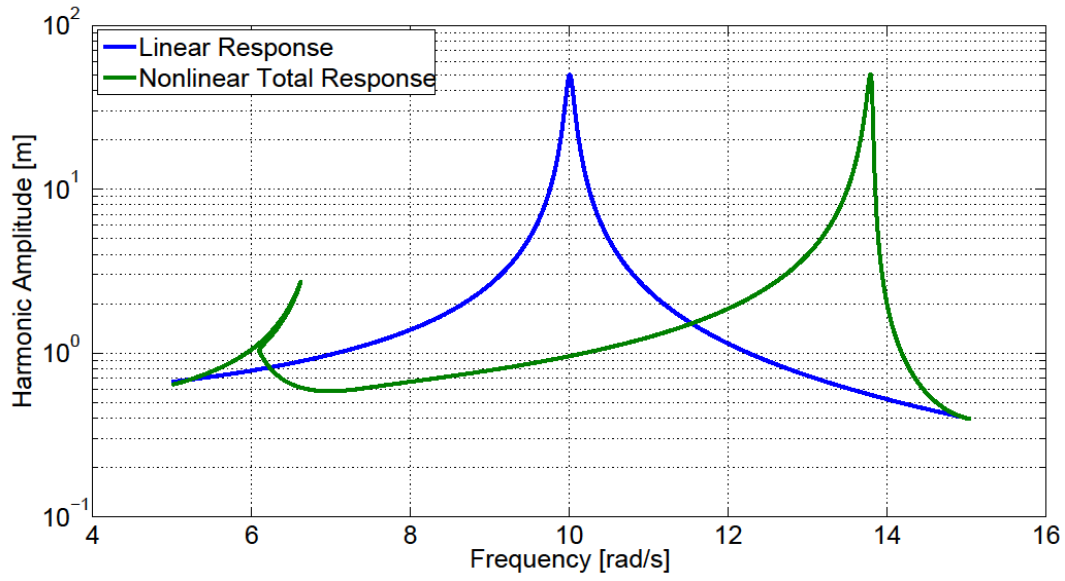
Figure 3.39 Linear and nonlinear total response curves for Case Study 3, Parameter Set 2
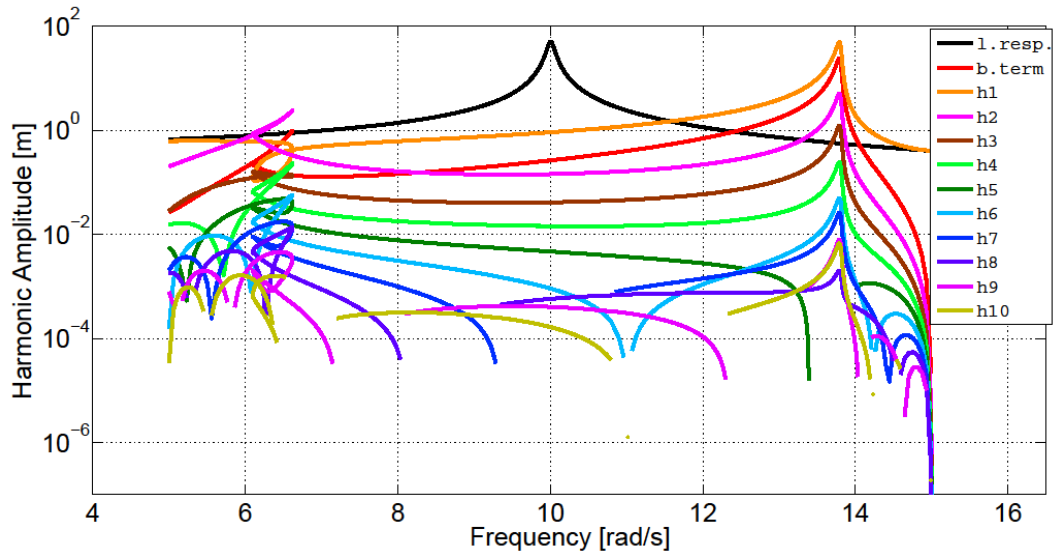
Figure 3.40 Amplitudes of Harmonics for Case Study 3, Parameter Set 2
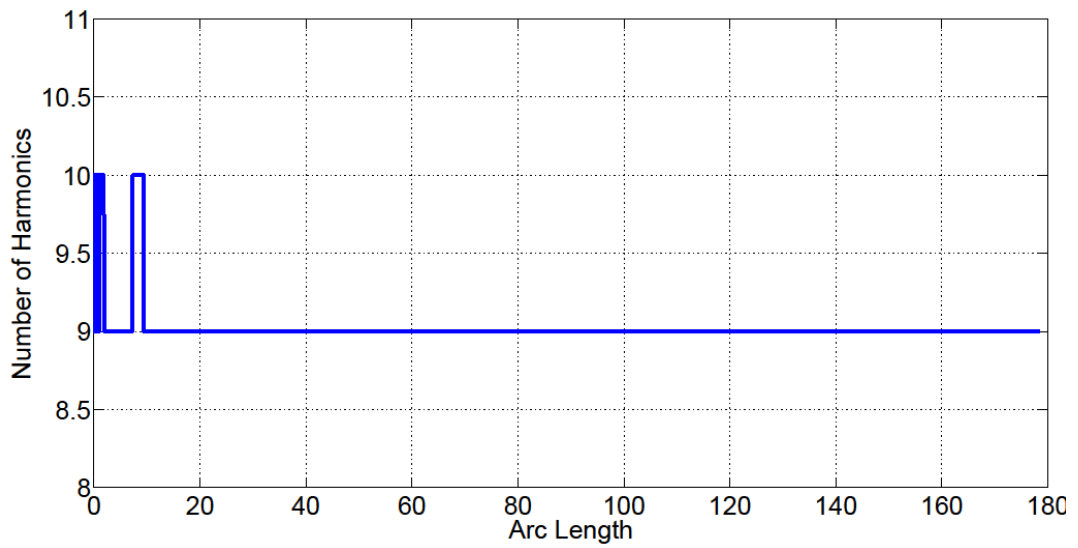
Figure 3.41 Number of Harmonics Used During Solution for Case Study 3, Parameter Set 2

For the final part of the study, the parameter set is changed as given in Table 3.7. The results obtained for this case are given in Figure 3.42, Figure 3.43 and Figure 3.44. It can be seen from these results that the number of retained harmonics decreased without a noticeable change in the total response.

Table 3.7 Parameter Set 3 for Case Study 3

M (kg)	k (N/m)	h (N/m)	δ (m)	k_g (N/m)	ρ_b	ρ_f	N_h^m
1	100	1	0.4	400	10^{-8}	10^{-4}	10
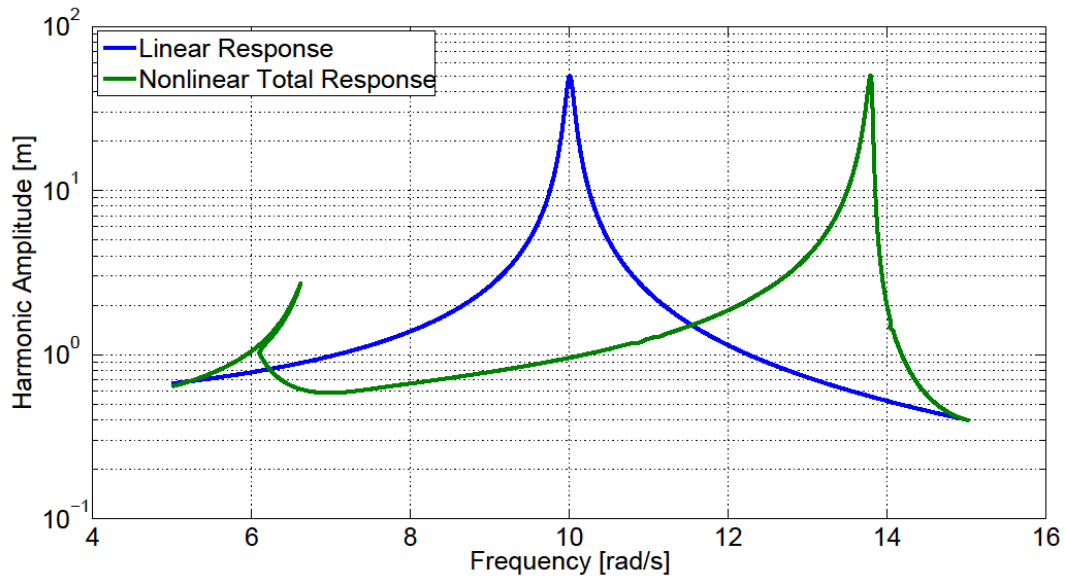
Figure 3.42 Linear and nonlinear total response curves for Case Study 3, Parameter Set 3

Figure 3.43 Amplitudes of Harmonics for Case Study 3, Parameter Set 3

Figure 3.44 Number of Harmonics Used During Solution for Case Study 3, Parameter Set 3

3.3.4 Case Study 4: Application of AHBM 2 on a MDOF System

The same system described in Section 3.2.2 is used for this study. For the first case, control parameters are taken as given in Table 3.8. Under the effect of these parameters, the response graphs are given in Figure 3.45 to Figure 3.52. The results show that, the control parameters do not let the algorithm to drop the number of used harmonics under 10 around the resonances.

Table 3.8 Control Parameters for Case Study 4, Parameter Set 1

ρ_b	ρ_f	N_h^m
10^{-14}	10^{-12}	10
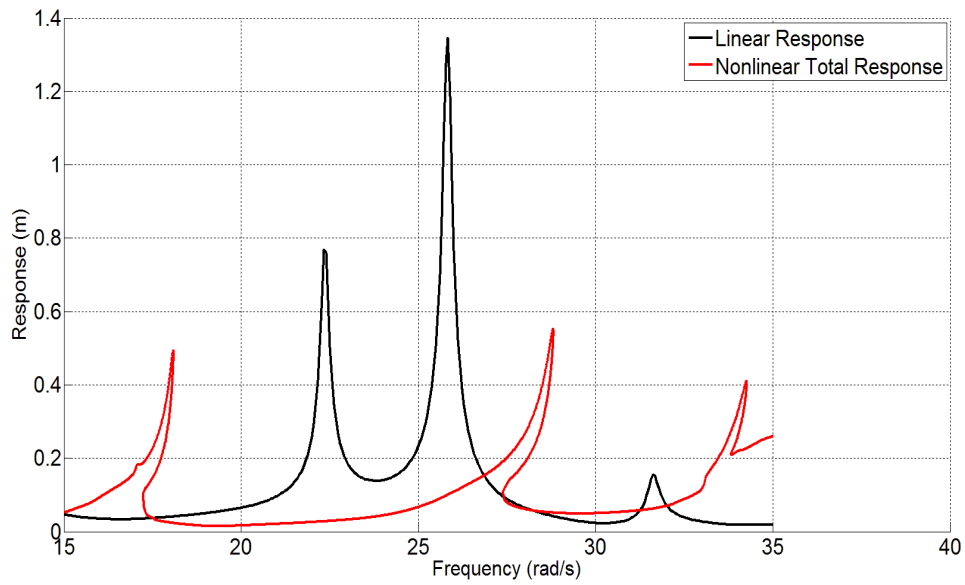
Figure 3.45 Total Response of the first DOF for Case Study 4, Parameter Set 1
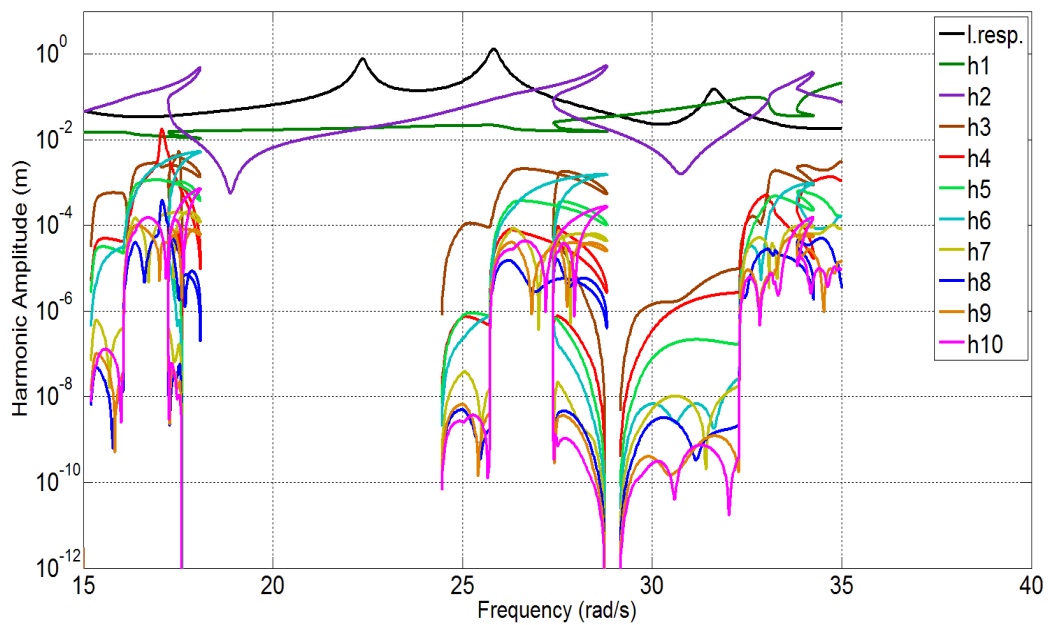
Figure 3.46 Harmonics of the first DOF for Case Study 4, Parameter Set 1

100
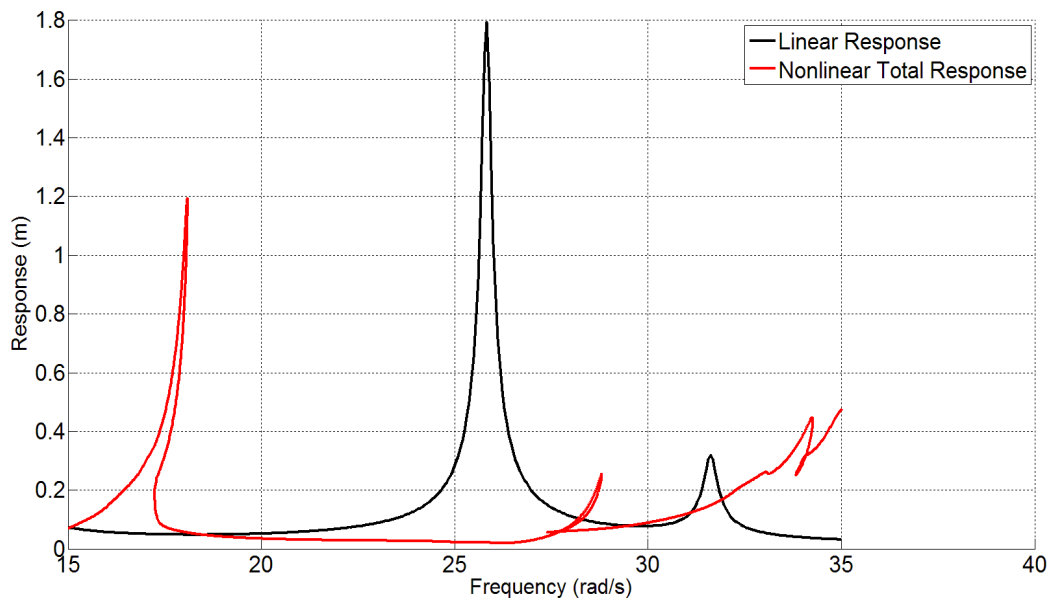
Figure 3.47 Total Response of the second DOF for Case Study 4, Parameter Set 1
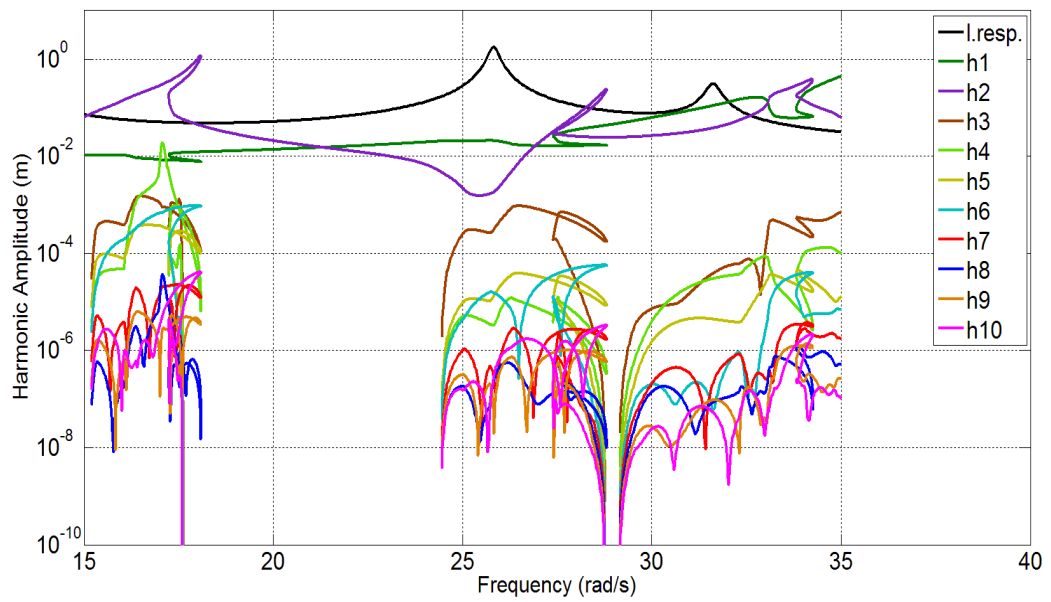
Figure 3.48 Harmonics of the second DOF for Case Study 4, Parameter Set 1
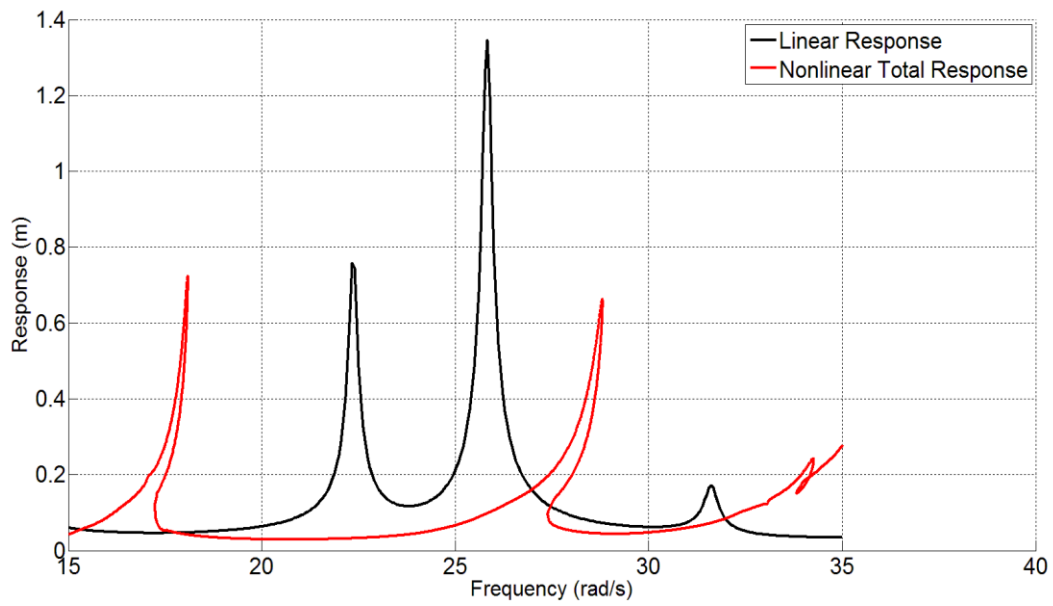
Figure 3.49 Total Response of the third DOF for Case Study 4, Parameter Set 1
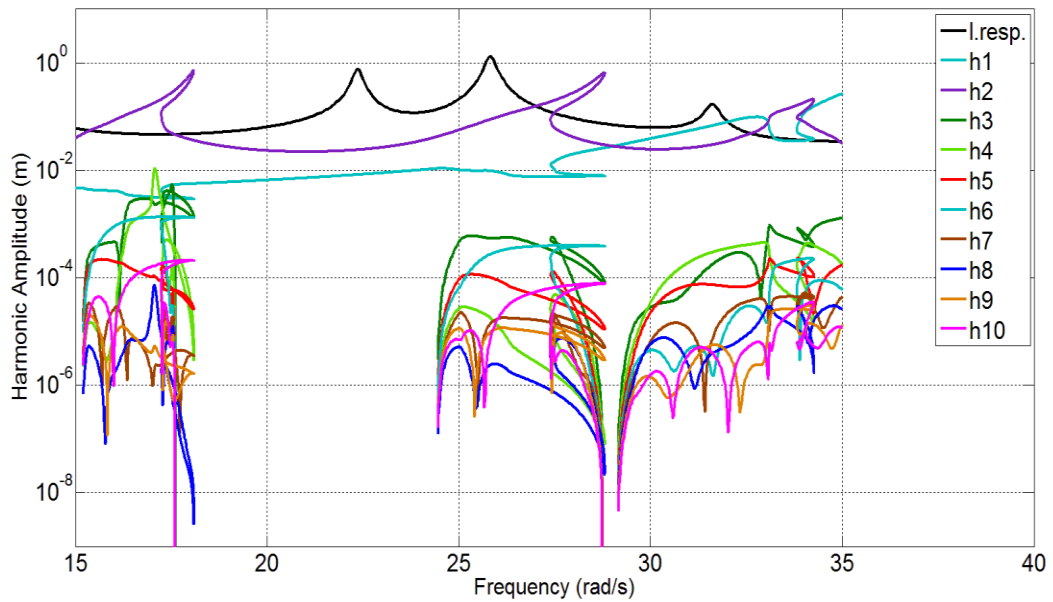
Figure 3.50 Harmonics of the third DOF for Case Study 4, Parameter Set 1

102
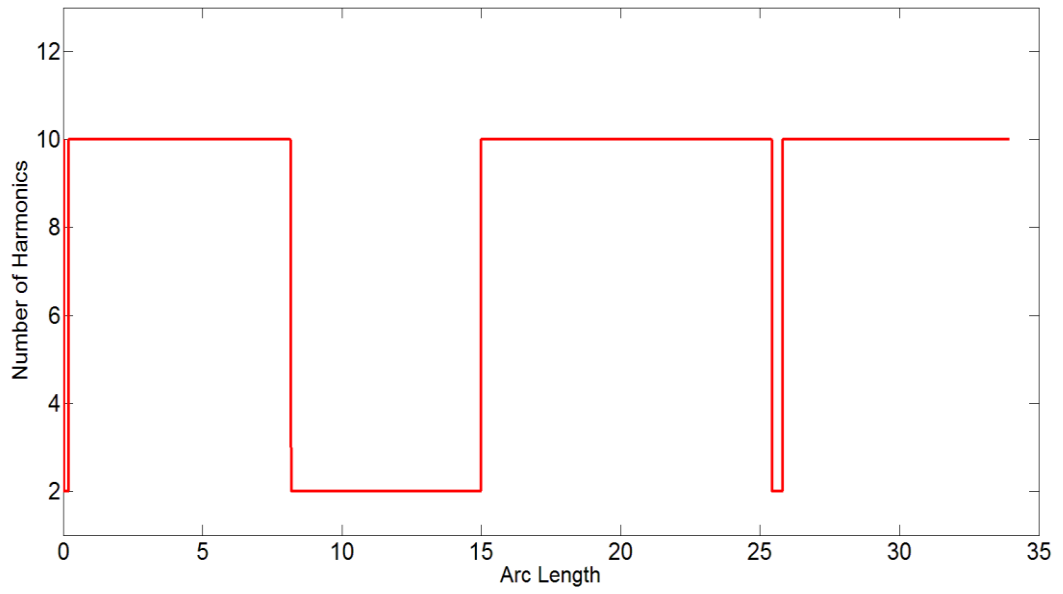
Figure 3.51 Number of harmonics used for Case Study 4, Parameter Set 1
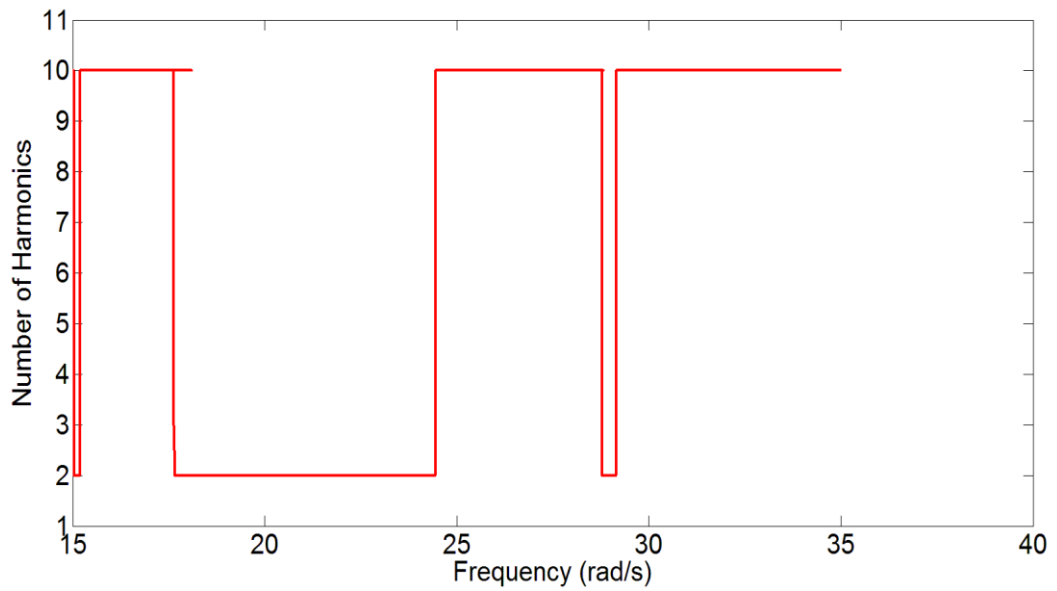
Figure 3.52 Number of harmonics used at each frequency for Case Study 4,
Parameter Set 1

For the next analysis, the parameters are changed as given in Table 3.9. The results obtained for this case are given in Figure 3.53 to Figure 3.60. The results show that the number of retained harmonics is decreased significantly for certain parts of the frequency spectrum.

Table 3.9 Control Parameters for Case Study 4, Parameter Set 2

ρ_b	ρ_f	N_h^m
10^{-10}	10^{-8}	10

Figure 3.53 Total Response of the first DOF for Case Study 4, Parameter Set 2

Figure 3.54 Harmonics of the first DOF for Case Study 4, Parameter Set 2

Figure 3.55 Total Response of the second DOF for Case Study 4, Parameter Set 2

Figure 3.56 Harmonics of the second DOF for Case Study 4, Parameter Set 2

Figure 3.57 Total Response of the third DOF for Case Study 4, Parameter Set 2

Figure 3.58 Harmonics of the third DOF for Case Study 4, Parameter Set 2
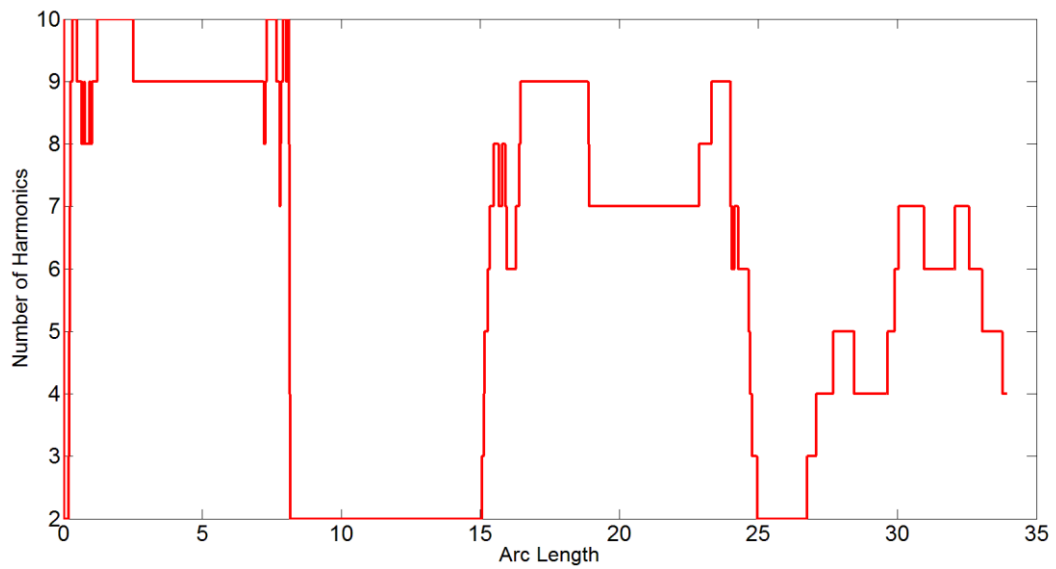
Figure 3.59 Number of harmonics used for Case Study 4, Parameter Set 2

107

Figure 3.60 Number of harmonics used at each frequency for Case Study 4, Parameter Set 2

3.4 AHBM 3: Yümer's Method

In 2010, Yümer [6] presented an AHBM, which is initially intended to be used in vibration analysis of bladed disks. Like the method presented by Jaumoillé et. al, it is a global and an incremental method. But since the threshold criterion does not require the computation of system response in order to decide which harmonics to be used, the method is still computationally economical.

In order to achieve adaptiveness, the method traces the nonlinear forcing vector. At the end of each solution step, a test is performed with the following criterion:

$$|f_0|+|f_{s1}|+|f_{c1}|+\ldots+|f_{sk}|+|f_{ck}| \geq a\left(\left|f_{s(k+1)}\right|+\left|f_{c(k+1)}\right|+\ldots+\left|f_{sN_h^m}\right|+\left|f_{cN_h^m}\right|\right), \qquad (3.21)$$

where the subscripts 0, s and c indicate the bias term, sine and cosine components, of the nonlinear forcing, respectively. Subscript k stands for the harmonic number,

108

N_h^m is the maximum number of harmonics allowed in the solution, a is an accuracy parameter set by the user. When the test starts, k is set to 1. Then, k is increased one by one until the criterion given in Equation (3.21) is satisfied. It can be seen from the equation that, increasing a also increases the accuracy of the solution, whereas the opposite leads to a more coarse solution.

In order to evaluate the criterion given in Equation (3.21), one needs to calculate a forcing vector having N_h^m harmonics even when the response is represented with less harmonics. This can be achieved by evaluating the following integrals for $j = 1, 2, 3 \ldots N_h^m$.

$$\begin{aligned}
\{f_{Nsj}\} &= \frac{1}{\pi} \int_0^{2\pi} f_N\left(q, \dot{q}, \theta\right) \sin(j\theta) d\theta \\
\{f_{Ncj}\} &= \frac{1}{\pi} \int_0^{2\pi} f_N\left(q, \dot{q}, \theta\right) \cos(j\theta) d\theta
\end{aligned} \tag{3.22}$$

Even when the response does not contain N_h^m harmonics, these integrals are able to give an idea about the harmonic content required by the nonlinear elements in the system.

As with the method presented by Jaumoillé et al. the incremental behavior of this method may sometimes cause the algorithm to reach saturation too early when the increase in the nonlinear forcing components is not smooth.

3.4.1   Case Study 5: Application of AHBM 3 on a SDOF System

The same system described in Section 3.2.1 is used for this study. For the first case, the control parameters are taken as given in Table 3.10. Under the effect of these parameters, the response graphs come out as given in figures between Figure 3.61 and Figure 3.62. The results show that, the control parameters do not let the

algorithm to drop the number of used harmonics under 10 almost throughout the frequency range. The number of harmonics drops only at a few points.

Table 3.10 Parameters for Case Study 5, Parameter Set 1

M (kg)	k (N/m)	h (N/m)	δ (m)	k_g (N/m)	a	N_h^m
1	100	1	0.4	400	10^3	10
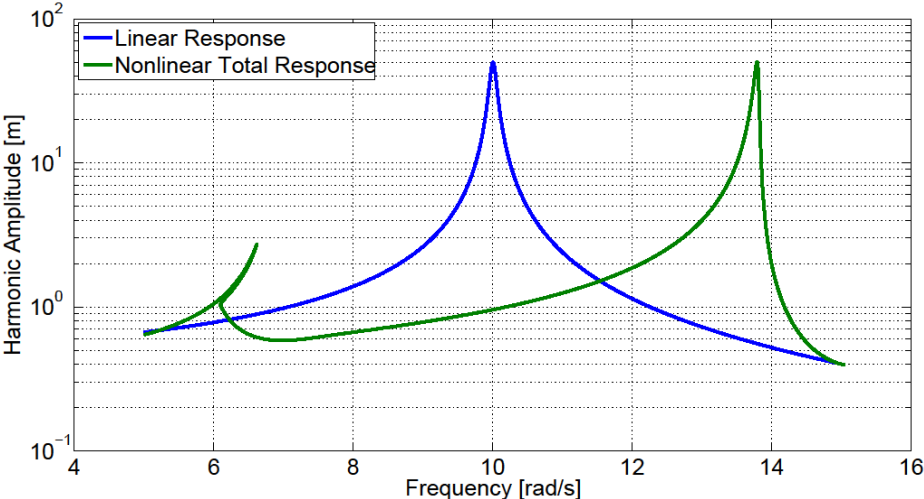
Figure 3.61 Linear and nonlinear total response curves for Case Study 5, Parameter Set 1
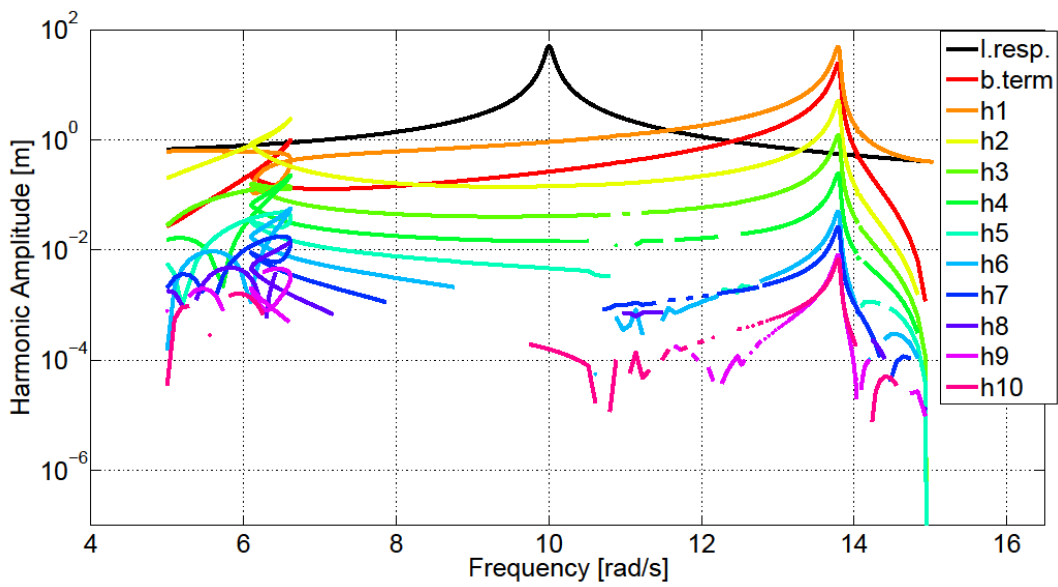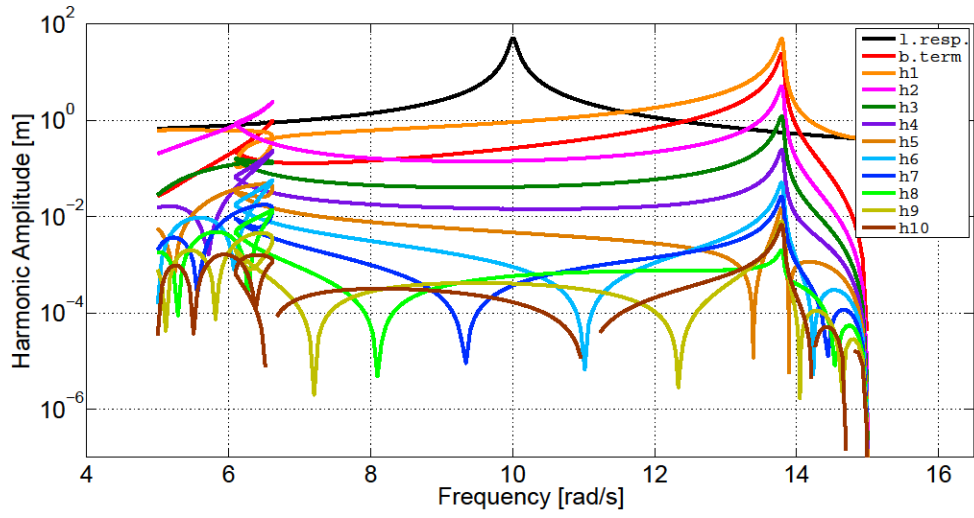
Figure 3.62 Amplitudes of Harmonics for Case Study 5, Parameter Set 1
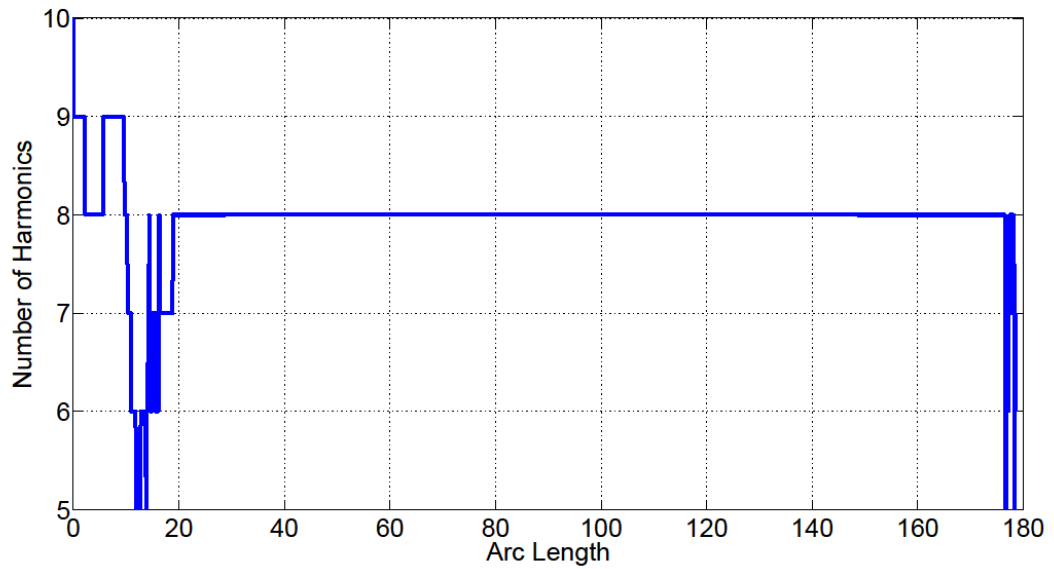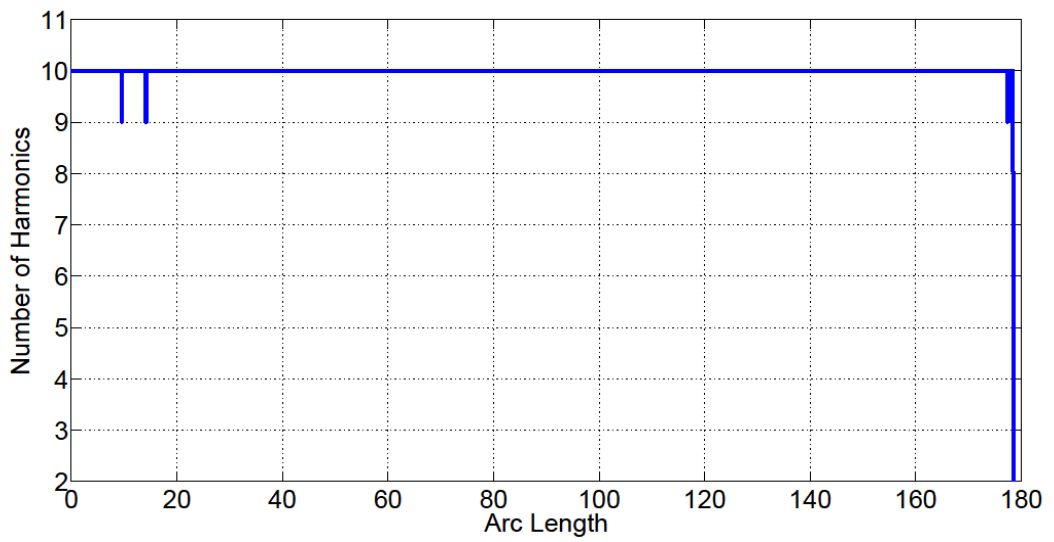

Figure 3.63 Number of harmonics used for Case Study 5, Parameter Set 1

111

For the next analysis, the parameters are changed as given in Table 3.11 The results obtained for this parameter set are given in Figure 3.64 to Figure 3.66.

The results show that the number of retained harmonics decreases considerably while no detectable change occurs in the total response. At most seven harmonics are used, especially around the first resonance peak (super-harmonic peak around 6 rad/s), which decreases to 4 around the fundamental resonance.

Table 3.11 Modified Parameters for Case Study 5, Parameter Set 2

M (kg)	k (N/m)	h (N/m)	δ (m)	k_g (N/m)	a	N_h^m
1	100	1	0.4	400	10^1	10
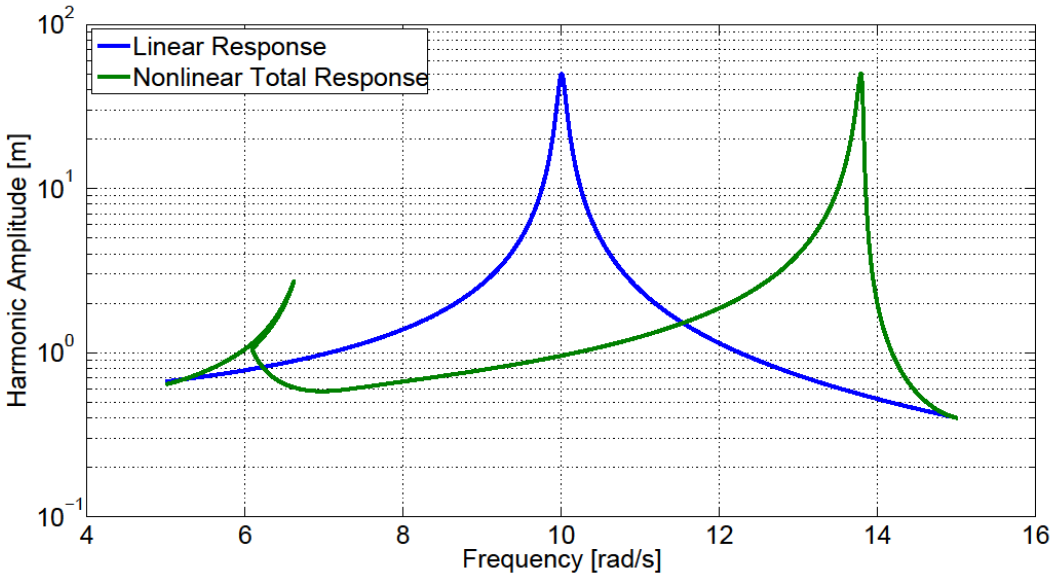
Figure 3.64 Linear and nonlinear total response curves for Case Study 5, Parameter Set 2
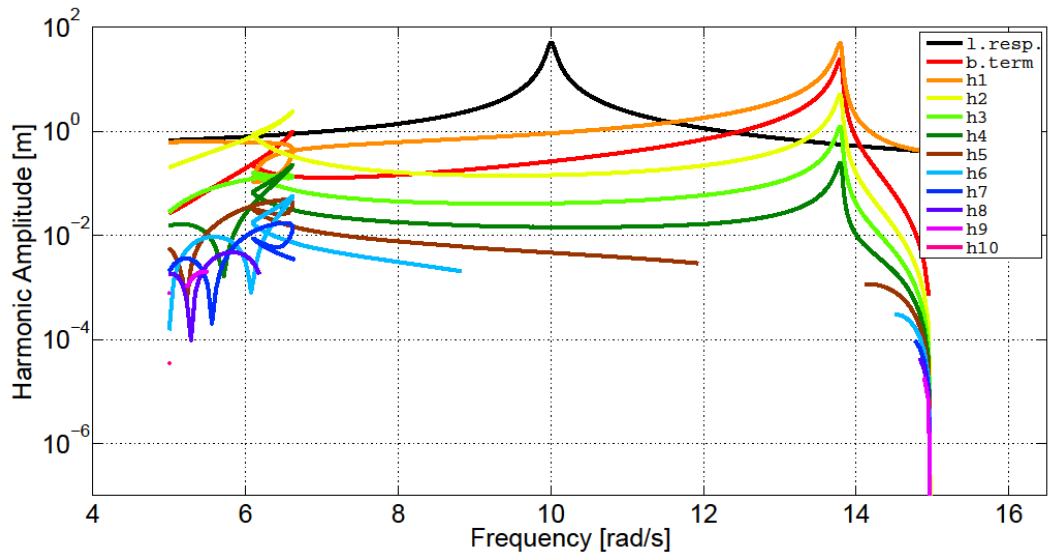
Figure 3.65 Amplitudes of Harmonics for Case Study 5, Parameter Set 2
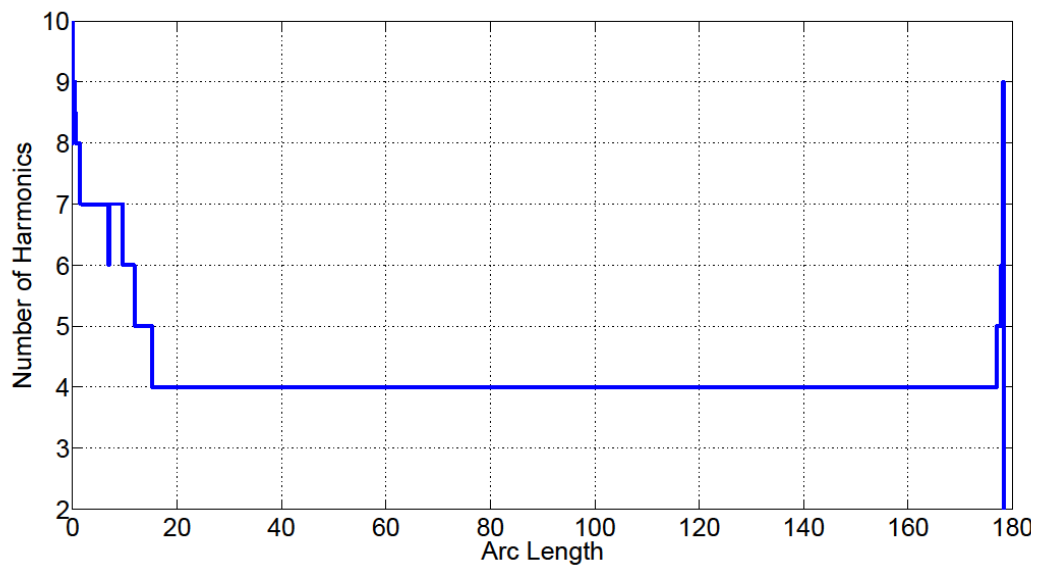
Figure 3.66 Number of harmonics used for Case Study 5, Parameter Set 2

113

For the final part of the study analysis, the parameters are changed as given in Table 3.12. The results obtained for this parameter set are given in Figure 3.67 to Figure 3.69. For this case, the harmonics retained in the solution decrease even further as expected, reaching to a minimum of 2.

Table 3.12 Modified parameters for Case Study 5, Parameter Set 3

M (kg)	k (N/m)	h (N/m)	δ (m)	k_g (N/m)	a	N_h^m
1	100	1	0.4	400	2	10
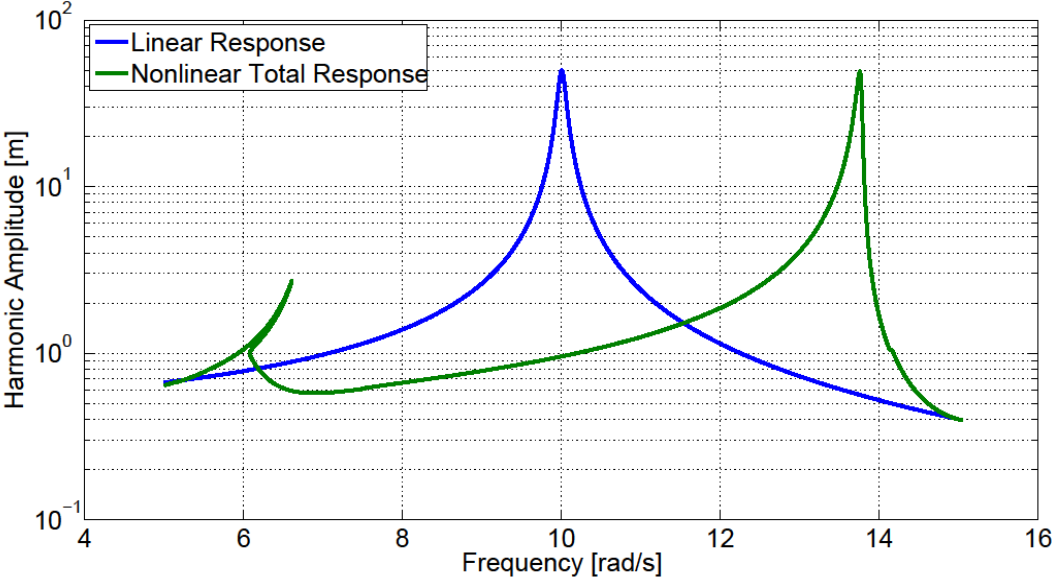
Figure 3.67 Linear and nonlinear total response curves for Case Study 5, Parameter Set 3

114
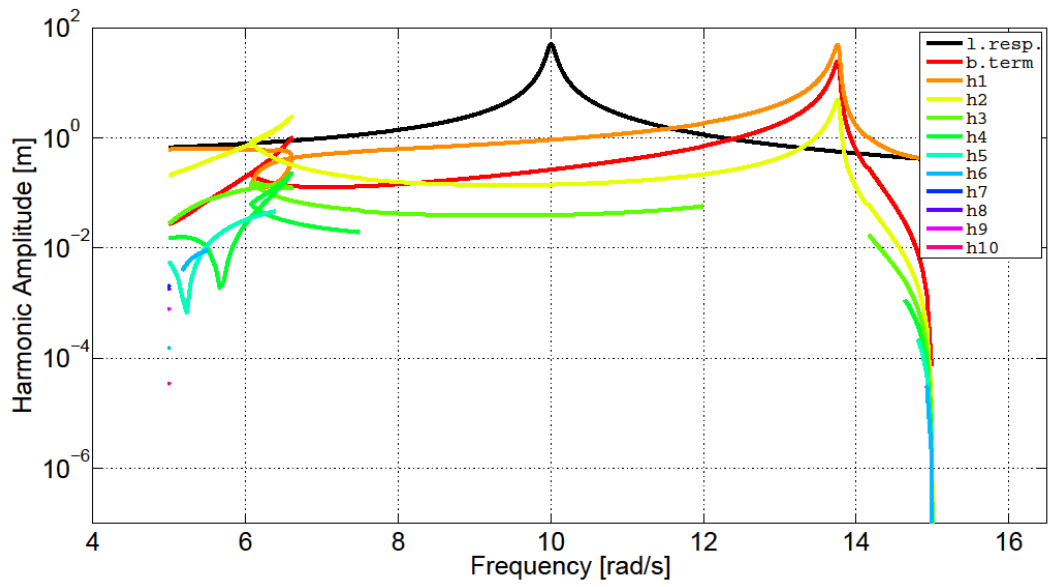
Figure 3.68 Amplitudes of Harmonics for Case Study 5, Parameter Set 3
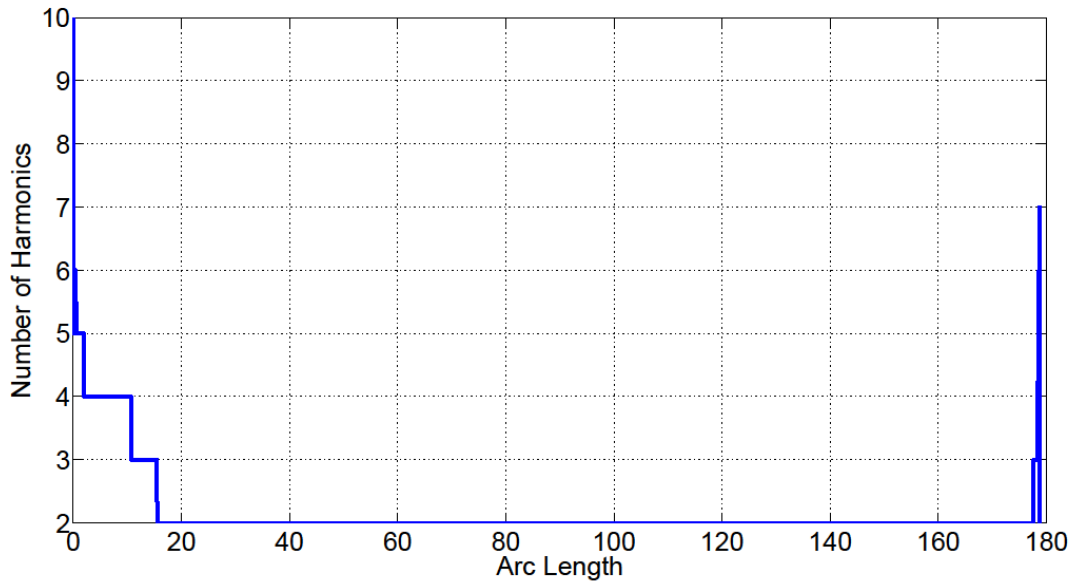
Figure 3.69 Number of harmonics used for Case Study 5, Parameter Set 3

3.4.2 Case Study 6: Application of AHBM 3 on a MDOF System

The same system described in Section 3.2.2 is used for this study. In the first parameter set, the control parameter and the maximum number of harmonics are taken as $a = 10^8$ and $N_h^m = 10$. The obtained results are given in Figure 3.70 to Figure 3.77. The figures indicate that the results are similar to those obtained by AHBM 2. The algorithm retained all the available harmonics in the solution except for the regions between the resonances where the system behaves almost as a hardened linear system.
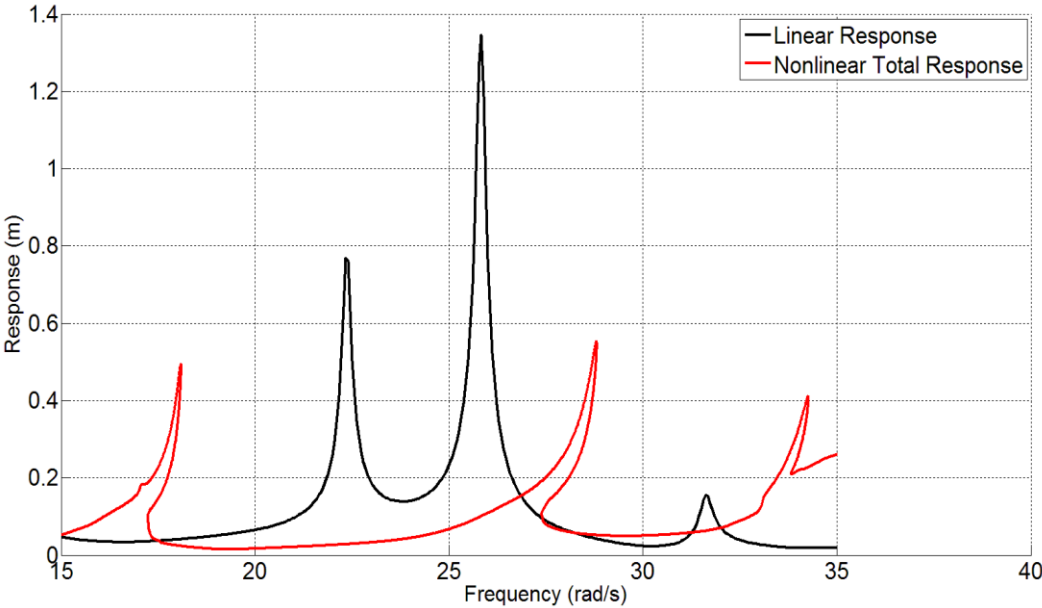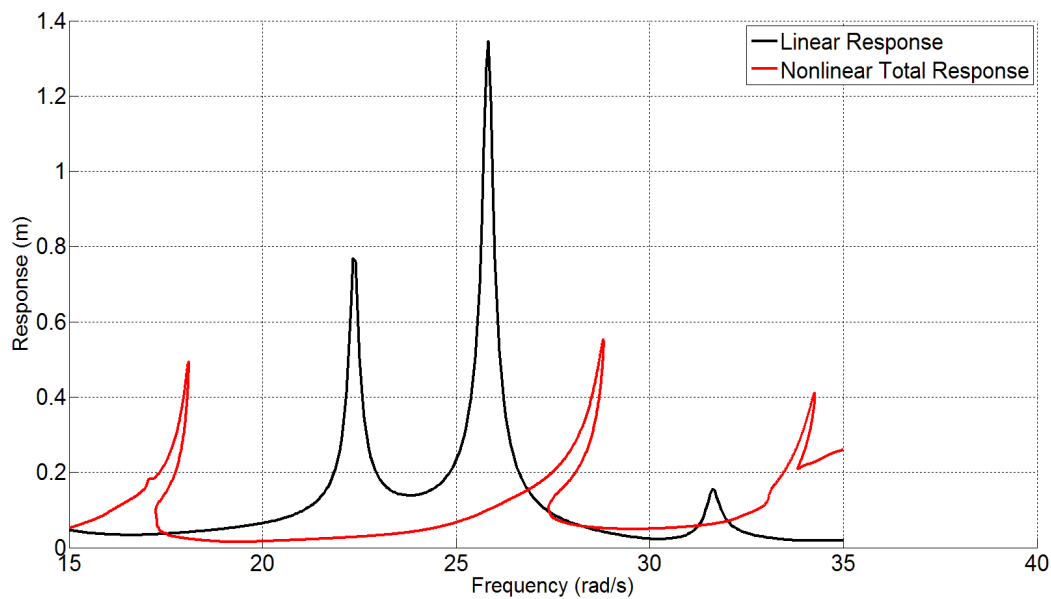

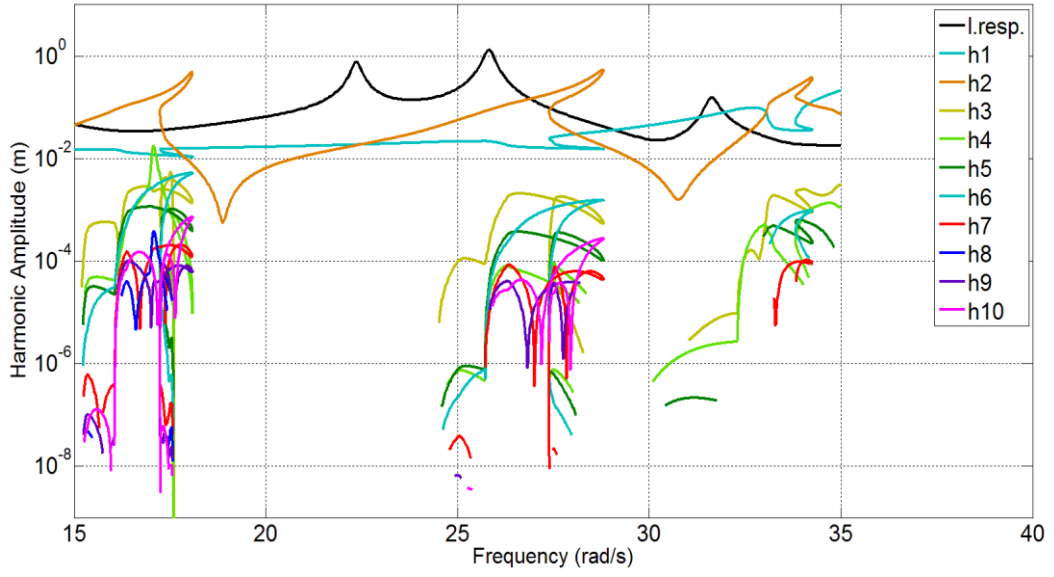**Figure 3.70** Total Response of the first DOF for Case Study 6, Parameter Set 1
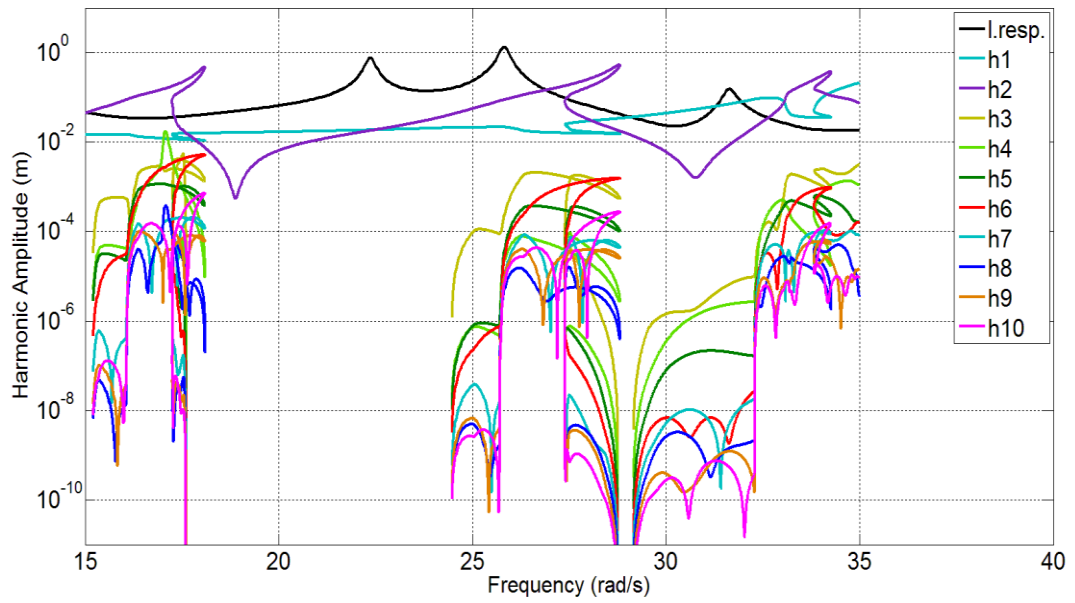
Figure 3.71 Harmonics of the first DOF for Case Study 6, Parameter Set 1
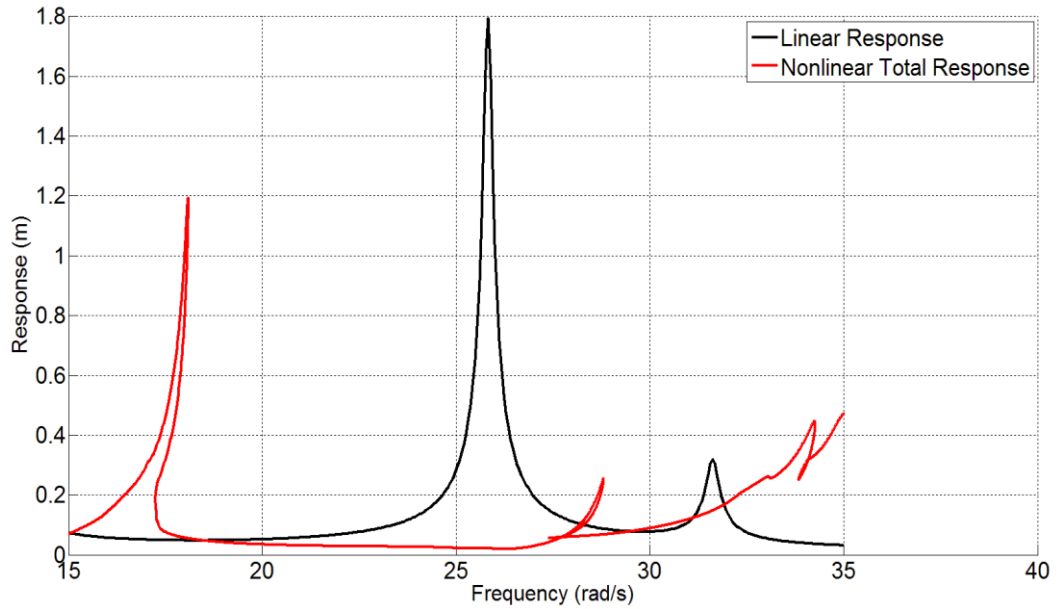
Figure 3.72 Total Response of the second DOF for Case Study 6, Parameter Set 1
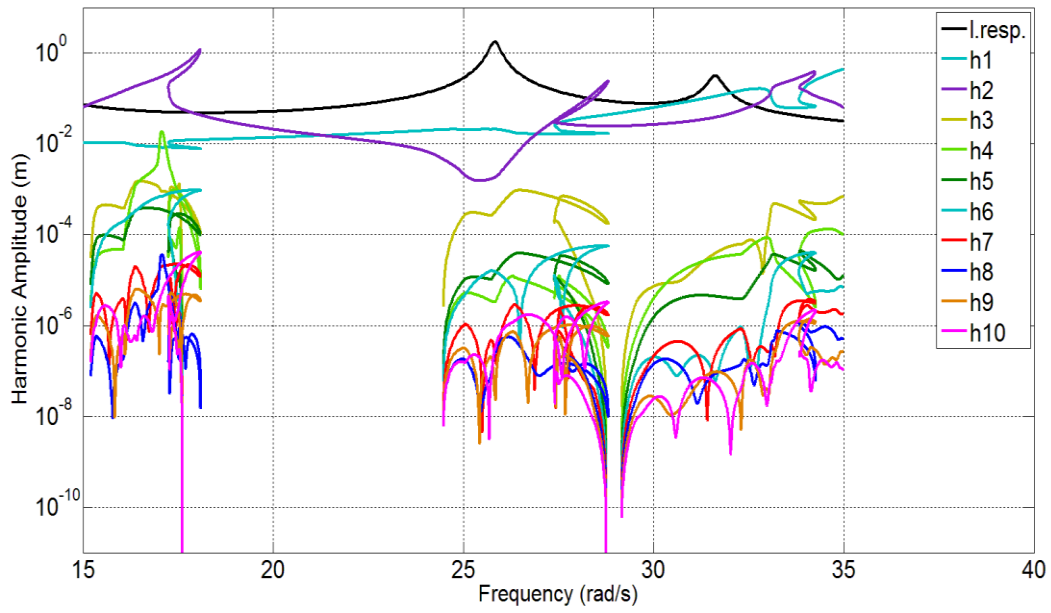
Figure 3.73 Harmonics of the second DOF for Case Study 6, Parameter Set 1
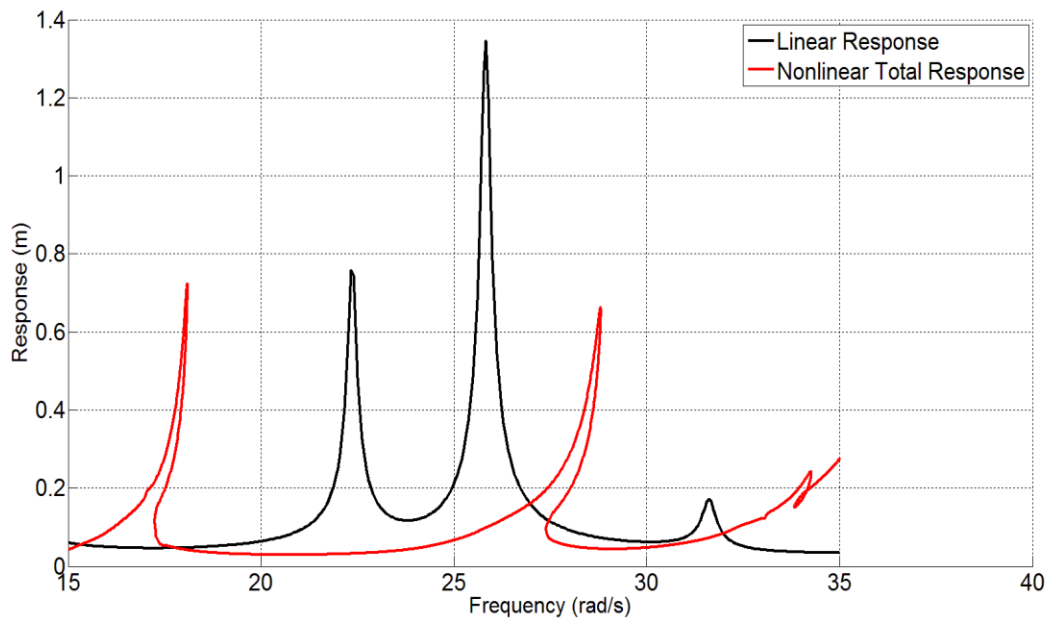
Figure 3.74 Response of the third DOF for Case Study 6, Parameter Set 1

118
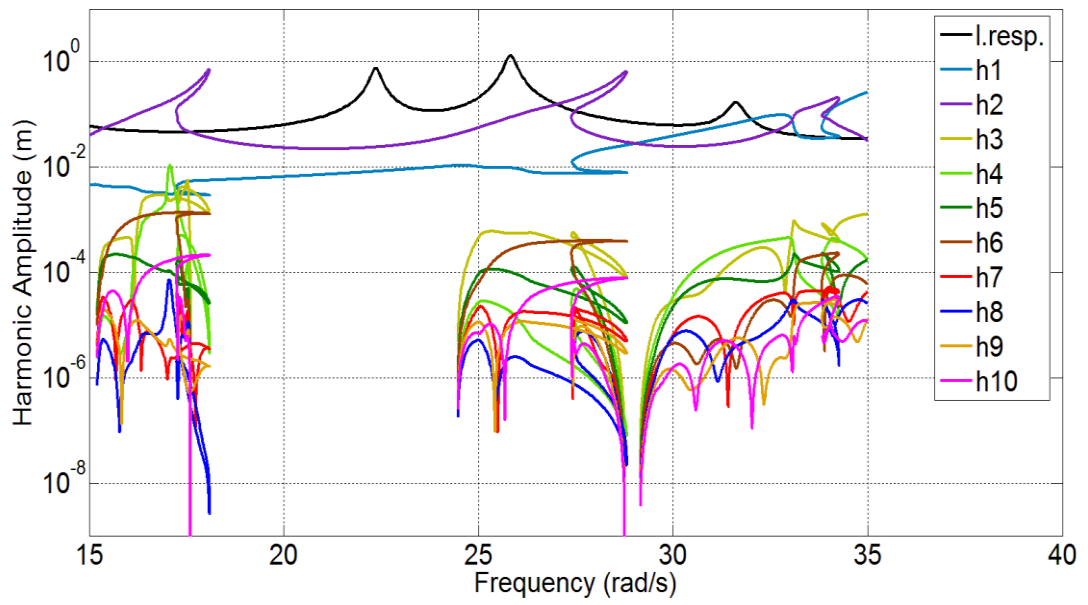
Figure 3.75 Harmonics of the third DOF for Case Study 6, Parameter Set 1
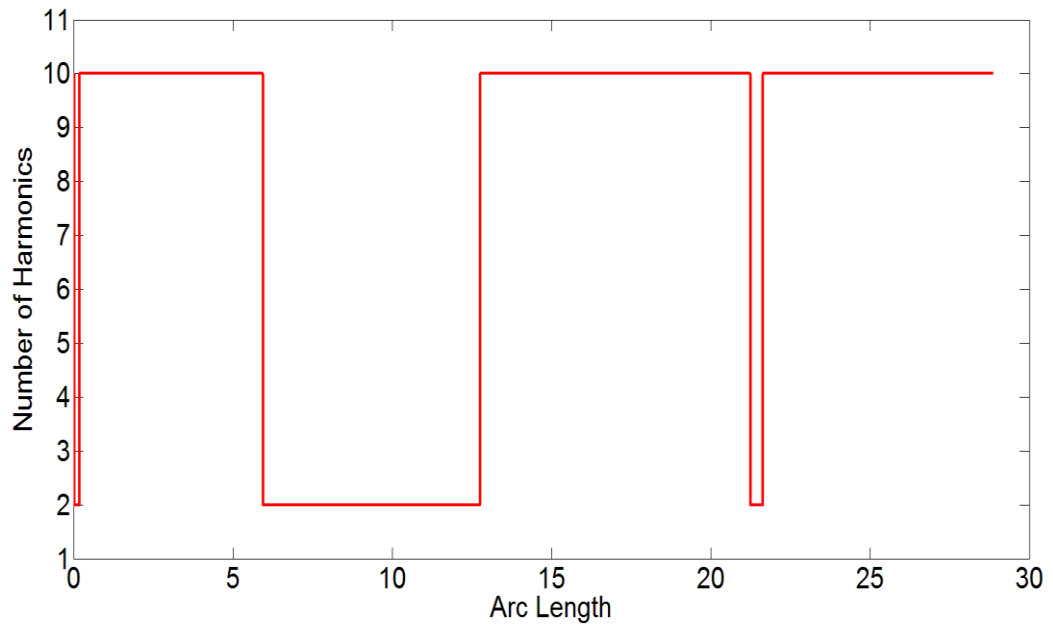
Figure 3.76 Number of harmonics used for Case Study 6, Parameter Set 1

119
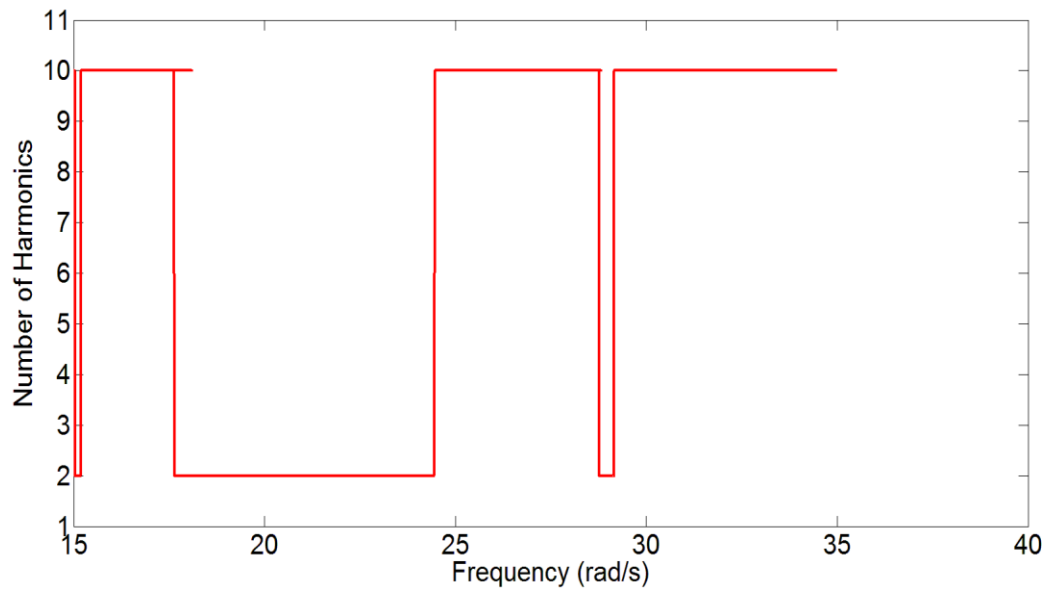
Figure 3.77 Number of harmonics used at each frequency for Case Study 6, Parameter Set 1

For the second part of the study, the control parameter and the maximum number of harmonics are taken as $a = 100$ and $N_h^m = 10$, respectively. The obtained results are given in Figure 3.78 to Figure 3.85. The results show that for this case, the number of retained harmonics changed considerably, reaching up to $N_h^m = 10$ only in certain parts of the nonlinear frequency response curve.
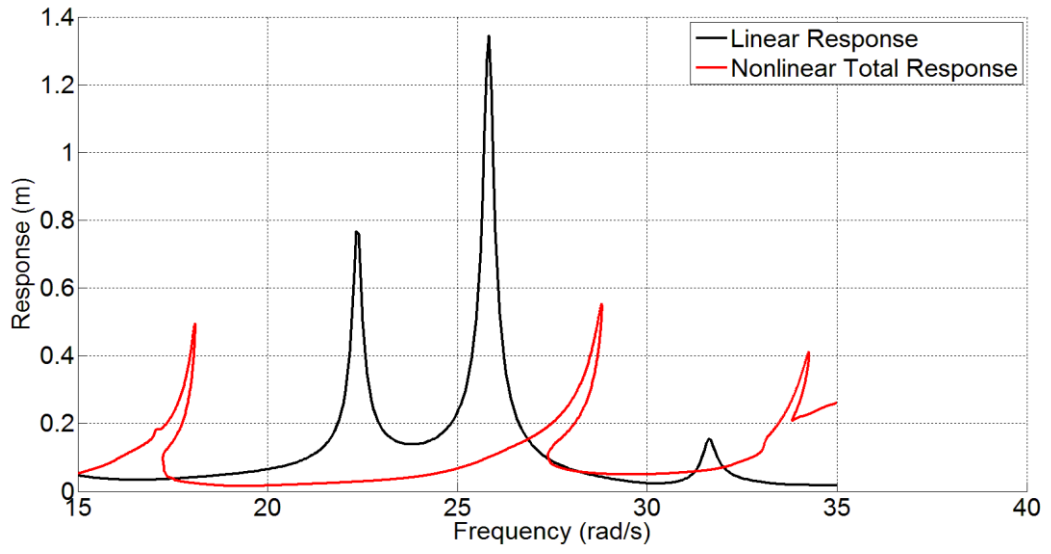
Figure 3.78 Response of the first DOF for Case Study 6, Parameter Set 2
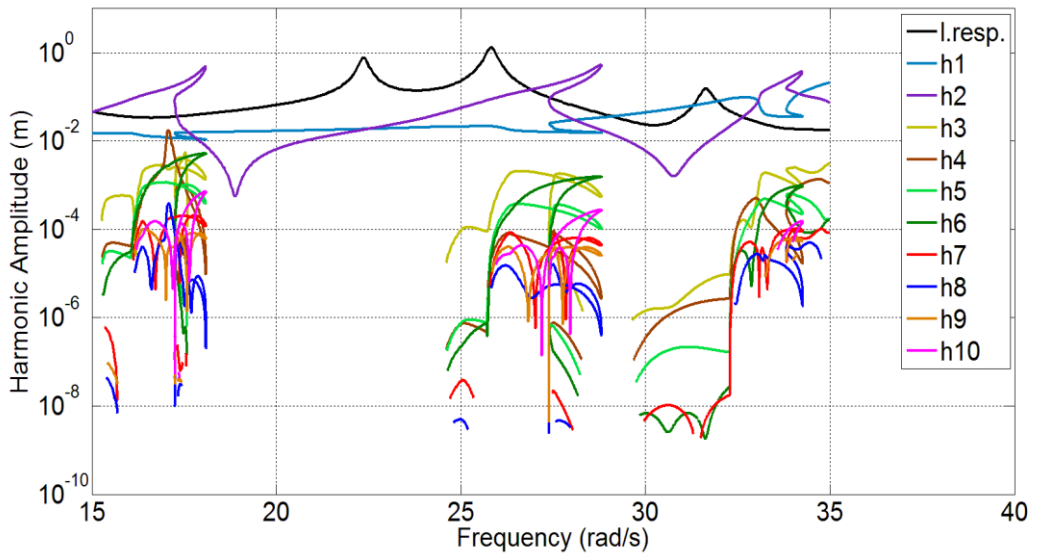
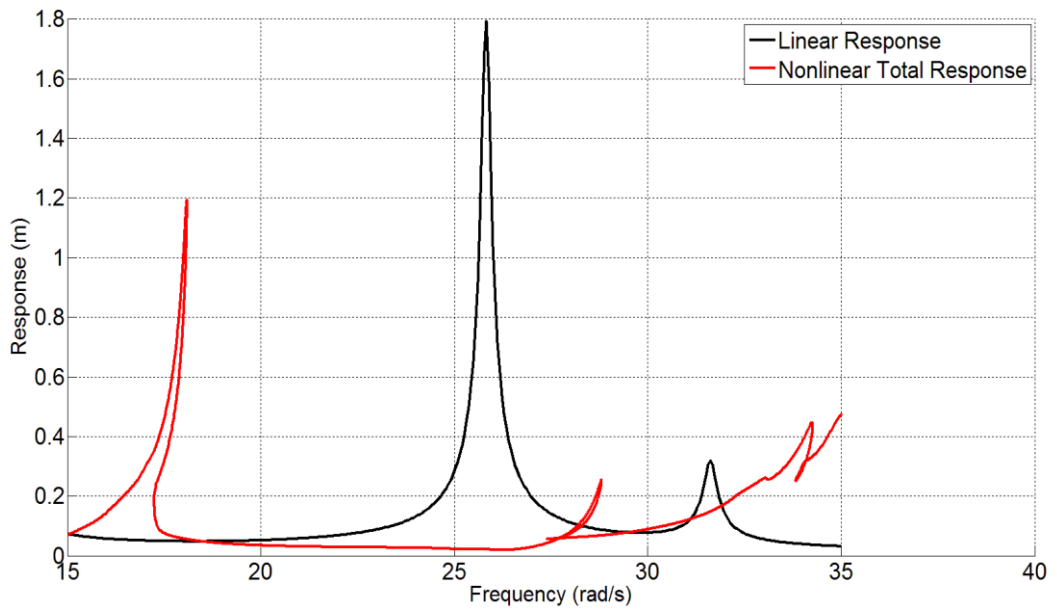**Figure 3.79** Harmonics of the first DOF for Case Study 6, Parameter Set 2

121
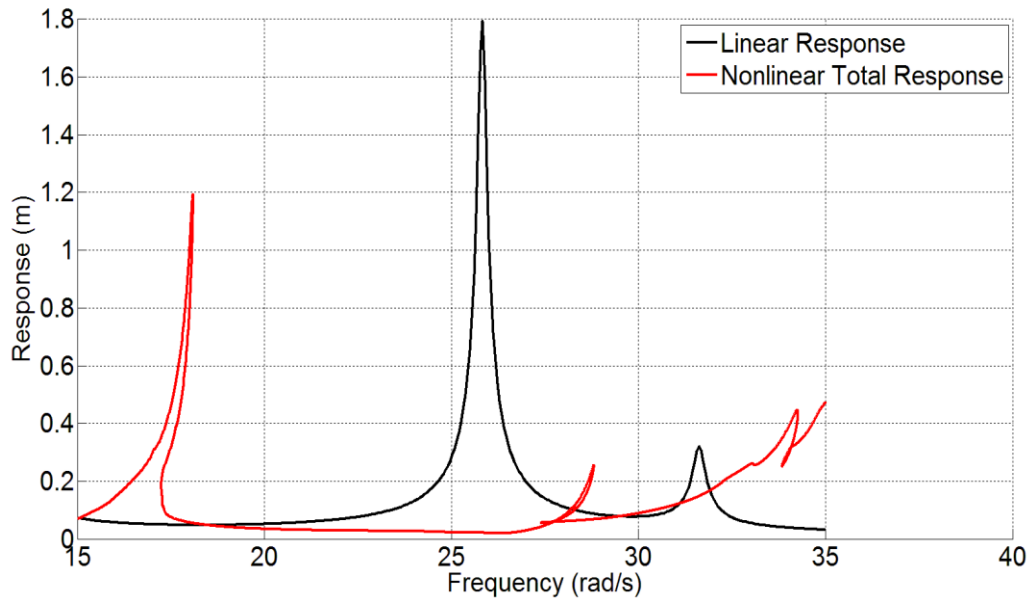
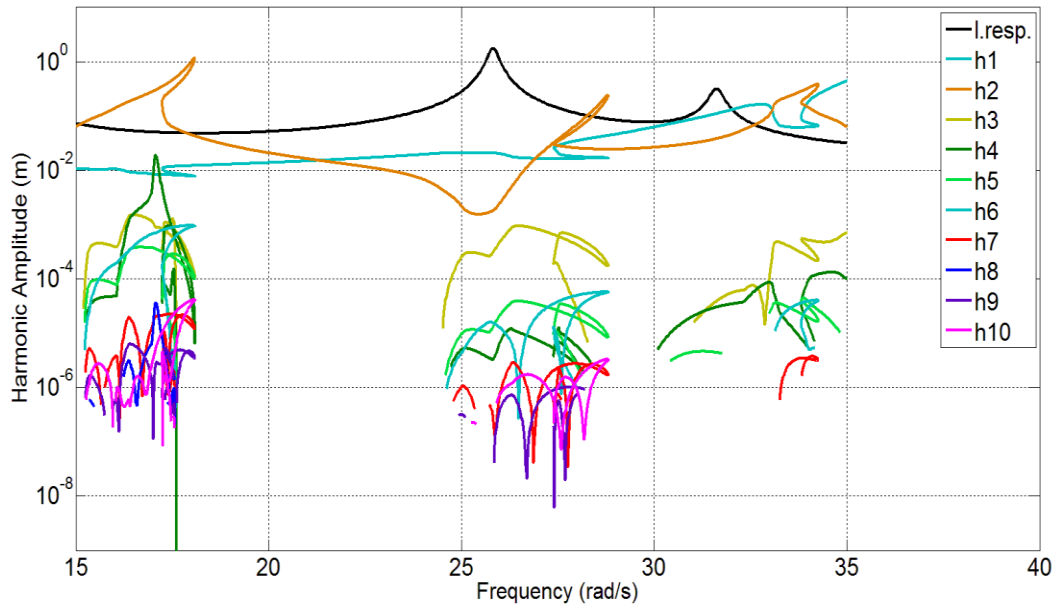**Figure 3.80** Response of the second DOF for Case Study 6, Parameter Set 2
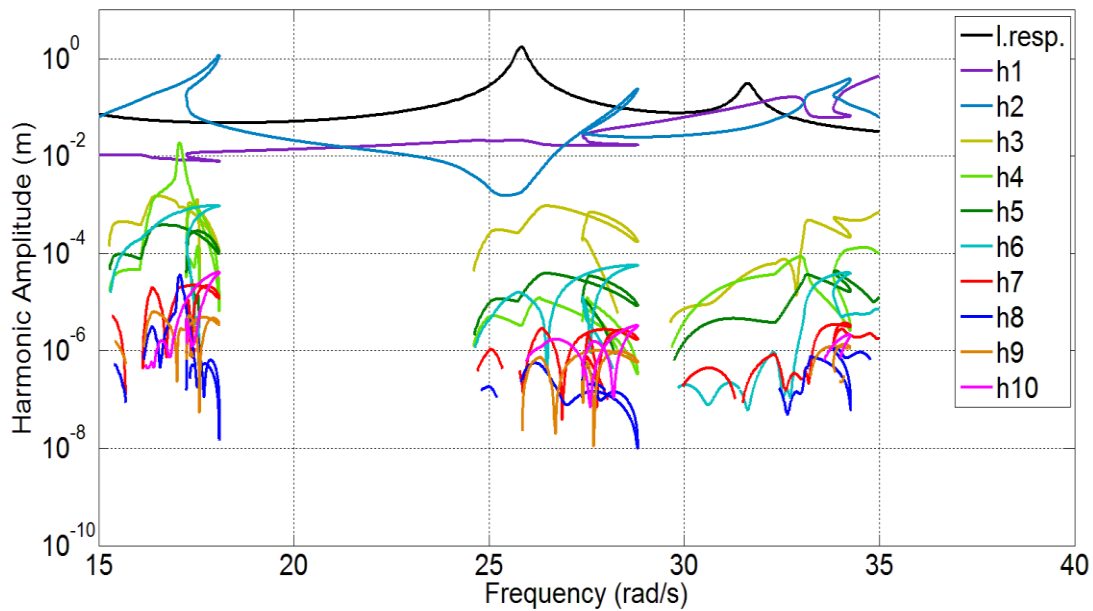
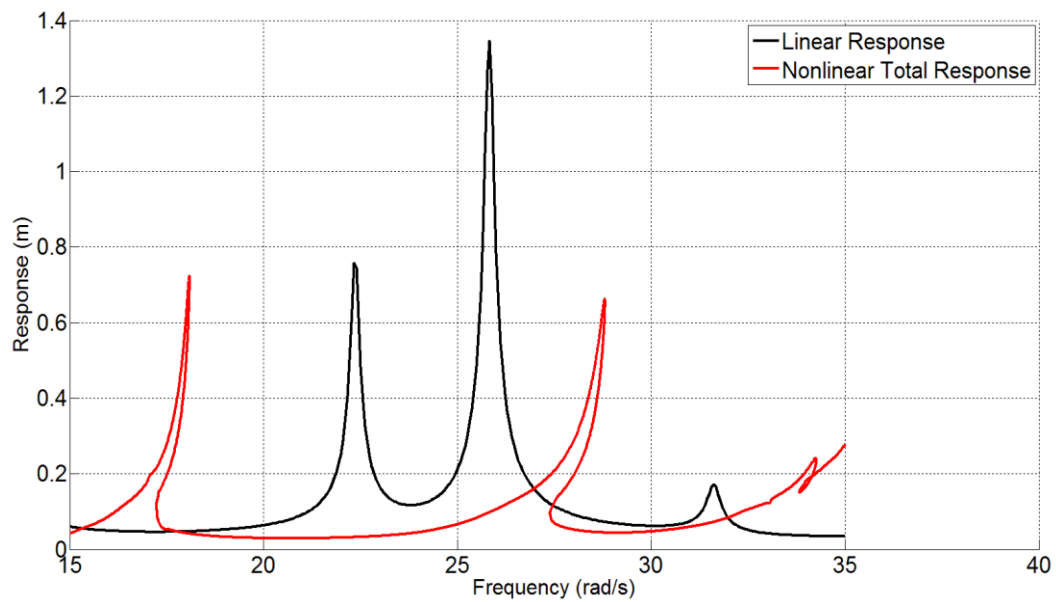**Figure 3.81** Harmonics of the second DOF for Case Study 6, Parameter Set 2
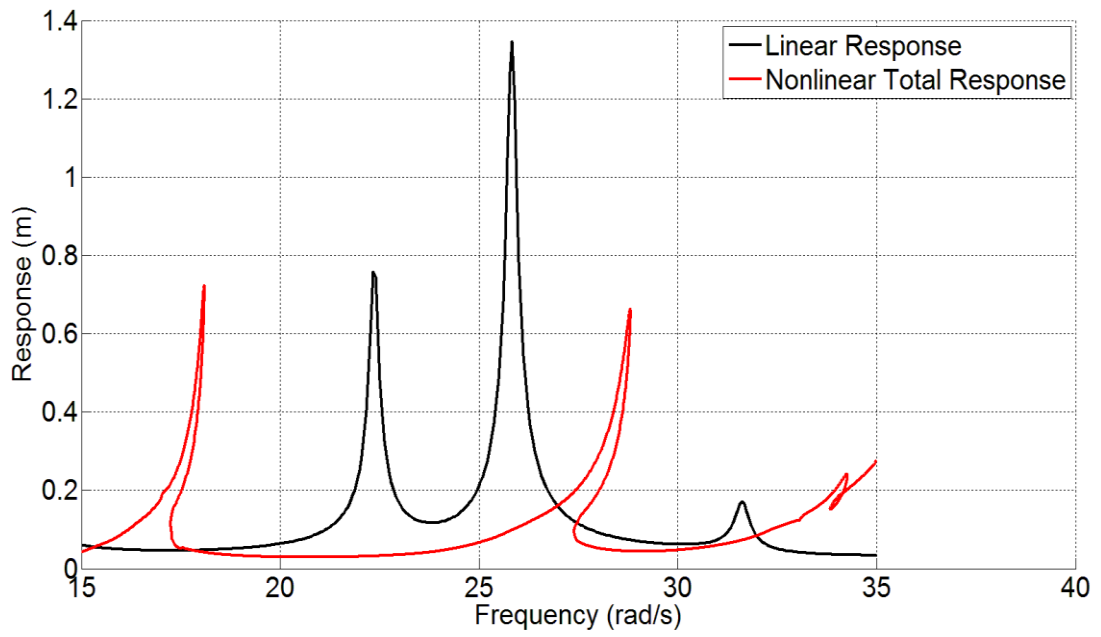
Figure 3.82 Response of the third DOF for Case Study 6, Parameter Set 2
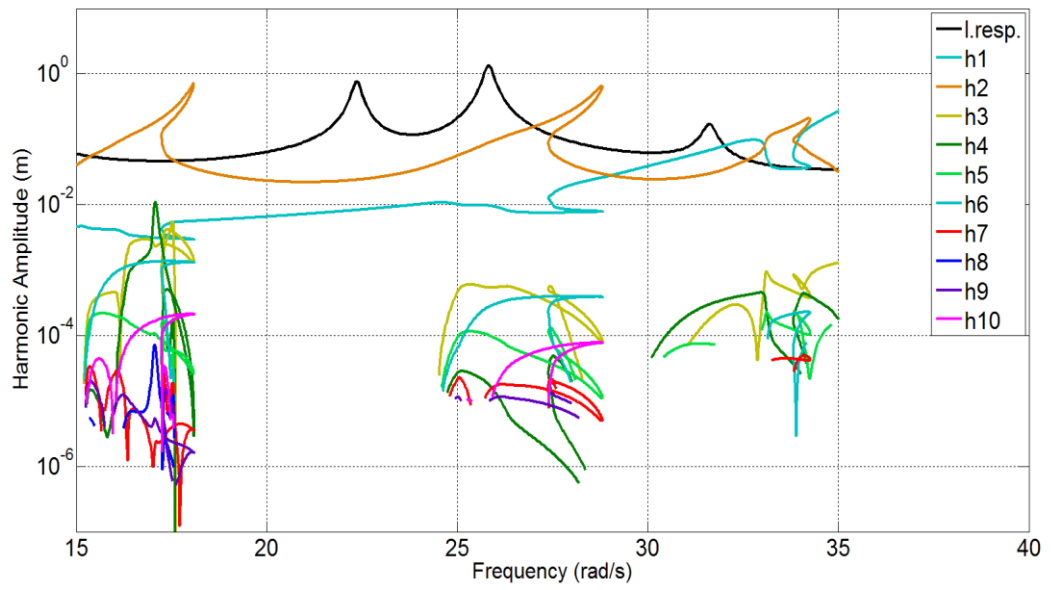

**Figure 3.83** Harmonics of the third DOF for Case Study 6, Parameter Set 2

123

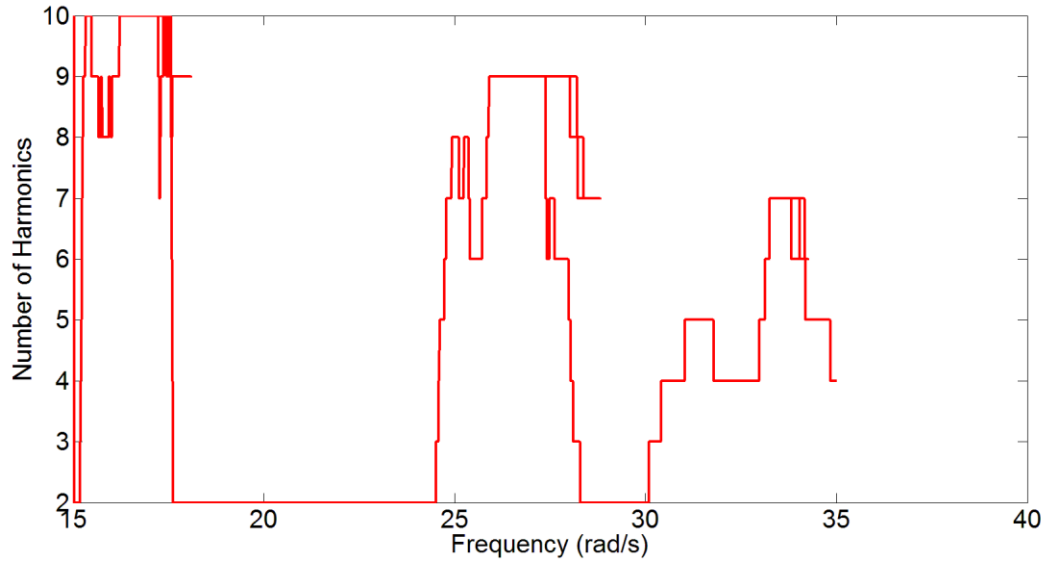**Figure 3.84** Number of harmonics used for Case Study 6, Parameter Set 2
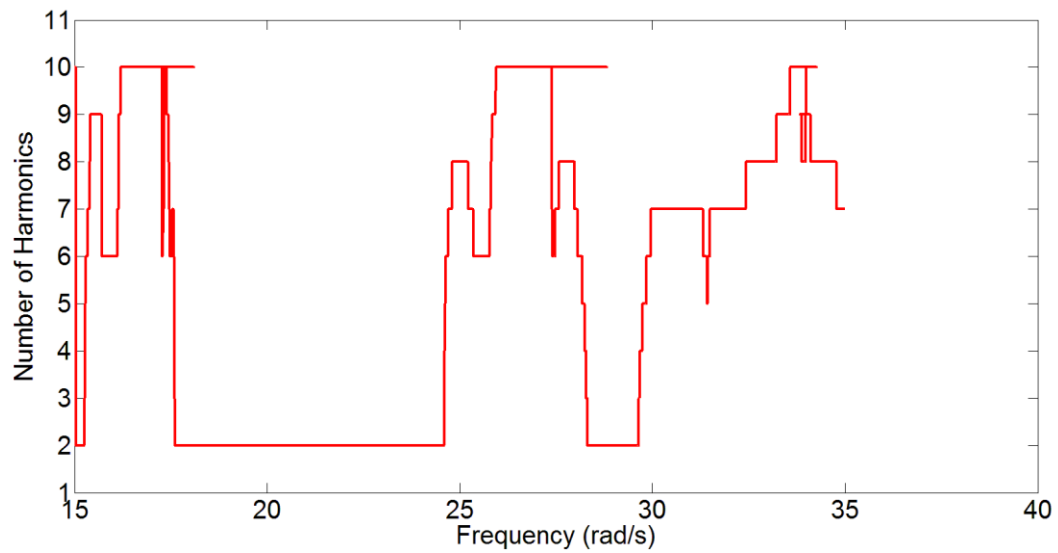
Figure 3.85 Number of harmonics used at each frequency for Case Study 6, Parameter Set 2

3.5 AHBM 4: The Newly Proposed Method - Pseudo-Response Based Adaptive Harmonic Balance Method

A new AHBM is presented in this section. This new method is actually an extension of AHBM 3. Although being global like AHBM 3, it is not an incremental method. Therefore it may be useful for the cases where the decrease in magnitude in higher harmonics does not follow an order. Due to its dependence of the newly introduced pseudo-response concept, the method is named as Pseudo-Response Based Adaptive Harmonic Balance Method (PRB-AHBM).

Similar to Grolet and Thouverez's Method and Yümer's Method, the new algorithm requires the user to assign a maximum number of harmonics r, and a threshold value ε_t to be used in the solution. Assume that a solution for the Fourier coefficients of the response is calculated by using a certain solution point i. From this solution, using the expressions given in Equation (3.22) one can construct a new nonlinear forcing vector even if the response does not have r harmonics. Then, by using the newly constructed nonlinear forcing vector the first criterion, given by the following relation is evaluated for $1 \leq k \leq r$ and $1 \leq d \leq n$:

$$\varepsilon_{f,k}^d = \frac{\sqrt{f_{Nsk}^{d\,2} + f_{Nck}^{d\,2}}}{\sqrt{f_{Ns1}^{d\,2} + f_{Nc1}^{d\,2}}}, \tag{3.23}$$

where $\varepsilon_{f,k}^d$ stands for the ratio of forcing magnitudes for the kth harmonic of DOF d, f_{Nsk}^d and f_{Nsk}^d stand for the sine and cosine components of the kth harmonic of DOF d, respectively. $\varepsilon_{f,k}^d$ represents a simple magnitude comparison between the fundamental harmonic and higher harmonics. During the evaluation of the criterion given in Equation (3.23), one obtains r $\varepsilon_{f,k}^d$ values for each DOF. Since the method is global, different numbers of harmonics for different DOFs is not required. However, as can be seen from the given criterion, the proposed method can be

readily used as a local method as well. In order to suppress the dependence on DOFs, the following ratio is defined:

$$\varepsilon_{f,k} = \max\left(\varepsilon_{f,k}^{1} \quad , \quad \varepsilon_{f,k}^{2} \quad , \quad \cdots \quad \varepsilon_{f,k}^{n} \right). \tag{3.24}$$

Then $\varepsilon_{f,k}$ values obtained for each harmonics are compared to the threshold value ε_{t}. Higher harmonics with ε_{f}^{k} less than ε_{t} are excluded from the solution. However, the bias term and the first harmonic are always included. All the remaining harmonic numbers are stored in a row matrix $\left[H_{ret} \right]$. For example, when the bias term, the first and third harmonics are retained, $\left[H_{ret} \right] = \begin{bmatrix} 0 & 1 & 3 \end{bmatrix}$.

After the evaluation of the first criterion, the excluded harmonics are removed from the nonlinear forcing matrix and the external forcing matrix. Treating the nonlinear forces as linear, i.e. calculating them by using the nonlinear response obtained at the previous frequency point, one can calculate a pseudo-response as follows which does not require any iterations.

$$
\begin{Bmatrix} \{q_0\} \\ \{q_{s1}\} \\ \{q_{c1}\} \\ \{q_{sh_3}\} \\ \{q_{ch_3}\} \\ \vdots \\ \{q_{sh_m}\} \\ \{q_{ch_m}\} \\ \vdots \end{Bmatrix} = \begin{pmatrix} [K] & [0] & [0] & \cdots & [0] & \cdots \\ [0] & [\Lambda(\omega)] & [0] & \cdots & [0] & \cdots \\ [0] & [0] & [\Lambda(h_3 \cdot \omega)] & \cdots & [0] & \cdots \\ \vdots & \vdots & \vdots & \ddots & \vdots & \vdots \\ [0] & [0] & [0] & \cdots & [\Lambda(h_m \cdot \omega)] & \cdots \\ \vdots & \vdots & \vdots & \cdots & \vdots & \ddots \end{pmatrix}^{-1} \begin{Bmatrix} \{F_0\}-\{f_{N0}\} \\ \{F_{s1}\}-\{f_{Ns1}\} \\ \{F_{c1}\}-\{f_{Nc1}\} \\ \{F_{sh_3}\}-\{f_{Nsh_3}\} \\ \{F_{ch_3}\}-\{f_{Nch_3}\} \\ \vdots \\ \{F_{sh_m}\}-\{f_{Nsh_m}\} \\ \{F_{ch_m}\}-\{f_{Nch_m}\} \\ \vdots \end{Bmatrix}, \tag{3.25}
$$

h_m represents $\left[H_{ret} \right]_{(1,m)}$ and the square matrix on the right hand side is the same as the block diagonal matrix defined in Equation (2.16) and Equation (2.17), evaluated

126

for the selected harmonics. This matrix can be replaced by the block diagonal matrix given in Equation (2.47) and Equation (2.44) which contains receptance matrices calculated for the retained harmonics. Using this pseudo-response vector given on the left hand side of Equation (3.25), the second criterion is evaluated for $h_k \in H_{ret}$:

$$\varepsilon_{pr,h_k}^d = \frac{\sqrt{q_{sh_k}^{d\ 2} + q_{ch_k}^{d\ 2}}}{\sqrt{q_{s1}^{d\ 2} + q_{c1}^{d\ 2}}}. \tag{3.26}$$

Similarly, the following ratio is defined in order to have a global method:

$$\varepsilon_{pr,h_k} = \max\left(\varepsilon_{pr,h_k}^1 \quad , \quad \varepsilon_{pr,h_k}^2 \quad , \quad \cdots \quad \varepsilon_{pr,h_k}^d\right). \tag{3.27}$$

ε_{pr,h_k} values obtained for each harmonic are compared to the threshold value ε_t. The harmonics with ε_{pr,h_k} ratio smaller than ε_t are excluded from the solution. If more flexibility is required by the user, a threshold value other than ε_t can be defined for pseudo-response. By this second criterion, a further reduction on the harmonics can be obtained, based on a response-like reference. It should be noted that all the AHBMs available does not consider the response of the structure. However, structure itself may as well behave like a filter; hence, it may filter out the forcing at particular frequencies. The proposed PRB-AHBM considers this fact and performs a second reduction which removes unnecessary harmonics from the response calculation. Moreover, since pseudo-based response calculation used, the computational time required by the proposed method is kept at minimum. After all, the main motivation of the AHBMs is to decrease the computational time required by retaining the accuracy of the solution. The remaining harmonics are included in the numerical solution scheme for the current solution point.

In the end, a global and a non-incremental method is presented with two threshold criteria, which are fairly easy for a computer to evaluate. Also, compared to other methods, the physical meanings of the threshold criteria are simpler, so it is easy for the user to come up with a ε_t ratio and obtain the required accuracy with fewer trials. Since the first harmonic is generally the largest harmonic in magnitude, one can easily identify that ε_t must take a value between 0 and 1. Making ε_t closer to 0 forces the algorithm to include more harmonics in the solution.

3.5.1 AHBM 5: An Extension of the Newly Proposed Method

In the nonlinear vibration response of a dynamic system, for some special cases, the first harmonic may not necessarily be the largest in amplitude. For these cases, applying PRB-AHBM as it is described in Section 3.5 can prevent the solution scheme from excluding some unnecessary harmonics having relatively small amplitudes, compared to the dominant harmonic which has the maximum amplitude. In this case, the computational efficiency would drop. This shortcoming can be overcome by making a small modification in the criteria used.

Instead of using Equation (3.24) and Equation (3.26) as they are defined in Section 3.5, one can change the definitions of and ε_{pr,h_k}^d as:

$$\varepsilon_{f,k}^d = \frac{\sqrt{f_{Nsk}^{d\ 2} + f_{Nck}^{d\ 2}}}{f_{\max}}, \tag{3.28}$$

where

$$f_{\max} = \max\left(\sqrt{f_{Ns1}^{d\ 2} + f_{Nc1}^{d\ 2}} \quad \sqrt{f_{Ns2}^{d\ 2} + f_{Nc2}^{d\ 2}} \quad \cdots \quad \sqrt{f_{Nsr}^{d\ 2} + f_{Ncr}^{d\ 2}}\right), \tag{3.29}$$

and

$$\varepsilon_{pr,h_k}^d = \frac{\sqrt{q_{sh_k}^{d\ 2} + q_{ch_k}^{d\ 2}}}{q_{\max}}, \tag{3.30}$$

where

$$q_{\max} = \max\left(\sqrt{q_{s1}^{d\,2} + q_{c1}^{d\,2}} \quad \sqrt{q_{s2}^{d\,2} + q_{c2}^{d\,2}} \quad \cdots \quad \sqrt{q_{sr}^{d\,2} + q_{cr}^{d\,2}}\right). \tag{3.31}$$

By making these changes, it is guaranteed that the method compares the amplitudes of harmonics with the maximum harmonic and applies the harmonic selection criteria accordingly. In return, the method is more likely to exclude harmonics that do not make a significant contribution to the total response.

3.5.2 Case Study 7: Application of AHBM 4 on a SDOF System

The same system given in Section 3.2.1 was investigated with AHBM 4 under the effect of following parameters: $\varepsilon_t = 10^{-6}$ and $N_h^m = 10$. The results for this parameter set are given in Figure 3.86 to Figure 3.89. The results indicate that the method does not allow the number of harmonics to decrease under 9 except for one point in this case.
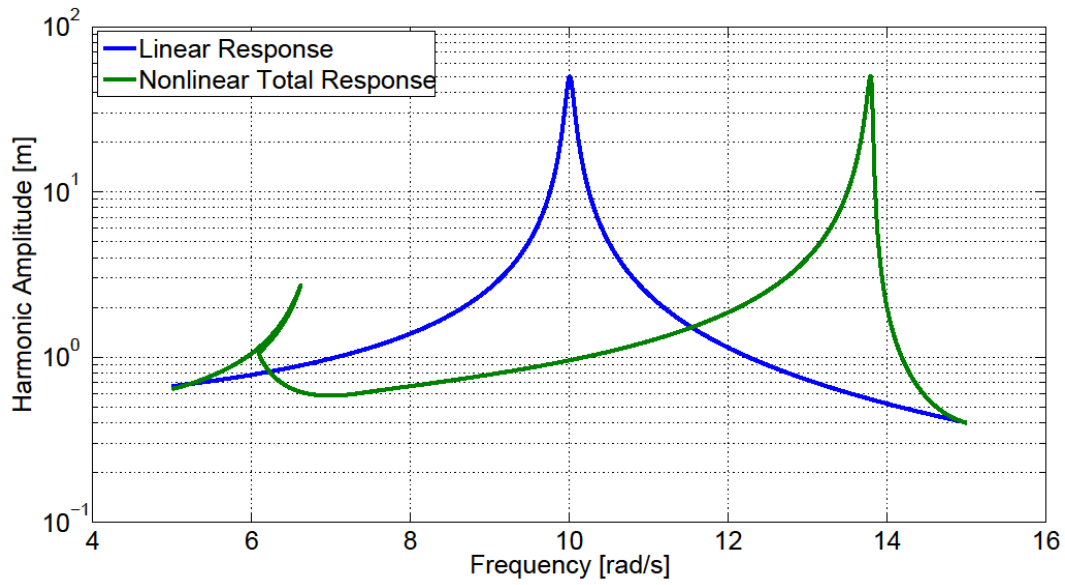
Figure 3.86 Linear and nonlinear total response curves for Case Study 7, Parameter Set 1
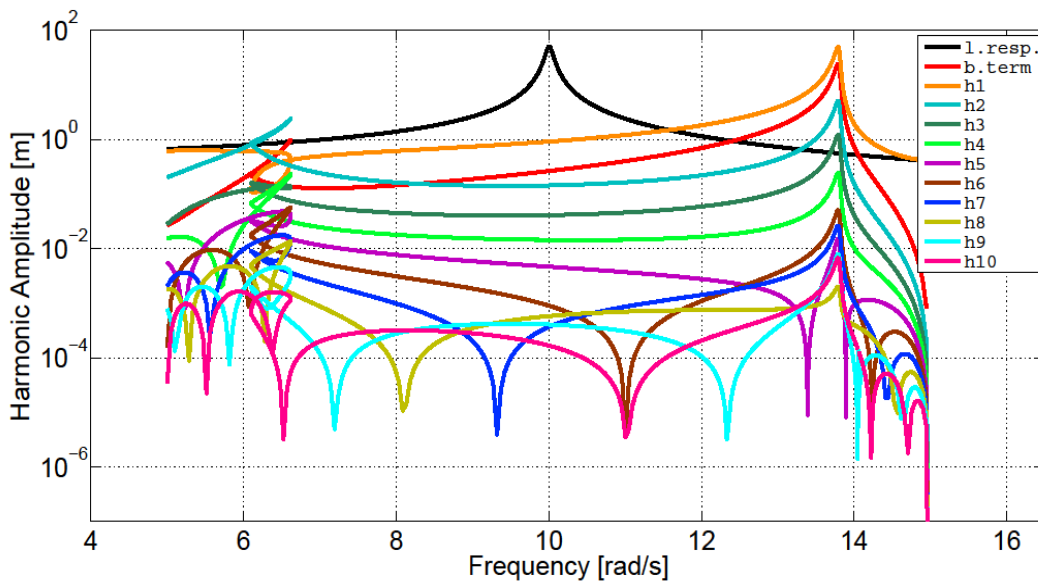
Figure 3.87 Amplitudes of Harmonics for Case Study 7, Parameter Set 1
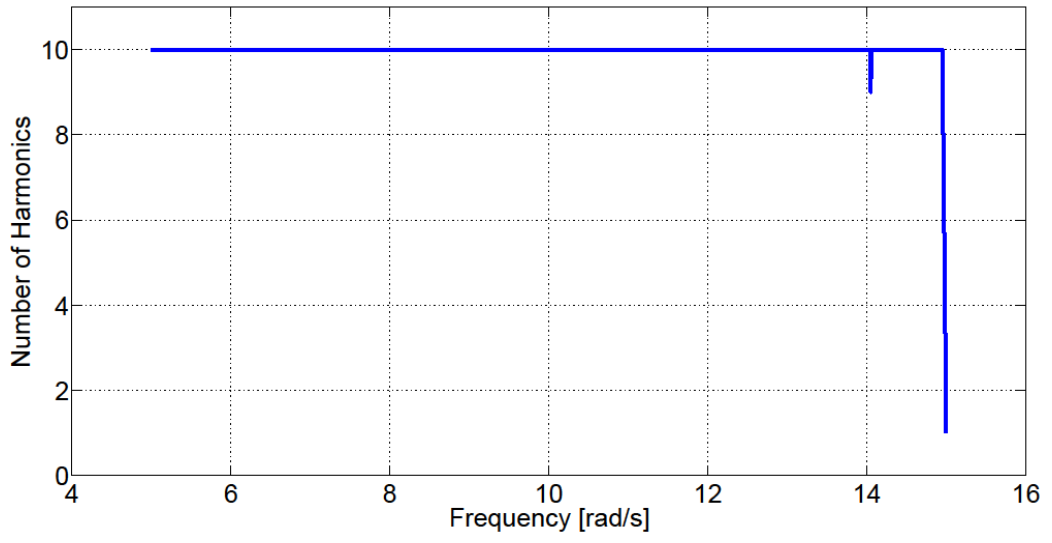
Figure 3.88 Number of harmonics used at each frequency Case Study 7, Parameter Set 1
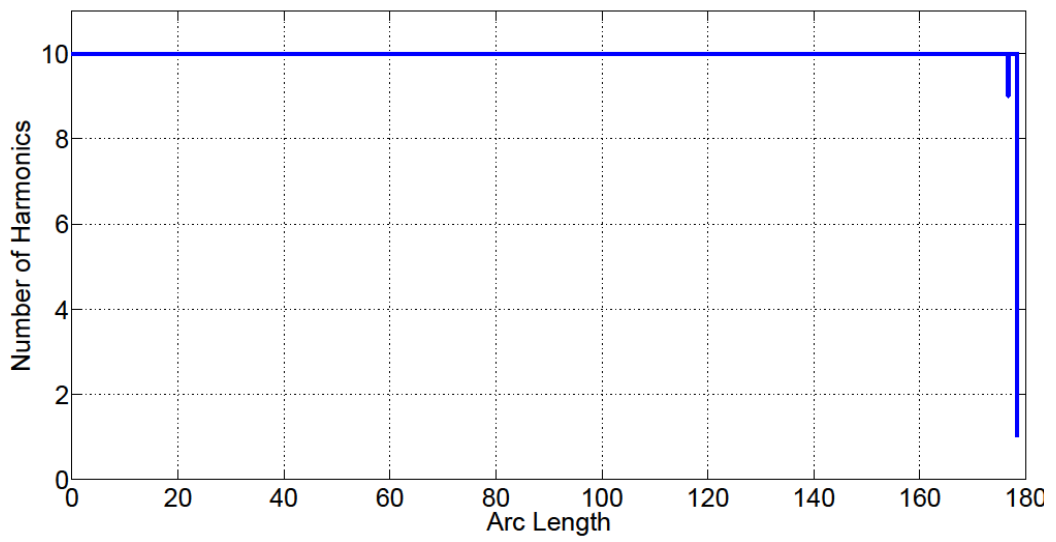
Figure 3.89 Number of harmonics used for Case Study 7, Parameter Set 1

For the second part of the study, control parameter is changed as $\varepsilon_t = 10^{-2}$. Results obtained with this parameter set are given in Figure 3.90 to Figure 3.93. From the results it can be seen that, compared to the first set of results, the retained number of harmonics decreased as expected. However the change in the total response is marginal.
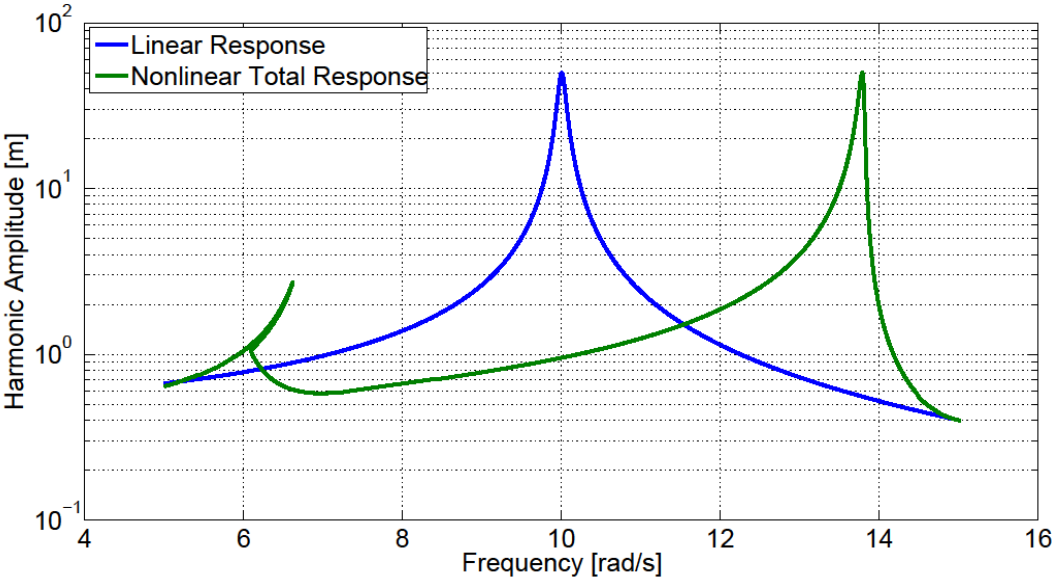
Figure 3.90 Linear and nonlinear total response curves for Case Study 7, Parameter Set 2
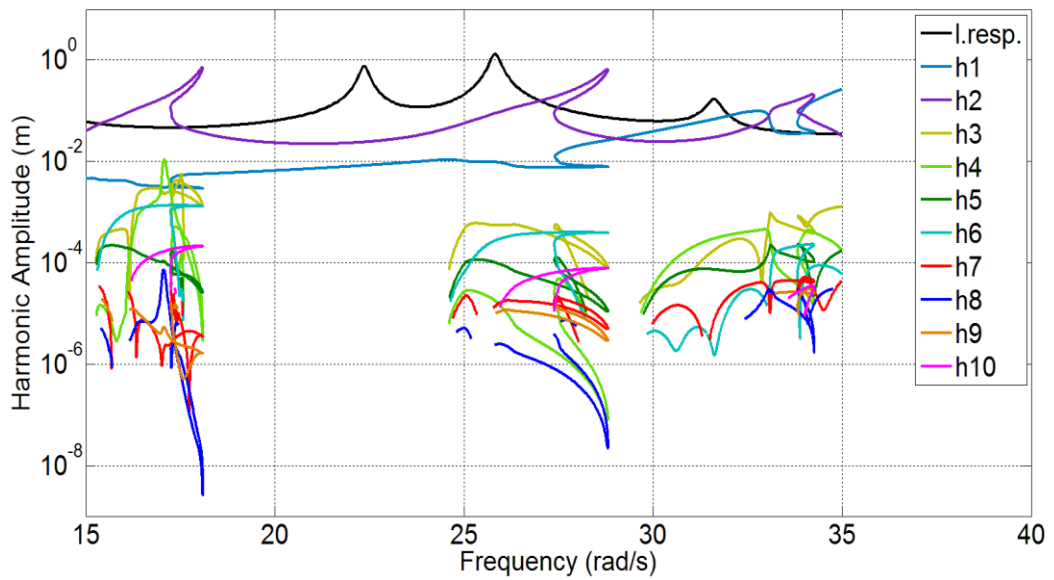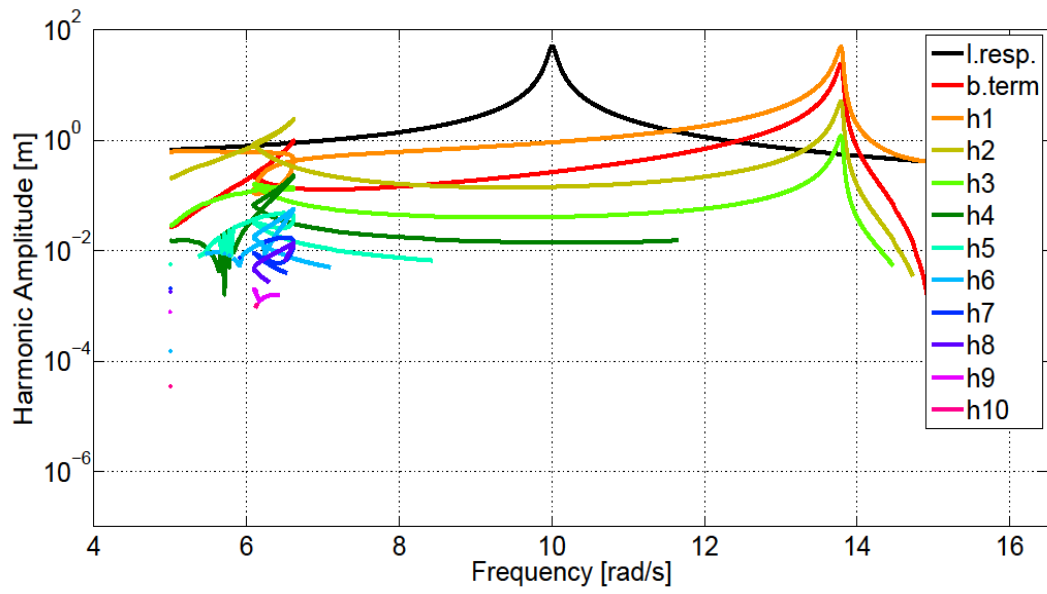
Figure 3.91 Amplitudes of Harmonics for Case Study 7, Parameter Set 2
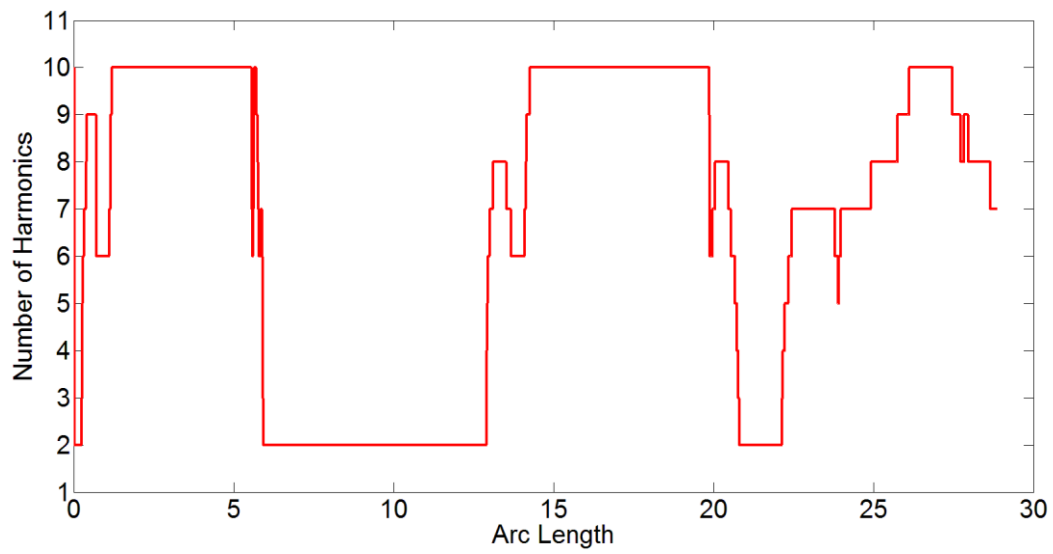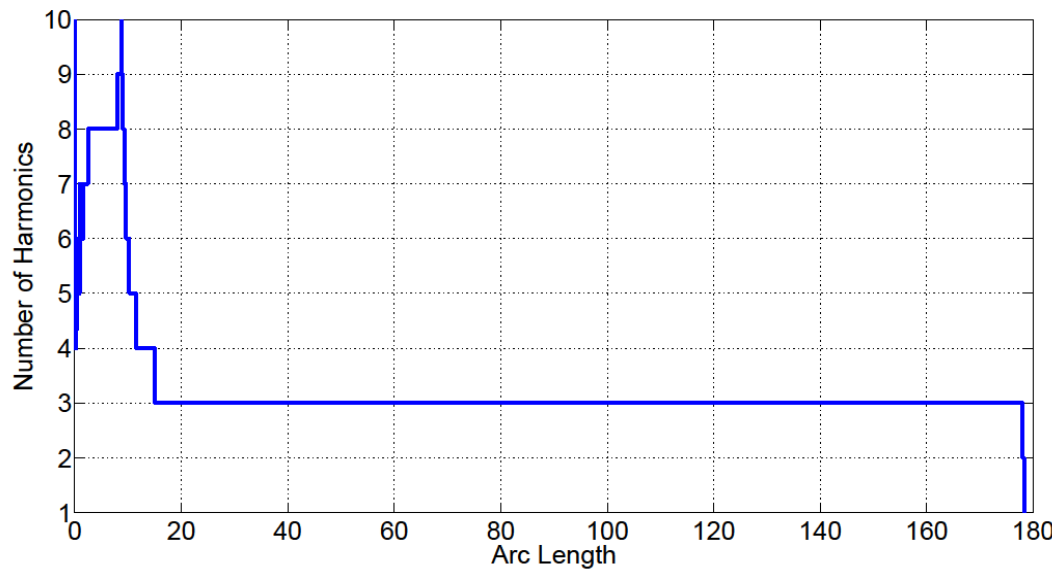

Figure 3.92 Number of harmonics used for Case Study 7, Parameter Set 2
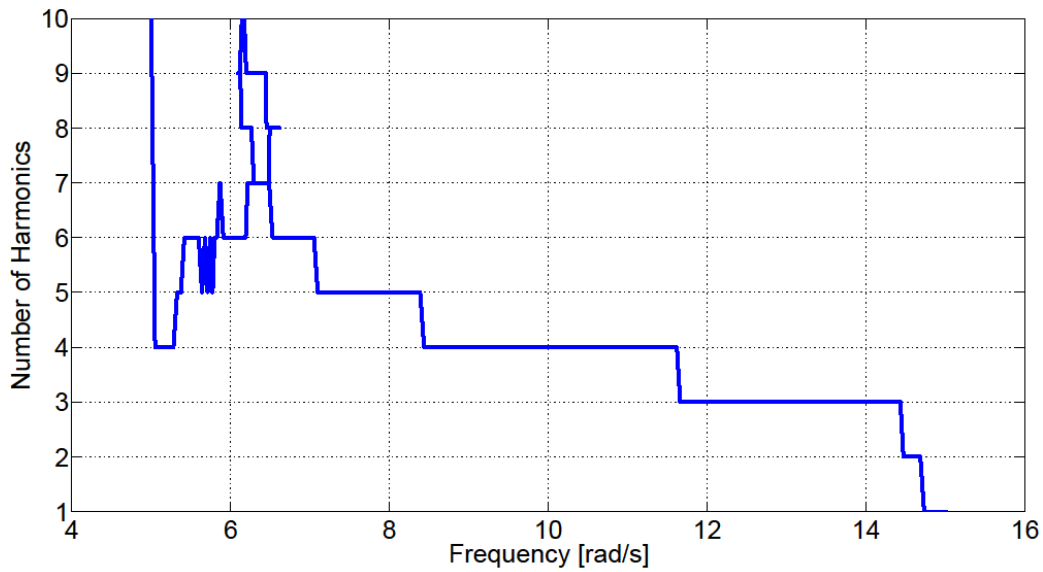
Figure 3.93 Number of harmonics used at each frequency Case Study 7, Parameter Set 2

3.5.3   Case Study 8: Application of AHBM 4 on a MDOF System

The same system described in Section 3.2.2 is used for this study. For the first part of the study, the control parameter is taken as $\varepsilon_t = 10^{-10}$ and the maximum number of harmonics is taken as $N_h^m = 10$. The results obtained are given in Figure 3.94 to Figure 3.101. The results show similarity with those obtained with AHBM 2 and AHBM 3. The algorithm retained all the available harmonics in the solution except for the regions where the system behaves almost linear. In Figure 3.102 and Figure 3.103 the effect of each threshold criterion on the number of harmonics can be found. Since the control parameter is chosen very small, the second criterion does not have a visible effect on the number of harmonics.
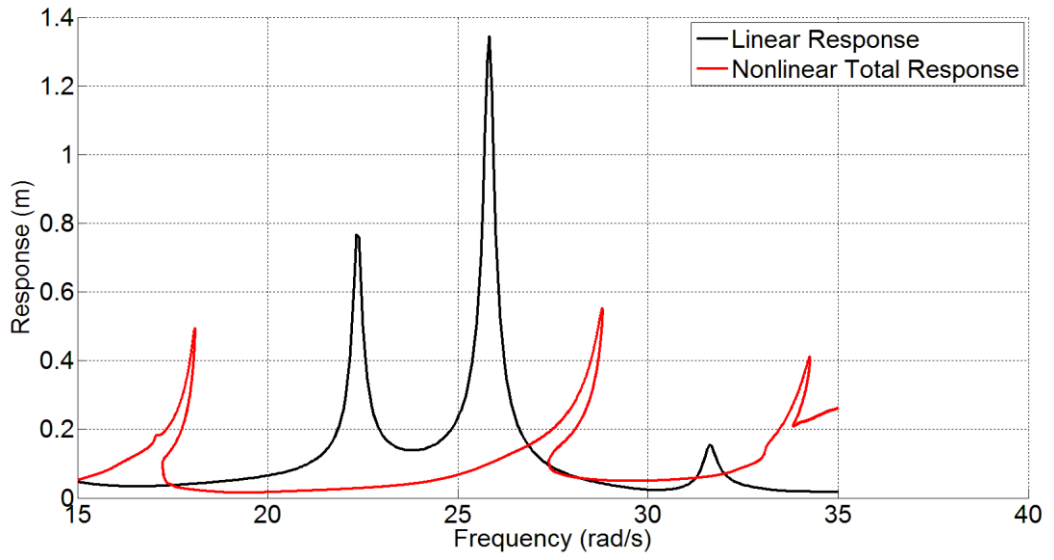
Figure 3.94 Response of the first DOF for Case Study 8, Parameter Set 1
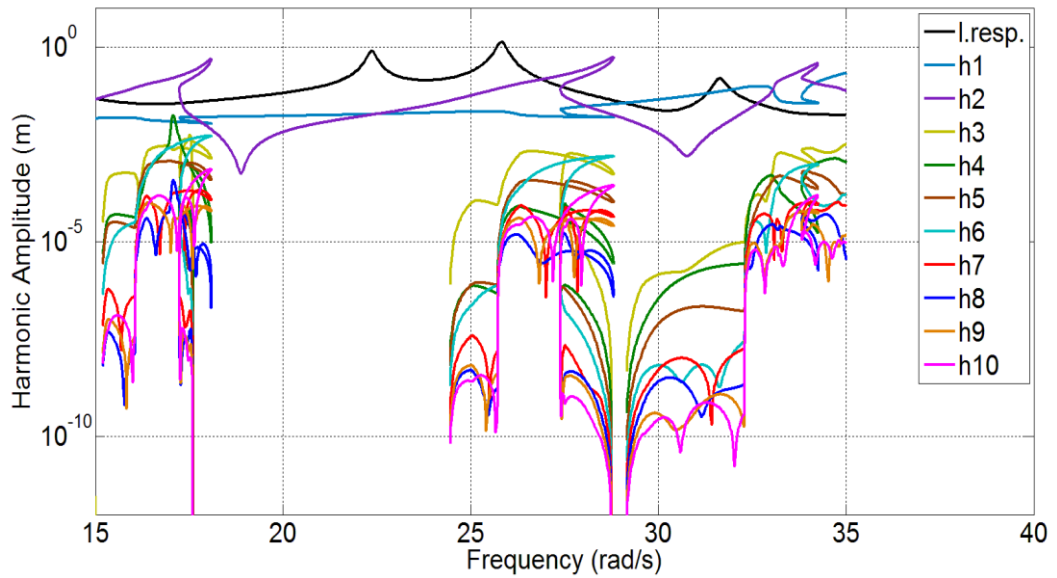
Figure 3.95 Harmonics of the first DOF for Case Study 8, Parameter Set 1

135
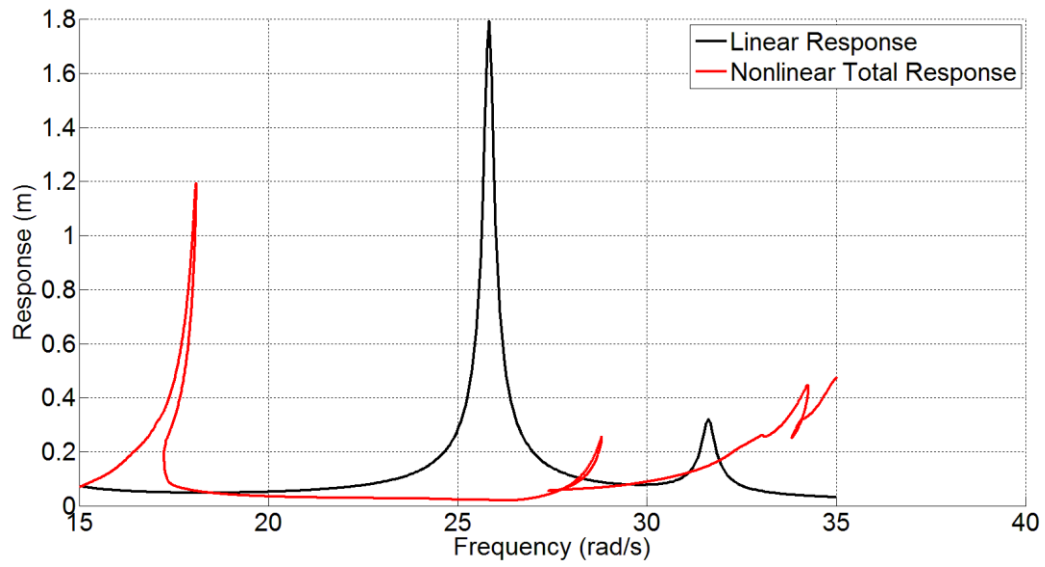
Figure 3.96 Response of the second DOF for Case Study 8, Parameter Set 1
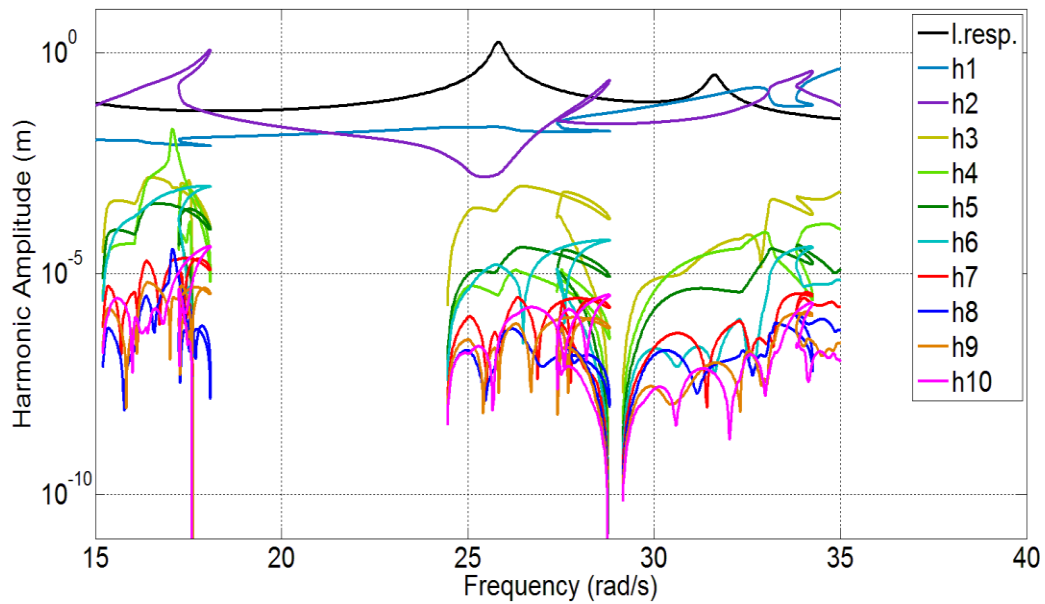
Figure 3.97 Harmonics of the second DOF for Case Study 8, Parameter Set 1

136
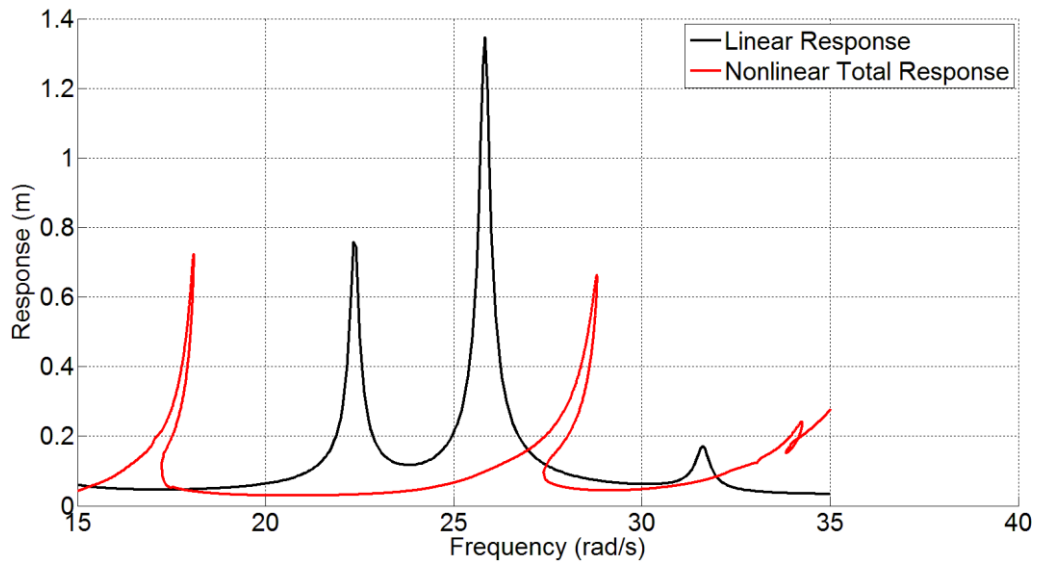
Figure 3.98 Response of the third DOF for Case Study 8, Parameter Set 1
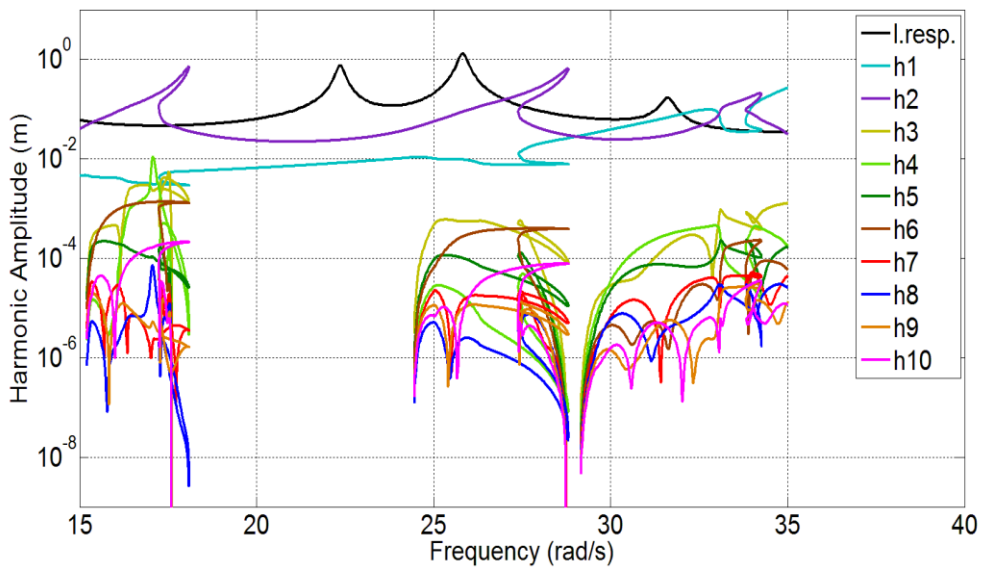
Figure 3.99 Harmonics of the third DOF for Case Study 8, Parameter Set 1

137
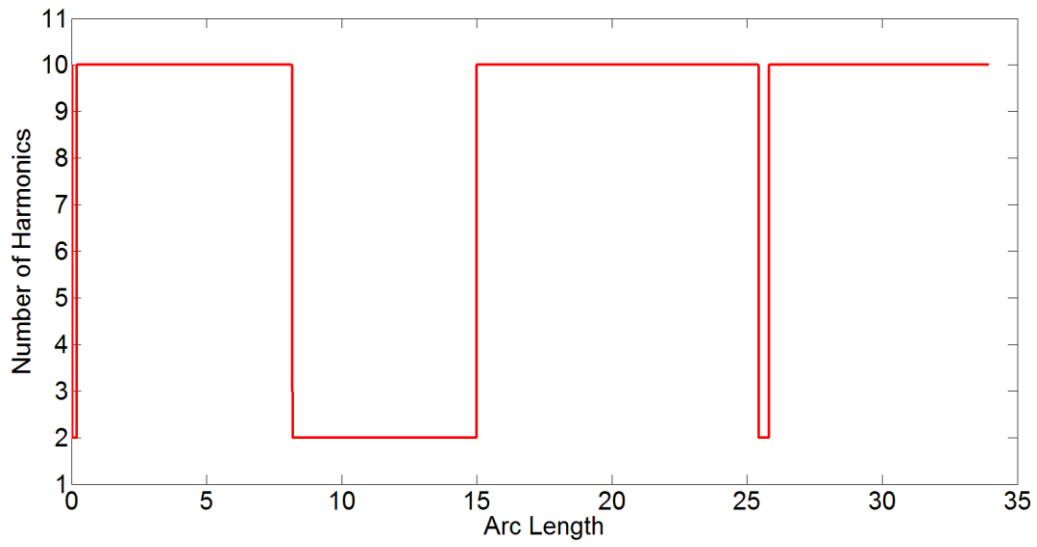
Figure 3.100 Number of harmonics used for Case Study 8, Parameter Set 1
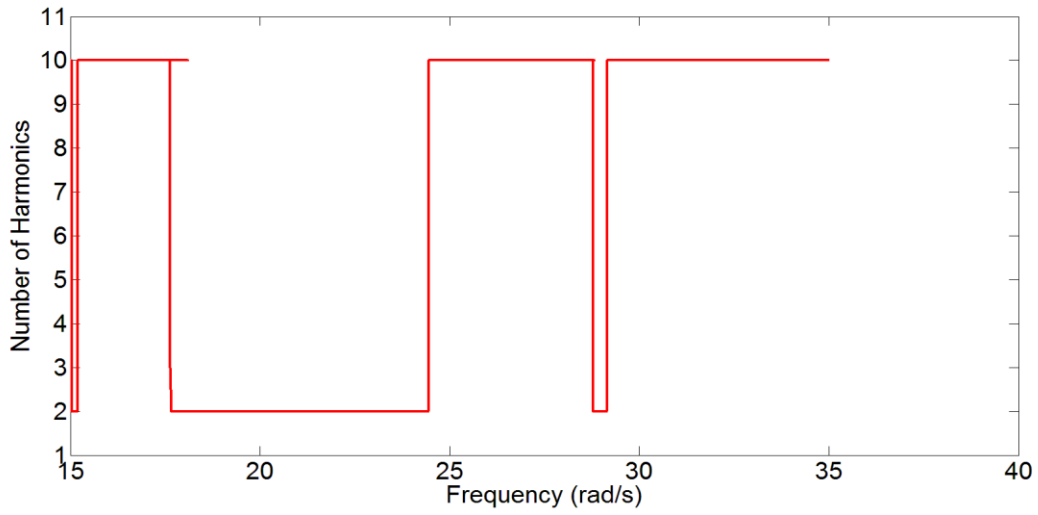
Figure 3.101 Number of harmonics used at each frequency for Case Study 8, Parameter Set 1
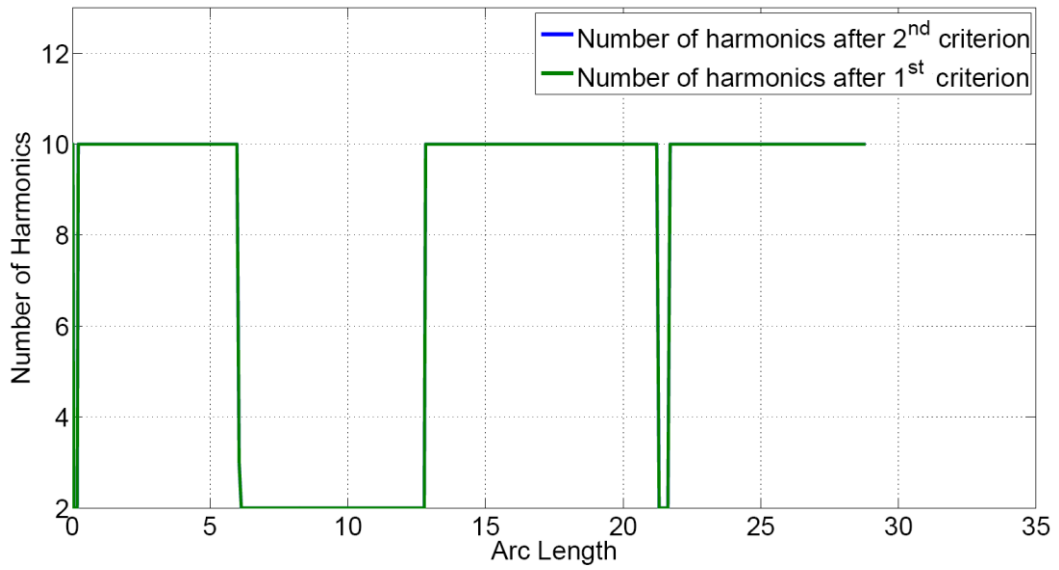
Figure 3.102 The change in harmonics due to application of threshold criteria
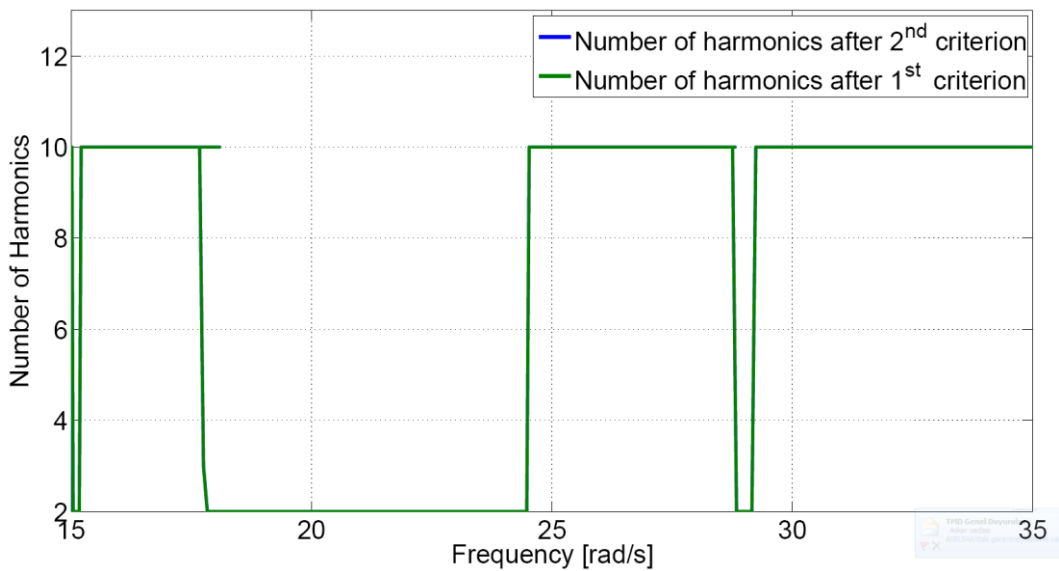
Figure 3.103 The change in harmonics due to application of threshold criteria at each frequency

139

For the second part of the study, the parameters are altered as $\varepsilon_t = 10^{-2}$ and $N_h^m = 10$. Results for this set of parameters are given in Figure 3.104 to Figure 3.113. As expected, the number of retained harmonics decreased considerably for this case. The computational time decreased as well; whereas, there is no considerable change in the total response. In Figure 3.112 and Figure 3.113 the effect of each threshold criterion on the number of harmonics can be seen clearly. The second criterion proves to be effective.
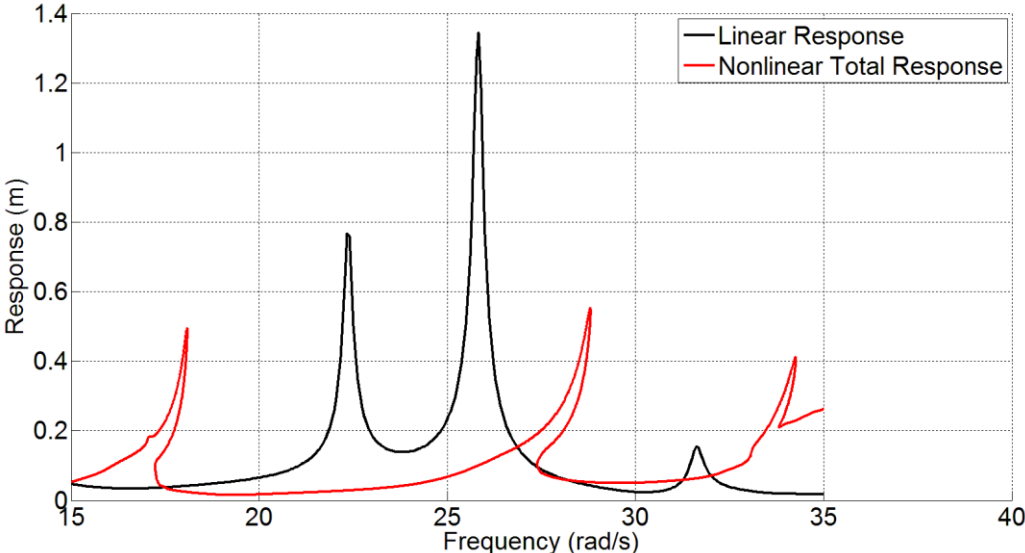
Figure 3.104 Response of the first DOF for Case Study 8, Parameter Set 2
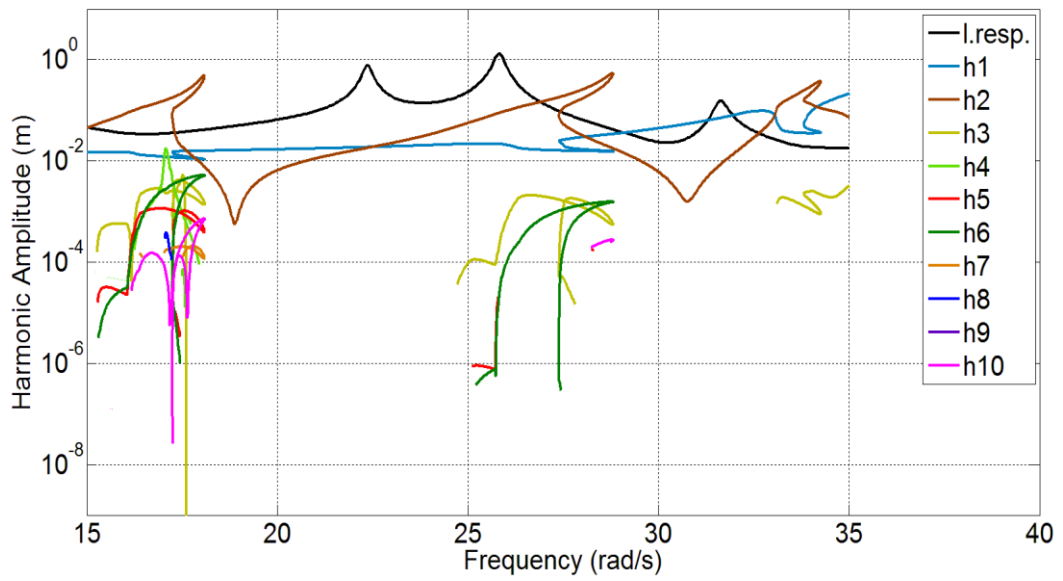
Figure 3.105 Harmonics of the first DOF for Case Study 8, Parameter Set 2
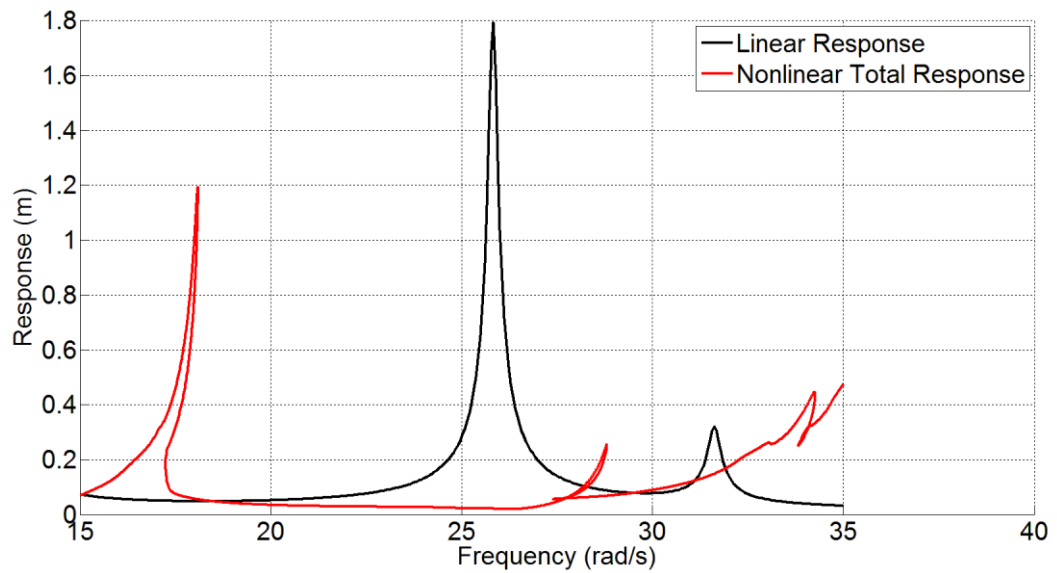
Figure 3.106 Response of the second DOF for Case Study 8, Parameter Set 2

141
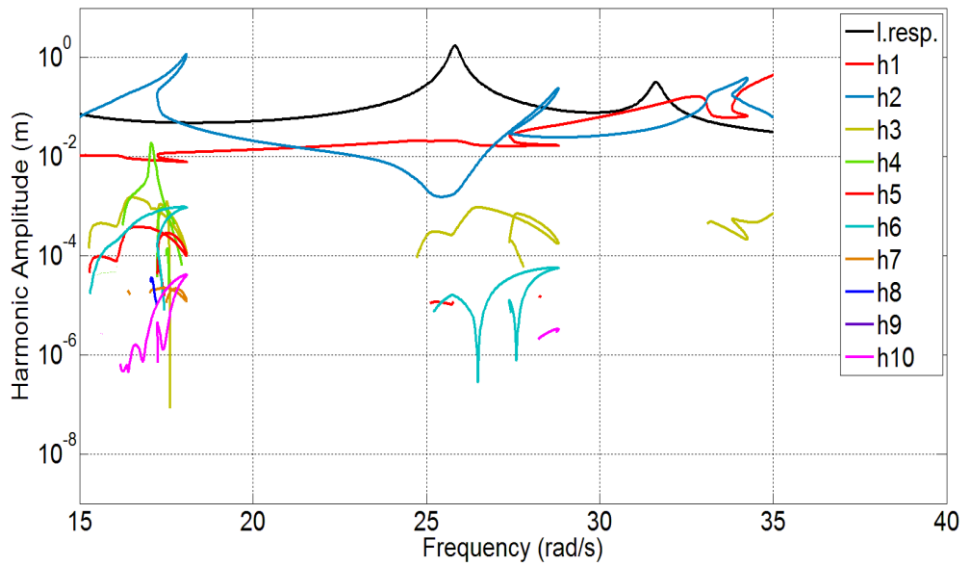
Figure 3.107 Harmonics of the second DOF for Case Study 8, Parameter Set 2
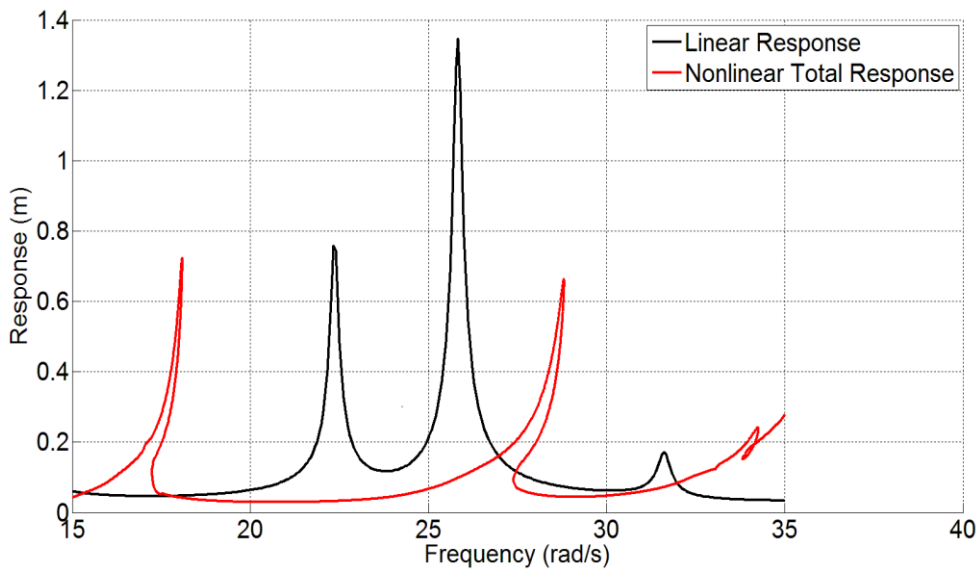
Figure 3.108 Response of the third DOF for Case Study 8, Parameter Set 2

142
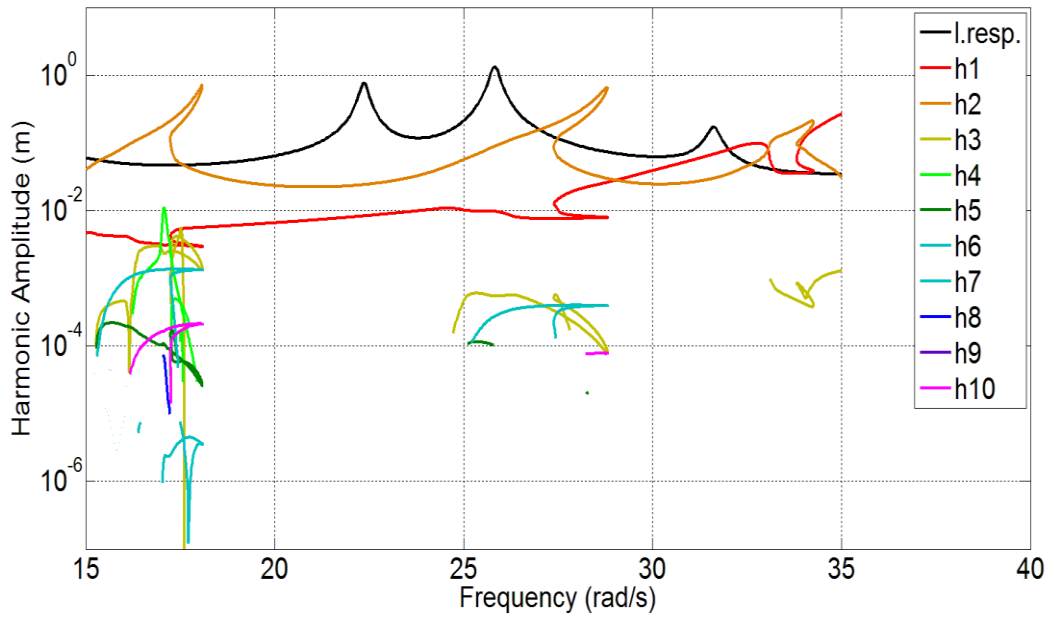
Figure 3.109 Harmonics of the third DOF for Case Study 8, Parameter Set 2
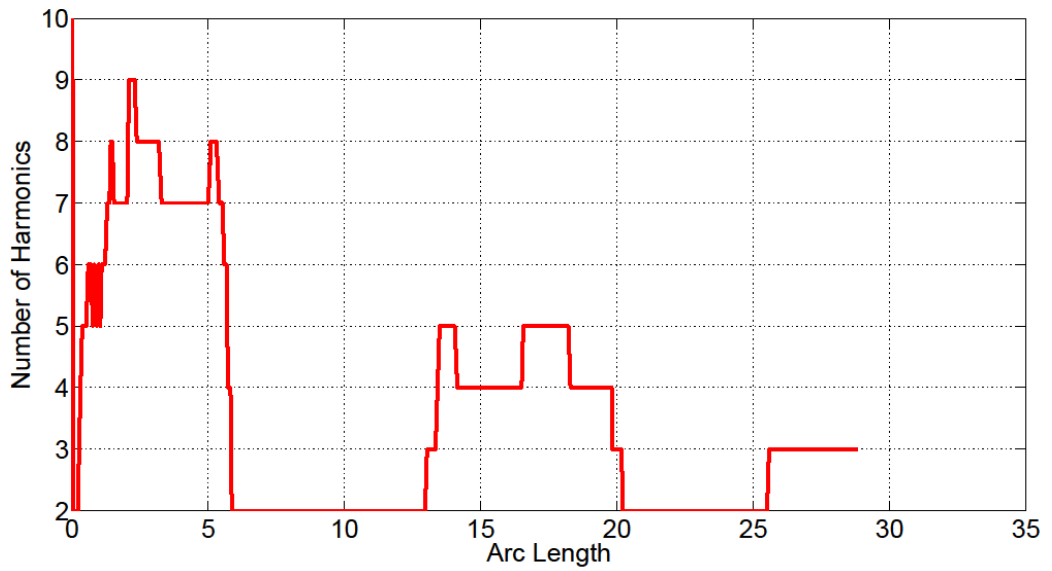
Figure 3.110 Number of harmonics used for Case Study 8, Parameter Set 2
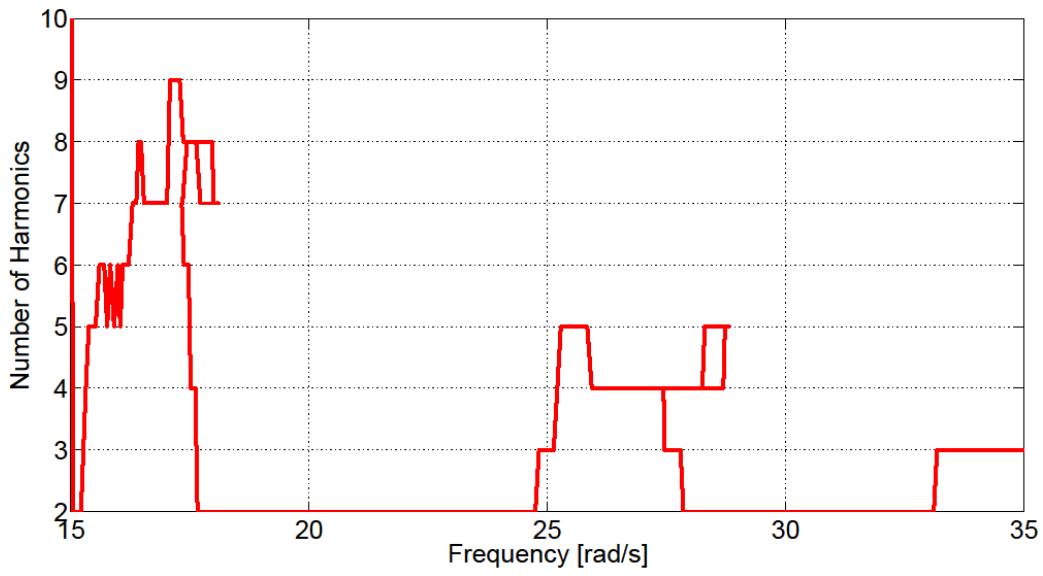
Figure 3.111 Number of harmonics used at each frequency for Case Study 8, Parameter Set 2
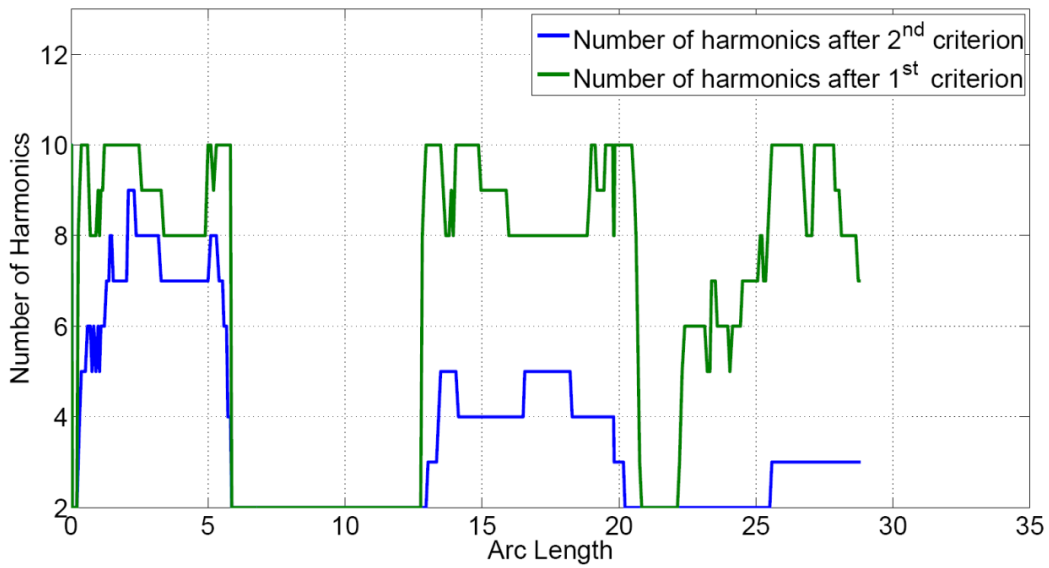
Figure 3.112 The change in harmonics due to application of threshold criteria
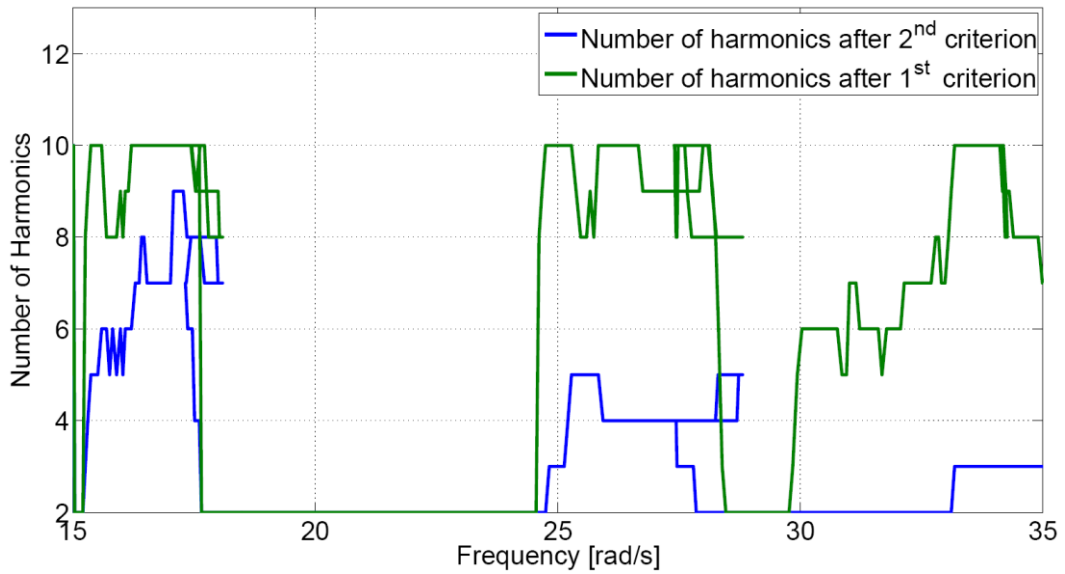
Figure 3.113 The change in harmonics due to application of threshold criteria at each frequency

3.5.4   Case Study 9: Application of AHBM 5 on a MDOF System

The aim of this case study is to demonstrate the difference between AHBM 4 and AHBM 5. The same system described in Section 3.2.2 is used for this study. For the first case, the control parameter is taken as $\varepsilon_t = 10^{-10}$ and the maximum number of harmonics is $N_h^m = 10$. The results are given in Figure 3.114 to Figure 3.120. The results indicate that, in this first part of the study, the results are not different from those obtained with AHBM 4. This is because the threshold parameter is chosen too low.
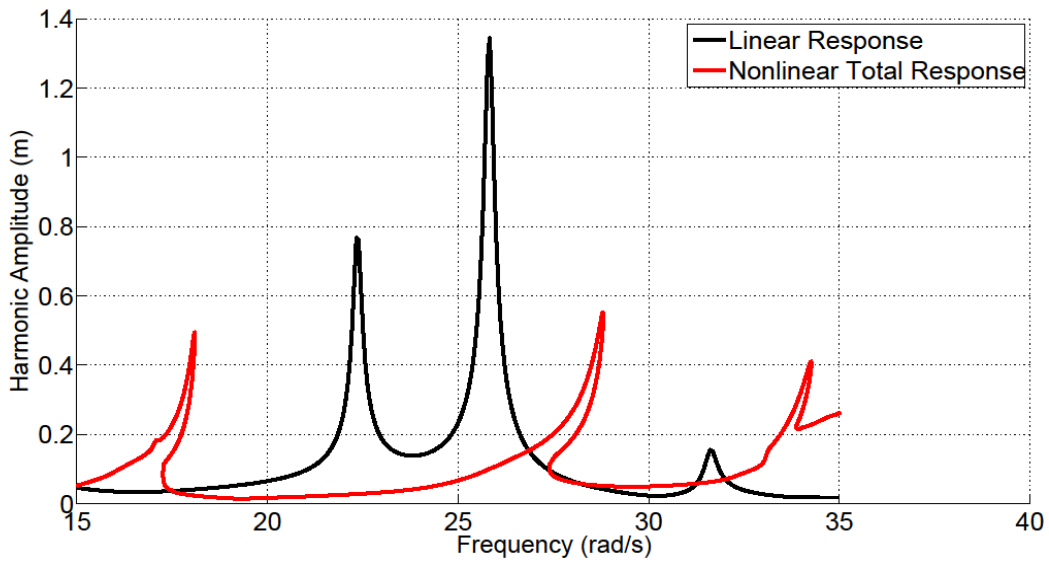
Figure 3.114 Response of the first DOF for Case Study 9, Parameter Set 1
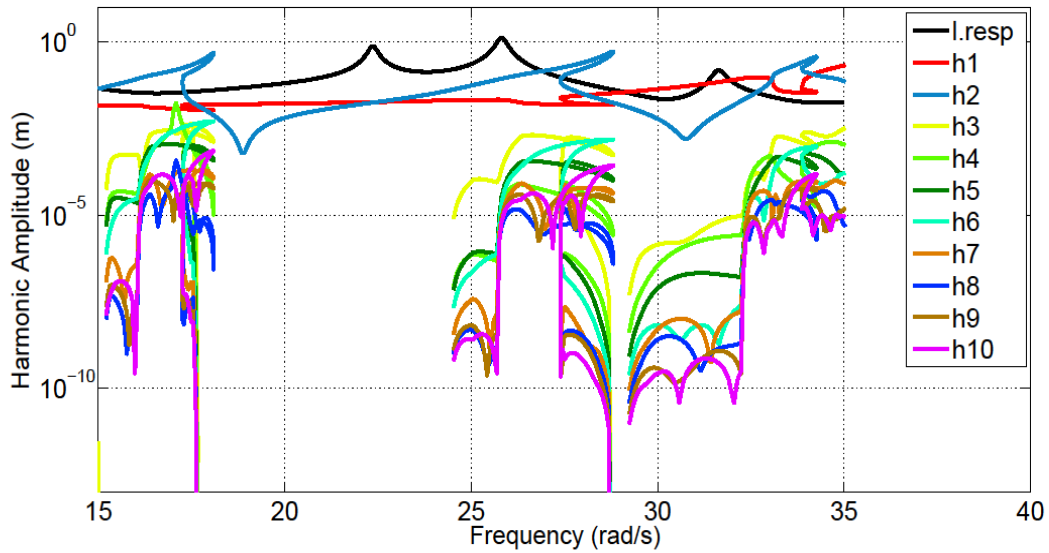
Figure 3.115 Harmonics of the first DOF for Case Study 9, Parameter Set 1

146
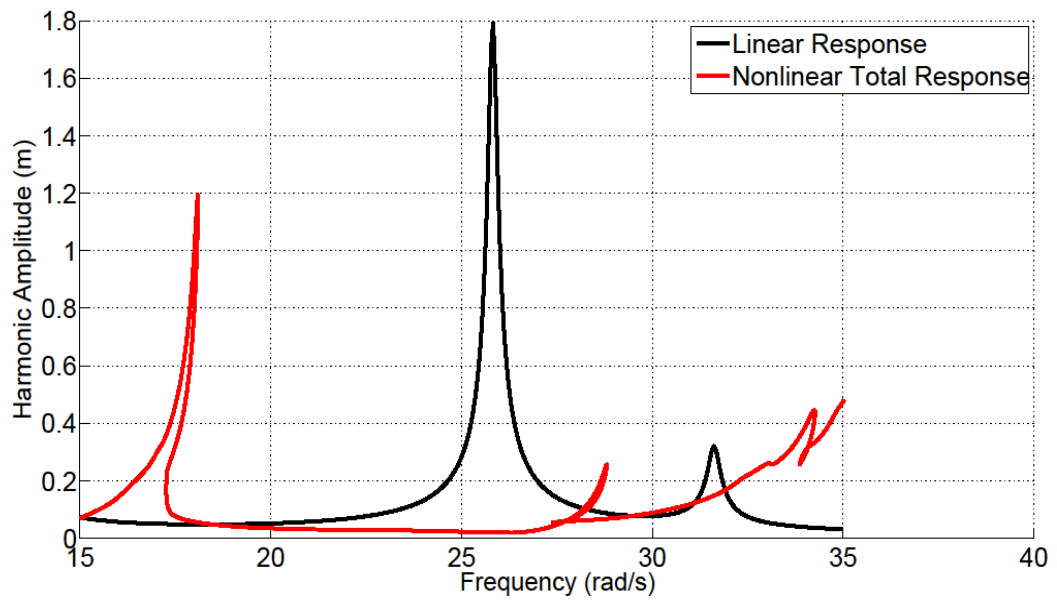
Figure 3.116 Response of the second DOF for Case Study 9, Parameter Set 1
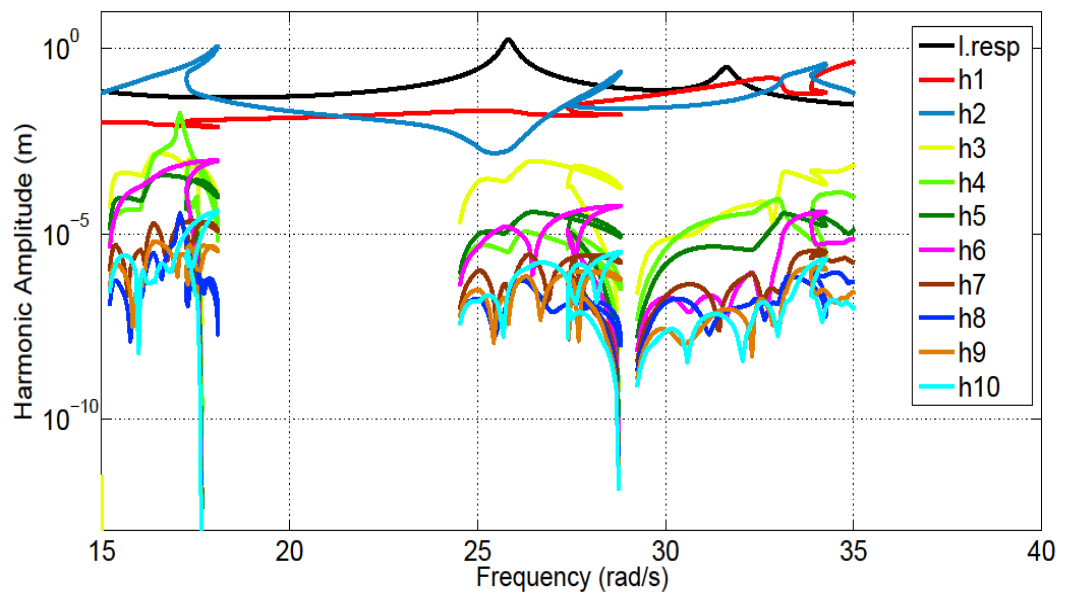
Figure 3.117 Harmonics of the second DOF for Case Study 9, Parameter Set 1
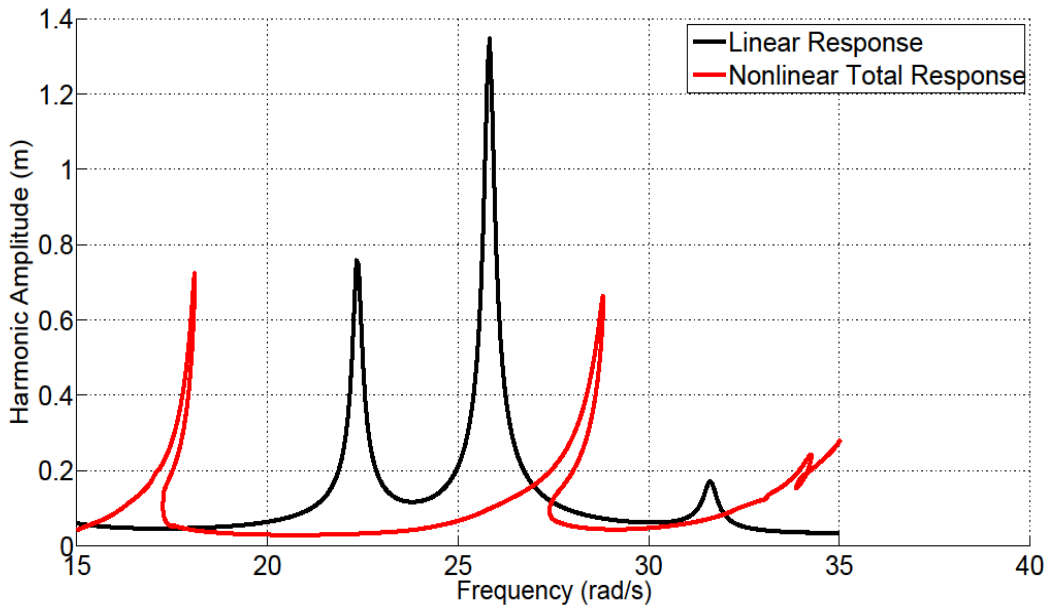
Figure 3.118 Response of the third DOF for Case Study 9, Parameter Set 1
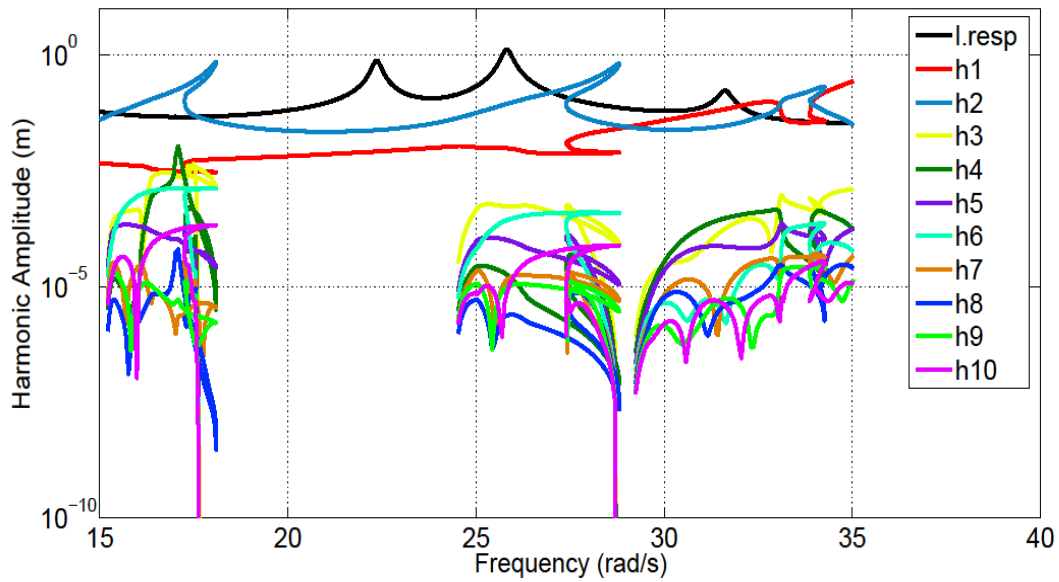
Figure 3.119 Harmonics of the third DOF for Case Study 9, Parameter Set 1

148
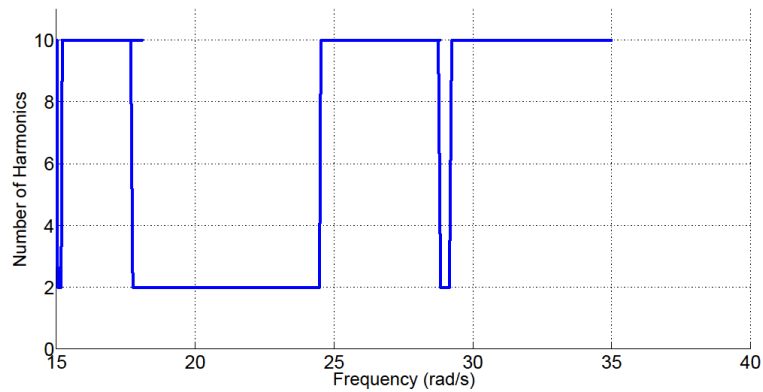
Figure 3.120 Number of harmonics used at each frequency for Case Study 9, Parameter Set 1

For the second part of the study the threshold parameter is set to $\varepsilon_t = 10^{-2}$. The results obtained are given in Figure 3.121 to Figure 3.127. It can be clearly seen from the results that, due to its algorithm AHBM 5 tends to exclude more harmonics from the solution scheme, eventually reducing the computational time, as expected.
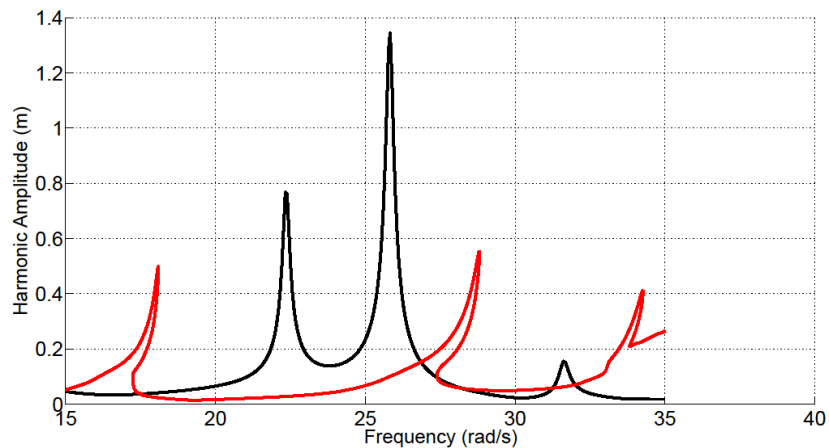
Figure 3.121 Response of the first DOF for Case Study 9, Parameter Set 2
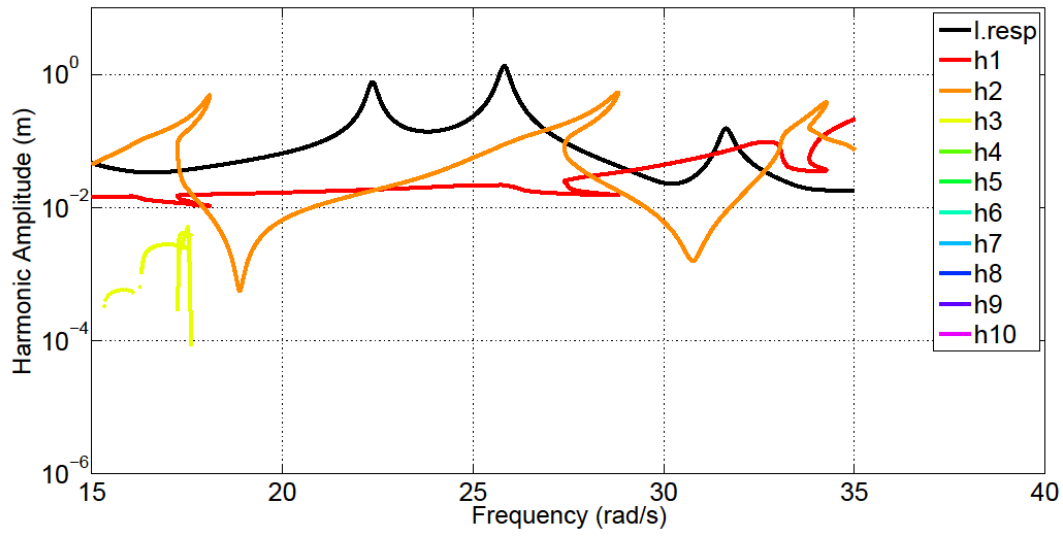
Figure 3.122 Harmonics of the first DOF for Case Study 9, Parameter Set 2
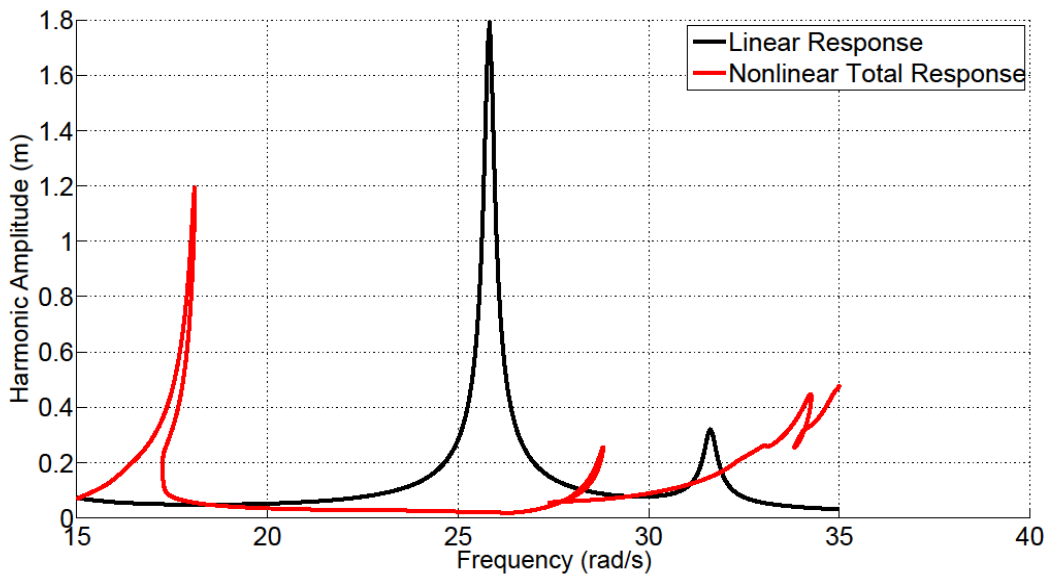
Figure 3.123 Response of the second DOF for Case Study 9, Parameter Set 2
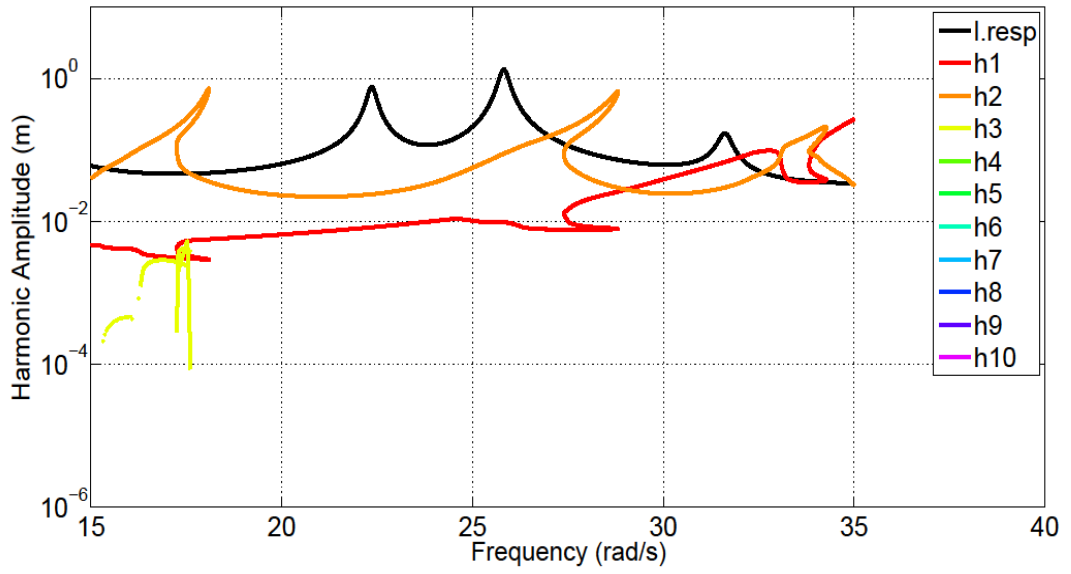
Figure 3.124 Harmonics of the second DOF for Case Study 9, Parameter Set 2
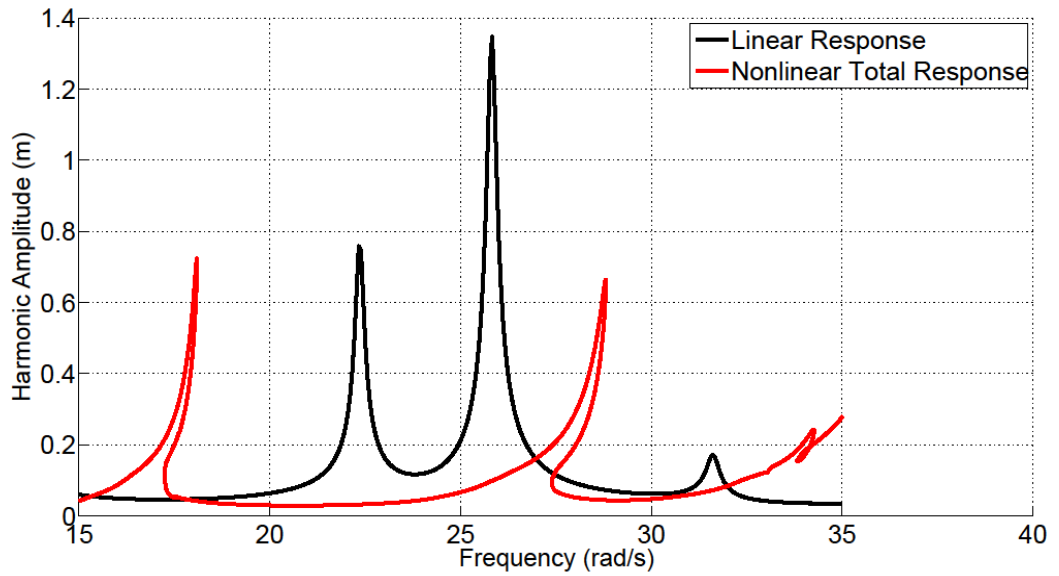
Figure 3.125 Response of the third DOF for Case Study 9, Parameter Set 2
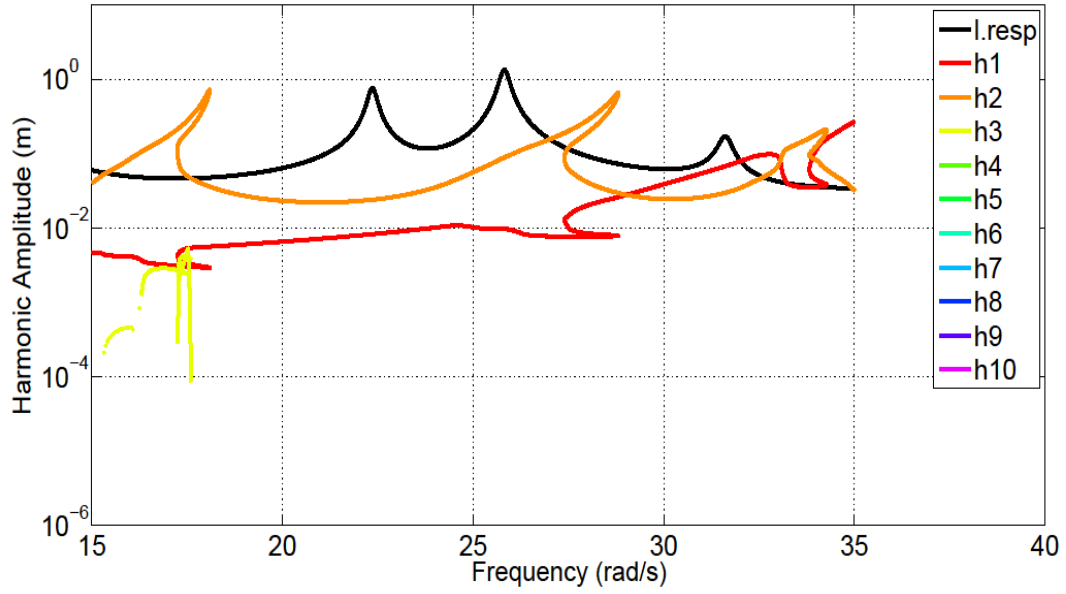
Figure 3.126 Harmonics of the third DOF for Case Study 9, Parameter Set 2
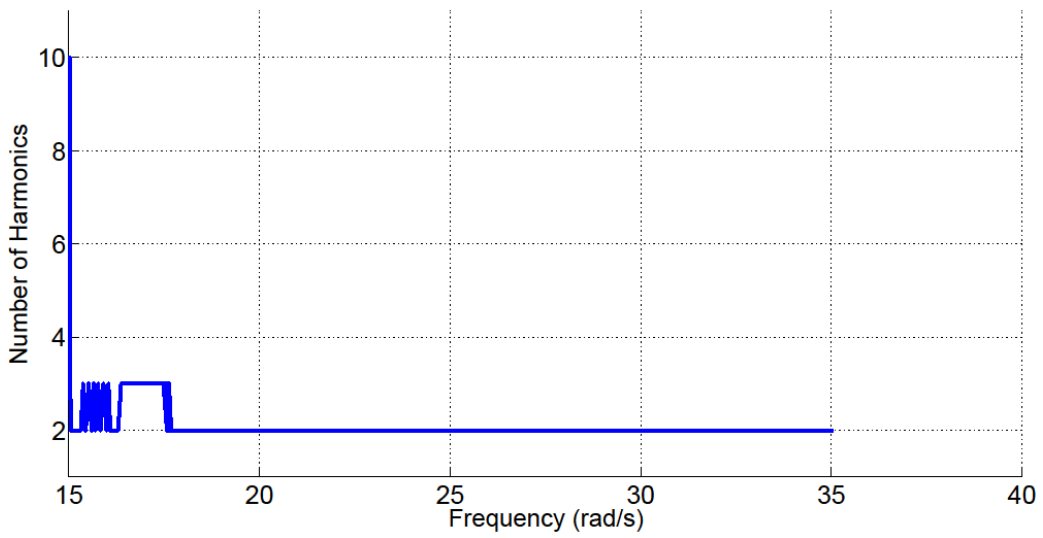
Figure 3.127 Number of harmonics used at each frequency for Case Study 9, Parameter Set 2

CHAPTER 4

THE COMPARISON OF ADAPTIVE HARMONIC BALANCE METHODS

4.1 Introduction

In Chapter 3, existing AHBMs from literature were presented, a new AHBM is introduced and a variant of this method is derived. In Chapter 4, the aim is to compare these methods in terms of their effectiveness and efficiency. For this purpose, in Section 4.2 the methodology of the comparison and metrics used for evaluation are explained. In the following sections, two case studies, which are conducted in the manner described in Section 4.2 are given. Results of the case studies are presented and explained in detail.

4.2 Methodology of the Study

As stated before, the aim of this chapter is to compare the presented AHBMs in terms of accuracy of their solutions and computational time required. With the purpose of making a fair comparison, the methods which obtain the same order of accuracy using the shortest time are pointed out as the most effective ones.

In the field of structural dynamics, the main concern is the magnitude of oscillations throughout a certain frequency spectrum. Therefore, in the case of a nonlinear frequency response obtained by HBM, it is natural for one to be interested in the total response and the contribution made to the total response by each harmonic, rather than the harmonics themselves. For this reason, in the methodology which will be described in the remaining of this section, the error in total response is used as a measure of solution accuracy.

In the case studies, after the discrete nonlinear dynamic system to be analyzed is chosen with the intention of forming an absolute reference from which the AHBMs are to be evaluated, a 10-harmonic classical HBM solution is performed at the first step. After the amplitudes of each harmonic are examined, it is decided that a 10 harmonic solution is sufficient to express the response to an acceptable degree. Therefore, the total response curve obtained from this solution, i.e. with 10 harmonics, is assumed to be correct. Then, analyses are performed for the same dynamic system by using the AHBMs. With the purpose of forming a data repository for each adaptive method, the analyses are repeated for various sets of control parameters. Accuracies of the total response curves obtained from AHBMs are evaluated by calculating how much these curves deviate from the total response obtained from the 10 harmonic solution, i.e. the error they make, at the chosen frequencies. Since it is very difficult to measure the distance between points inside the unstable region and also it is difficult to observe the unstable region in a real-life experiment, the frequency points inside that part are excluded from the error calculations.

When comparing two different total response values, one obtained from the classical solution and the other from an AHBM solution, one must guarantee that these points correspond to the same frequency. Otherwise, the comparison loses its physical meaning. In order to make the frequencies correspond, the step size is taken as constant in the arc length continuation scheme. When the frequencies failed to overlap, even with the constant step size, linear interpolation is performed. To prevent the interpolation from making inaccurate estimations, the step size is chosen as a small value; hence the distance between two neighboring solution points is significantly decreased. After the error values are obtained for all of the chosen frequency points, integral error and relative error values are computed for each case. For computing the integral error, the trapz function of MATLAB® is used. Since the step size is chosen as a small value, it is considered that the number of partitions to

be used in the trapezoidal rule and the accuracy obtained sufficient to give an idea about the order of integral error.

The amounts of time spent during solution are measured by the tic-toc function of MATLAB®. To make the comparison fair, all of the analyses are performed on the same Dell XPS 15-L502X laptop computer having a 2.0 GHz Intel Core i7-2630 (quad core) processor and 4 GB of 667 MHz DDR3 RAM.

4.3   Case Study 1

In this section, the 2-DOF system, which is used in the error analysis, is presented. In the following sub-sections, Section 4.3.1 to Section 4.3.3, the results obtained from the analyses performed on this 2-DOF system are demonstrated and in Section 4.3.4, the results are compared with each other.

The studied system is illustrated in Figure 3.18. Parameters of the system and parameters of the piecewise linear stiffness elements are given in Table 3.3 and Table 3.4, respectively. The system, parameters of which are given in Table 4.1, is illustrated in Figure 4.1.
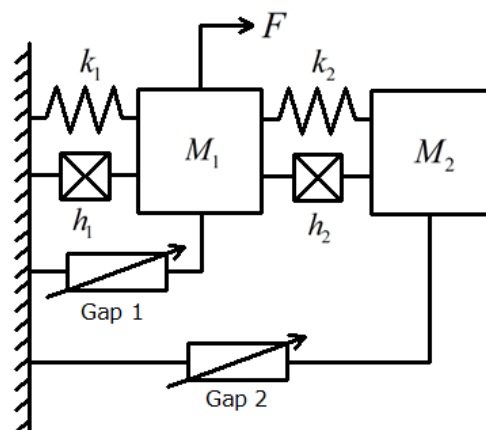
Figure 4.1 A 2-DOF system with gap nonlinearity

Table 4.1 Parameters for the 2-DOF System

M_1 (kg)	M_2 (kg)	k_1, k_2 (N/m)	h_1, h_2 (N/m)	F (N)
1	0.75	5000	50	$30\sin(\theta) + 30\sin(2\theta) + 30\sin(3\theta)$

Studying the linear part of the system, one can find the natural frequencies as 48.21 rad/s and 119.76 rad/s. The frequency range in consideration is selected between 35 rad/s and 65 rad/s which covers the first resonance frequency. Since a 3-harmonic excitation is applied to the first DOF, in the frequency response plot one can expect to see two super-harmonic resonances located at 39.92 rad/s and 59.88 rad/s, the points where 2ω and 3ω are equal to the second natural frequency. In addition, one more peak should appear at 48.21 rad/s, at the first natural frequency.

Parameters of the nonlinear elements used the model are given in Table 4.2. Gap nonlinearity is chosen for this study, since, as it is shown in the previous chapters, it excites higher harmonics in certain frequency intervals, whereas outside these intervals, the system acts like a linear structure. Therefore the adaptive algorithms are forced to change the number of retained harmonics frequently. The results obtained from the 10-harmonic classical solution are given in Figure 4.2 and Figure 4.3.

Table 4.2 Parameters for Nonlinear Elements

	δ (m)	k_g (N/m)
Gap 1	0.05	500
Gap 2	0.1	500
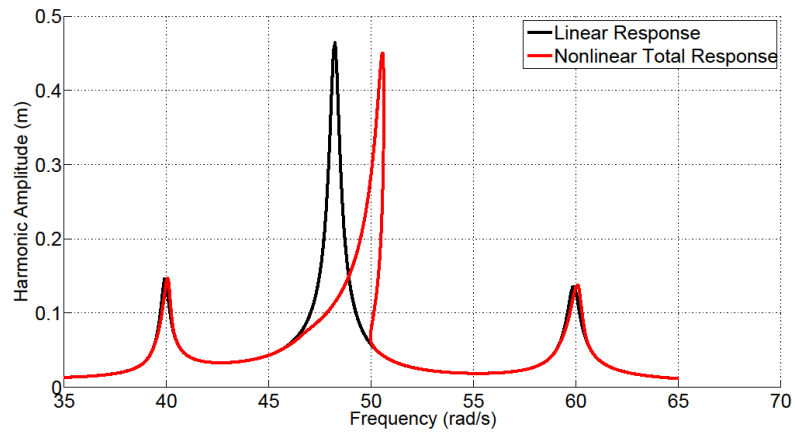
Figure 4.2 Total Response of the First DOF
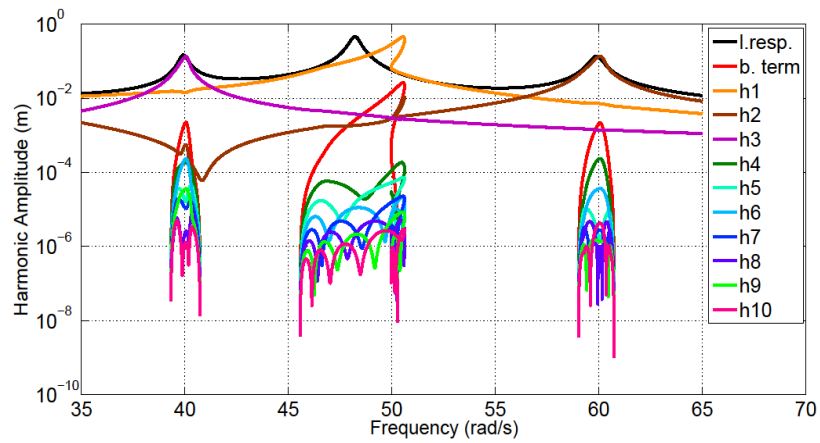
Figure 4.3 Amplitudes of harmonics for the first DOF

For the error analysis, the frequency response curve is studied in 3 parts, as shown in Figure 4.4. As explained in the previous section, the unstable region is excluded from the error analysis.

For comparison, the following parameters are used:

1. Maximum error around the first peak (Region 1)

2. Maximum error around the primary resonance (Region 2)

3. Maximum error around the third peak (Region 3)

4. Maximum relative error around primary resonance (Region 2)

5. Integral error (all regions combined)
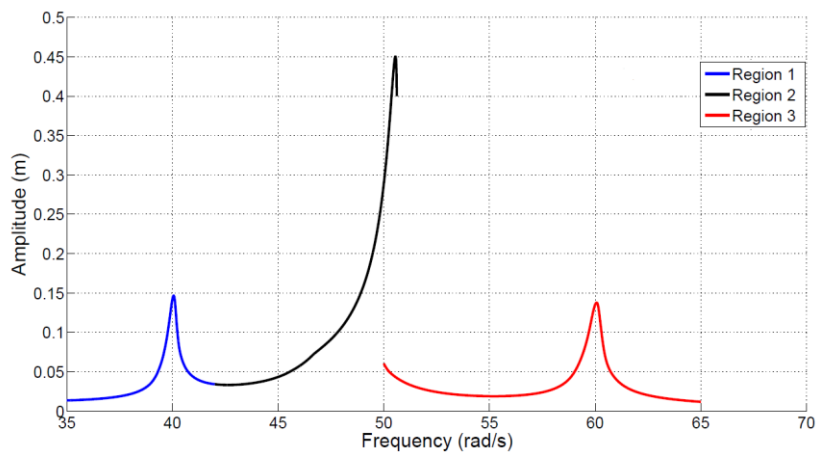
Figure 4.4 Regions defined for error analysis

4.3.1 Results Obtained by AHBM 1: Jaumouille´, Sinou and Petitjean's Method

As explained in Chapter 3, this method uses a threshold value, ε, to adjust the number of harmonics retained. Due to its definition, ε must be greater than 0 and less than 1. Making ε smaller forces the algorithm to retain more harmonics.

For this study, analyses are carried out for ε values ranging between 10^{-2} and 10^{-30}. The resulting maximum absolute error, maximum relative error, integral error values

and amounts of time spent for computation are given in Table 4.3, Table 4.4 and Table 4.5. The percentages of reduction obtained in computational time with respect to the 10-harmonic classical HBM solution are given in Table 4.6.

Table 4.3 Maximum Absolute Error Values for AHBM 1

ε	Time (sec)	Max. Err 1	Max. Err 2	Max. Err 3
1.00E-02	654.3	1.45E-04	1.21E-04	3.80E-05
1.00E-04	776.6	1.45E-04	1.21E-04	3.69E-05
1.00E-06	976.1	1.13E-04	7.71E-05	3.50E-05
1.00E-08	1293.9	1.12E-04	7.71E-05	3.37E-05
1.00E-10	1934.8	1.12E-04	7.71E-05	3.37E-05
1.00E-12	2228.0	1.12E-04	7.71E-05	3.37E-05
1.00E-14	2569.6	1.12E-04	7.71E-05	3.37E-05
1.00E-16	2894.4	1.12E-04	7.71E-05	3.37E-05
1.00E-20	3061.5	1.12E-04	7.71E-05	3.37E-05
1.00E-25	3082.2	1.12E-04	6.73E-05	3.07E-05
1.00E-30	3069.6	1.12E-04	6.73E-05	3.07E-05

Table 4.4 Maximum Relative Error Values for AHBM 1

ε	Time (sec)	Max. Err 1 (Rel)	Max. Err 2 (Rel)	Max. Err 3 (Rel)
1.00E-02	654.3	1.192E-03	3.02E-04	3.02E-04
1.00E-04	776.6	1.192E-03	3.02E-04	2.77E-04
1.00E-06	976.1	9.26E-04	2.64E-04	2.67E-04
1.00E-08	1293.9	9.26E-04	2.64E-04	2.67E-04
1.00E-10	1934.8	9.26E-04	2.64E-04	2.67E-04
1.00E-12	2228.0	9.26E-04	2.64E-04	2.67E-04
1.00E-14	2569.6	9.26E-04	2.64E-04	2.67E-04
1.00E-16	2894.4	9.26E-04	2.64E-04	2.67E-04
1.00E-20	3061.5	9.26E-04	2.64E-04	2.67E-04
1.00E-25	3082.2	9.28E-04	2.65E-04	2.81E-04
1.00E-30	3069.6	9.28E-04	2.65E-04	2.81E-04

Table 4.5 Integral Error Values for AHBM 1

ε	Time (sec)	Total Integral Error
1.00E-02	654.3	2.14E-04
1.00E-04	776.6	2.04E-04
1.00E-06	976.1	1.45E-04
1.00E-08	1293.9	1.43E-04
1.00E-10	1934.8	1.43E-04
1.00E-12	2228	1.43E-04
1.00E-14	2569.6	1.43E-04
1.00E-16	2894.4	1.43E-04
1.00E-20	3061.5	1.43E-04
1.00E-25	3082.2	1.40E-04
1.00E-30	3069.6	1.40E-04

Table 4.6 Reductions in computational time obtained by AHBM 1

ε	Reduction in Time (%)
1.00E-02	84.3
1.00E-04	81.4
1.00E-06	76.6
1.00E-08	69.0
1.00E-10	53.7
1.00E-12	46.6
1.00E-14	38.5
1.00E-16	30.7
1.00E-20	26.7
1.00E-25	26.2
1.00E-30	26.5

It can be seen from the results that, as the control parameter gets smaller, the solution time increases considerably. However there is no considerable change in the error. Normally, it is expected that, lowering the control parameter would cause more harmonics to be retained, therefore increase the accuracy. The reasons for this unusual behavior are explained in the remaining of this section.

In Figure 4.5 and Figure 4.6, absolute error and retained harmonics plots are given for the cases where ε is taken as 10^{-8} and 10^{-20}.
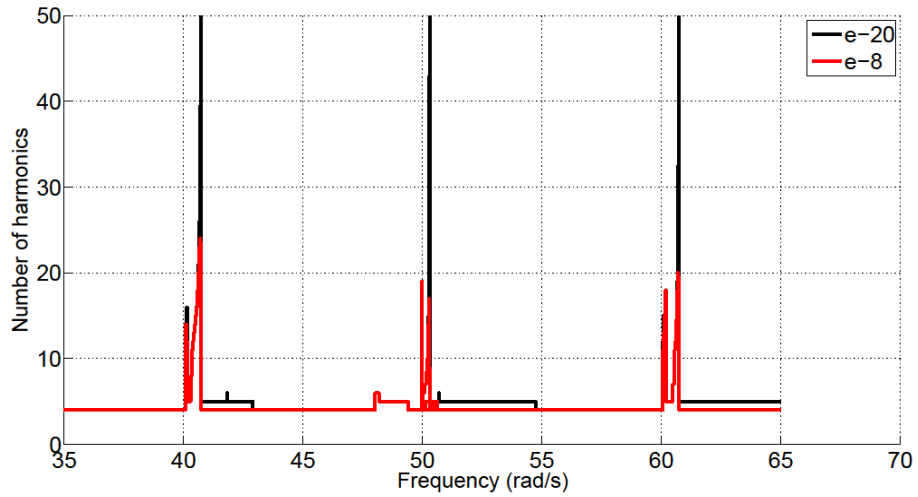
Figure 4.5 Number of Harmonics used by AHBM 1, Case Study 1 Selected Cases
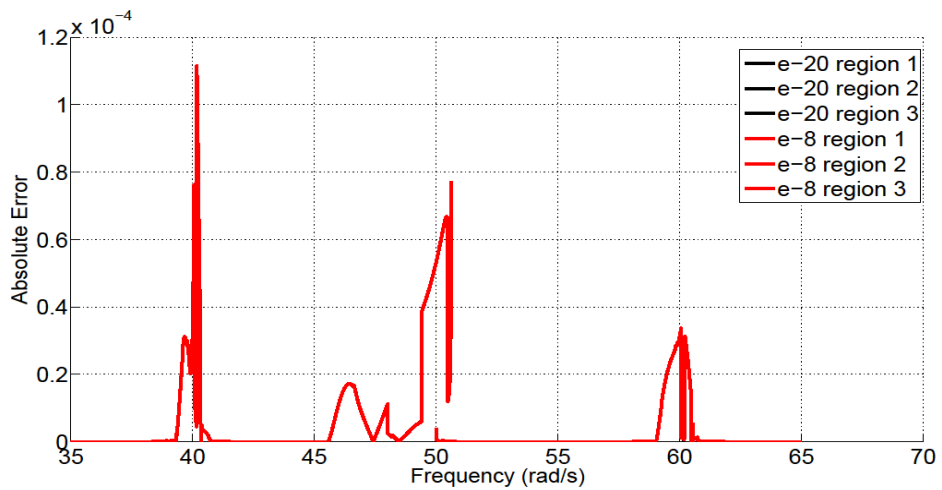
Figure 4.6 Error Plots for AHBM 1, Case Study 1 Selected Cases

From Figure 4.5 , it can be seen that changing ε causes a significant change in the number of harmonics only in the neighborhood of the resonances. In other regions, the numbers of retained harmonics are close. Also in Figure 4.5 near 40 rad/s one can see that the algorithm increases the number of harmonics first. Then a drop occurs until the number of harmonics starts to increase again. The same phenomenon can also be spotted around other resonances. When the drop occurs, the error increases rapidly and reaches to a maximum. Since the algorithm forms this drop for every value of ε , the maximum error values do not change significantly. For the case where $\varepsilon = 10^{-20}$, the number of harmonics reach up to 50 at 3 points however, as shown in Figure 4.6, since this number is unnecessarily high for the current case study, it does not make a very large impact on the accuracy.

In Table 4.3, Table 4.4 and Table 4.5, a small increase in the error values can be spotted for higher values of ε. The reason for this can be seen in Figure 4.7 and Figure 4.8. As ε decreases, the algorithm changes the number of harmonics more rapidly. This causes the error to drop faster after making a peak. Also, another drop in the error occurs in a small region between 45 rad/s and 50 rad/s. However, these differences hardly make a noticeable difference as ε gets smaller than 10^{-6}.
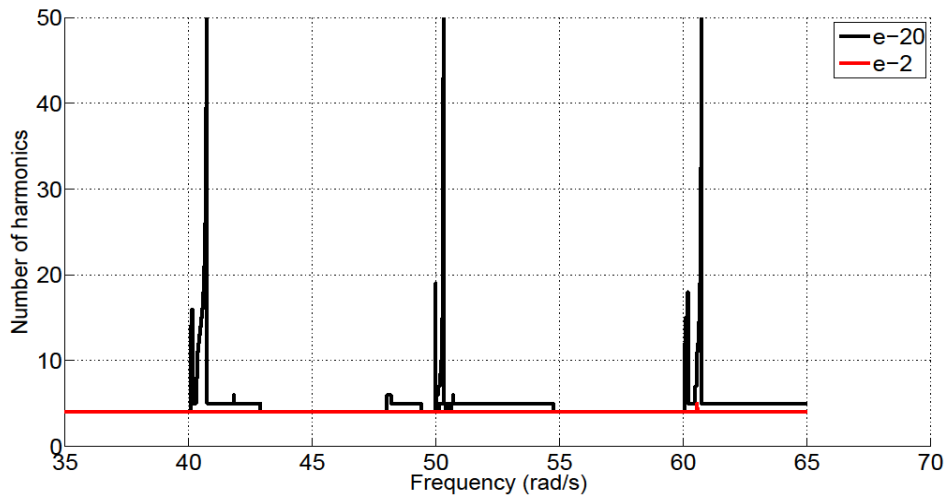
Figure 4.7 Number of Retained Harmonics for AHBM 1, Case Study 1
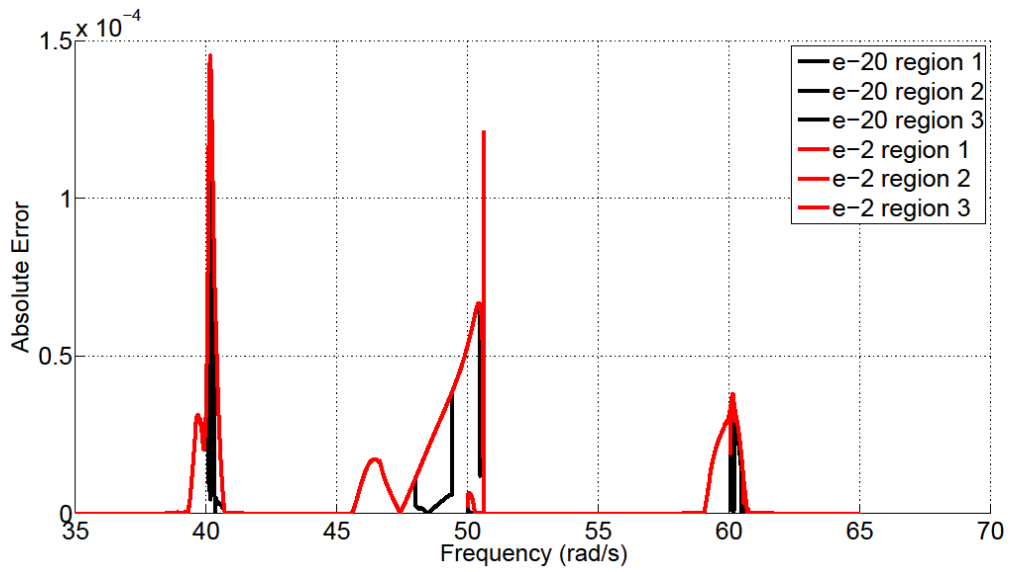
Figure 4.8 Error Plots for AHBM 1, Case Study 1 Selected Cases

4.3.2 Results Obtained By AHBM 2: Grolet and Thouverez's Method

As explained in Chapter 3, this method uses two threshold values, ρ_f and ρ_b, to adjust the number of harmonics retained. Due to their definitions, ρ_f must be smaller than ρ_b and both must lie in between 0 and 1. Choosing ρ_f and ρ_b smaller and close to each other forces the algorithm to include more harmonics in the solution. To prevent the algorithm from using too many harmonics a maximum number of harmonics must be defined. For this study, it is selected as 10.

In this study, analyses are carried out with ρ_f values ranging between 10^{-20} and 10^{-9}, ρ_b values ranging between 10^{-15} and 10^{-2}. Values lower than 10^{-20} and 10^{-15} are not be included in the study, since they resulted in numerical instability. The resulting maximum absolute error, maximum relative error, integral error values and amounts of time spent for computation can be seen in Table 4.7, Table 4.8 and Table 4.9. The percentages of reduction obtained in computational time with respect to the 10-harmonic classical HBM solution are given in Table 4.10.

It can be seen from the results that error values change significantly around the primary resonance. However, around super-harmonic resonances, i.e. region 1 and region 3, there is no significant difference. The algorithm uses similar number of harmonics in these parts of the response curve.

Table 4.7 Maximum Absolute Error Values for AHBM 2

ρ_f	ρ_b	Time (sec)	Max. Err 1	Max. Err 2	Max. Err 3
1.00E-20	1.00E-15	3187.5	2.11E-03	4E-05	2.26E-03
1.00E-20	1.00E-12	2811.5	2.11E-03	3.9E-05	2.33E-03
1.00E-20	1.00E-10	2350.0	2.11E-03	7.3E-05	2.33E-03
1.00E-20	1.00E-08	2326.1	2.14E-03	5.1E-04	2.47E-03
1.00E-20	1.00E-06	2086.0	2.14E-03	8.5E-04	2.5E-03
1.00E-18	1.00E-15	3006.9	2.11E-03	4E-05	2.26E-03

Table 4.7 (continued) Maximum Absolute Error Values for AHBM 2

ρ_f	ρ_b	Time (sec)	Max. Err 1	Max. Err 2	Max. Err 3
1.00E-18	1.00E-12	2827.2	2.11E-03	3.9E-05	2.33E-03
1.00E-18	1.00E-10	2366.5	2.11E-03	7.3E-05	2.23E-03
1.00E-18	1.00E-08	2319.2	2.11E-03	5.1E-04	2.47E-03
1.00E-18	1.00E-06	2251.3	2.14E-03	5.1E-04	2.47E-03
1.00E-15	1.00E-12	2937.3	2.09E-03	4E-05	1.8E-03
1.00E-15	1.00E-10	2309.2	2.09E-03	7.1E-05	1.82E-03
1.00E-15	1.00E-08	2128.4	2.14E-03	5.1E-04	2.47E-03
1.00E-15	1.00E-06	2092.7	2.14E-03	5.1E-04	2.47E-03
1.00E-15	1.00E-02	2061.7	2.14E-03	5.1E-04	2.47E-03
1.00E-12	1.00E-10	2164.0	2.09E-03	9.8E-05	1.65E-03
1.00E-12	1.00E-09	1875.2	2.09E-03	1.9E-04	2.5E-03
1.00E-12	1.00E-08	1776.8	2.14E-03	2.4E-04	2.47E-03
1.00E-12	1.00E-06	1690.0.	2.14E-03	2.4E-04	2.47E-03
1.00E-10	1.00E-06	1384.8	2.14E-03	1.953E-02	8.54E-03
1.00E-09	1.00E-02	1353.0	2.14E-03	1.953E-02	1.89E-02

Table 4.8 Maximum Relative Error Values for AHBM 2

ρ_f	ρ_b	Time (sec)	Max. Err 1 (Rel)	Max. Err 2 (Rel)	Max. Err 3 (Rel)
1.00E-20	1.00E-15	3187.5	1.56E-01	8.12E-04	5.19E-02
1.00E-20	1.00E-12	2811.5	1.56E-01	7.88E-04	5.21E-02
1.00E-20	1.00E-10	2350.0	1.56E-01	8.13E-04	5.39E-02
1.00E-20	1.00E-08	2326.1	1.59E-01	6.50E-03	5.85E-02
1.00E-20	1.00E-06	2086.0	1.59E-01	8.00E-03	5.85E-02
1.00E-18	1.00E-15	3006.9	1.56E-01	8.12E-04	5.19E-02
1.00E-18	1.00E-12	2827.2	1.56E-01	7.88E-04	5.21E-02
1.00E-18	1.00E-10	2366.5	1.56E-01	8.13E-04	5.39E-02
1.00E-18	1.00E-08	2319.2	1.59E-01	6.50E-03	5.85E-02
1.00E-18	1.00E-06	2251.3	1.59E-01	6.50E-03	5.85E-02
1.00E-15	1.00E-12	2937.3	1.55E-01	7.94E-04	3.72E-02
1.00E-15	1.00E-10	2309.2	1.55E-01	7.94E-04	4.07E-02

Table 4.8 (continued) Maximum Relative Error Values for AHBM 2

ρ_f	ρ_b	Time (sec)	Max. Err 1 (Rel)	Max. Err 2 (Rel)	Max. Err 3 (Rel)
1.00E-15	1.00E-08	2128.4	1.59E-01	6.50E-03	5.85E-02
1.00E-15	1.00E-06	2092.7	1.59E-01	6.50E-03	5.85E-02
1.00E-15	1.00E-02	2061.7	1.59E-01	6.50E-03	5.85E-02
1.00E-12	1.00E-10	2164.0	1.55E-01	1.38E-03	4.26E-02
1.00E-12	1.00E-09	1875.2	1.55E-01	1.61E-03	5.77E-02
1.00E-12	1.00E-08	1776.8	1.59E-01	3.00E-03	5.85E-02
1.00E-12	1.00E-06	1690.0	1.59E-01	3.00E-03	5.85E-02
1.00E-10	1.00E-06	1384.8	1.59E-01	4.45E-02	4.10E-01
1.00E-09	1.00E-02	1353.0	1.59E-01	5.15E-02	6.85E-01

Table 4.9 Integral Error Values for AHBM 2

ρ_f	ρ_b	Time (sec)	Total Integral Error
1.00E-20	1.00E-15	3187.5	0.00634
1.00E-20	1.00E-12	2811.5	0.00644
1.00E-20	1.00E-10	2350.0	0.00651
1.00E-20	1.00E-08	2326.1	0.01432
1.00E-20	1.00E-06	2086.0	0.01745
1.00E-18	1.00E-15	3006.9	0.00634
1.00E-18	1.00E-12	2827.2	0.00644
1.00E-18	1.00E-10	2366.5	0.00651
1.00E-18	1.00E-08	2319.2	0.01432
1.00E-18	1.00E-06	2251.3	0.01676
1.00E-15	1.00E-12	2937.3	0.00773
1.00E-15	1.00E-10	2309.2	0.00788
1.00E-15	1.00E-08	2128.4	0.01458
1.00E-15	1.00E-06	2092.7	0.01676
1.00E-15	1.00E-02	2061.7	0.01677
1.00E-12	1.00E-10	2164.0	0.00789
1.00E-12	1.00E-09	1875.2	0.01057
1.00E-12	1.00E-08	1776.8	0.0146
1.00E-12	1.00E-06	1690.0	0.01678
1.00E-10	1.00E-06	1384.8	0.06979
1.00E-09	1.00E-02	1353.0	0.09511

Table 4.10 Reductions in computational time obtained by AHBM 2

ρ_f	ρ_b	Reduction in Time (%)
1.00E-20	1.00E-15	23.7
1.00E-20	1.00E-12	32.7
1.00E-20	1.00E-10	43.7
1.00E-20	1.00E-08	44.3
1.00E-20	1.00E-06	50.0
1.00E-18	1.00E-15	28.0
1.00E-18	1.00E-12	32.3
1.00E-18	1.00E-10	43.3
1.00E-18	1.00E-08	44.5
1.00E-18	1.00E-06	46.1
1.00E-15	1.00E-12	29.7
1.00E-15	1.00E-10	44.7
1.00E-15	1.00E-08	49.0
1.00E-15	1.00E-06	49.9
1.00E-15	1.00E-02	50.6
1.00E-12	1.00E-10	48.2
1.00E-12	1.00E-09	55.1
1.00E-12	1.00E-08	57.4
1.00E-12	1.00E-06	59.5
1.00E-10	1.00E-06	66.8
1.00E-09	1.00E-02	67.6

4.3.2.1 Results Obtained by AHBM 3: Yümer's Method

As explained in Chapter 3, this method uses a threshold ratio, a, to adjust the number of harmonics retained. Due its definition, a must be chosen greater than 1. Choosing the parameter a larger, forces the algorithm to include more harmonics in the solution. To prevent the algorithm from using too many harmonics, a maximum number of harmonics is defined, which is chosen as 10, for this study. The results are given in Table 4.11, Table 4.12 and Table 4.13. The percentages of reduction obtained in computational time with respect to the 10-harmonic classical HBM solution are given in Table 4.14.

Table 4.11 Maximum Absolute Error Values for AHBM 3

a	Time (sec)	Max. Err1	Max. Err 2	Max. Err 3
2	233.5	1.30E-01	1.32E-02	1.31E-01
5	291.6	1.30E-01	1.32E-02	1.31E-01
10	335.1	1.30E-01	1.32E-02	1.31E-01
20	431.5	1.30E-01	1.32E-02	1.31E-01
30	456.6	1.30E-01	1.32E-02	1.31E-01
40	521.6	1.30E-01	1.32E-02	1.31E-01
50	519.4	1.30E-01	1.32E-02	1.31E-01
60	540.3	1.30E-01	1.32E-02	1.31E-01
70	576.0	1.30E-01	1.32E-02	1.31E-01
80	612.2	1.30E-01	1.32E-02	1.31E-01
90	607.7	1.30E-01	1.32E-02	1.31E-01
100	614.7	1.30E-01	1.32E-02	1.31E-01
200	616.2	1.30E-01	1.32E-02	1.31E-01
400	645.2	1.30E-01	1.32E-02	1.31E-01
600	650.2	1.30E-01	1.32E-02	1.31E-01
800	630.2	1.30E-01	1.32E-02	1.31E-01
1000	685.8	1.30E-01	1.32E-02	1.31E-01
2000	681.6	1.30E-01	1.32E-02	1.31E-01
10000	688.6	1.30E-01	1.32E-02	1.31E-01
100000	674.8	1.30E-01	1.32E-02	1.31E-01
1000000	627.5	1.30E-01	1.32E-02	1.31E-01

Table 4.12 Maximum Relative Error Values for AHBM 3

a	Time (sec)	Max. Err 1 (Rel)	Max. Err 2 (Rel)	Max. Err 3 (Rel)
2	233.5	0.8871064	0.38671	0.95172
5	291.6	0.8871064	0.38671	0.95172
10	335.1	0.8871064	0.38671	0.95172
20	431.5	0.8871064	0.38671	0.95172
30	456.6	0.8871064	0.38671	0.95172
40	521.6	0.8871064	0.38671	0.95172
50	519.4	0.8871064	0.38671	0.95172
60	540.3	0.8871064	0.38671	0.95172
70	576.0	0.8871064	0.38671	0.95172
80	612.2	0.8871064	0.38671	0.95172

Table 4.12 (continued) Maximum Relative Error Values for AHBM 3

a	Time (sec)	Max. Err 1 (Rel)	Max. Err 2 (Rel)	Max. Err 3 (Rel)
90	607.7	0.8871064	0.38671	0.95172
100	614.7	0.8871064	0.38671	0.95172
200	616.2	0.8871064	0.38671	0.95172
400	645.2	0.8871064	0.38671	0.95172
600	650.2	0.8871064	0.38671	0.95172
800	630.2	0.8871064	0.38671	0.95172
1000	685.8	0.8871064	0.38671	0.95172
2000	681.6	0.8871064	0.38671	0.95172
10000	688.6	0.8871064	0.38671	0.95172
100000	674.8	0.8871064	0.38671	0.95172
1000000	627.5	0.8871064	0.38671	0.95172

Table 4.13 Integral Error Values for AHBM 3

a	Time (sec)	Total Integral Error
2	233.5	0.469949
5	291.6	0.465767
10	335.1	0.464304
20	431.5	0.464199
30	456.6	0.464197
40	521.6	0.464191
50	519.4	0.464191
60	540.3	0.46419
70	576.0	0.464189
80	612.2	0.464187
90	607.7	0.464184
100	614.7	0.464304
200	616.2	0.464183
400	645.2	0.464126
600	650.2	0.464126
800	630.2	0.464125
1000	685.8	0.464125
2000	681.6	0.464125
10000	688.6	0.464125
100000	674.8	0.464125
1000000	627.5	0.464125

Table 4.14 Reductions in computational time obtained by AHBM 3

a	Reduction in Time (%)
2	94.4
5	93.0
10	92.0
20	89.7
30	89.1
40	87.5
50	87.6
60	87.1
70	86.2
80	85.3
90	85.4
100	85.3
200	85.2
400	84.5
600	84.4
800	84.9
1000	83.6
2000	83.7
10000	83.5
100000	83.8
1000000	85.0

The results given in Table 4.11, Table 4.12 and Table 4.13 indicate that the computational times are relatively low, as desired. However the error values are significantly high and they tend to stay constant, although the control parameter changes.

The reasons for such results are investigated and it is observed that the algorithm failed to increase the harmonics used near the secondary (super-harmonic) resonances located at 39.92 and 59.88 rad/s. Therefore, the accuracy around those regions is poor, although it is quite high near the primary resonance. However, since region 2 starts from 42 rad/s, the error values belonging to region 2 turn out to be

high as well. Another important point is that, as the value of *a* increases, the algorithm increases the number of retained harmonics around the primary resonance only. Around the secondary resonances, a single harmonic representation is used and the same amount of error is introduced, regardless of parameter *a*. This phenomenon is illustrated in the overlapping response and absolute error curves shown in Figure 4.9 and Figure 4.10.
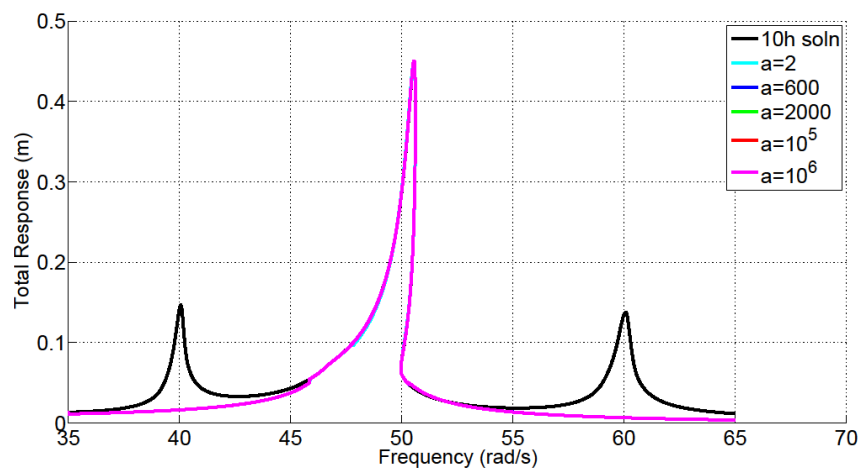
Figure 4.9 Total Response Plots for AHBM 3, Case Study 1 Selected Cases
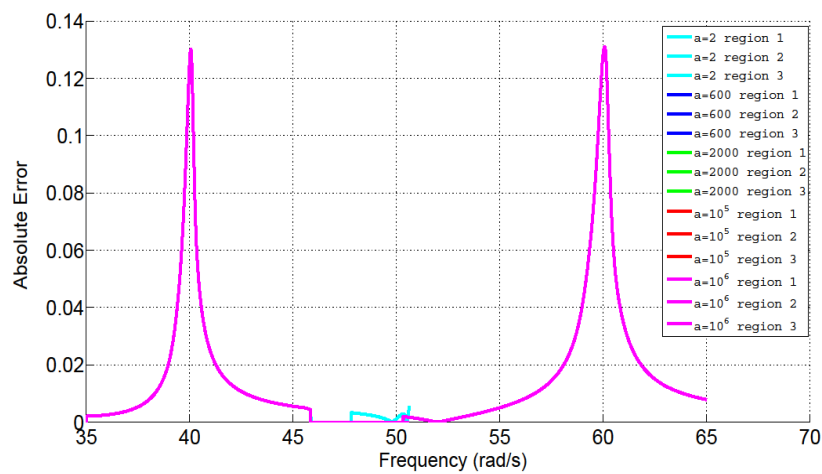
Figure 4.10 Error Plots for AHBM 3, Case Study 1 Selected Cases

4.3.3 Results Obtained by AHBM 4: Forcing Based Adaptive Harmonic Balance Method (FB-AHBM)

Since Yümer's Method generated error values that are very high, a modified version of Yümer's Method is studied. The main idea of the modification is to make the algorithm always retain the harmonics of external forcing inside the response representation, so that when the external forcing contains more than one harmonic component, causing super-harmonic resonances to occur in the frequency response, high accuracy can be achieved. The modification naturally increases the computational time, however since the computational time employed by Yümer's Method is very low, a reasonable increase is tolerable. The modified method is named as Forcing Based Adaptive Harmonic Balance Method (FB-AHBM).

The results obtained by FB-AHBM are summarized in Table 4.15, Table 4.16 and Table 4.17. The data presented in the tables clearly show that the modified method has much more accuracy at the expense of an acceptable increase in the computational time. The percentages of reduction obtained in computational time with respect to the 10-harmonic classical HBM solution are given in Table 4.18.

Table 4.15 Maximum Absolute Error Values for AHBM 4

a	Time (sec)	Max. Err 1	Max. Err 2	Max. Err 3
2	510.09	1.10E-04	7.74E-04	3.39E-05
5	591.4	4.79E-05	7.74E-04	3.30E-05
10	673.3	3.54E-05	7.74E-04	5.63E-05
20	798.6	2.76E-07	6.48E-05	3.89E-05
30	872.2	2.76E-07	6.48E-05	3.96E-06
40	907.3	2.76E-07	8.69E-06	2.80E-06
50	940.0	2.76E-07	8.69E-06	2.61E-06
60	949	2.76E-07	8.69E-06	1.24E-06
70	973.6	2.76E-07	8.72E-06	1.03E-06
80	992.6	2.76E-07	8.72E-06	8.88E-07
90	1011.6	2.76E-07	8.71E-06	8.47E-07
100	1053.5	2.76E-07	3.29E-06	8.43E-07

172

Table 4.15 (continued) Maximum Absolute Error Values for AHBM 4

a	Time (sec)	Max. Err 1	Max. Err 2	Max. Err 3
200	1068.5	2.76E-07	6.41E-07	8.27E-07
300	1069.3	2.76E-07	4.50E-07	8.31E-07
400	1097.3	2.76E-07	4.07E-07	8.31E-07
500	1101.8	2.76E-07	4.08E-07	8.31E-07
600	1093.5	2.76E-07	4.07E-07	8.31E-07
700	1096.2	2.76E-07	4.08E-07	8.31E-07
800	1110.6	2.76E-07	4.07E-07	8.31E-07
1000	1106.6	2.76E-07	4.07E-07	8.31E-07
2000	1123.2	2.76E-07	4.07E-07	8.31E-07
10000	1124.5	2.76E-07	4.07E-07	8.31E-07
100000	1119.2	2.76E-07	4.07E-07	8.31E-07
1000000	1131.0	2.76E-07	4.07E-07	8.31E-07

Table 4.16 Maximum Relative Error Values for AHBM 4

a	Time (sec)	Max. Err 1 (Rel)	Max. Err 2 (Rel)	Max. Err 3 (Rel)
2	510.9	9.27E-04	1.93E-03	3.22E-04
5	591.4	3.92E-04	1.93E-03	2.75E-04
10	673.3	2.71E-04	1.93E-03	7.74E-06
20	798.6	5.41E-06	1.61E-04	5.34E-06
30	872.2	5.41E-06	1.62E-04	3.11E-05
40	907.3	5.41E-06	2.06E-05	2.42E-05
50	940.0	5.41E-06	2.06E-05	2.30E-05
60	949.0	5.41E-06	2.06E-05	1.24E-05
70	973.6	5.41E-06	2.10E-05	1.05E-05
80	992.6	5.41E-06	2.10E-05	9.24E-06
90	1011.6	5.41E-06	2.09E-05	8.59E-06
100	1053.5	5.41E-06	1.35E-05	7.93E-06
200	1068.5	5.41E-06	1.60E-06	6.02E-06
300	1069.3	5.41E-06	1.11E-06	6.05E-06
400	1097.3	5.41E-06	1.02E-06	6.05E-06
500	1101.8	5.41E-06	1.02E-06	6.05E-06
600	1093.5	5.41E-06	1.02E-06	6.05E-06
700	1096.2	5.41E-06	1.02E-06	6.05E-06
800	1110.6	5.41E-06	1.02E-06	6.05E-06
1000	1106.6	5.41E-06	1.02E-06	6.05E-06

Table 4.16 (continued) Maximum Relative Error Values for AHBM 4

a	Time (sec)	Max. Err 1 (Rel)	Max. Err 2 (Rel)	Max. Err 3 (Rel)
2000	1123.2	5.41E-06	1.02E-06	6.05E-06
10000	1124.5	5.41E-06	1.02E-06	6.05E-06
100000	1119.2	5.41E-06	1.02E-06	6.05E-06
1000000	1131.0	5.41E-06	1.02E-06	6.05E-06

Table 4.17 Integral Error Values for AHBM 4

a	Time (sec)	Total Integral Error
2	510.9	2.01E-04
5	591.4	1.58E-04
10	673.3	1.27E-04
20	798.6	2.03E-05
30	872.2	1.62E-05
40	907.3	9.86E-06
50	940.0	9.22E-06
60	949.0	8.16E-06
70	973.6	6.91E-06
80	992.6	5.09E-06
90	1011.6	2.07E-06
100	1053.5	9.62E-07
200	1068.5	2.63E-07
300	1069.3	1.87E-07
400	1097.3	1.67E-07
500	1101.8	1.65E-07
600	1093.5	1.65E-07
700	1096.2	1.65E-07
800	1110.6	1.65E-07
1000	1106.6	1.64E-07
2000	1123.2	1.65E-07
10000	1124.5	1.64E-07
100000	1119.2	1.64E-07
1000000	1131.0	1.64E-07

Table 4.18 Reductions in computational time obtained by AHBM 4

a	Reduction in Time (%)
2	87.8
5	85.8
10	83.9
20	80.9
30	79.1
40	78.3
50	77.5
60	77.3
70	76.7
80	76.2
90	75.8
100	74.8
200	74.4
300	74.4
400	73.7
500	73.6
600	73.8
700	73.7
800	73.4
1000	73.5
2000	73.1
10000	73.1
100000	73.2
1000000	72.9

4.3.4 Results Obtained by AHBM 5: Pseudo-Response Based Adaptive Harmonic Balance Method (PRB-AHBM)

As explained in Section 3.5, this method uses a threshold ratio, ε_t, to adjust the number of harmonics retained. Due its definition, ε_t must be chosen between 0 and 1. Choosing the parameter ε_t smaller forces the algorithm to include more harmonics in the response representation. To prevent the algorithm from using too many harmonics, a maximum number of harmonics is defined, which is selected as 10. At this part of the study the first version of this method, presented in Section 3.5 is used,

i.e. harmonic selection based on the comparison to the first harmonic. Results are given in Table 4.19, Table 4.20 and Table 4.21. The percentages of reduction obtained in computational time with respect to the 10-harmonic classical HBM solution are given in Table 4.22.

Table 4.19 Maximum Absolute Error Values for AHBM 5

ε_t	Time (sec)	Max. Err 1	Max. Err 2	Max. Err 3
5.00E-02	403.6	1.41E-04	1.95E-02	2.92E-03
2.00E-02	407.9	1.41E-04	1.95E-02	8.60E-05
1.00E-02	447.8	1.41E-04	5.649E-03	5.05E-05
5.00E-03	456.2	1.06E-04	7.74E-04	3.38E-05
1.00E-03	505.7	2.68E-05	7.74E-04	1.38E-05
5.00E-04	545.0	1.32E-05	7.74E-04	1.38E-05
1.00E-04	713.2	2.64E-06	6.48E-05	5.96E-06
5.00E-05	793.0	1.68E-06	1.62E-05	3.30E-06
1.00E-05	1028.7	2.76E-07	2.14E-06	8.53E-07
5.00E-06	1066.5	2.76E-07	4.16E-07	8.47E-07
1.00E-06	1041.6	2.76E-07	4.07E-07	8.31E-07
5.00E-07	1080.5	2.76E-07	4.07E-07	8.31E-07
1.00E-10	1033.0	2.76E-07	4.07E-07	8.31E-07

Table 4.20 Maximum Relative Error Values for AHBM 5

ε_t	Time (sec)	Max. Err 1 (Rel)	Max. Err 2 (Rel)	Max. Err 3 (Rel)
5.00E-02	403.6	1.18E-03	4.45E-02	5.31E-02
2.00E-02	407.9	1.18E-03	4.44E-02	8.54E-04
1.00E-02	447.8	1.20E-03	1.40E-02	6.44E-04
5.00E-03	456.2	1.14E-03	1.93E-03	4.14E-04
1.00E-03	505.7	4.24E-04	1.93E-03	2.41E-04
5.00E-04	545.0	2.34E-04	1.93E-03	2.41E-04
1.00E-04	713.2	4.99E-05	1.61E-04	1.11E-04
5.00E-05	793.0	3.23E-05	6.60E-05	6.47E-05
1.00E-05	1028.7	5.41E-06	1.46E-05	1.28E-05
5.00E-06	1066.5	5.41E-06	8.23E-06	6.27E-06
1.00E-06	1041.6	5.41E-06	1.89E-06	6.05E-06
5.00E-07	1080.5	5.41E-06	1.68E-06	6.05E-06
1.00E-10	1033.0	5.41E-06	1.02E-06	6.05E-06

Table 4.21 Integral Error Values for AHBM 5

ε_t	Time (sec)	Total Int. Error
5.00E-02	403.6	1.50E-02
2.00E-02	407.9	3.43E-03
1.00E-02	447.8	1.48E-03
5.00E-03	456.2	2.26E-04
1.00E-03	505.7	1.54E-04
5.00E-04	545.0	1.47E-04
1.00E-04	713.2	2.50E-05
5.00E-05	793.0	1.67E-05
1.00E-05	1028.7	5.94E-07
5.00E-06	1066.5	2.50E-07
1.00E-06	1041.6	1.67E-07
5.00E-07	1080.5	1.65E-07
1.00E-10	1033.0	1.64E-07

Table 4.22 Reductions in computational time obtained by AHBM 5

ε_t	Reduction in Time (%)
5.00E-02	90.3
2.00E-02	90.2
1.00E-02	89.3
5.00E-03	89.1
1.00E-03	87.9
5.00E-04	86.9
1.00E-04	82.9
5.00E-05	81.0
1.00E-05	75.4
5.00E-06	74.5
1.00E-06	75.1
5.00E-07	74.1
1.00E-10	75.3

For the second part of this study, the second variant of PRB-AHBM, explained in Section 3.5.1 is employed, i.e. harmonic selection based on the comparison to the

177

harmonic with maximum amplitude. Results are presented in Table 4.23, Table 4.24 and Table 4.25. The percentages of reduction obtained in computational time with respect to the 10-harmonic classical HBM solution are given in Table 4.26.

From the tables, it can be seen that the second variant of PRB-AHBM is better, since it achieves shorter computational times at the expense of a small decrease in accuracy, compared to the first variant. This is an expected result since the algorithm is more prone to excluding harmonics.

Table 4.23 Maximum Absolute Error Values for AHBM 6

ε_t	Time (sec)	Max. Err 1	Max. Err 2	Max. Err 3
5.00E-02	403.4	1.41E-04	1.95E-02	2.92E-03
2.00E-02	404.5	1.41E-04	1.95E-02	7.84E-04
1.00E-02	425.8	1.41E-04	5.65E-03	9.49E-05
5.00E-03	435.4	1.41E-04	7.74E-04	9.47E-05
1.00E-03	449.3	1.06E-04	7.74E-04	5.86E-05
5.00E-04	502.8	7.76E-05	7.74E-04	3.39E-05
1.00E-04	628.0	8.03E-06	6.48E-05	8.94E-06
5.00E-05	729.3	4.39E-06	1.62E-05	6.35E-06
1.00E-05	1074.4	6.59E-07	2.14E-06	1.28E-06
5.00E-06	1030.3	6.73E-07	4.16E-07	8.47E-07
1.00E-06	1091.7	2.76E-07	4.07E-07	8.31E-07
5.00E-07	1124.9	2.76E-07	4.07E-07	8.31E-07
1.00E-10	1043.4	2.76E-07	4.07E-07	8.31E-07

Table 4.24 Maximum Relative Error Values for AHBM 6

ε_t	Time (sec)	Max. Err 1 (Rel)	Max. Err 2 (Rel)	Max. Err 3 (Rel)
5.00E-02	403.4	1.18E-03	4.45E-02	5.31E-02
2.00E-02	404.5	1.18E-03	4.45E-02	1.05E-02
1.00E-02	425.8	1.18E-03	1.40E-02	8.65E-04
5.00E-03	435.4	1.18E-03	1.93E-03	8.68E-04
1.00E-03	449.3	1.14E-03	1.93E-03	7.14E-04
5.00E-04	502.8	7.82E-04	1.93E-03	4.14E-04
1.00E-04	628.0	1.42E-04	1.61E-04	1.52E-04
5.00E-05	729.3	8.13E-05	6.60E-05	7.69E-05

Table 4.24 (continued) Maximum Relative Error Values for AHBM 6

ε_t	Time (sec)	Max. Err 1 (Rel)	Max. Err 2 (Rel)	Max. Err 3 (Rel)
1.00E-05	1074.4	1.27E-05	1.46E-05	1.57E-05
5.00E-06	1030.3	1.31E-05	8.23E-06	8.10E-06
1.00E-06	1091.7	5.41E-06	1.89E-06	6.05E-06
5.00E-07	1124.9	5.41E-06	1.68E-06	6.05E-06
1.00E-10	1043.4	5.41E-06	1.02E-06	6.05E-06

Table 4.25 Integral Error Values for AHBM 6

ε_t	Time (sec)	Total Int. Error
5.00E-02	403.4	1.69E-02
2.00E-02	404.5	3.78E-03
1.00E-02	425.8	1.48E-03
5.00E-03	435.4	2.26E-04
1.00E-03	449.3	2.30E-04
5.00E-04	502.8	2.25E-04
1.00E-04	628.0	3.17E-05
5.00E-05	729.3	2.10E-05
1.00E-05	1074.4	8.82E-07
5.00E-06	1030.3	3.13E-07
1.00E-06	1091.7	1.69E-07
5.00E-07	1124.9	1.66E-07
1.00E-10	1043.4	1.64E-07

Table 4.26 Reductions in computational time obtained by AHBM 6

ε_t	Reduction in Time (%)
5.00E-02	90.3
2.00E-02	90.3
1.00E-02	89.8
5.00E-03	89.6
1.00E-03	89.2
5.00E-04	88.0
1.00E-04	85.0
5.00E-05	82.5
1.00E-05	74.3

Table 4.26 (continued) Reductions in computational time obtained by AHBM 6

ε_t	Reduction in Time (%)
5.00E-06	75.3
1.00E-06	73.9
5.00E-07	73.1
1.00E-10	75.0

4.3.5 Comparison

In this section, an overall comparison of the tabulated data given in the previous sections is presented. As explained in Section 4.3, 5 criteria are used for evaluation, which are presented in graphical form. In these plots, the horizontal axis is the computational time, and the vertical axis is the error. Therefore, the method for which the curves lie closest to the lower left corner are more favorable methods since they manage to achieve greater accuracy in a shorter time. Results are given in Figure 4.11 to Figure 4.15. From the figures, one can see that the methods which make lesser error in shorter time are the newly proposed FB-AHBM, the first variant of PRB-AHBM and the second variant of PRB-AHBM.
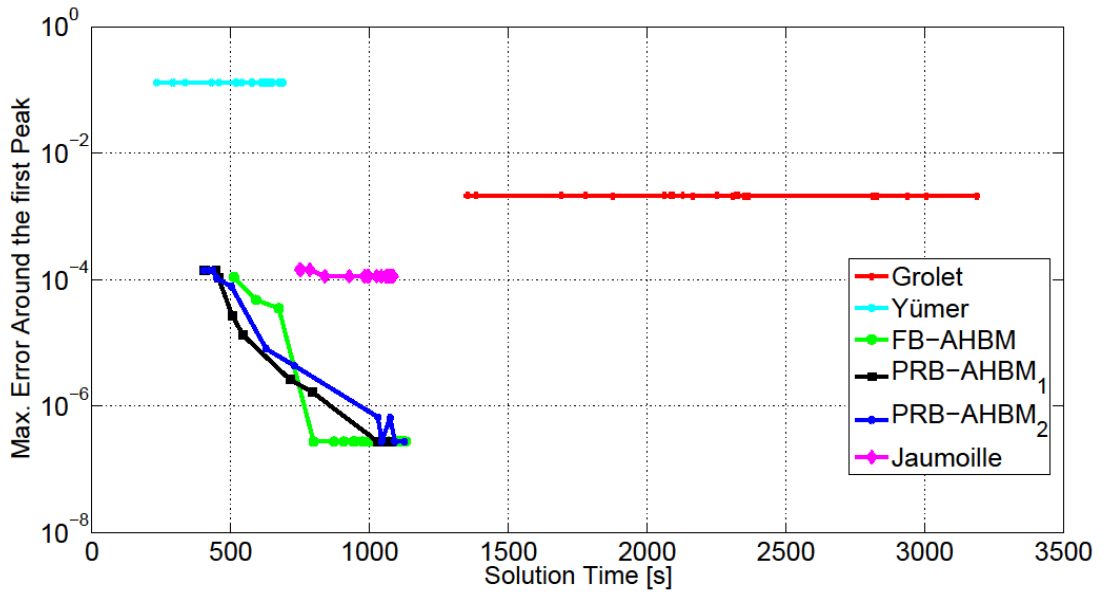
Figure 4.11 Computational Time vs Maximum Error in Region 1
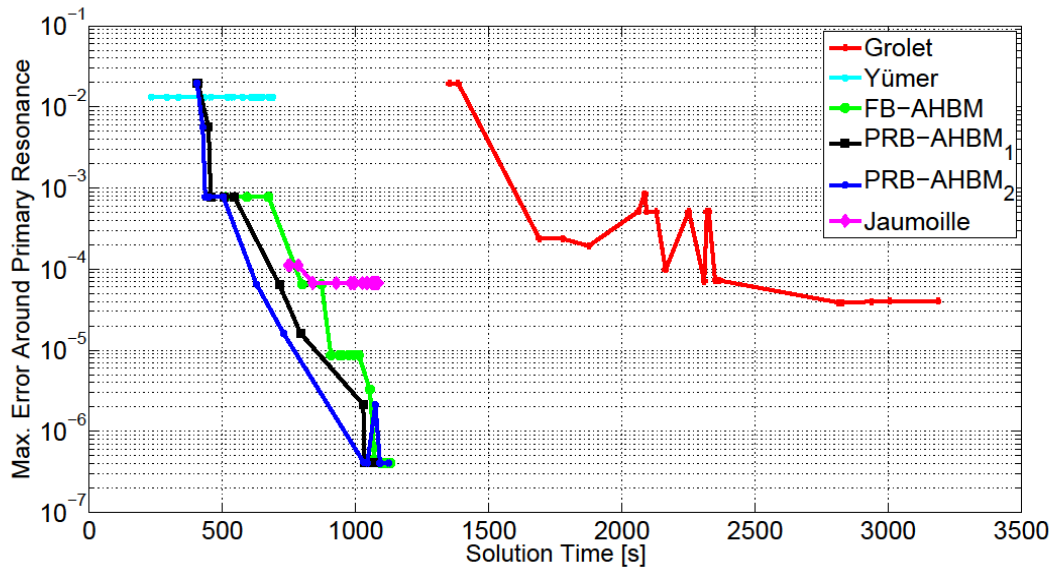
Figure 4.12 Computational Time vs Maximum Error in Region 2
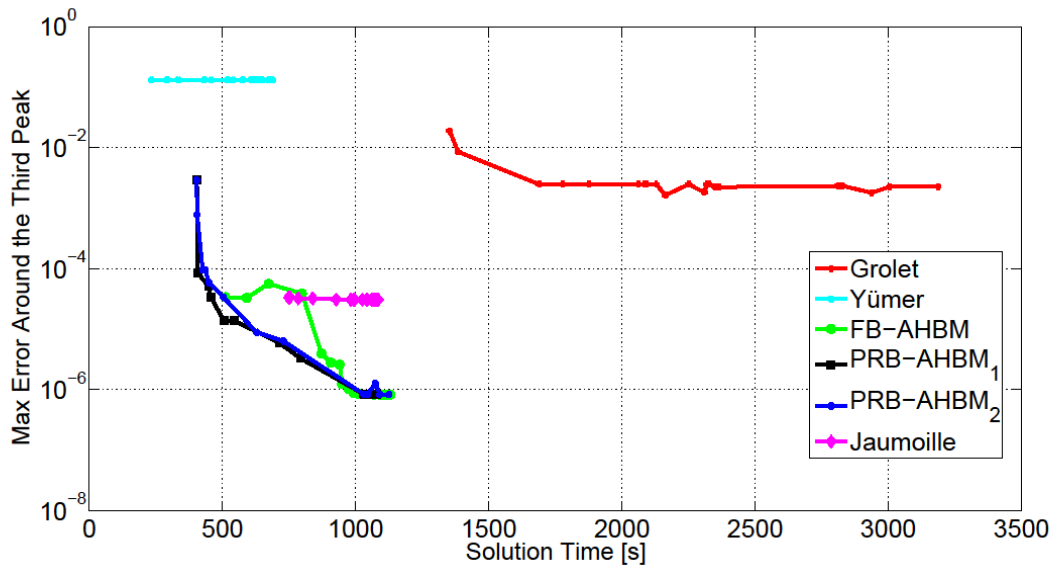
Figure 4.13 Computational Time vs Maximum Error in Region 3
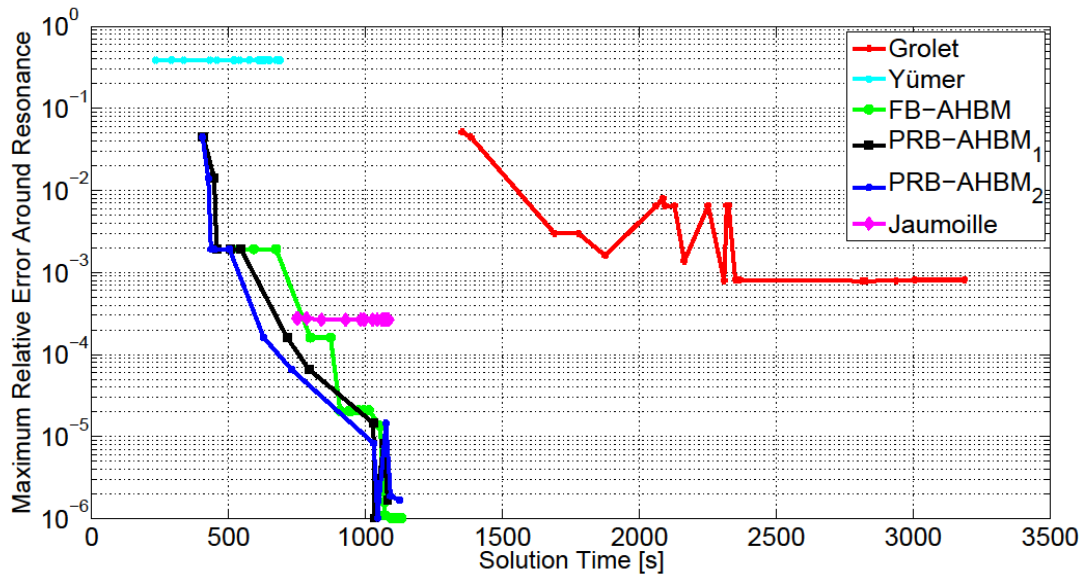
Figure 4.14 Computational Time vs Maximum Relative Error in Region 2
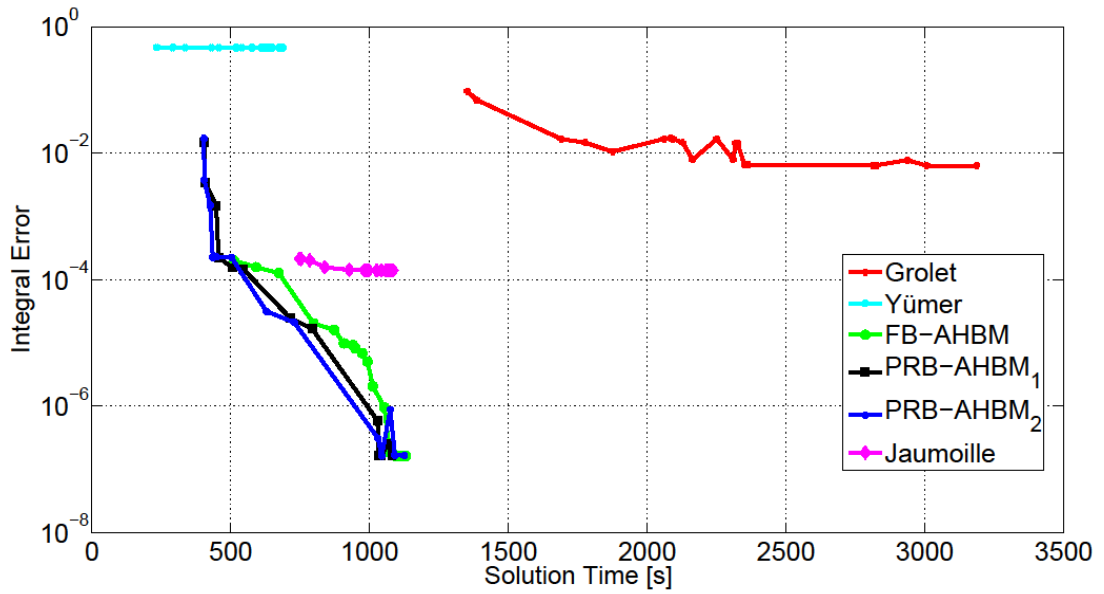
Figure 4.15 Computational Time vs Integral Error

4.4 Case Study 2

This study is carried out in order to present a comparison between the two PRB-AHBMs and FB-AHBM, which are proposed in this study, since these methods performed better than the other methods considered here. This section aims to emphasize the differences between them.

The system to be analyzed is illustrated in Figure 4.16. The parameters of the system are given in Table 4.27.
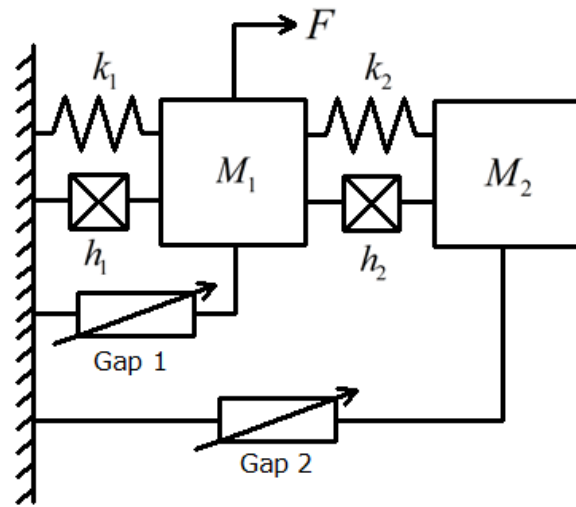
Figure 4.16 A 2-DOF System with gap nonlinearity

Table 4.27 Parameters of the 2-DOF System

M_1 (kg)	M_2 (kg)	k_1, k_2 (N/m)	h_1, h_2 (N/m)	F (N)
0.1	2	2000, 10000	40, 200	$30\sin(\theta)+1\sin(2\theta)+1\sin(3\theta)+...$ $+1\sin(4\theta)+1\sin(5\theta)$

The natural frequencies of the system are located at 28.37 rad/s and 252.41 rad/s. The frequency range in consideration is between 24 rad/s and 32 rad/s. These parameters are selected intentionally, so that the natural frequencies are far away from each other and there are no superharmonic peaks located inside the frequency range of interest. Parameters for the nonlinear elements are given in Table 4.28.

The plots obtained from the 10-harmonic classical solution are given in Figure 4.17 and Figure 4.18.

Table 4.28 Parameters for Nonlinear Elements

	δ (m)	k_g (N/m)
Gap 1	0.05	500
Gap 2	0.1	500
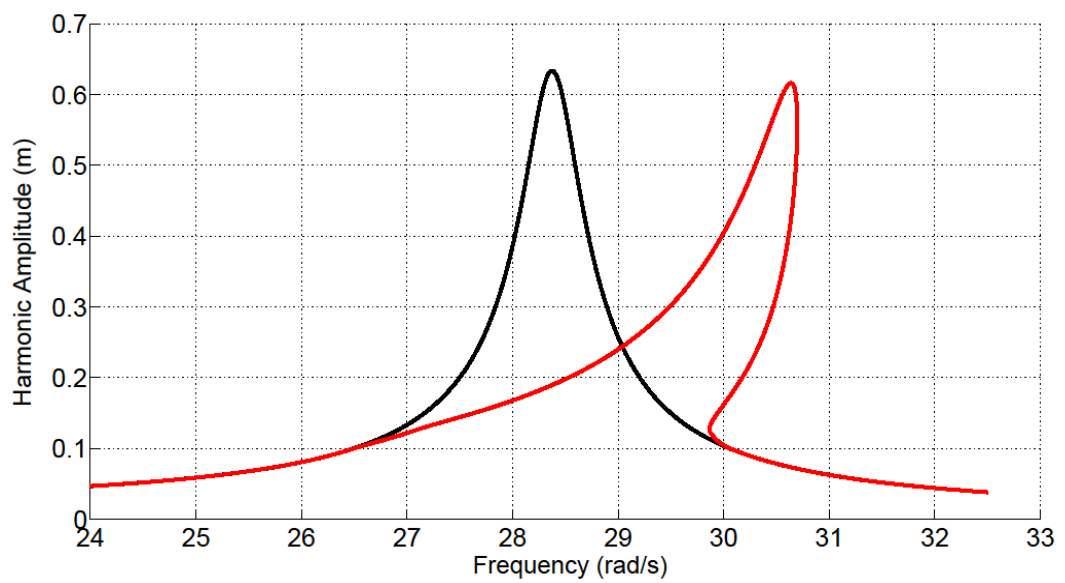
Figure 4.17 Total Response of the First DOF
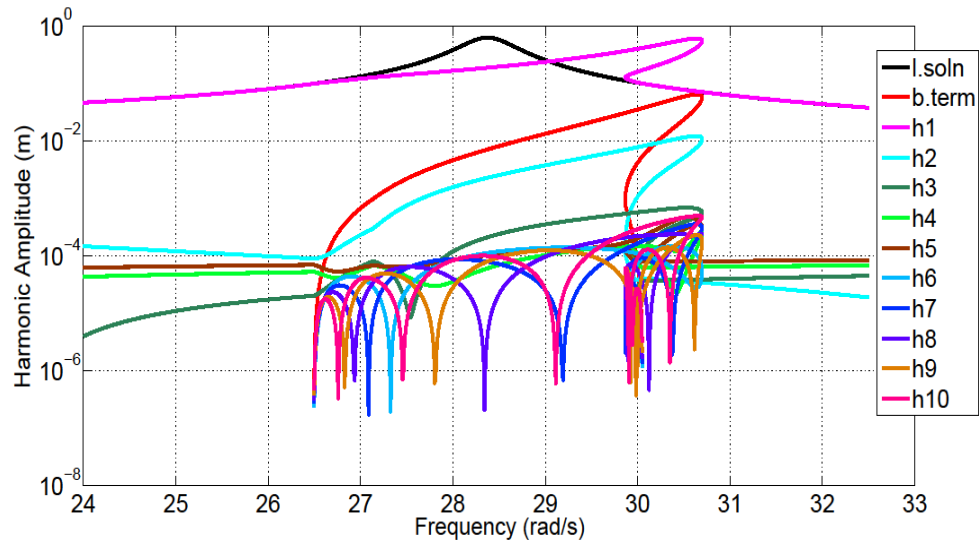
Figure 4.18 Amplitudes of harmonics for the First DOF

For the error analysis, the frequency response curve is studied in 2 parts as shown in Figure 4.19. The unstable region is excluded as in the previous comparisons.

The evaluation criteria are defined as follows:

1. Maximum error around the resonance (Region 1)
2. Maximum error in linear region (Region 2)
3. Maximum relative error around resonance (Region 1)
4. Integral error (all regions combined)

In addition to the solution time measured by the processor, total number of harmonics used throughout the solution is also included as a measure of computational effort spent.
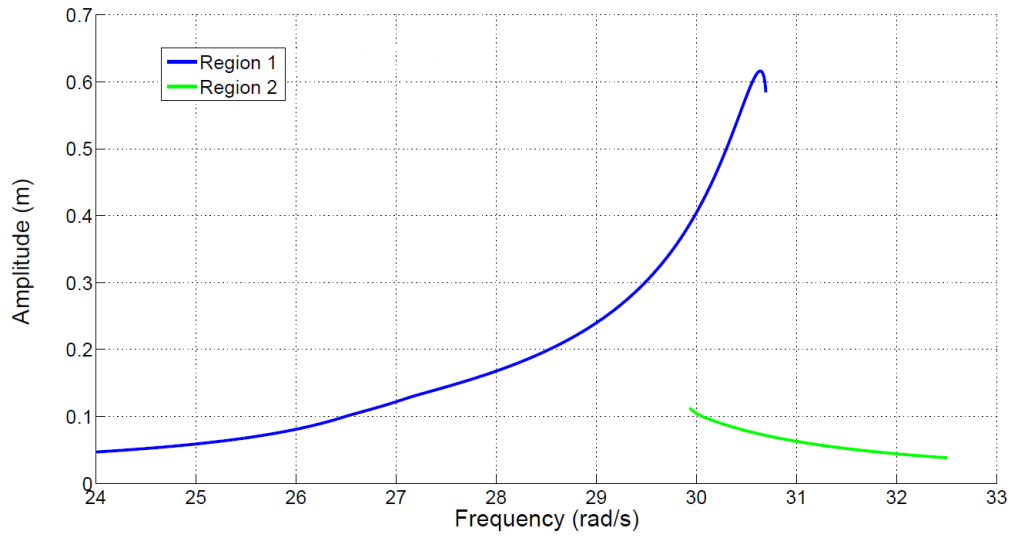
Figure 4.19 Regions defined for error analysis

4.4.1 Results Obtained by AHBM 4: FB-AHBM

As explained in Chapter 3, this method uses a threshold ratio, a to adjust the number of harmonics retained. Due its definition, a must be chosen greater than 1. Selecting parameter a larger forces the algorithm to include more harmonics in the solution. To prevent the algorithm from using too many harmonics, a maximum number of harmonics, i.e. 10 harmonics for this study, is defined. The results are given in Table 4.29, Table 4.30 and Table 4.31. The percentages of reduction obtained in computational time with respect to the 10-harmonic classical HBM solution are given in Table 4.32.

It can be seen from the tables that, since the method always retains the forcing harmonics in the solution, the time spent for solution and the total number of harmonics used do not drop below a certain margin. For this case study, the algorithm is forced to retain a minimum of 5 harmonics at each solution step, even though the higher harmonics in the forcing are relatively small, compared to the first

187

harmonic. Therefore, in the end, even the crudest solution includes 5822 harmonics; as result of which, the accuracy always stays above a certain value.

Table 4.29 Maximum Absolute Error Values for AHBM 4

a	Time (sec)	Max. Err 1	Max. Err 2	Total # of harmonics
2	169.9	3.58E-04	6.25E-05	5822
5	191.5	3.58E-04	5.56E-05	5884
10	196.6	3.58E-04	4.29E-05	5991
20	231.0	3.58E-04	2.29E-05	6589
30	267.0	2.55E-04	1.77E-05	7175
40	294.6	2.12E-04	1.76E-05	7546
50	314.9	2.12E-04	1.45E-05	7922
60	326.6	2.12E-04	1.45E-05	8091
70	322.2	2.12E-04	1.45E-05	8189
80	335.2	2.12E-04	1.45E-05	8303
90	306.3	2.12E-04	1.88E-06	8383
100	358.4	2.12E-04	1.65E-06	8476
200	353.2	2.70E-06	2.01E-06	8979
400	400.7	5.51E-07	9.46E-07	9100
600	400.1	5.51E-07	9.46E-07	9103
800	378.7	5.51E-07	1.71E-07	9106
1000	372.2	5.51E-07	1.71E-07	9106
2000	389.2	5.51E-07	1.71E-07	9109
10000	392.6	5.51E-07	1.71E-07	9110
100000	405.5	5.51E-07	1.71E-07	9110
1000000	419.3	5.51E-07	1.71E-07	9110

Table 4.30 Maximum Relative Error Values for AHBM 4

a	Time (sec)	Max. Err1 (Rel)	Max. Err6 (Rel)	Total # of harmonics
2	169.9	7.09E-04	5.87E-04	5822
5	191.5	7.09E-04	5.21E-04	5884
10	196.6	7.09E-04	3.86E-04	5991
20	231.0	6.13E-04	2.15E-04	6589

Table 4.30 (continued) Maximum Relative Error Values for AHBM 4

a	Time (sec)	Max. Err1 (Rel)	Max. Err6 (Rel)	Total # of harmonics
30	267.0	5.23E-04	1.62E-04	7175
40	294.6	5.23E-04	1.62E-04	7546
50	314.9	5.39E-04	1.32E-04	7922
60	326.6	5.39E-04	1.31E-04	8091
70	322.2	5.36E-04	1.31E-04	8189
80	335.2	3.47E-04	1.31E-04	8303
90	306.3	3.47E-04	1.74E-05	8383
100	358.4	3.47E-04	1.51E-05	8476
200	353.2	7.00E-06	1.85E-05	8979
400	400.7	5.50E-06	8.60E-06	9100
600	400.1	5.50E-06	8.60E-06	9103
800	378.7	5.50E-06	1.71E-06	9106
1000	372.2	5.50E-06	1.71E-06	9106
2000	389.2	5.50E-06	1.71E-06	9109
10000	392.6	5.50E-06	1.71E-06	9110
100000	405.5	5.50E-06	1.71E-06	9110
1000000	419.3	5.50E-06	1.71E-06	9110

Table 4.31 Integral Error Values for AHBM 4

a	Time (sec)	Total Integral Error	Total # of harmonics
2	169.9	3.95E-04	5822
5	191.5	3.92E-04	5884
10	196.6	3.87E-04	5991
20	231.0	3.46E-04	6589
30	267.0	3.56E-04	7175
40	294.6	2.65E-04	7546
50	314.9	2.56E-04	7922
60	326.6	2.07E-04	8091
70	322.2	1.51E-04	8189
80	335.2	1.03E-04	8303
90	306.3	7.69E-05	8383
100	358.4	4.74E-05	8476
200	353.2	5.84E-07	8979

Table 4.31 (continued) Integral Error Values for AHBM 4

a	Time (sec)	Total Integral Error	Total # of harmonics
400	400.7	7.35E-08	9100
600	400.1	6.86E-08	9103
800	378.7	5.55E-08	9106
1000	372.2	5.55E-08	9106
2000	389.2	5.07E-08	9109
10000	392.6	4.98E-08	9110
100000	405.5	4.98E-08	9110
1000000	419.3	4.98E-08	9110

Table 4.32 Reductions in computational time obtained by AHBM 4

a	Reduction in Time (%)
2	79.6
5	77.0
10	76.4
20	72.2
30	67.9
40	64.6
50	62.2
60	60.8
70	61.3
80	59.7
90	63.2
100	56.9
200	57.6
400	51.9
600	51.9
800	54.5
1000	55.3
2000	53.2
10000	52.8
100000	51.3
1000000	49.6

4.4.2 Results Obtained by AHBM 6: PRB-AHBM

As explained in Section 3.5, this method uses a threshold ratio, ε_t, to adjust the number of harmonics retained. Due to its definition, ε_t must be chosen between 0 and 1. Selecting parameter ε_t smaller forces the algorithm to include more harmonics in the response representation. To prevent the algorithm from using too many harmonics a maximum number of harmonics is defined, which is chosen as 10. At this part of the study, the second version of this method, presented in Section 3.5.1 is used. Results can be found in Table 4.33, Table 4.34 and Table 4.35. The percentages of reduction obtained in computational time with respect to the 10-harmonic classical HBM solution are given in Table 4.36.

It can be seen from the tables that, this method is more flexible in terms of computational time and accuracy. The number of harmonics and computational time could be reduced up to only 595 and 23.7 seconds, respectively. The method is suitable for obtaining the most precise solutions that can be obtained by FB-AHBM as well as much more crude ones. It is easier to find an optimum between computational time and accuracy by simply changing the control parameter ε_t.

Table 4.33 Maximum Absolute Error Values for AHBM 4

ε_t	Time (sec)	Max. Err 1	Max. Err 2	Total # of harmonics
5.00E-02	23.8	1.44E-02	4.87E-03	595
2.00E-02	29.9	2.72E-03	6.53E-03	770
1.00E-02	56.7	2.20E-03	2.00E-04	1690
9.00E-03	57.9	2.20E-03	2.05E-04	1702
8.00E-03	58.3	2.20E-03	4.06E-04	1711
7.00E-03	55.5	2.20E-03	2.05E-04	1725
6.00E-03	55.2	2.20E-03	2.05E-04	1737
5.00E-03	56.3	2.20E-03	2.05E-04	1759
4.00E-03	64.8	2.20E-03	2.04E-04	2040
3.00E-03	73.7	3.05E-04	1.99E-04	2435
2.00E-03	84.5	3.05E-04	1.99E-04	2732

Table 4.33 (continued) Maximum Absolute Error Values for AHBM 4

ε_t	Time (sec)	Max. Err 1	Max. Err 2	Total # of harmonics
1.00E-03	102.5	3.05E-04	1.84E-04	3717
9.00E-04	111.9	3.05E-04	1.15E-04	4014
8.00E-04	127.1	3.16E-04	6.69E-05	4506
7.00E-04	137.9	2.70E-04	5.19E-05	4851
6.00E-04	154.7	5.58E-04	5.18E-05	5287
5.00E-04	197.1	1.88E-04	5.14E-05	6286
1.00E-04	330.0	4.76E-05	1.06E-05	8682
5.00E-05	350.6	1.95E-05	1.85E-06	8976
1.00E-05	357.0	2.56E-06	1.93E-07	9096
5.00E-06	357.6	2.56E-06	1.71E-07	9100
1.00E-06	356.8	5.51E-07	1.71E-07	9110

Table 4.34 Maximum Relative Error Values for AHBM 6

ε_t	Time (sec)	Max. Err 1 (Rel)	Max. Err 2 (Rel)	Total # of harmonics
5.00E-02	23.8	2.70E-02	4.37E-02	595
2.00E-02	29.9	1.24E-02	5.87E-02	770
1.00E-02	56.7	4.94E-03	1.80E-03	1690
9.00E-03	57.9	4.36E-03	1.84E-03	1702
8.00E-03	58.3	3.84E-03	3.65E-03	1711
7.00E-03	55.5	3.76E-03	1.84E-03	1725
6.00E-03	55.2	3.76E-03	1.84E-03	1737
5.00E-03	56.3	3.76E-03	1.84E-03	1759
4.00E-03	64.8	3.76E-03	1.84E-03	2040
3.00E-03	73.7	1.22E-03	1.79E-03	2435
2.00E-03	84.5	1.22E-03	1.79E-03	2732
1.00E-03	102.5	9.00E-04	1.71E-03	3717
9.00E-04	111.9	7.78E-04	1.10E-03	4014
8.00E-04	127.1	7.74E-04	7.25E-04	4506
7.00E-04	137.9	7.74E-04	5.79E-04	4851
6.00E-04	154.7	9.24E-04	4.65E-04	5287
5.00E-04	197.1	7.66E-04	4.62E-04	6286
1.00E-04	330.0	1.64E-04	9.56E-05	8682
5.00E-05	350.6	7.43E-05	1.84E-05	8976
1.00E-05	357.0	2.54E-05	1.74E-06	9096
5.00E-06	357.6	2.54E-05	1.71E-06	9100
1.00E-06	356.8	5.50E-06	1.71E-06	9110

Table 4.35 Integral Error Values for AHBM 6

ε_t	Time (sec)	Total Integral Error	Total # of harmonics
5.00E-02	23.8	1.65E-02	595
2.00E-02	29.9	3.15E-03	770
1.00E-02	56.7	1.22E-03	1690
9.00E-03	57.9	1.15E-03	1702
8.00E-03	58.3	1.10E-03	1711
7.00E-03	55.5	1.05E-03	1725
6.00E-03	55.2	1.02E-03	1737
5.00E-03	56.3	9.93E-04	1759
4.00E-03	64.8	7.49E-04	2040
3.00E-03	73.7	4.92E-04	2435
2.00E-03	84.5	5.06E-04	2732
1.00E-03	102.5	4.05E-04	3717
9.00E-04	111.9	3.76E-04	4014
8.00E-04	127.1	3.32E-04	4506
7.00E-04	137.9	2.93E-04	4851
6.00E-04	154.7	2.80E-04	5287
5.00E-04	197.1	2.50E-04	6286
1.00E-04	330.0	1.41E-05	8682
5.00E-05	350.6	2.37E-06	8976
1.00E-05	357.0	1.10E-07	9096
5.00E-06	357.6	1.07E-07	9100
1.00E-06	356.8	4.98E-08	9110

Table 4.36 Reductions in computational time obtained by AHBM 6

ε_t	Reduction in Time (%)
5.00E-02	97.1
2.00E-02	96.4
1.00E-02	93.2
9.00E-03	93.0
8.00E-03	93.0
7.00E-03	93.3
6.00E-03	93.4
5.00E-03	93.2
4.00E-03	92.2

Table 4.36 (continued) Reductions in computational time obtained by AHBM 6

ε_t	Reduction in Time (%)
3.00E-03	91.2
2.00E-03	89.8
1.00E-03	87.7
9.00E-04	86.6
8.00E-04	84.7
7.00E-04	83.4
6.00E-04	81.4
5.00E-04	76.3
1.00E-04	60.4
5.00E-05	57.9
1.00E-05	57.1
5.00E-06	57.1
1.00E-06	57.1

4.4.3 Comparison

In this section, an overall comparison of the tabulated data given in the previous sections is presented. As explained in Section 4.4, four criteria are used for evaluation, each one of which is presented in a graphical form. As explained before, methods having plots closer to the lower left hand corner are more favorable, since greater accuracy is obtained with less computational time. Results are given in Figure 4.20 to Figure 4.23.

The results presented in the graphs indicate that using PRB-AHBM, it is more possible and easy to obtain a wide range of accuracies and with less or similar computational times. A desired precision can be obtained in relatively shorter time, especially when an average precision is required.
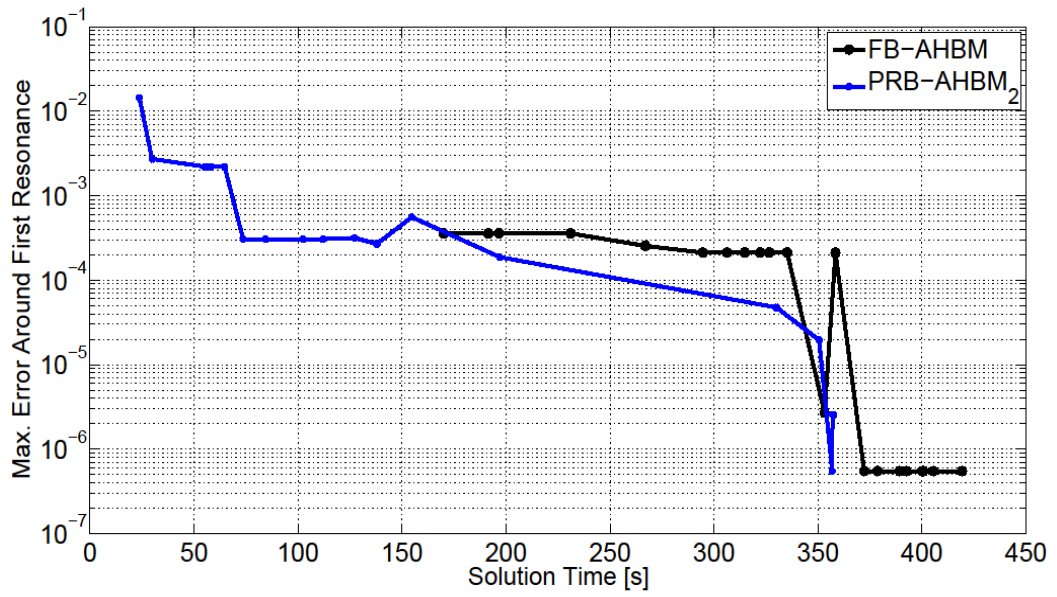
Figure 4.20 Computational Time vs Maximum Error in Region 1
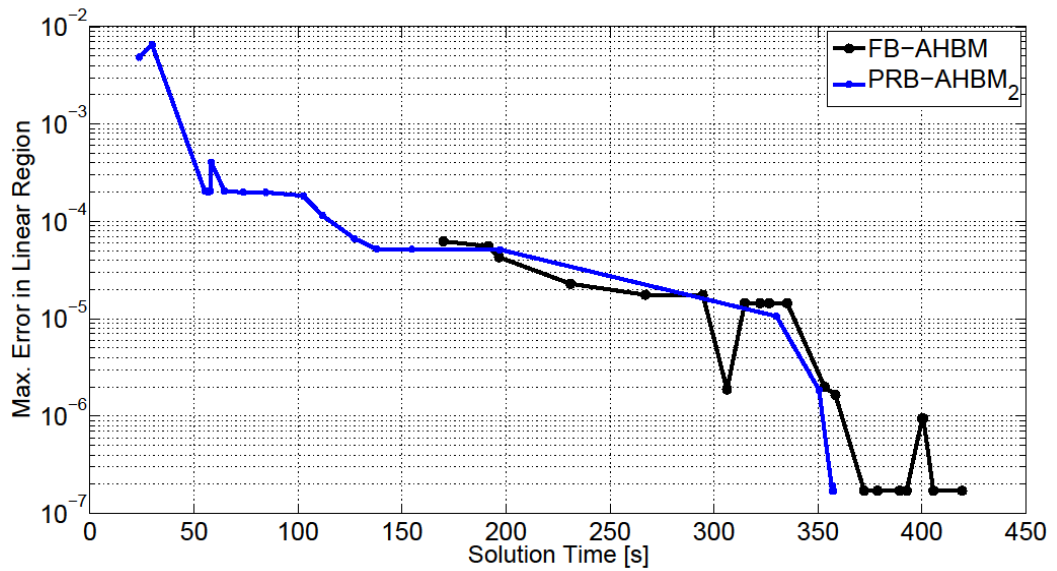
Figure 4.21 Computational Time vs Maximum Error in Region 2

195
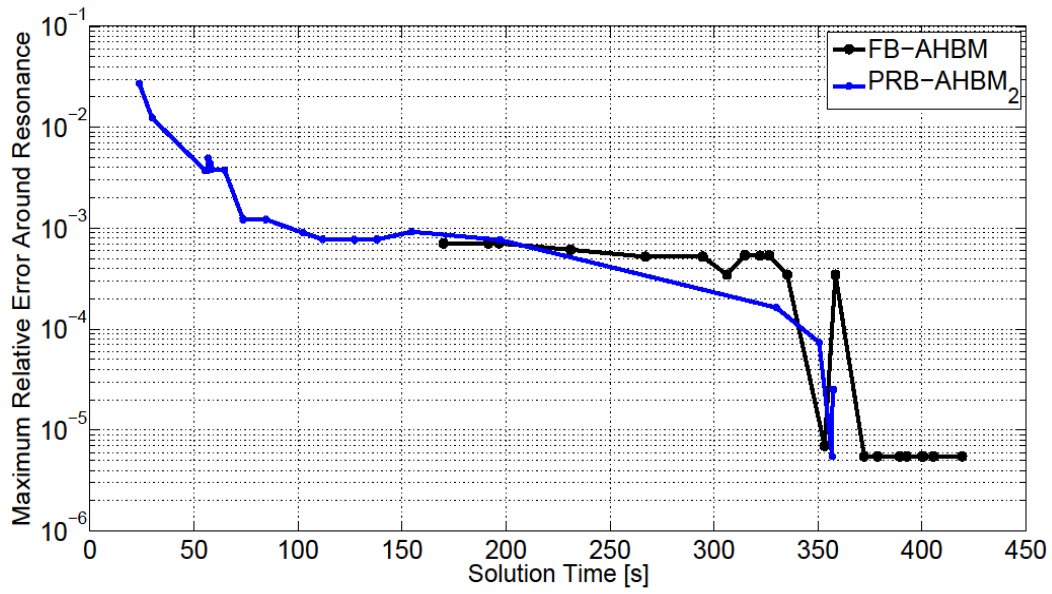
Figure 4.22 Computational Time vs Maximum Relative Error in Region 1
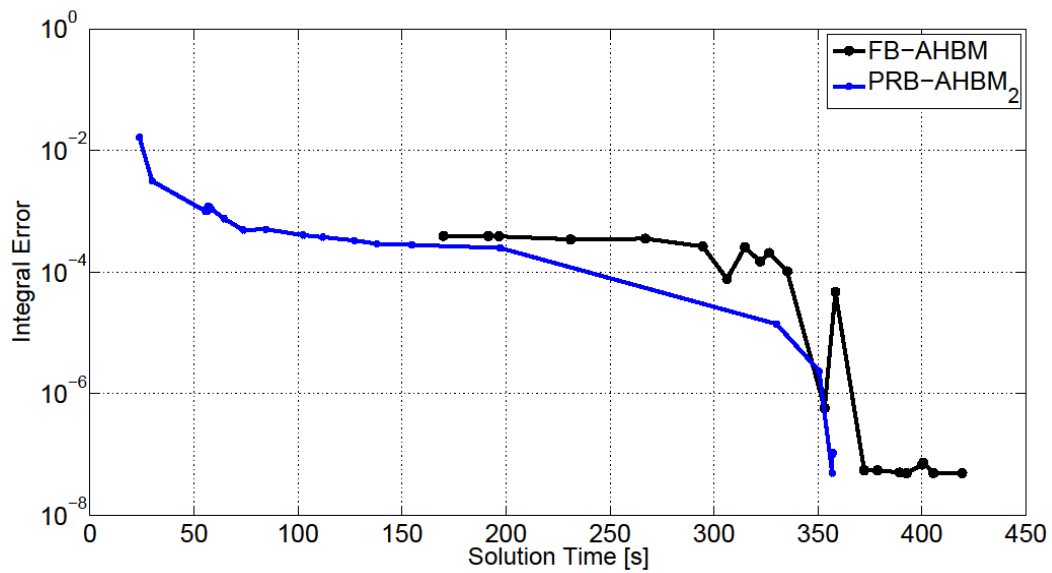
Figure 4.23 Computational Time vs Integral Error

196

CHAPTER 5

CONCLUSION

5.1   Conclusions

The main objective of this thesis is to investigate and compare the effectiveness of Adaptive Harmonic Balance Methods (AHBMs) that are currently in use for in structural dynamics and to introduce new Adaptive Harmonic Balance methods, which address the deficiencies of the existing ones.

In this thesis, first of all the theoretical background of the application of the Harmonic Balance Method (HBM) in nonlinear vibrations is explained in detail, together with the solution and path following methods. At the end of Chapter 2, case studies are given in order to demonstrate the classical HBM. In Chapter 3, AHBMs currently available in literature and used in the field of structural dynamics are presented. Furthermore, a new AHBM, namely PRB-AHBM, with two alternatives is developed and a new method based on the modification of Yümer's method, namely FB-AHBM, is proposed. Chapter 4 deals with the comparison of the mentioned AHBMs through two case studies. For all the studies presented, the same MATLAB codes that are written for each method are used.

The conclusions made from this study can be summarized as follows:

1. AHBM 1, created by Jaumoille, Sinou and Petitjean, is a favorable method for lightly nonlinear systems. However, there are cases where it can fail to increase the number of harmonics when needed. The method increases the number of harmonics starting from 1 at every solution step. When the number of harmonics needs to be increased, forming the tangent predictor by adding

zeros may end up with a very rough prediction and may cause convergence problems. Even when the solutions converge, the results may end up inaccurate.

2. In the case studies presented in this thesis, highly nonlinear small scale systems are analyzed. Also, in many of the examples, nonlinearities are distributed over every DOF. In a large scale system with local nonlinearities AHBM 2, created by Grolet et al., could prove to be more effective for the case where it is combined with a condensation method, such as the receptance method. Reducing the system by using condensation and then applying a second reduction by altering the harmonic number seperately for each DOF may work effectively. However, writing the code for this complex algorithm can be difficult and time consuming.

3. There are cases where Yümer's Method fails to include necessary harmonics inside the response representation and produces inaccurate results. In this thesis, a system with a multi-harmonic forcing and a gap nonlinearity caused inaccuracy. However, for a system with piecewise linear stiffness, this was not the case.

4. The newly introduced Forcing Based Adaptive Harmonic Balance Method (FB-AHBM) turned out to be a suitable method for analyzing small scale systems. However, it tends to work inefficiently when the harmonic content of the external forcing and the response of the analyzed system are not similar to each other. Therefore, it requires the user to have an insight about the system to be analyzed, which is a setback.

5. Unlike FB-AHBM, the newly proposed Pseudo-Response Based Adaptive Harmonic Balance Method (PRB-AHBM) does not require the user to have

any prior knowledge about the harmonic content of the analyzed system. Its threshold criteria solely depend on the ratio of response and forcing amplitudes and it does not require significant mathematical manipulations. Also, in the case studies presented, it has been seen that PRB-AHBM performs efficiently and accurately for the case studies considered in this study.

5.2 Future Recommendations

For future work, the following items can be considered:

- PRB-AHBM is a global method, i.e., it assigns the same number of harmonics for each DOF. A local version of the method may be introduced, so that the method performs more efficiently on large scale nonlinear systems. It should be developed method is a local method if the final part, which determines the maximum number of harmonics, is removed and the number of harmonics obtained for each DOF is stored.

- In this thesis, Newton's Method is used for solving the nonlinear algebraic equations. For the purpose of forming initial guesses, the tangent predictor is utilized. Quasi-Newton methods and other predictors may be tested, in order to accelerate the numerical solution process.

REFERENCES

[1] A. LaBryer and P. J. Attar, "A harmonic balance approach for large-scale problems in nonlinear structural dynamics," *Comput. Struct.*, vol. 88, no. 17–18, pp. 1002–1014, Sep. 2010.

[2] E. Sarrouy and J. Sinou, "Non-Linear Periodic and Quasi-Periodic Vibrations in Mechanical Systems-On the use of the Harmonic Balance Methods," in *Advances in Vibration Analysis Research*, D. F. Ebrahimi, Ed. InTech, 2011, pp. 419–434.

[3] Y. Kim and S. Choi, "A multiple harmonic balance method for the internal resonant vibration of a non-linear Jeffcott rotor," *J. Sound Vib.*, vol. 208, pp. 745–761, 1997.

[4] V. Jaumouillé, J.-J. Sinou, and B. Petitjean, "An adaptive harmonic balance method for predicting the nonlinear dynamic responses of mechanical systems—Application to bolted structures," *J. Sound Vib.*, vol. 329, no. 19, pp. 4048–4067, Sep. 2010.

[5] A. Grolet and F. Thouverez, "On a new harmonic selection technique for harmonic balance method," *Mech. Syst. Signal Process.*, vol. 30, pp. 43–60, Jul. 2012.

[6] M. E. Yümer, "On the Non-Linear Vibration and Mistuning Identification of Bladed Disks," Middle East Technical University, 2010.

[7] L. Z. L. Zhu and C. E. Christoffersen, "Adaptive harmonic balance analysis of oscillators using multiple time scales," *3rd Int. IEEE-NEWCAS Conf. 2005.*, pp. 1–4, 2005.

[8] M. M. Gourary, K. K. Gullapalli, B. J. Mulvaney, S. G. Rusakov, S. L. Ulyanov, and M. M. Zharov, "A New Computational Approach to Simulate Highly Nonlinear Systems by Harmonic Balance Method," 2000.

[9] R. C. Maple, P. I. King, P. D. Orkwis, and J. Mitch Wolff, "Adaptive harmonic balance method for nonlinear time-periodic flows," *J. Comput. Phys.*, vol. 193, no. 2, pp. 620–641, Jan. 2004.

[10] A. Nayfeh and D. Mook, *Nonlinear oscillations*, 2nd ed. New York: John Wiley & Sons Inc., 1995.

[11] M. M. Gourary, S. G. Rusakov, S. L. Ulyanov, M. M. Zharov, K. K. Gullapalli, and B. J. Mulvaney, "Adaptive Harmonic Balance Analysis (AHBA)."

[12] D. J. Lucia, P. S. Beran, and W. a. Silva, "Reduced-order modeling: new approaches for computational physics," *Prog. Aerosp. Sci.*, vol. 40, no. 1–2, pp. 51–117, Feb. 2004.

[13] H. Huang and K. Ekici, "A discrete adjoint harmonic balance method for turbomachinery shape optimization," *Aerosp. Sci. Technol.*, vol. 1, pp. 1–10, Jul. 2014.

[14] M. C. Pauzin, S. Mensah, B. Cochelin, and J. P. Lefebvre, "High order harmonic balance formulation of free and encapsulated microbubbles," *J. Sound Vib.*, vol. 330, no. 5, pp. 987–1004, Feb. 2011.

[15] K. Ekici, R. E. Kielb, and K. C. Hall, "The effect of aerodynamic asymmetries on turbomachinery flutter," *J. Fluids Struct.*, vol. 36, no. January 2009, pp. 1–17, Jan. 2013.

[16] R. E. Mickens and D. Semwogerere, "Consider the non-linear, one-dimensional oscillator differential equation," *J. Sound Vib.*, vol. 195, no. 3, pp. 528–530, 1996.

[17] H. S. Y. Ghan, K. W. Chung, and Z. Xut, "STRONGLY NON-LINEAR OSCILLATORS," vol. 31, no. 1, pp. 59–72, 1996.

[18] G. von Groll and D. Ewins, "The harmonic balance method with arc-length continuation in rotor/stator contact problems," *J. Sound Vib.*, no. August, pp. 1–12, 2001.

[19] J.-J. Sinou and a. W. Lees, "A non-linear study of a cracked rotor," *Eur. J. Mech. - A/Solids*, vol. 26, no. 1, pp. 152–170, Jan. 2007.

[20] J.-J. Sinou and a. W. Lees, "The influence of cracks in rotating shafts," *J. Sound Vib.*, vol. 285, no. 4–5, pp. 1015–1037, Aug. 2005.

[21] M. Guskov, J. J. Sinou, and F. Thouverez, "Multi-dimensional harmonic balance applied to rotor dynamics," *Mech. Res. Commun.*, vol. 35, no. 8, pp. 537–545, Dec. 2008.

[22] D. Laxalde and F. Thouverez, "Complex non-linear modal analysis for mechanical systems: Application to turbomachinery bladings with friction interfaces," *J. Sound Vib.*, vol. 322, no. 4–5, pp. 1009–1025, 2009.

[23] E. Ciğeroğlu and H. N. Özgüven, "Nonlinear vibration analysis of bladed disks with dry friction dampers," *J. Sound Vib.*, vol. 295, no. 3–5, pp. 1028–1043, Aug. 2006.

[24] K. Sanliturk and D. Ewins, "Modelling two-dimensional friction contact and its application using harmonic balance method," *J. Sound Vib.*, vol. 193, pp. 511–523, 1996.

[25] B. Şayin, "Application of Structural Modification Method to Nonlinear Vibration Analysis of Bladed Disks," Middle East Technical University, 2013.

[26] a. Al-Shyyab and a. Kahraman, "Non-linear dynamic analysis of a multi-mesh gear train using multi-term harmonic balance method: Sub-harmonic motions," *J. Sound Vib.*, vol. 279, no. 1–2, pp. 417–451, Jun. 2005.

[27] Y. Shen, S. Yang, and X. Liu, "Nonlinear dynamics of a spur gear pair with time-varying stiffness and backlash based on incremental harmonic balance method," *Int. J. Mech. Sci.*, vol. 48, no. 11, pp. 1256–1263, Nov. 2006.

[28] M. a. AL-Shudeifat, E. a. Butcher, and C. R. Stern, "General harmonic balance solution of a cracked rotor-bearing-disk system for harmonic and sub-harmonic analysis: Analytical and experimental approach," *Int. J. Eng. Sci.*, vol. 48, no. 10, pp. 921–935, Oct. 2010.

[29] D. D. Quinn, "Modal analysis of jointed structures," *J. Sound Vib.*, vol. 331, no. 1, pp. 81–93, Jan. 2012.

[30] J. X. Zhou and L. Zhang, "Incremental harmonic balance method for predicting amplitudes of a multi-d.o.f. non-linear wheel shimmy system with combined Coulomb and quadratic damping," *J. Sound Vib.*, vol. 279, no. 1–2, pp. 403–416, Jan. 2005.

[31] E. H. Boutyour, E. M. Daya, and M. Potier-Ferry, "A harmonic balance method for the non-linear vibration of viscoelastic shells," *Comptes Rendus Mécanique*, vol. 334, no. 1, pp. 68–73, Jan. 2006.

[32] N. Jacques, E. M. Daya, and M. Potier-Ferry, "Nonlinear vibration of viscoelastic sandwich beams by the harmonic balance and finite element methods," *J. Sound Vib.*, vol. 329, no. 20, pp. 4251–4265, Sep. 2010.

[33] S. Leadenham and a. Erturk, "M-shaped asymmetric nonlinear oscillator for broadband vibration energy harvesting: Harmonic balance analysis and experimental validation," *J. Sound Vib.*, pp. 1–15, Jul. 2014.

[34] Y. M. Chen, J. K. Liu, and G. Meng, "Incremental harmonic balance method for nonlinear flutter of an airfoil with uncertain-but-bounded parameters," *Appl. Math. Model.*, vol. 36, no. 2, pp. 657–667, Feb. 2012.

[35] M. Ye, S. Dou, W. Zhang, and Z. Zeng, "Nonlinear identification of systems with parametric excitation," *Sci. China Technol. Sci.*, vol. 54, no. 8, pp. 2080–2089, Jun. 2011.

[36] Y. M. Fu, J. W. Hong, and X. Q. Wang, "Analysis of nonlinear vibration for embedded carbon nanotubes," *J. Sound Vib.*, vol. 296, no. 4–5, pp. 746–756, Oct. 2006.

[37] K. Y. Xu, X. N. Guo, and C. Q. Ru, "Vibration of a double-walled carbon nanotube aroused by nonlinear intertube van der Waals forces," *J. Appl. Phys.*, vol. 99, no. 6, p. 064303, 2006.

[38] F. Albertson and J. Gilbert, "Harmonic Balance Method Used for Calculating the Steady State Oscillations of a Simple One-Cylinder Cold Engine," *J. Sound Vib.*, vol. 241, no. 4, pp. 541–565, Apr. 2001.

[39] C. Fritz, S. Farner, and J. Kergomard, "Some aspects of the harmonic balance method applied to the clarinet," *Appl. Acoust.*, vol. 65, no. 12, pp. 1155–1180, Dec. 2004.

[40] J. Alvarez, M. Meraz, F. J. Valdes-Parada, and J. Alvarez-Ramirez, "First-harmonic balance analysis for fast evaluation of periodic operation of chemical processes," *Chem. Eng. Sci.*, vol. 74, pp. 256–265, May 2012.

[41] V. Marinca and N. Herisanu, *Nonlinear Dynamical Systems in Engineering: Some Approximate Approaches*. Berlin: Springer, 2012.

[42] T. M. Cameron and J. H. Griffin, "An Alternating Frequency/Time Domain Method for Calculating the Steady-State Response of Nonlinear Dynamic Systems," *J. Appl. Mech.*, vol. 56, no. 1, p. 149, Mar. 1989.

[43] S. L. Lau and Y. K. Cheung, "Amplitude Incremental Variational Principle for Nonlinear Vibration of Elastic Systems," *J. Appl. Mech.*, vol. 48, no. 4, p. 959, Dec. 1981.

[44] K. Y. Sze, S. H. Chen, and J. L. Huang, "The incremental harmonic balance method for nonlinear vibration of axially moving beams," *J. Sound Vib.*, vol. 281, no. 3–5, pp. 611–626, Mar. 2005.

[45] A. A. Ferri, "On the Equivalence of the Incremental Harmonic Balance Method and the Harmonic Balance-Newton Raphson Method," *J. Appl. Mech.*, vol. 53, no. 2, p. 455, Jun. 1986.

[46] Y. K. Cheung, S. H. Chen, and S. L. Lau, "Application of the incremental harmonic balance method to cubic non-linearity systems," *J. Sound Vib.*, vol. 140, no. 2, pp. 273–286, Jul. 1990.

[47] C. Pierre, A. A. Ferri, and E. H. Dowell, "Multi-Harmonic Analysis of Dry Friction Damped Systems Using an Incremental Harmonic Balance Method," *J. Appl. Mech.*, vol. 52, no. 4, p. 958, Dec. 1985.

[48] S. L. Lau and W.-S. Zhang, "Nonlinear Vibrations of Piecewise-Linear Systems by Incremental Harmonic Balance Method," *J. Appl. Mech.*, vol. 59, no. 1, p. 153, Mar. 1992.

[49] A. Y. T. Leung and S. K. Chui, "Non-linear vibration of coupled duffing oscillators by an improved incremental harmonic balance method," *J. Sound Vib.*, vol. 181, no. 4, pp. 619–633, Apr. 1995.

[50] S. L. Lau and S. W. Yuen, "The Hopf bifurcation and limit cycle by the incremental harmonic balance method," *Comput. Methods Appl. Mech. Eng.*, vol. 91, no. 1–3, pp. 1109–1121, Oct. 1991.

[51] A. Raghothama and S. Narayanan, "Non-linear dynamics of a two-dimensional airfoil by incremental harmonic balance method," *J. Sound Vib.*, vol. 226, pp. 493–517, 1999.

[52] A. Raghothama and S. Narayanan, "Bifurcation and chaos in geared rotor bearing system by incremental harmonic balance method," *J. Sound Vib.*, vol. 226, pp. 469–492, 1999.

[53] A. Raghothama and S. Narayanan, "Bifurcation and chaos of an articulated loading platform with piecewise non-linear stiffness using the incremental harmonic balance method," *Ocean Eng.*, vol. 27, no. 10, pp. 1087–1107, Oct. 2000.

[54] L. Xu, M. W. Lu, and Q. Cao, "Bifurcation and chaos of a harmonically excited oscillator with both stiffness and viscous damping piecewise linearities by incremental harmonic balance method," *J. Sound Vib.*, vol. 264, no. 4, pp. 873–882, Jul. 2003.

[55] R. R. Pušenjak and M. M. Oblak, "Incremental harmonic balance method with multiple time variables for dynamical systems with cubic non-linearities," *Int. J. Numer. Methods Eng.*, vol. 59, no. 2, pp. 255–292, Jan. 2004.

[56] Y. M. Chen, J. K. Liu, and G. Meng, "Relationship between the homotopy analysis method and harmonic balance method," *Commun. Nonlinear Sci. Numer. Simul.*, vol. 15, no. 8, pp. 2017–2025, Aug. 2010.

[57] W. Lu, F. Ge, X. Wu, and Y. Hong, "Nonlinear dynamics of a submerged floating moored structure by incremental harmonic balance method with FFT," *Mar. Struct.*, vol. 31, pp. 63–81, Apr. 2013.

[58] B. S. Yuste, "Comments on the method of harmonic balance in which Jacobi elliptic functions are used," *J. Sound Vib.*, vol. 145, no. 3, pp. 381–390, Mar. 1991.

[59] J. Garcia-Margallo, J. D. Bejarano, and S. B. Yuste, "Generalized fourier series for the study of limit cycles," *J. Sound Vib.*, vol. 125, no. 1, pp. 13–21, Aug. 1988.

[60] B. S. Yuste and J. D. Bejarano, "Construction of approximate analytical solutions to a new class of non-linear oscillator equations," *J. Sound Vib.*, vol. 110, no. 2, pp. 347–350, Oct. 1986.

[61] J. Garcia-Margallo and J. D. Bejarano, "Generalized Fourier series and limit cycles of generalized van der Pol oscillators," *J. Sound Vib.*, vol. 136, no. 3, pp. 453–466, Feb. 1990.

[62] A. Elías-Zúñiga, "Application of Jacobian Elliptic Functions to the Analysis of the Steady-State Solution of the Damped Duffing Equation with Driving Force of Elliptic Type," *Nonlinear Dyn.*, vol. 42, no. 2, pp. 175–184, Oct. 2005.

[63] M. Belhaq and F. Lakrad, "on the Elliptic Harmonic Balance Method for Mixed Parity Non-Linear Oscillators," *J. Sound Vib.*, vol. 233, no. 5, pp. 935–937, Jun. 2000.

[64] F. Lakrad and M. Belhaq, "Periodic Solutions of Strongly Non-Linear Oscillators By the Multiple Scales Method," *J. Sound Vib.*, vol. 258, no. 4, pp. 677–700, Dec. 2002.

[65] L. Cveticanin, G. M. Abd El-Latif, a. M. El-Naggar, and G. M. Ismail, "Periodic solution of the generalized Rayleigh equation," *J. Sound Vib.*, vol. 318, no. 3, pp. 580–591, Dec. 2008.

[66] Y. M. Chen and J. K. Liu, "Elliptic harmonic balance method for two degree-of-freedom self-excited oscillators," *Commun. Nonlinear Sci. Numer. Simul.*, vol. 14, no. 3, pp. 916–922, Mar. 2009.

[67] Y. Kim and S. Noah, "Quasi-periodic response and stability analysis for a non-linear Jeffcott rotor," *J. Sound Vib.*, vol. 190, pp. 239–253, 1996.

[68] T. C. Kim, T. E. Rook, and R. Singh, "Super- and sub-harmonic response calculations for a torsional system with clearance nonlinearity using the harmonic balance method," *J. Sound Vib.*, vol. 281, no. 3–5, pp. 965–993, Mar. 2005.

[69] J. F. Dunne and P. Hayward, "A split-frequency harmonic balance method for nonlinear oscillators with multi-harmonic forcing," *J. Sound Vib.*, vol. 295, no. 3–5, pp. 939–963, Aug. 2006.

[70] N. Coudeyras, J. J. Sinou, and S. Nacivet, "A new treatment for predicting the self-excited vibrations of nonlinear systems with frictional interfaces: The Constrained Harmonic Balance Method, with application to disc brake squeal," *J. Sound Vib.*, vol. 319, no. 3–5, pp. 1175–1199, Jan. 2009.

[71] P. Bonello and P. Minh Hai, "A receptance harmonic balance technique for the computation of the vibration of a whole aero-engine model with nonlinear bearings," *J. Sound Vib.*, vol. 324, no. 1–2, pp. 221–242, Jul. 2009.

[72] A. LaBryer and P. J. Attar, "High dimensional harmonic balance dealiasing techniques for a Duffing oscillator," *J. Sound Vib.*, vol. 324, no. 3–5, pp. 1016–1038, Jul. 2009.

[73] a. Y. T. Leung and Z. Guo, "Forward residue harmonic balance for autonomous and non-autonomous systems with fractional derivative damping," *Commun. Nonlinear Sci. Numer. Simul.*, vol. 16, no. 4, pp. 2169–2183, Apr. 2011.

[74] a. Y. T. Leung and Z. Guo, "Residue harmonic balance approach to limit cycles of non-linear jerk equations," *Int. J. Non. Linear. Mech.*, vol. 46, no. 6, pp. 898–906, Jul. 2011.

[75] M. Xiao, W. X. Zheng, and J. Cao, "Approximate expressions of a fractional order Van der Pol oscillator by the residue harmonic balance method," *Math. Comput. Simul.*, vol. 89, pp. 1–12, Mar. 2013.

[76] J. Didier, J.-J. Sinou, and B. Faverjon, "Nonlinear vibrations of a mechanical system with non-regular nonlinearities and uncertainties," *Commun. Nonlinear Sci. Numer. Simul.*, vol. 18, no. 11, pp. 3250–3270, Nov. 2013.

[77] E. Ciğeroğlu, *ME709 Lecture Notes*, Spring Sem. Middle East Technical University, 2012.

[78] J. D. García-Saldaña and A. Gasull, "A theoretical basis for the Harmonic Balance Method," *J. Differ. Equ.*, vol. 254, no. 1, pp. 67–80, Jan. 2013.

[79] C. Kelley, *Solving nonlinear equations with Newton's method*, 1st ed. Philadelphia: Society for Industrial and Applied Mathematics, 2003.

[80] C. T. Kelley, *Iterative Methods for Linear and Nonlinear Equations*, 1st ed. Philadelphia: Society for Industrial and Applied Mathematics, 1995.

[81] C. G. Broyden, "A Class of Methods for Solving Nonlinear Simultaneous Equations," *Math. Comput.*, vol. 19, no. 92, p. 577, Oct. 1965.

[82] A. Niet, "Step-size control and corrector methods in numerical continuation of ocean circulation and fill-reducing orderings in multilevel ILU methods," University of Groningen, 2002.

[83] C. H. Menq, J. H. Griffin, and J. Bielak, "The influence of microslip on vibratory response, Part II: a comparison with experimental results," *J. Sound Vib.*, vol. 107, no. 2, pp. 295–307, 1986.

[84] E. Cigeroglu, N. An, and C.-H. Menq, "Forced Response Prediction of Constrained and Unconstrained Structures Coupled Through Frictional Contacts," *J. Eng. Gas Turbines Power*, vol. 131, no. 2, p. 022505, 2009.

[85] K. Worden and G. Tomlinson, *Nonlinearity in Structural Dynamics: Detection, Identification and Modelling*, 1st ed. Bristol: Institute of Physics Publishing, 2001.

[86] I. Senjanovi ć and Y. Fan, "Some Advances of the Harmonic Balance Method," *J. Sound Vib.*, vol. 191, no. 2, pp. 295–307, Mar. 1996.

[87] S. C. Chapra, *Applied Numerical Methods with MATLAB for Engineers and Scientists*, 3rd ed. New York: McGraw Hill, 2012.